Doctorate Program in Molecular Oncology
and Endocrinology
Doctorate School in Molecular Medicine

XX cycle - 2004–2007
Coordinator: Prof. Giancarlo Vecchio

"Anaplastic thyroid carcinoma: novel therapeutic targets and strategies"

Silvana Libertini

University of Naples Federico II
Dipartimento di Biologia e Patologia Cellulare e Molecolare
"L. Califano"

Administrative Location

Dipartimento di Biologia e Patologia Cellulare e Molecolare "L. Califano"
Università degli Studi di Napoli Federico II

Partner Institutions

Italian Institutions
Università di Napoli "Federico II", Naples, Italy
Istituto di Endocrinologia ed Oncologia Sperimentale "G. Salvatore", CNR, Naples, Italy
Seconda Università di Napoli, Naples, Italy
Università del Sannio, Benevento, Italy
Università di Genova, Genoa, Italy
Università di Padova, Padua, Italy

Foreign Institutions
Johns Hopkins School of Medicine, Baltimore, MD, USA
Johns Hopkins Krieger School of Arts and Sciences, Baltimore, MD, USA
National Institutes of Health, Bethesda, MD, USA
Ohio State University, Columbus, OH, USA
Université Paris Sud XI, Paris, France
Universidad Autonoma de Madrid, Spain
Centro de Investigaciones Oncologicas (CNIO), Spain
Universidade Federal de Sao Paulo, Brazil
Albert Einstein College of Medicine of Yeshiwa University, USA

Supporting Institutions
Università di Napoli "Federico II", Naples, Italy
Ministero dell'Istruzione, dell'Università e della Ricerca
Istituto Superiore di Oncologia (ISO)
Terry Fox Foundation, Canada
Istituto di Endocrinologia ed Oncologia Sperimentale "G. Salvatore", CNR, Naples, Italy
Centro Regionale di Competenza in Genomica (GEAR)

Faculty

Italian Faculty

Giancarlo Vecchio, MD, Co-ordinator
Salvatore Maria Aloj, MD
Francesco Beguinot, MD
Maria Teresa Berlingieri, PhD
Angelo Raffaele Bianco, MD
Bernadette Biondi, MD
Francesca Carlomagno, MD
Gabriella Castoria, MD
Angela Celetti, MD
Annamaria Cirafici, PhD
Mario Chiariello, MD
Vincenzo Ciminale, MD
Annamaria Colao, MD
Alma Contegiacomo, MD
Sabino De Placido, MD
Monica Fedele, PhD
Pietro Formisano, MD
Alfredo Fusco, MD
Massimo Imbriaco, MD
Paolo Laccetti, MD
Antonio Leonardi, MD
Barbara Majello, PhD
Rosa Marina Melillo, MD
Claudia Miele, PhD
Francesco Oriente, MD
Roberto Pacelli, MD
Giuseppe Palumbo, PhD
Silvio Parodi, MD
Giuseppe Portella, MD
Giorgio Punzo, MD
Antonio Rosato, MD
Massimo Santoro, MD
Giampaolo Tortora, MD
Donatella Tramontano, PhD
Giancarlo Troncone, MD
Bianca Maria Veneziani, MD
Giuseppe Viglietto, MD
Roberta Visconti, MD

Foreign Faculty

National Institutes of Health (USA)
Michael M. Gottesman, MD
Silvio Gutkind, PhD
Stephen Marx, MD
Ira Pastan, MD
Phil Gorden, MD

Johns Hopkins School of Medicine (USA)
Vincenzo Casolaro, MD
Pierre Coulombe, PhD
James G. Herman MD
Robert Schleimer, PhD

Johns Hopkins Krieger School of Arts and Sciences (USA)
Eaton E. Lattman, MD

Ohio State University, Columbus (USA)
Carlo M. Croce, MD

Albert Einstein College of Medicine of Yeshiwa University (USA)
Luciano D'Adamio, MD
Nancy Carrasco

Université Paris Sud XI (France)
Martin Schlumberger, MD

Universidad Autonoma de Madrid (Spain)
Juan Bernal, MD, PhD
Pilar Santisteban

Centro de Investigaciones Oncologicas (Spain)
Mariano Barbacid, MD
Universidade Federal de Sao Paulo (Brazil)
Janete Maria Cerutti
Rui Maciel

“Anaplastic thyroid carcinoma: novel therapeutic targets and strategies”

TABLE OF CONTENTS

LIST OF PUBLICATIONS

This dissertation is based upon the following publications:

-Libertini S, Iacuzzo I, Ferraro A, Vitale M, Bifulco M, Fusco A, Portella G.
Lovastatin enhances the replication of the oncolytic adenovirus dl1520 and its antineoplastic activity against anaplastic thyroid carcinoma cells.
Endocrinology. 2007 Nov;148(11):5186-94. Epub 2007 Aug 9.

-Chieffi P, Cozzolino L, Kisslinger A, Libertini S, Staibano S, Mansueto G, De Rosa G, Villacci A, Vitale M, Linardopoulos S, Portella G, Tramontano D.
Aurora B expression directly correlates with prostate cancer malignancy and influence prostate cell proliferation.
Prostate. 2006 Feb 15;66(3):326-33.

-Perruolo G, Libertini S, Santopietro S, Troncone G, Raciti GA, Oriente F, Portella G, Miele C, Beguinot F.
Raised expression of the antiapoptotic protein ped/pea-15 increases susceptibility to chemically induced skin tumor development.
Oncogene. 2005 Oct 27;24(47):7012-21.

-Sorrentino R, Libertini S, Pallante PL, Troncone G, Palombini L, Bavetsias V, Spalletti-Cernia D, Laccetti P, Linardopoulos S, Chieffi P, Fusco A, Portella G
Aurora B overexpression associates with the thyroid carcinoma undifferentiated phenotype and is required for thyroid carcinoma cell proliferation.
J Clin Endocrinol Metab. 2005 Feb;90(2):928-35. Epub 2004 Nov 23.

-Chieffi P, Troncone G, Caleo A, Libertini S, Linardopoulos S, Tramontano D, Portella G.
Aurora B expression in normal testis and seminomas.
J Endocrinol. 2004 May;181(2):263-70.

-Portella G, Pacelli R, Libertini S, Cella L, Vecchio G, Salvatore M, Fusco A.
ONYX-015 enhances radiation-induced death of human anaplastic thyroid carcinoma cells.
J Clin Endocrinol Metab. 2003 Oct;88(10):5027-32.

ABSTRACT

Anaplastic thyroid carcinoma (ATC) is one of the most aggressive human malignancies, with a mean survival of only 6 months. Therefore, novel therapeutic approaches are desperately required.

- *dl*1520 is a replication competent adenovirus that, due to lack of a functional *E1B-55kD* gene, can complete its life cycle solely in tumoural cells. We previously demonstrated that *dl*1520 efficiently kills ATC cells, but high multiplicity of infection (MOI) are required to obtain a significant antineoplastic effect. One of the major limiting factor in the efficient adenoviral transduction is the presence on cell surface of CAR receptor. Inhibition of the Raf/MEK/ERK pathway up-regulates CAR expression in cancer cells, thus improving adenoviral entry and cell killing by adenoviral mutants. To enhance its oncolytic activity, we decided to combine *dl*1520 with lovastatin, a drug that, blocking mevalonate synthesis, inhibits Raf/MEK/ERK pathway. However, lovastatin does not up-regulate CAR levels but, acting on viral genes expression, enhances viral replication. Indeed, lovastatin enhances *in vitro* and *in vivo dl*1520 effects, thus suggesting its potential role as *dl*1520 adjuvant in ATC therapy.

- A common feature of anaplastic thyroid carcinoma is represented by aneuploidy. Aberrant expression of Aurora B occurs in solid tumours and it is associated with chromosome instability and carcinogenesis. Therefore, Aurora B expression has been evaluated in cell lines and samples from human thyroid carcinoma, showing that its expression paralleles the malignant phenotype. To establish a molecular target for ATC, Aurora B expression has been inhibited by RNAi or a specific inhibitor, showing that Aurora B inhibition blocks cell proliferation and cell survival.

1. BACKGROUND

THYROID CARCINOMA

Thyroid cancers originating from follicular cell epithelium include papillary thyroid carcinoma, follicular carcinoma, and anaplastic thyroid carcinoma (ATC). Well differentiated thyroid carcinomas (WDTC: papillary and follicular) account for 80-85% of all thyroid carcinomas while ATC accounts for a small fraction (1-7%). Despite the small percentage, ATC is responsible for more than half of the 1200 deaths per year attributed to thyroid cancer (Ain *et al*. 1998).

At molecular level, papillary carcinoma presents an high percentage of rearrangements of RET gene and/or B-RAF mutations (Grieco *et al.* 1990, Xu *et al.* 2003) while follicular carcinomas frequently show RAS genes activating mutations (Suarez *et al.* 1990) and PAX 8-PPAR-1 rearrangements (Kroll *et al.* 2000). Alterations of the p53 tumour suppressor gene and beta-catenin are a peculiar feature of anaplastic carcinomas (Ito *et al.* 1992, Garcia Rostan *et al.* 1999, Nikiforov *et al.* 2004).

Several studies have documented a series of molecular abnormalities associated with the progression of normal to benign to well-differentiated to anaplastic thyroid carcinoma. The evidences available so far suggest that the early stages of thyroid cancer development may be the consequence of the activation of proto-oncogenes or growth factor receptors, such as gsp, ras, ret, and the thyrotropin (TSH) receptor. Inappropriate expression of these genes is associated with the development of neoplasms ranging from benign toxic adenomas (TSH receptor), to differentiated follicular (ras, B-Raf) and papillary (met, NTRK, ret, PAX8-PPAR1) carcinomas. In contrast, alterations in tumour suppressor genes such as p53 or Rb are solely observed in poorly differentiated forms of thyroid cancer, suggesting that they represent relatively late genetic events (Segev *et al*. 2003).

Usually, thyroid cancer is a well treatable disease with a good prognosis. Current therapeutic protocols include surgery to remove the thyroid gland in part or totally, followed, if necessary, by application of ^{131}I. This radioisotope is accumulated in remnant or even disseminated thyrocytes by the thyroidal sodium/iodide symporter (NIS) and destroys them by internal radiation. Another widely used therapeutic measure is the administration of thyroxine (T_4) to suppress the production of the thyrotrophic growth factor TSH via hypothalamic and hypophyseal feedback; this aims to reduce the proliferation rate of residual thyroid tissue or metastases. In contrast, external radiation or chemotherapy, being less potent, are of minor importance (Schmultzler and Koehrle 2000).

These therapeutic measures are so far the only ones with proven efficiency and prognostic relevance. They are successfully applied for WDTCs

but they are unsuccessful for anaplastic thyroid carcinoma, that is one of the most malignant solid tumour in the human body, leading to death within a few months after diagnosis.

THERAPEUTIC APPROACHES FOR ATC

The individual failure of all modalities in the management of anaplastic thyroid carcinoma has prompted the application of multimodality regimens, with old and new drugs in different combinations, including vascular targeting agents (in table 1, VTA), histone deacetilase inhibitors (HDACI), PPARgamma agonist (PPARγA), reverse transcriptase inhibitors (RTI) and farnesyl-transferase inhibitors (FTI). These approaches are summarized in table 1.

Table 1 – Novel therapeutic approaches for anaplastic thyroid carcinoma

Class of drug	Drug 1	Drug 2	Drug 3	Effect	In vitro/ in vivo	Reference
VTA	anti VEGF2	Irinotecan or Paclitaxel	/	No potentiation	Both	Kim *et al.* 2006, Gomez-Rivera *et al.* 2007
VTA	anti EGF	/	/	/	Both	Schiff *et al.* 2004
VTA	anti EGF	anti VEGF	Doxorubucin	Potentiation	Both	Prichard *et al.* 2007
VTA	anti EGF/VEGF	Paclitaxel	/	Synergistic	Both	Kim *et al.* 2005
VTA	Combretastatin A4	/	/	/	Both	Randal *et al.* 2000, Dowlati *et al.* 2002
VTA	Combretastatin A4	Manumicin or Carboplatin	Paclitaxel	Synergistic	Both	Yeung *et al.* 2007
VTA	Combretastatin A4	/	/	/	One patient still alive after 36 months	Randal *et al.* 2000
VTA	Fumagillin	/	/	/	Both	Hama *et al.* 1997, Nahari *et al.* 2007
HDACI	Trichostatin A	/	/	/	In vitro	Greenberg *et al.* 2001
HDCAI	Sodium butyrate	/	/	/	In vitro	Greenberg *et al.* 2001
HDACI	Acid valproic	Doxorubicin	/	Potentiation	In vitro	Catalano *et al.* 2006
HDACI	Acid valproic	Paclitaxel	/	Potentiation	In vitro	Catalano *et al.* 2007
HDACI	SAHA	/	/	/	Both	Mitsiades *et al.* 2005, Luong *et al.* 2006
HDACI	Depsipeptide (FR901228)	P53 gene therapy	/	Potentiation	In vitro	Kitazono *et al.* 2001, Imanishi *et al.* 2002, Furuya *et al.* 2004
PPARγA	RS5444	Paclitaxel	/	Potentiation	Both	Copland *et al.* 2006
RTI	nevirapine	/	/	Differentiation	Both	Landriscina *et al.* 2005
RTI	efavirenz	/	/	Differentiation	Both	Landriscina *et al.* 2005
RTI	nevirapine	/	/	Restore of radioiodine uptake in distal metastatic	One patient	Modoni *et al.* 2007
FTI	Manumycin A	Paclitaxel	/	Synergistic	Both	Xu *et al.* 2001, Yeung *et al.* 2007
FTI	Manumycin A	Paclitaxel	Minocycline	Synergistic	Both	She and Jim 2006

Some of these agents have been proposed for different lesions, such as vascular targeting agents, that seek to starve the tumour by inhibiting angiogenesis, or farnesyltransferase inhibitors, that act on genes (*e.g.* Ras) frequently mutated in tumours. Others agents are more specific for ATC, since they seek to redifferentiate thyroid tumours, at least to such a degree that established treatment protocols, especially radioiodine therapy, may be applicable again. The classification is not so strict, indeed some drugs, initially designed as antineoplastic agent, can also induce differentiation, and therefore be used to restore sensitivity to radioiodine uptake.

GENE THERAPY

Another proposed approach for ATC treatment is gene therapy. Gene therapy seeks to treat cancer by introducing genes that will result in destruction of the tumour from within or will enhance an immune response against it. Viruses are frequently chosen as vehicles for such genes because they have evolved very efficient mechanisms of gene transfer (transduction) and expression. For safety reasons, such virus vectors are generally replication-defective but, unfortunately, this limits the efficacy of treatment by restricting the number of cells the therapeutic gene is delivered to (reviewed by Walther and Stein 2000). For this reason, the use of replication-competent viruses has been proposed. There are 3 general mechanisms used to achieve tumour selective viral replication:

1) deletion of viral genes that are dispensable upon infection of neoplastic cells but are critical for viral replication in non neoplastic cells,
2) placement of tumour specific promoters upstream of viral genes that are critical for efficient viral replication,
3) delivery of virus entry into cells based on the expression of antigens that are unique or overexpressed on the tumour cell surface.

It is worth to note that the replication of these viruses results in lysis of the host cells with amplification of the "input dose", since the infection continues until abrogated by an immune system response or a lack of susceptible cells. Consequently, oncolytic viral therapy is capable of increasing the therapeutic index between tumour cells and normal cells when viral replication proceeds preferentially in tumour cells.

The role of immune system is controversial. Oncolytic viruses can be administered locally, by direct intratumoural inoculation, or systemically, by intravascular administration. The immune system could antagonize the effectiveness of oncolytic viruses administered intravascularly by limiting viral delivery to the tumour while, on the other hand, once the virus has reached its target and begins replicating within and destroying tumour cells, the immune response can theoretically augment tumour reduction by redirecting the cytotoxic T lymphocytes response from viral antigens to tumour antigens, also against distal metastasis. In fact, viruses administered by direct intratumoural inoculation elicit a systemic immune response that prevents tumour formation and causes regression of existing tumours at distant sites (Todo *et al.* 1999).

These data suggest that the best targets for replication competent viruses are locally advanced cancers, such as glioblastoma, ovarian cancer, head and neck cancer and anaplastic thyroid carcinoma.

Gene therapy for anaplastic thyroid carcinoma

Several approaches of gene therapy have been studied for poorly differentiated and anaplastic thyroid carcinomas, such as differentiating therapy to restore radioiodine uptake (see Spitzweg and Morris 2001), suicide therapy, replication selective viruses.

In suicide gene therapy, gene transfer is used to introduce into the tumour a vector coding for a `sensitising enzyme'. A chemotherapeutic agent is then applied as a non-toxic prodrug, which is activated only in those cells that express the sensitising enzyme. The most widely used system for suicide therapy is the prodrug ganciclovir (GCN) together with herpes simplex virus type 1 thymidine kinase (HSV1-TK). GCN is a nucleotide analogue, and HSV1-TK, in contrast to normal mammalian TK, preferentially phosphorylates GCN. Monophosphorylated GCN is then converted to its triphosphate by cellular kinases and interferes with cell propagation by competition with normal nucleotides during replication. Growing cells will be destroyed preferentially, which limits the side effects on normal tissue. As the thyroid gland is a very slowly growing tissue, gene therapy using GCN and the TK gene might be a method of choice in this case. In 2005, Barzon et colleagues published the first report of gene therapy for ATC using suicide therapy. Two patients with end-stage anaplastic thyroid carcinoma were treated by direct intratumour injection of retroviral vector producer cells followed by ganciclovir. The retroviral vector carried the human IL-2 gene and the suicide gene thymidine kinase of herpes simplex virus type 1. Treatment was safe and associated with only mild adverse events. Radiological evaluation of injected tumour masses demonstrated local tumour necrosis.

The most used replication defective viruses are adenoviral mutants; to better understand their function, I will briefly summarize their life cycle.
The Ad genome is composed of a linear double-stranded DNA molecule of approximately 36 kb. Adenoviral infection of permissive cells involves two distinct virus–cell interactions. Cell surface attachment is mediated by binding of the knob domain of the viral fiber protein to the cellular coxsackie–adenovirus receptor (CAR) (Bergelson *et al*. 1997; Tomko *et al.* 2000). Internalization, via receptor-mediated endocytosis, involves interactions between the Arg-Gly-Asp peptide sequence of the viral penton protein with the cellular *a*v*b*3 and *a*v*b*5 integrin receptors. Ad genes are transcribed in a complex temporal manner and have been divided into three groups: early, intermediate, and late (Fields 1996). Early viral gene expression commences at the E1 locus and includes gene products that promote entry into cell cycle. E1A binds members of the cellular pRb family. This interaction results in the displacement of Rb-bound E2F family members, that are then free to activate transcription of E2F-responsive genes involved in stimulating cell cycle

progression. The expression of E1A induces an apoptotic cellular antiviral response through p53-dependent and independent pathways. To circumvent premature cell death during viral replication, the viral E1B-55kD protein binds to and inhibits p53 (Yew and Berk 1992) while the E1B-19kD protein functions as a viral homolog of the cellular antiapoptotic factor Bcl2 (White 1992). The remaining early regions encode proteins involved in viral DNA synthesis (E2), modulation of host immune response and cell lysis (E3), and regulation of viral gene expression, mRNA transport, DNA replication, and apoptosis (E4). The intermediate and late gene products encode viral structural proteins and proteins involved in virion assembly.

A well designed replication competent virus is HILMI. As already mentioned, a sizable fraction of undifferentiated or poorly differentiated thyroid cancers were shown to contain mutations in beta-catenin, an oncogenic protein involved in the aetiology of cancers of many tissues. Abbosh *et al.* (2007) developed HILMI, a conditionally replicative adenovirus that, by virtue of TCF response elements, drives E1A and E1B expression and replicates specifically in cells with an active Wnt/beta-catenin pathway. Several thyroid cancer cell lines, derived from undifferentiated or anaplastic tissues, were susceptible to cell killing by HILMI. Furthermore, viral replication in ATC cells as xenograft tumours in nude mice was observed, and prolonged survival of mice with ATC tumours was observed following administration of the HILMI therapeutic vector. Clinical trial are now necessary to establish its therapeutical effect.

Already studied in clinic is *dl*1520, the first replication competent adenovirus described. *dl*1520 (also called ONYX-015) contains alterations in the *E1B-55kD* gene, that result in complete abrogation of E1B-55kD protein expression (Bischoff *et al.* 1996). E1B-55kD binds and inhibits the p53 tumour suppressor protein, thereby inhibiting p53-dependent apoptosis and enabling the cell to enter the S phase of the cell cycle, a requirement for efficient replication of viral DNA. *dl*1520 lacks the ability to inactivate p53 and therefore it was expected to replicate only in cells lacking functional p53. This has generated considerable hopes for its clinical use, because more than 50% of tumours have a mutant *TP53* gene and even more possess defects in one of the genes that modulate p53 expression (White 2006, Fulci *et al.* 1998, Fulci and Van Meir 1999). In spite of this early enthusiasm (Bischoff *et al*. 1996; Heise *et al*. 1997; Rogulski *et al*. 2000), there have been reports contradicting the mechanism of *dl*1520 selectivity based on findings that cells with a normal *TP53* gene support its replication. Recently, it has been shown that E1B-55K mediates late-viral RNA transport and *dl*1520 tumour-selective replication is determined by a unique property of tumour cells to efficiently export late viral RNA in the absence of E1B-55kD. Thus, loss of E1B-55kD-mediated late viral RNA export, rather than p53 degradation, is the major determinant of *dl*1520 selective replication in neoplastic cells (Parato *et al.* 2005).

The safety and antitumour efficacy of *dl*1520 have been tested in numerous phase I and II clinical trials with multiple tumour types and several

routes of administration (for a review, see Nemunaitis *et al.* 2007). In all cases, safety was demonstrated, with the most common associated toxicity being flulike symptoms. Although preclinical cancer models have demonstrated the antitumour capabilities of *dl*1520, there are few examples of complete tumour eradication. A multimodal cancer therapy approach utilizing oncolytic viruses in conjunction with chemotherapy or radiotherapy was the next logical step. Several studies *in vitro* and *in vivo*, utilizing various human tumour models, have demonstrated enhanced to synergistic effects of *dl*1520 in combination with different drugs (see table 2). Several mechanism can explain the augmented therapeutic effects of combined treatment:

- the virus may be increasing the cell-killing effects of the drug sensitising cells to antineoplastic agents,
- the drug may enhance virus replication,
- the two different therapies may be acting on different cell populations within the tumour.

*dl*1520 has also been used in conjunction with chemotherapeutic agents in clinical trials with evidence for potential synergistic antitumour activity (see table 2). It is worth to note that in all tested clinical approaches there is not a significant increase in toxicity compared with single treatment.

Table 2- *dl*1520 plus chemotherapy

Drug	Effect/Comment	Tumour type	In vitro/ in vivo/ clinical trial	Reference
Cisplatin + paclitaxel	Synergistic	NSCLC	In vitro	You *et al.* 2000
Doxorubicin	Synergistic	Thyroid	In vitro	Portella *et al.* 2002
Paclitaxel	Synergistic	Thyroid	In vitro	Portella *et al.* 2002
5-fluorouracil	Enhanced	HNSCC	In vivo	Heise *et al.* 1997
5-fluorouracil	Enhanced	Colon	In vivo	Heise *et al.* 1997
Cisplatin	Enhanced	HNSCC	In vivo	Heise *et al.* 1997
5-fluorouracil + cisplatin	Enhanced	HNSCC	In vivo	Heise *et al.* 2000
5-fluorouracil + cisplatin	Enhanced	Ovarian	In vivo	Heise *et al.* 2000
5-fluorouracil + cisplatin	Enhanced, with no improved toxicity	HNSCC	Phase II	Khuri *et al.* 2000, Lamont *et al.* 2000
leucovorin and 5-fluorouracil	Enhanced, with no improved toxicity	gastrointestinal carcinoma metastatic to the liver	Phase II	Reid *et al.* 2002
gemcitabine	Enhanced, with no improved toxicity	unresectable pancreatic carcinoma	Phase I/II	Hecht *et al.* 2003

Finally**,** in November 2005, China approved world's first oncolytic virus therapy for cancer treatment, with Shanghai Sunway Biotech's genetically modified adenovirus H101. This virus is considered the Chinese version of *dl*1520, being the only difference between the two viruses a slightly larger deletion in H101's E3 gene, which affects immune response. In its phase III trial, Sunway reported a 79% response rate for H101 plus chemotherapy, compared with 40% for chemotherapy alone (Yu and Fang 2007**)**.

We have previously demonstrated an antineoplastic activity of *dl*1520 against ATC cell lines (Portella *et al.* 2002, Portella *et al.* 2003). It is worth to note that high multiplicity of infection (MOI) were used in these previous studies, highlighting the need to enhance viral transduction in order to obtain a significant killing effect. CAR receptor is a major limiting factor in the efficient transduction of tumour cells, since it is not ubiquitously expressed and many tumour types exhibit variable levels of CAR expression (Bergelson *et al*. 1997; Fechner *et al.* 1999; Tomko *et al.* 2000). Moreover, recent observation suggest that expression of this receptor, that physiologically participates in formation of cell-cell adhesion, is frequently reduced in highly malignant cancer cells. This raises the possibility that those tumours representing the greatest therapeutic challenge might be the least susceptible to infection with oncolytic adenovirus. It has been reported that treatment of cells with histone deacetilase inhibitors up-regulates CAR and αv integrin levels, increasing the number of infected cells and the antitumour effect of the replicant selective adenovirus OBP-301 (Kitazono *et al.* 2001, Goldsmith *et al.* 2003, Watanabe *et al.* 2006). Anders *et al*. (2003) showed that inhibition of the Raf/MEK/ERK pathway up-regulates CAR expression in cancer cells, thus improving adenoviral entry and cell killing by *dl*1520. To enhance viral transduction, we decided to combine *dl*1520 with lovastatin, a statin that, acting on mevalonate pathway, behaves as Raf/MEK/ERK pathway inhibitor.

Statins as antineoplastic drugs

Increasing evidences suggest that statins might be useful for cancer treatment. Statins, or 3-hydroxy-3-methylglutaryl coenzyme A (HMG-CoA) reductase inhibitors, are commonly-used drugs for the treatment of hypercholesterolemia. They act inhibiting the rate-limiting step of the mevalonate pathway, that is the conversion of HMG-CoA to mevalonate, catalyzed by HMG-CoA reductase. They have a marked beneficial action on the lipid profile but also have effects unrelated to lipid reduction, since mevalonate is precursor not only of cholesterol but also of dolicol, ubiquinone and prenylic groups (geranyl-geranylpyrophospate GPP and farnesylpyrophosphate FPP). Geranylgeranyl transferase and farnesyl transferase use GPP and FPP, respectively, for posttranslational modifications of cellular proteins. These include Ras, nuclear lamins, and many small GTP-binding proteins such as members of the Rab, Rac, and Rho families. Indeed, to be active, some proteins must first undergo prenylation to properly associate with the plasma membrane. This association is achieved by the addition of a farnesyl (*e.g.,* Ras) or a geranylgeranyl moiety (*e.g.,* Rho) to the COOH terminus of the proteins. Blockade of mevalonate pathway results in decreased levels of all its downstream products and, thus, may have significant influences on many critical cellular functions, such as cell proliferation, differentiation and migration (Chan *et al*. 2003). Indeed, *in vitro* and *in vivo* studies have demonstrated that statins inhibit tumour growth, induce apoptosis or decrease metastatic potential in a variety of tumour cells, including melanoma

(Shellman *et al.* 2005), glioma (Koyuturk *et al.* 2004), neuroblastoma (Girgert 1999), leukemia (Dimitroulakos *et al.* 2000), breast (Koyuturk *et al.* 2007) and pancreatic cell lines (Kusama *et al.* 2001). Additionally, several clinical trials have also assessed the antitumour activity of statins (for a review, see Hindler *et al*. 2006). Moreover, increasing evidence suggest that statins might enhance the antitumour activity of various chemotherapeutic agents (see table 3).

Table 3 – Statin for the treatment of cancer: summary of human clinical trials

Drug	No. of patients	Type of cancer	Result	Reference
Fluvastatin	12	Pediatric tumours	22 months' survival of two patients with anaplastic astrocytoma	Lopez-Aguilar *et al.* 1999
Pravastin + fluorouracil	91	Advanced hepatocellular carcinoma	Median survival rate: 18 months in the statin group vs. 9 months in the control group ($p < .006$)	Kawata *et al.* 2001
Lovastatin	1	Acute myeloblastic leukemia	Statin therapy leads to an apparent control of the leukemic blast cells	Minden *et al.* 2001
Pravastastin	58	Hepatocellular carcinoma	Median survival rate: 7.2 months in the statin group vs. 5 months in the octreotide group and 3.5 months in the gemcitabine group	Lersch *et al.* 2004
Statin and neoadjuvant chemoradiation	349	Non metastatic rectal cancer	Complete response rate: 30% in the statin group vs. 17% in the control group ($p= .10$)	Katz *et al.* 2005
Lovastatin	26	HNSCC	Stable disease in 23% of the patients	Knox *et al.* 2005

It is important to note that recent study by Wang *et al.* (2003) has shown that at a higher dose (50microM) lovastatin induces apoptosis of ATC cells, whereas at a lower doses (10-25microM) it promotes 3-D cytomorphological differentiation and increases secretion of thyroglobulin, a differentiation marker of thyrocytes. These data have further encouraged us to evaluate the effects of the combined treatment .

To treat anaplastic thyroid carcinoma it is also important to identify novel therapeutic targets. To this purpose, we focused our attention on Aurora B kinase, that belongs to Aurora kinase family genes.

AURORA KINASES

Mitosis is an extraordinary complex biological process, by which a complete copy of the duplicated genome is precisely segregated into two daughter cells. All mitosis phases are strictly controlled by phosphorylation events performed by several evolutionary conserved serine/threonine kinases, known as mitotic kinases, such as cyclin-dependent kinases, NIMA-related kinases and Aurora-Ipl1 related kinases. Three paralogues of Aurora kinases are present in mammals: Aurora A, Aurora B and Aurora C. These are very similar in sequence, in particular within the carboxyterminal catalytic domain, in which human Aurora A and B share 71% identity. However, the three Auroras differ in the length and sequence of the amino-terminal domain and have very distinct expression patterns, localizations, functions. Aurora-A kinases are associated with centrosomes and are involved in their positioning, recruitment of components at the forming mitotic spindle and microtubules stability while Aurora B and Aurora C are chromosomal passenger proteins. Moreover, Aurora A and Aurora B are expressed ubiquitously while Aurora C is expressed only in testis.

The genes encoding the three human Aurora kinases map to regions that are affected by chromosomal abnormalities in different cancer types, and overexpression of each of the three human Auroras has been detected in tumour cell lines (Carmena and Earnshaw 2003).

Aurora B

The Aurora B gene lies on human chromosome 17p13 and codifies for a 41KDa serin-treonin kinase. Aurora B expression and activity in proliferating tissues are cell cycle regulated: expressions peaks at G2-M transition and kinase activity is maximal during mitosis.

Aurora B is a one of the component of the Cromosomal Passenger Complex. The CPC proteins show a very dynamic localization during mitosis that gave them their name (Earnshaw and Bernat, 1991): they initially paint the entire chromatin during the onset of mitosis, move from the chromosome arms toward the inner centromeric chromatin (in between the kinetochores, the sites of microtubule attachment)during prometaphase, relocalize to the microtubules of the central spindle at the metaphase–anaphase transition, and finally concentrate at the midbody during telophase/cytokinesis. This localization correlates with the diverse functions of the CPC during mitosis: modifying histones at the chromatin, correcting misattachments while at the centromere, and regulating cytokinesis at the central spindle (and later midbody). Given the correlation between localization and function, it is apparent that timely and

proper localization of the CPC is the key to allowing Aurora-B to exert its diverse functions during mitosis (Vader *et al.* 2006).

The CPC can be regarded as a complex in which the binding of a nonenzymatic protein to its enzymatic partner is essential for functioning of the kinase. The CPC contains three nonenzymatic subunits, all of which are essential for the activity, localization, stability, and substrate specificity of Aurora-B. In human cells, these non enzymatic subunits are Survivin, the inner centromere protein (INCENP), and Borealin. Recent evidence suggests that two distinct passenger complexes exist during mitosis: one containing all four CPC members and another consisting of INCENP and Aurora-B (Gassmann *et al*. 2004). Of these two complexes, the quaternary CPC functions during chromosome alignment and cytokinesis, whereas the INCENP–Aurora-B complex might be responsible for modifying Histone H3 (Gassmann *et al*., 2004). Aurora-B is a histone kinase, a spindle checkpoint kinase and a cytokinesis kinase.

Histone kinase - Aurora-B is responsible for the mitotic phosphorylation of not only the celebrated Ser10 residue in the tail of histone H3 but also of Ser28 in H3 and of Ser7 in CENP-A. These phosphorylation events are thought to be necessary for chromosome condensation, although the only direct evidence comes from Tetrahymena. It is quite likely, however, that these phosphorylations might only initiate the recruitment of condensation and segregation proteins on chromosomes (Goto *et al.* 2002).

Spindle checkpoint kinase - Aurora-B phosphorylates, inactivating and targeting it to the kinetochores, the microtubule depolymerase MCAK (mitotic centromere-associated kinesin). MCAK can then be locally activated by a phosphatase, presumably PP1, to correct any incorrect kinetochore attachments to the spindle. In the absence of Aurora-B, MCAK does not localize to kinetochores and incorrect attachments persist (Andrews *et al.* 2004).

A speculative model postulate that the dynamic interplay between Aurora B, MCAK and PP1 could constitute a phosphorylation-dependent tensiometer. The key to this model is a dynamic, metastable localization of Aurora B. The asymmetric localisation of Aurora B on the centromere axis results in asymmetric phosphorylation of factors that promote microtubule dynamics, such as MCAK, causing asymmetric force production and thus directional movement of the chromosome. A force-balanced stationary chromosome can occur only transiently, unless Aurora B localization becomes fixed between the middle of centromeres or the its kinase activity is inhibited. At anaphase, Aurora B leaves the centromere and force generation can proceed unhindered (Giet *et al.* 2005).

Cytokinesis kinase – Phosphorylation has a dramatic effect on intermediate filament stability and some intermediate filaments participating in cleavage furrow dynamics, such as vimentin, desmin, myosin II, are Aurora B substrates. For instance, Aurora-B phosphorylates Ser72 in vimentin: in the absence of Ser72 phosphorylation, the two daughter cells remain associated through long bridges of cytoplasm, and cytokinesis fails (Goto *et al.* 2003).

Moreover, Aurora-B also phosphorylates MgcRacGAP, a GTPase-activating protein (GAP) required for cytokinesis. Phosphorylation in Ser387 occurs in the midbody and activates its GAP activity towards RhoA. MgcRacGAP and RhoA seem to regulate cortical movement during cytokinesis (Minoshima *et al.* 2005)

Aurora B and cancer

Aurora B is involved in chromosome segregation, spindle-checkpoint and cytokinesis, and alteration of each of these steps could induce aneuploidy, that is one of main feature and driving force of cancer cells.

In vitro studies performed with several Aurora B inhibitors/dominant negative/RNAi, show that Aurora B deficiency interfere with cell cycle. Treated cells cannot divide after mitosis and become tetraploidy, with 2 centrosomes. Moreover, cells expressing catalytically inactive Aurora B do not arrest in mitosis in the presence of nocodazole or taxol, underling a role for Aurora B in mitotic checkpoint. These observations concur with Aurora B presumed roles: spindle checkpoint suppression let cells go on mitosis, despite many of the chromosome are oriented in a syntelic manner (both kinetocore attached to the same pole) while the missed fosforilation of clivage furrow components prevents the cytokinesis. The effects of longer depletion of Aurora B seem to be cell line dependent. Some cells either enter additional cell cycles but, because of cell division failure, they become massively polyploidy, whereas others undergo apoptosis or arrest in a pseudo G1 state. These different fates are probably not a reflection of differing requirements for Aurora-kinase activity in these cell lines, but rather of the status of the p53-dependent post-mitotic checkpoint (Margolis *et al*. 2003). Briefly, it seems that p53 can also respond to a failed cell division by inducing a G1-like arrest following an abnormal mitosis. In this manner, p53 might act as a 'back-up' to the spindle-checkpoint system to prevent the propagation of cells with an abnormal genome. Consistently, p53 is required to prevent endoreplication in U2OS cells following exposure to the Aurora inhibitor ZM447439 (Ditchfield *et al.* 2003).

One report from Ota *et al*. (2002) strongly suggests a direct link between Aurora B and carcinogenesis. The authors transfected Chinese hamster embryo (CHE) cells, carrying wild type p53 or a G245S mutation in both allele of p53 (CHEp53$^{-/-}$), with Aurora B. The mutation in p53 abrogates the p53-dependent G1 checkpoint. Stable clones overexpressing Aurora B were isolated and injected in nude mice. Notably, the authors could use only CHEp53$^{-/-}$ tranfected cells, since they could not isolate any stable clone from CHE with wt p53. Nontransfected cells induce tumours when injected in nude mice, but they don't metastasize whereas mice injected with Aurora B overexpressing CHE p53$^{-/-}$ cells formed more aggressive tumours that, also, developed metastases. In a recent paper, Kanda *et at.* (2005) showed that, although Aurora B overexpression is not oncogenic in BALB/c 3T3 A31-1-1 cells, Aurora-B kinase activity augments Ras-mediated cell transformation,

suggesting that the overexpression of Aurora-B may contribute to the generation of a transformed phenotype, by potentiating oncogene activity during carcinogenesis.

Aurora B expression has been studied in different human cancer and it has been shown that its expression directly correlates with malignancy in several human cancers, such as non small cell lung carcinoma (Smith *et al*. 2005, Vischioni *et al.* 2006), mesothelioma (Lopez-Rios *et al.* 2006), glioblastoma (Araki *et al*. 2004, Zeng *et al.* 2007), oral cancer (Qi *et al.* 2007) and hepatocellular carcinoma (Kurai *et al.* 2005). In previous papers, we have demonstrated that Aurora B is overexpressed in seminoma (Chieffi *et al.* 2004) and that Aurora B expression directly correlates with Gleason grade in prostate cancer (Chieffi *et al.* 2006).

Despite the established role of Aurora B in different types of cancers, information regarding its expression in normal and neoplastic thyroid are very limitate. A recent paper by Ito *et colleagues* (2003) demonstrated that survivin expression is significantly linked to the dedifferentiation of thyroid carcinoma, being survivin expression low in normal tissue, stronger in papillary and follicular carcinomas and very strong in anaplastic thyroid.

This observation, the high aneuploidy of thyroid carcinoma and the availability of specific inhibitors led us to analyse the expression of Aurora B in anaplastic thyroid carcinoma.

Aurora kinases inhibitors represent a novel and interesting class of drugs with a broad therapeutic index. Indeed, Aurora kinases are only expressed and active during mitosis, therefore non-proliferating cells would not be adversely affected by these drugs. Furthermore, cells lacking a p53-mediated post-mitotic checkpoint are highly responsive to Aurora(s) inhibition. Clinical trial will be soon underway to test the effect of Aurora-kinase inhibitors in patient with cancer, animal studies suggest that the major side effect is neutropenia, dose depending and reversible.

Anaplastic thyroid carcinoma are characterized by high incidence of p53 mutation, therefore Aurora B could represent a novel therapeutic target for the treatments of this dismal disease.

2. AIMS OF THE STUDY

Novel therapeutic approaches are desperately required for anaplastic thyroid carcinoma, that is one of the most aggressive human neoplasia.

We have previously demonstrated that the oncolytic adenovirus *dl*1520 is active against ATC cells and tumour xenografts, although a high viral multiplicity of infection are required. In the present thesis, I have decided to evaluate whether the combination of *dl*1520 with lovastatin, a drug that blocks mevalonate pathway, could enhance viral cell killing activity .

Aneuploidy is a common feature of anaplastic thyroid carcinoma and the serine threonine kinase Aurora B is involved in chromosomal instability. Therefore, I have decided to evaluate the expression levels of Aurora B in ATC cell lines, experimental models of thyroid carcinogenesis and human samples, validating Aurora B as potential therapeutic target.

3. MATERIALS AND METHODS

Cell lines

See Sorrentino *et al*., 2005 and Libertini *et al.,* 2007

Plamids, transfections, Aurora B inhibitor

PCMV-AurB construct was obtained as follows: mRNA from human testis (Clontech, USA) was reverse transcribed using random hexamers as primers and MuLV reverse transcriptase (Applied Biosystems, Foster City, CA) to yeld cDNA. The forward: 5'CTCTGGATCCATGGCCCAGAAGGAGAAC3'; and the Reverse: 5'ACAGGGATCCTCAGGCGACAGATTGAAG3' primers were used to amplify the human Aurora B gene (Accession: NM 004217). The PCR product was cloned into the Bam H1 site of the pcDNA His-tagged (Invitrogen Life Technologies).The pCMV-AurB sense and antisense constructs were obtained by inserting the Aurora B cDNA in both sense and antisense orientation in the pCMV vector under the trascriptional control of the cytomegalovirus promoter. The vector also carries the gene for G418 resistance. The transfection was performed according to the calcium phosphate transfection protocol. After 36 hours, the cells were tripsinized and expanded, stable transfectants were generated after selection with 400 μg/ml geneticin (G418) (Life Technologies, Italy). Five and six independent clones were isolated from pCMV-AurB sense and antisense and from control transfections, respectively. The integration of the contruct was confirmed by Southern blot assay. In pCMV-AurB antisense transfected clones a decreased synthesis of Aurora B protein was confirmed by Western Blot. Clones carrying sense or antisense plasmid were then selected for further experiments.

For the synthesis of Aurora kinase inhibitor was followed the methodology described elsewhere. The quinazolin derivative: N-[4-(6,7-dimethoxy-quinazolin-4-ylamino)-phenyl]-benzamide was dissolved in DMSO at a concentration of 10mM. $1x10^3$ ARO cells were plated in a 96 well plate and after 24 hours the cells were treated with 5, 10, 15 μM of the inhibitor. Cell proliferation was evaluated after 24 and 48 hours by using the Cell Titer 96 ® Aqueous cell proliferation assay (Promega). Soft agar colony assays were performed according to a previously described technique.

RNA interference and transfection of RNA Oligonucleotides

For design of siRNA oligos targeting Aurora B, the sequence AAG GAGAACUCCUACCCCUGG (RNAi) was selected, corresponding to the nucleotides located 67-87 bp of the human Aurora B gene. As a control of siRNA oligo, the following aspecific sequence was used AAG GUC CCC AUC CUC AAG AGG (RNAc). The siRNAs were purchased from Pharmacon Research (USA). Approximately, $6*10^5$ cells were plated per 6-well plate in media containing 10% fetal bovine serum to give 30–50% confluence.

Transfection of the RNA oligonucleotides was performed after 24 hours to result in a final RNA concentration of 200nM. Transfections were performed by Oligofectamine (Invitrogen, Carlsbad, CA).

Preparation of adenoviruses and adenovirus infection

*dl*1520 (ONYX-015), a gift from Dr. A. Balmain and Dr I. Ganly, is a chimaeric human group C adenovirus (Ad2 and Ad5) that has a deletion between nucleotides 2496 and 3323 in the E1B region that encodes the 55-kDa protein. In addition, there is a C to T transition at position 2022 in region E1B that generates a stop codon at the third codon of the protein. Viral stocks were expanded in the human embryonic kidney cell line HEK-293 (American Type Culture Collection) and purified as previously reported. Stocks were stored at -70°C after the addition of glycerol to a concentration of 50% vol/vol. Virus titre was determined by plaque-forming units (pfu) on the HEK-293 cells.
Cells were detached, counted, and plated in 6 well plate at 70% cell density. After 24 hours cells were infected with AdGFP, a non replicating E1 and E2-deleted adenovirus encoding green fluorescent protein, diluted in growth medium at different MOIs, medium was replaced after 2 hours. Cells were washed 24 hours after infection, then trypsinised, washed, and resuspended in 300µl of PBS and analyzed for GFP expression on a FACS cytometer (Dako Cytomation, U.S.A.) and Summit V4.3 software (Dako).
For the evaluation of lovastatin effects on adenoviral entry and GFP expression, the cells were treated for 16h with 10 µM lovastatin and then infected for 24 h with AdGFP. Cells were harvested and prepared for FACS analysis as previously described. For the evaluation of the cytoxic effects of the *dl*1520 virus, 1 x10^3 cells were seeded in 96-well plates, and 24 hours later lovastatin was added to the incubation medium. After additional 16 hours, medium was replaced with a medium containing or not lovastatin plus *dl*1520 at different MOIs. After 14 days, the media were fixed with 50% TCA and stained with 0.4 % sulforhodamine B in 1% acetic acid. The bound dye was solubilised in 200 µl of 10 mM unbuffered Tris solution and the optical density was determined at 490 nm in a microplate reader (Biorad). The percent of survival rates of treated cells were calculated by assuming the survival rate of untreated cells to be 100%.

Quantitative PCR of dl1520

To quantify the amount of *dl*1520 virus genome upon lovastatin treatment, ATC cells were treated with 10µM lovastatin for 16 hours and then media replaced with a medium containing different MOIs of *dl*1520 alone or with lovastatin. After 24 hours of infection, cell media were collected and viral DNA extracted using a QIAamp DNA mini kit (Valencia, CA, USA). Viral DNA was then quantified by Real-Time PCR using assay-specific primer and probe. A Real Time-based assay was developed using the following primers: 5'-GCCACCGAGACGTACTTCAGCCTG-3' (Upstream primer) and 5'-TTG TAC GAG TAC GC G GTA TCCT-3' (Downstream primer) for the

amplification of 143 bp sequence of the viral hexon gene (from bp 99 to 242 bp). For quantification, a standard curve was constructed by assaying serial dilutions of *dl*1520 virus ranging from 0.1 pfu to 100 pfu.
To quantify the amount of *dl*1520 virus genome in tumour xenografts, total DNA was extracted from 20 mg of each sample using a DNA Purification System (Promega Corporation, Madison,WI, USA). DNA was resuspended in 200 μL of water and 2 μl used for the Real Time PCR-based assay. For each experiment the DNA was extracted from three different samples of each treatment group.

Quantitative RT-PCR of dl1520 gene expression

Cells were infected with 10 or 100 pfu of *dl*1520, in the presence or in the absence of 10 μM of lovastatin, and harvested at 24 hours post infection. Cells were dissolved in 1 ml Trizol (Invitrogen). RNA quality was evaluated by agarose gel electrophoresis, DNAse treatment was performed. 1 μg of total RNA was reverse transcribed and the expression of *E1A 13 S* and *Penton* genes monitored using Real Time PCR with the following specific primers:
E1A 13 S Forward: 5'-AATGGCCGCCAGTCTTTT-3'
E1A 13 S Reverse: 5'-ACACAGGACTGTAGACAA-3'
Penton Forward: 5'-TAACCAGTCACAGTCGCAAG-3'
Penton Reverse: 5'-CCCGCGCCTTAAACTTATT-3'.
To calculate the relative expression levels we used the $2^{-[delta][delta]Ct}$ method. Negative controls, samples without RT PCR or CDNA template were included in every PCR run, always resulting negative (data not shown).

Detection of cell-surface CAR receptor

Cells were grown in 6-well plates. After 48 hours cells were detached in PBS-EDTA 10mM, washed with PBS and then incubated 1.5 h in FACS buffer with a mouse anti-CAR monoclonal antibody RmcB (1:250). After washing, the cells were incubated in FACS buffer containing the secondary antibody conjugated to fluorescein isothiocyanate [FITC] (Sigma,1:100) and analyzed for CAR expression on a Cyan cytometer (Dako Cytomation, U.S.A.) and Summit V4.3 software (Dako).

Human thyroid tissue samples, semiquantitative RT-PCR, Real Time RT-PCR and immunohistochemistry

Normal and neoplastic human thyroid tissue were obtained from surgical specimens and immediately frozen in liquid nitrogen. Thyroid tumours were collected at the Laboratoire d'Histologie et de Cytologie, Centre Hospitalier Lyon Sud, France and at the Laboratoire d'Anatomie Pathologique, Hospital de L' Antiquaille Lyon, France. The study was approved by the Ethics Committee of the Centre Hospitalier Lyon Sud and of the University Federico II Napoli and conducted in accordance to the principles of the Declaration of Helsinki as revised in 2000. In all cases written informed consent was obtained.

Total RNA was isolated and DNAse-digested using the Rneasy mini kit (Qiagen, Valencia, CA) according to the manufacturer's recommendations. Three μg of total RNA from each sample were reverse transcribed using random hexamers as primers and MuLV reverse transcriptase (Applied Biosystems, Foster City, CA) to yeld cDNA. Semiquantitative RT-PCR was carried out on cDNA using the GeneAmp PCR System 9600 (Applied Biosystems). RNA PCR Core kit (Applied Biosystems) was used to perform PCR reactions. The human ß-actin gene primers, amplifying a 109-bp cDNA fragment, were used as a control with the following program: 95°C for 10 min; 25 cycles of 95°C for 30 sec, 60°C for 30 sec and 72°C for 30 sec; 72°C for 5 min for a final extension. To amplify the AuroraB mRNA RT-PCR was performed using two primers that amplified a 128-bp nucleotide cDNA fragment encompassing exons 5 and 6 with the following program: 95°C for 10 min; 29 cycles of 95°C for 30 sec, 59.5°C for 30 sec and 72°C; final extension of 72°C for 5 min. Same primers were used for Real-Time RT-PCR and semiquantitative RT-PCR.

Quantitative PCR was performed in triplicate using iCycler (Bio-Rad, München, Germany) with SYBR® Green PCR Master Mix (Applied Biosystems) as follows: 95°C 10 min and 40 cycles (95°C 15 s and 60°C 1').

For Cxadr mRNA, an amplicon of 93 nucleotides scattered among sixth and seventh exon was selected. The primer sequences were:

Aurora B forward: 5'-CTGGAATATGCACCACTTGGA,

Aurora B reverse: 5'CGAATGACAGTAAG-ACAGGG;

ß-Actin-forward,5'-TCGTGCGTGACATTAAGGAG;

ß-Actin-reverse, 5'-GTCAGGCAGCTCGTA-GCTCT.

Cxadr forward 5'-ATGAAAAGGAAGTTCATCACGATA-3';

Cxadr reverse 5'-AATGATTACTGCCGATGTAGCTT-3'

Fold mRNA overexpression was calculated according to the formula $2^{(Rt-Et)}2^{(Rn-En)}$, where Rt is the threshold cycle number for the reference gene (β actin) in the tumour, Et for the experimental gene in the tumour, Rn for the reference gene in the normal sample and En for the experimental gene in the normal sample.

The cellular distribution of Aurora B protein was assessed by immuno-histochemical analysis. Aurora B expression was evaluated both in non-neoplastic and neoplastic thyroid tissues. H&E stained slides were retrieved from the files of the Department of Bio-Morphological Sciences at the University Federico II of Naples; in all cases the histological diagnosis was confirmed on review. Paraffin-embedded sections were obtained from these samples and Aurora B expression was evaluated Xylene dewaxed and alcohol rehydrated paraffin sections were placed in Coplin jars filled with a 0.01M tri-sodium citrate solution, and heated for 3 minutes in a conventional pressure cooker. After heating, slides were thoroughly rinsed in cool running water for 5 minutes and then washed in Tris-Buffered Saline (TBS) ph 7.4.

Aurora B protein was detected by using the polyclonal antibody raised in rabbit (n° 611082; BD Transduction Laboratories, USA). The incubation with the

primary antibody was followed by incubation with biotinylated anti-mouse immunoglobulins, and by peroxidase labelled streptavidine (LSAB-DAKO). The signal was developed by using diaminobencidine chromogen as substrate. Negative controls were run with normal rabbit serum instead of the primary antibody or the antibody was preadsorbed with the cognate peptide (10^{-6} M). Cases were scored by assessing the percentage of labelled cells, percentage of positive cells was evaluated by analysing 1000 neoplastic cells in five different high power fields.

Western blot analysis

See Sorrentino *et al*. 2005, Libertini *et al*. 2007

Tumorigenicity assays

Experiments were performed in six-week-old male athymic mice (Charles-River, Italy). All mice were maintained at the Dipartimento di Biologia e Patologia Animal Facility, in accordance with accepted standards of animal care and with the Italian regulations for the welfare of animals used in studies of experimental neoplasia. The studies were approved by Ethic Committee on animal care of the University Federico II Napoli.

Untransfected ARO cells ($5*10^6$) or respectively transfected with a plasmid containing Aurora B in the sense or antisense orientation were injected into the right flank of the mice. The animals were monitored for the appearance of tumours and tumour latency evaluated.

FRO cells ($4*10^6$) were injected into the right flank of 80 athymic mice. After 20 days, when tumours were clearly detectable, the animals were divided into four groups (20 animals/group), and tumour volume was evaluated.

In one experiments, two groups received lovastatin intratumourally, twice a week, for 7 weeks, at a final concentration of 10μM. After 16 hours, one of these group received *dl*1520 ($5*10^7$pfu) as well. The other groups were media or *dl*1520 alone administrated with same schedule.

In the second experiment, two groups received lovastatin in the drinking water (40mg/1000 ml) and after six days *dl*1520 ($5*10^7$pfu) was injected in the peritumoral area in a group treated with lovastatin and in an untreated group. Tumour diameters were measured with calipers every second day by two blind and neutral observers until the animals were sacrificed. No mouse showed signs of wasting or other indications of toxicity. Tumour volumes (V) were calculated by the formula of rotational ellipsoid: $V= A \times B^2/2$ (A= axial diameter, B= rotational diameter).

The amount of lovastatin administered was chosen considering that the average daily water intake for each mouse was 5–7.5 ml and 10 mg/kg/day was the best dose of lovastatin for obtaining biological effects in mice.

To evaluate the genome equivalent copies of *dl*1520 in tumour xenografts, 3 animals bearing FRO xenografts received lovastatin in the drinking water (40 mg /1000 ml) or intratumourally. After six days (*per os* administration) or 16

hours (intratumoural administration), *dl*1520 (5 x 10^7 pfu) was injected in the peritumoral area of the mice treated with lovastatin and in 3 untreated mice.
After 48 hours, animals were sacrificed, tumours excised, DNA extracted and viral replication evaluated by Real Time PCR. DNA quality was analysed by Real Time PCR of β actin gene.

Statistical analysis

Comparisons among different treatment groups in the experiments *in vivo* were made by the ANOVA method and the Bonferroni *post hoc* test using a commercial software (GraphPad Prism 4). Assessment of differences among rate of tumour growth in mice was made for each time point of the observation period; treatment groups were control, *dl*1520, lovastatin and lovastatin plus *dl*1520. The analysis of the cell killing effect *in vitro* was also made by ANOVA method and the Bonferroni post hoc test. For all the other experiments comparisons among groups were made by ANOVA method and *t test*.

4. RESULTS

Lovastatin enhances the cell killing effects of *dl*1520

To evaluate whether lovastatin could enhance oncolytic activity of *dl*1520, we infected two anaplastic cell lines, KAT-4 and FRO, characterized by a different sensitivity to adenoviral infection. KAT-4 cells were chosen as representative of ATC cells at low sensitivity, FRO cell line was chosen as representative of an intermediate infectivity (Libertini *et al.* 2007).

In both cell lines, the combined treatment enhanced the cell killing activity of *dl*1520. In FRO cells treated with 10 pfu/cell of *dl*1520, an additive and significant (2.5 μM) and highly significant (5μM) increase in cell killing was observed. In KAT-4 cells, a highly significant increase in cell killing was induced by lovastatin treatment at all MOIs and drug concentrations used (Fig.1).

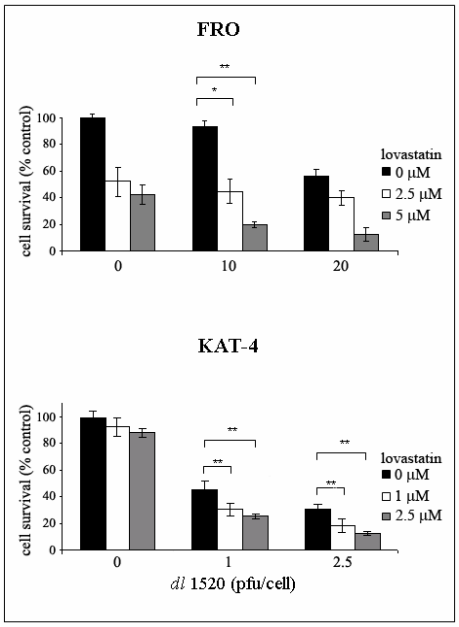

Figure 1 - Lovastatin treatment enhances the cell killing effects of *dl* 1520

FRO and KAT-4 cells were treated for 16 h with lovastatin, then medium was replaced with a medium containing or not lovastatin plus *dl*1520 at different MOIs. Survival was established after 14 days of infection.
In FRO cells kept in the presence of lovastatin, a highly significant increase (**$p < 0.01$*) in the cell killing activity of 10 pfu/cell of *dl*1520 was observed in association with 5 μM of lovastatin. In KAT-4 cells kept in the presence of 1 and 2.5 μM of lovastatin, a highly significant increase (**$p < 0.01$*) in combination with 1 and 2.5 pfu/cell of *dl*1520 was obtained. Viral concentration able to induce the same cell killing in the two cell lines were used.
The data are expressed as percentages of untreated control cells and are the mean of five different experiments, the bar represents the standard deviation.

Lovastatin slightly enhances adenoviral entry

Since *dl*1520 activity is enhanced by lovastatin, we have decided to evaluate whether lovastatin enhanced adenoviral entry in ATC cells. For this purpose we used AdGFP, a replication defective adenovirus transducing GFP. It's worth to note that we used different treatment conditions for the evaluation of lovastatin effects: antineoplastic effects of *dl*1520 were evaluated in the presence of lovastatin, whereas experiments designed to evaluate the effects of the drug on the early phases of viral infection were performed with a short treatment time.

KAT-4 and FRO cells were pre-treated with a non-cytotoxic concentration of lovastatin (10 μM) for 16 hours and then infected with AdGFP for other 24 hours at different MOIs. FACS analysis showed that lovastatin treatment induced a highly statistically significant increase (**p<0.01*), albeit modest, in the number positive cells ranging from 3 up to 10% (Fig.2, upper panel). Both cell lines showed a strong increase (up to 250%) in fluorescence to cell ratio upon lovastatin treatment (Fig.2, lower panel).

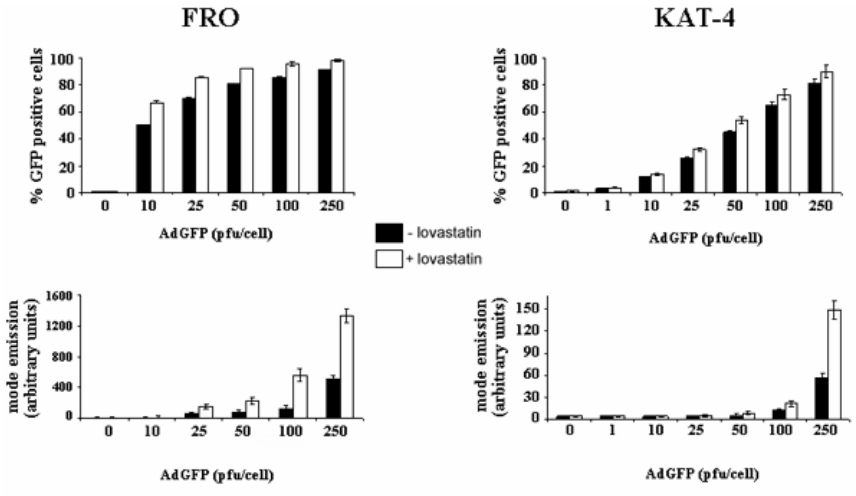

Figure 2 - Lovastatin enhances percentage of GFP positive cells and fluorescence to cell ratio

FRO and KAT-4 cells were treated with 10 μM of lovastatin for 16 hours and then infected with Ad GFP at different MOIs. FACS analysis was performed 24 hours after the infection. Lovastatin increased the percentage of Ad GFP positive KAT-4 and FRO cells (upper panel). Highly significant difference between treated and untreated cells is observed in both cell lines starting from 10pfu/cell point. Lovastatin treated cells showed an increase in fluorescence to cell ratio (lower panel). The difference is statistically high (**p<0.01) starting from 25 pfu/cell (FRO cells) or 50 pfu/cell (KAT-4 cells). The data are the mean of five different experiments, the bar represents the standard deviation.

Lovastatin does not change total and membrane CAR levels

Since adenoviral infection occurs via the attachment of the knob domain of the viral fiber protein to the cellular coxsackie–adenovirus receptor (CAR) and since pharmacological inhibitors of the Raf-MEK-ERK pathway upregulates CAR expression on the cell surface of cancer cells, we have analysed CAR expression after lovastatin treatment. By inhibiting Ras pathway, HMG-CoA reductase inhibitors act as Raf-MEK-ERK inhibitors. Cells at same confluence were treated for 16 or 24 hours with 5 or 10 μM of lovastatin, then harvested for proteins extraction or FACS analysis. As shown in figure 3A, total CAR expression were not modified by lovastatin treatment. Since the virus uses membrane CAR for its entry, we have evaluated CAR levels on cell surface by FACS analysis, again showing no differences (fig.3B). Moreover, preincubation with neutralizing anti-CAR antibody does not

decreased infectivity in lovastatin treated cells (data not shown). Therefore, we can affirm that lovastatin does not act on total and membrane CAR levels.

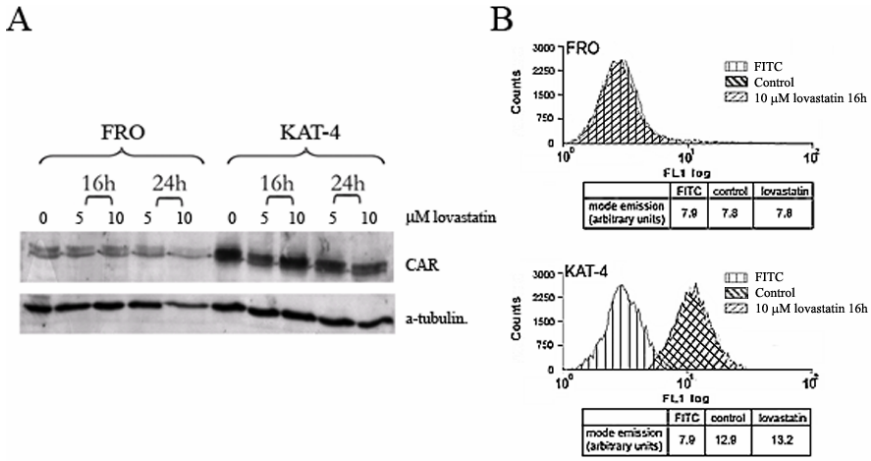

Figure 3 - Lovastatin does not modify total and membrane CAR levels

A- KAT-4 and FRO cells were treated with 0, 5 or 10 µM of lovastatin for 16 or 24 hours. Proteins were subjected to SDS-PAGE (10%). Equal amount of protein were loaded in each lane (50 µg).
B- KAT-4 and FRO cells were treated with 0 (control), 5 or 10 µM of lovastatin for 16 or 24 hours, then harvested and incubated with anti CAR (RmcB) monoclonal antibody. Background emission was assessed by incubating KAT-4 and FRO cells with fluorescein isothiocyanate (FITC)-labeled-mouse alone (FITC). At all times and lovastatin concentrations used, CAR expression was not modified. The figure represents CAR expression after 16 hours of 10µM lovastatin. The data are representative of three different experiments

It has been shown that lovastatin inhibits the invasiveness of ATC cell lines, lowering FAK (focal adhesion kinase) phosphorylation (Zhong *et al.* 2005). FAK is a non receptor tyrosine kinase, that plays a crucial role in integrins mediated cell adhesion. Integrins act as a coreceptor for Adenovirus type 2 (Ad2) and type 5 (Ad5), therefore the slight increase in adenoviral entry, observed after lovastatin treatment, could be due to changes in integrins pattern on cell surface.
The modest increase in adenoviral entry (3-10%) is not sufficient to explain lovastatin effects on fluorescence to cell ratio (Fig.2) and cell survival (Fig.1), therefore we decided not to further investigate this step.

Lovastatin enhances the expression of viral genes and viral replication

Increase in fluorescence to cell ratio suggests that lovastatin treatment could enhance viral gene expression. To monitor this step, we selected two genes, whose expression is correlated with different stages of the adenoviral life-cycle: *E1A 13 S,* representing genes transcribed from the immediate early region, and *Penton,* representing genes expressed from the late region. FRO and KAT-4 cells were infected, respectively, with a MOI of 100 and 10 pfu of *dl*1520 in the presence or in the absence of lovastatin (10 µM). The expression

levels of *E1A 13 S* and *Penton* gene were measured by Real Time RT-PCR at 24h. Co-treatment with lovastatin significantly (*$p<0.05$) enhanced the expression levels of *E1A 13 S* and *Penton* gene in both cell lines (Fig.4).

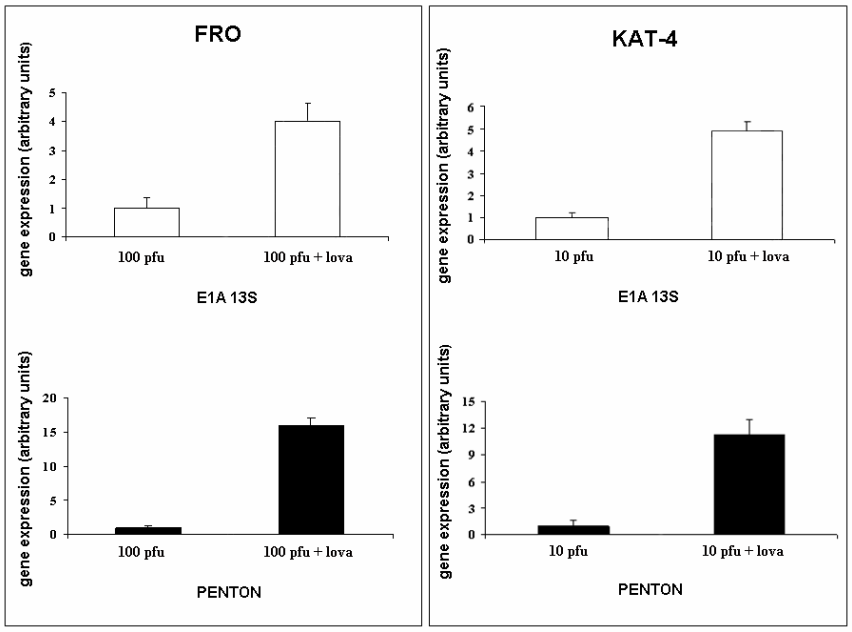

Figure 4 - Lovastatin increases viral gene expression in ATC cells

FRO and KAT-4 cells were treated with 10 μM of lovastatin, after 16 h cells were infected with *dl*1520. For FRO cells a MOI of 100 pfu was used, KAT-4 cells were infected with 10 pfu. After 24 h, the levels of expression of the early gene *E1A 13 S* and of late gene *Penton* were measured by Real Time RT PCR. The result is normalized to β-actin gene expression.
Lovastatin treatment significantly enhanced the expression levels of both genes. In FRO cells, a four fold increase of *E1A 13 S* expression levels and sixteen fold increase of Penton gene were obtained. In KAT-4 cells, a five fold increase of *E1A 13 S* expression levels and twelve fold increase in Penton expression levels were observed. The data are the mean of three different experiments, the bar represents the standard deviation.

Next, we quantified the amount of *dl*1520 virus genome by Real Time PCR in FRO and KAT-4 cells untreated, treated with lovastatin for 16 hours (lovastatin 16h) before infection, or kept in the presence of lovastatin after the infection (lovastatin) and infected with different MOIs (Fig.5).

In FRO cells infected at 10 pfu/cell, both lovastatin treatments induced an highly significant (**$p<0.01$) increase in viral replication, while at 1 pfu/cell no significant differences were observed. KAT-4 cells kept in the presence of lovastatin also showed a highly significant increase in viral replication (**$p<0.01$), whereas 16 hours pre-treatment did not modified viral replication. These results suggest that the increase in viral replication observed treating ATC cells with lovastatin is viral dose or lovastatin treatment time dependent. Therefore, it is possible that higher MOIs of *dl*1520 in combination with a 16 h lovastatin pre-treatment could result in enhanced viral replication in KAT-4. In conclusion of this part, we can affirm that lovastatin enhances viral gene

expression and, consequently, viral replication. Other drugs have been reported to enhance *dl*1520 activity, such as cisplatin and 5-fluorouracil, which potentiate the *dl*1520 virus without changing viral replication (Heise *et al.* 2000) or paclitaxel, that increases adenoviral entry and viral gene expression (AboulEl Hassan *et al.* 2006). Recent studies suggest that the stage of the cell cycle may influence the outcome of Ad infection (Seidman *et al.* 2001). It has been demonstrated that adenoviral binding is optimal during M phase, since both CAR and αv integrin expression showed increased cell surface expression at M phase. Statins induce apoptosis or a G1 arrest but not a G2 arrest (Sala *et al.* 2007, Sivaprasad *et al.* 2006) in neoplastic cells. We have shown that lovastatin does not change CAR levels, therefore other mechanisms are responsible for lovastatin effects on viral life cycle.

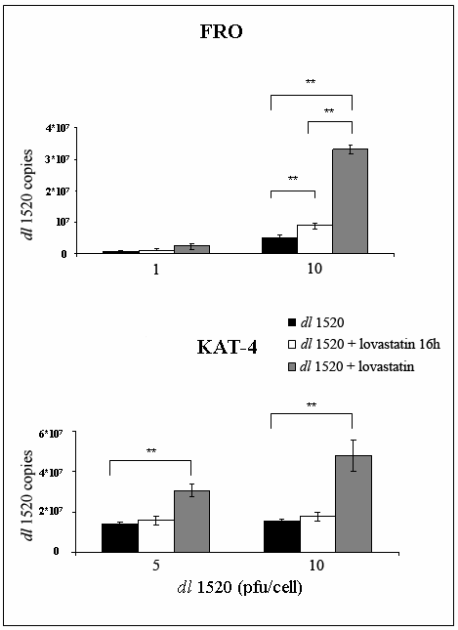

Figure 5 - Lovastatin treatment enhances the replication of the *dl*1520

FRO and KAT-4 cells were treated with lovastatin (10μM) for 16 hours and then infected with a medium containing *dl*1520 (lovastatin 16 h) or *dl*1520 plus lovastatin (lovastatin). Cells were harvested after 24 hours of infection.
FRO cells at 10 pfu/cell showed a highly significant increase (**$p<0.01$) of *dl* 1520 replication in both groups. KAT-4 cells at 5 and 10 pfu/cell showed a highly significant increase (**$p<0.01$) of *dl* 1520 replication only in the group kept in the presence of lovastatin.
The data are the mean of three different experiments, the bar represents the standard deviation.

Lovastatin per os in combination with *dl*1520 reduced the growth of ATC tumour xenografts

In order to demonstrate that the combined treatment lovastatin and *dl*1520 could potentially yield improved clinical efficacy, we have evaluated the effects of lovastatin treatment *in vivo.* We performed two different experiments: in the first one, lovastatin was given within the tumour, whereas in the second one was added in the drinking water. FRO cells ($4*10^6$) were injected into the right flank of athymic mice, and after 20 days, when tumours were clearly detectable (T=0), animals were randomised into four groups. In figure, tumour growth is expressed as a percentage of growth relative to the volume observed at T=0.

In the first experiment (Fig.6A), one group received *dl*1520 ($5*10^7$ pfu) or lovastatin (10μM) or both within the tumour. Animals that received both

treatments were treated one day with lovastatin and with virus after 16 hours, twice a week. The control group received same volume (100µl) of media. The treatment was performed for 7 weeks, twice a week.

In the second experiment (Fig.6B), after the randomisation, lovastatin was added in the drinking water of two groups and the animals received lovastatin until the end of the experiment. After six days, *dl*1520 was injected within the tumour (T=6), twice per week, for 6 weeks.

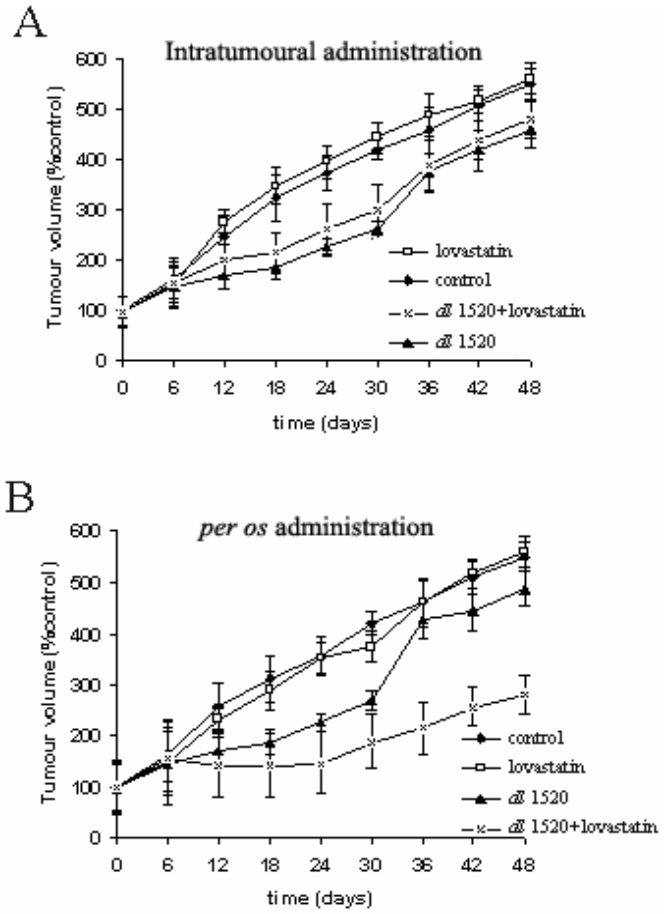

Figure 6 - Tumour growth

A- Intratumoral administration of lovastatin doesn't affect oncolytic activity of *dl*1520

Groups received twice a week intratumoral injection of 100 µl of media (control), *dl*1520 alone, lovastatin alone or *dl*1520 plus lovastatin (in this group lovastatin was given 16 hours prior to *dl*1520). No statistical differences between control and lovastatin and between *dl* 1520 alone or plus lovastatin were observed. The difference between control and *dl*1520 alone or plus lovastatin is statistically significant (*p<0.05) up to T=30.

B- *per os* administration of lovastatin enhances tumour growth delay induced by *dl*1520

Lovastatin and *dl*1520+lovastatin groups received lovastatin in the drinking water starting from T=0 until the end of the experiment. *dl*1520 and *dl*1520+lovastatin groups received *dl*1520 within the tumour twice a week, for 6 weeks, starting from T=6. Lovastatin treatment alone did not show statistically significant differences with the untreated control, whereas *dl* 1520 induced a statistically significant reduction (*$p<0.05$) in the initial phase of the treatment (up to T=30). The combination of *dl*1520+lovastatin significantly delayed tumour growth compared to *dl*1520 alone from T=36 (**$p<0.01$). Data are presented as mean ± SD.

As shown in figure 6A and 6B, *dl*1520 treatment was able to significantly reduce (*$p<0.05$) the growth of tumour xenografts in the initial phase of the treatment (up to T=30). As shown in figure 6A, locally administrated lovastatin did not affect *dl*1520 activity; conversely, the combination lovastatin plus *dl*1520 was able to induce a highly significant reduction (**$p<0.01$) in tumour growth until the end of experiment (Fig.6B).

Finally, we have evaluated by Real Time PCR the genome equivalent copies of *dl*1520 in animals bearing FRO xenografts and treated with *dl*1520 alone or plus lovastatin. As expected, *per os* administration of lovastatin was able to induce a ten fold increase in viral replication (Fig.7B) while no differences were observed in samples obtained from intratumorally injected animals (Fig.7A).

It is worth to note that the injection of lovastatin and the virus within the tumour did not increase the effects of *dl*1520, indicating that a constant lovastatin blood concentration should be obtained in order to enhance the effects of *dl*1520.

It is also important to note that lovastatin alone -administrated both locally and *per os*- did not affect tumour growth, confirming previous observations that statins can enhance antitumour activity of other drugs but, at concentrations compatible with life in animal models, do not show intrinsic antineoplastic effects.

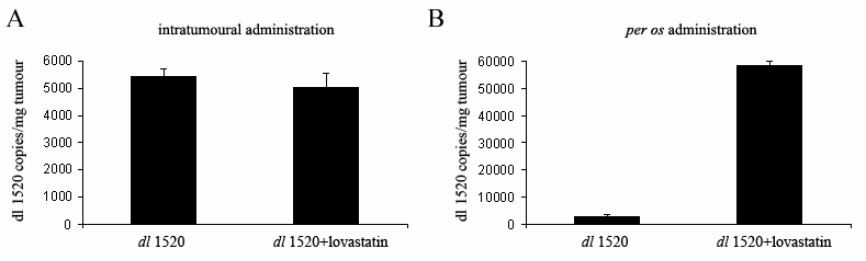

Figure 7 - Genome equivalent copies in tumour xenografts

per os administration of lovastatin increases by ten fold genome equivalent copies in tumour xenografts while intratumoural administration has no effect on viral replication.
The data are the mean of three different experiments, the bar represents the standard deviation.

The data presented here identify lovastatin as a promising agent for increasing the effects of oncolytic adenoviruses in ATC cells. It has been reported that HDAC inhibitors, such as FR901228 and valproic acid (Bieler *et al.* 2006), or MEK inhibitors, such as U0126 and PD184352 (Anders *et al.* 2003), increase the antineoplastic effects of oncolytic adenoviruses. However, these agents have been used in a limited number of clinical trials, whereas

statins have been widely used to reduce cardiovascular diseases without major adverse effects.

In the present study, in *in vitro* experiments, lovastatin was used at a final concentrations ranging from 5 to 10 μM and, in *in vivo* experiments, we have used a lovastatin concentration of 10 mg/kg/day. Although the therapeutic dose for the treatment of hypercholesterolemia is about 1 mg/kg/die, which yields serum levels of 0.1μM, it has been shown that serum concentrations of 2-4 μM of lovastatin are well tolerated in animal models and clinical trials of phase I and II have been performed using 25 mg/Kg/day with encouraging results (Hindler *et al*. 2006). All these data indicate that lovastatin at a dose of 10 mg/kg/day could be probably used in ATC patients in combination with *dl*1520 without major side effects.

In conclusion, we have identified lovastatin as a drug that increases adenoviral replication and enhances the effects of an oncolytic adenovirus *in vitro* and *in vivo* against ATC cells. Therefore, lovastatin could be useful in the context of gene therapy for anaplastic thyroid carcinoma.

In the second part of my study, I focused my attention on Aurora B, that plays a pivotal role in chromosomal instability and aneuploidy, common features in anaplastic thyroid carcinoma.

Aurora B is overexpressed in malignant thyroid carcinoma cells and in experimental model of thyroid carcinogenesis

Thyroid carcinoma cell lines derived from papillary (NPA and TPC1), follicular (FB1 and WRO) and anaplastic thyroid carcinomas (ARO, CAL 62, KAT-4, 8550-C, BHT101, KAT-18, FRO) were analyzed for Aurora B expression by Western blot. An Aurora B specific band of 41KDa was detected in all the samples. As shown in Figure 8, the highest expression levels were observed in the cell lines derived from anaplastic thyroid carcinoma, whereas only a faint band was observed in human thyroid primary culture cells (PrT). This data shows that Aurora B is more abundant in cell lines derived from more aggressive carcinoma. It's worth to note that we did not use nocodazole or other mitotic drug to block cells in mitosis, since we did not want to force Aurora B expression, but only to value normally expressed protein levels.

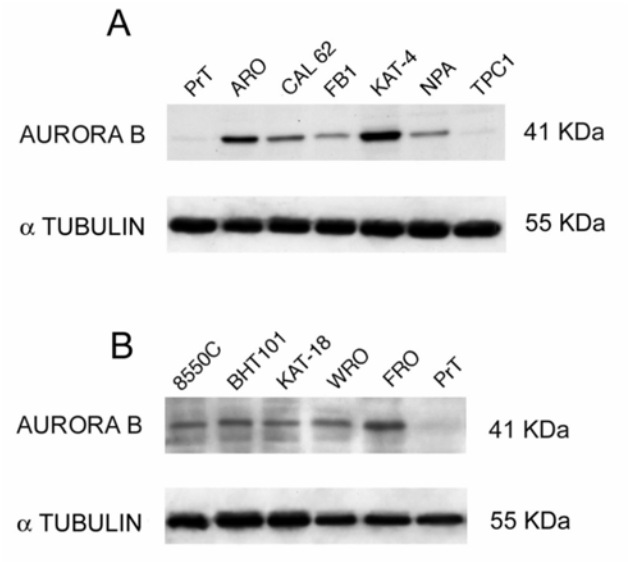

Figure 8- Aurora B expression in thyroid cell lines

Western blot analysis of Aurora B expression in human thyroid cells.
NPA and TPC arise from papillary thyroid carcinoma whereas WRO and FB1 originate from follicular thyroid carcinoma. The remaining cells originate from ATC. Primary culture of human thyroid (PrT) was used as control. In all lanes, equal protein amounts were loaded (50μg)

To confirm that Aurora B gene expression is increased in highly malignant thyroid carcinomas, Western Blot analysis was performed to evaluate its expression levels in thyroid glands from animal models of thyroid

carcinogenesis. We used transgenic mice lines, expressing RET/PTC3, HPV 16 E7 and LT SV40 oncogenes under the transcriptional control of the thyroglobulin promoter. Overexpression of these oncogenes in the thyroid gland of transgenic mice causes, respectively, papillary, follicular and anaplastic thyroid carcinoma. As control of non neoplastic proliferation, thyroid glands of animals treated for 2 and 4 weeks with the goitrogenic agent propylthiouracil (PTU) were used. Furthermore, the thyroid gland of a 6 months old wild type mouse was used as a control (Fig 9).
It is important to note that in the glands of animals treated with the goitrogenic agent PTU, known to stimulate a reversible hyperplasia of the gland, a very low expression of Aurora B was observed despite the intense mitotic activity of the follicular cells. These data indicate that Aurora B increased expression is associated to the late stages of thyroid tumour progression and suggest that the Aurora B overexpression could contribute to thyroid tumour progression.

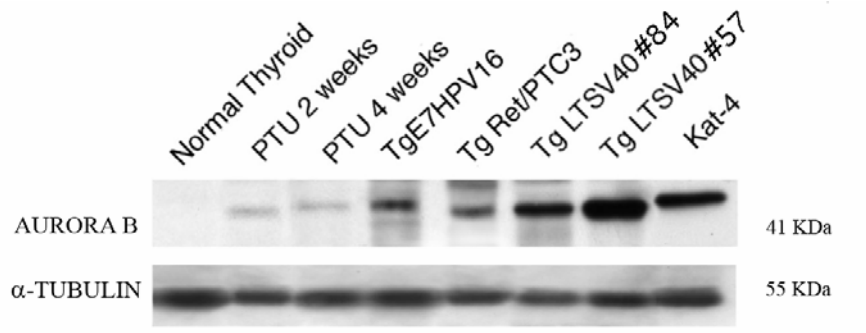

Figure 9 - Aurora B expression in experimental models of carcinogenesis
Western blot analysis of Aurora B expression in thyroid excised from different experimental models *Normal thyroid*: normal thyroid gland excised from a 6 months old wild type mouse; *PTU 2 and 4 weeks*: Thyroid gland excised from a mouse treated for 2 or 4 weeks with PTU; *Tg E7 HPV16*: Follicular carcinoma of a transgenic mouse expressing in the gland HPV 16 oncogene; *Tg Ret/PTC3*: Papillary carcinoma of a transgenic mouse expressing in the gland RET/PTC3 oncogene; *Tg LTSV40*: Anaplastic thyroid carcinomas obtained from two transgenic mice (#84, #57); *KAT-4*: Positive control cells.

Aurora B is overexpressed in human anaplastic thyroid carcinoma

In order to evaluate the expression of Aurora B in human thyroid carcinoma tissues, a panel of matched tumour/normal tissues was analysed by RT-PCR. No significant differences in Aurora B gene expression were observed in papillary carcinomas matched with normal thyroid tissue (Fig.10A), whereas an increased Aurora B expression was observed in anaplastic thyroid carcinomas with respect to the normal thyroid tissue (Fig.10B). Quantitative PCR was performed to confirm overexpression of Aurora B in anaplastic thyroid carcinomas. About 15 fold mRNA overexpression was observed in ATC samples with respect to the β-actin

reference gene, whereas in papillary thyroid carcinoma samples only a two fold increase was observed (Fig.10C)

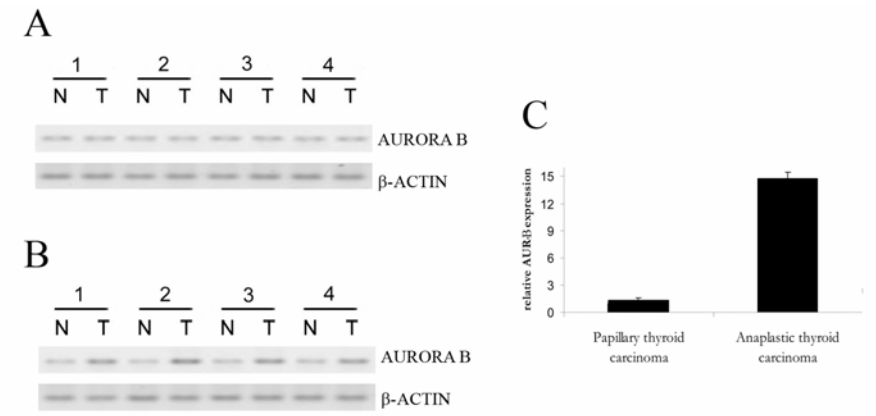

Figure 10 – Real Time analysis of Aurora B expression in matched tumour/normal tissues

A Papillary thyroid carcinomas matched with normal thyroid tissues.
B Anaplastic thyroid carcinomas matched with normal thyroid tissues. Levels of Aurora B were increased in the anaplastic thyroid carcinomas.
C Real Time PCR analysis of Aurora B expression in papillary thyroid carcinomas and in anaplastic thyroid carcinomas. A 15 fold increase of Aurora B expression was observed in anaplastic thyroid carcinomas.

Immunohistochemical analysis of Aurora B expression was performed on samples from normal thyroid, adenoma (5 cases), follicular (5 cases), papillary (10 cases) and anaplastic thyroid carcinomas (15 cases). Three cases of nodular goitre and three of Hashimoto's thyroiditis were used as non neoplastic proliferation control. In normal thyroid tissue, few positive cells for Aurora B staining were observed. Conversely, all of thyroid anaplastic carcinoma examined showed a very high expression of Aurora B (Fig.11C and 11D). Positive cells were irregularly distributed throughout the tumour. Occasionally, a heterogeneous pattern of expression was seen, with areas showing strong labelling adjacent to areas with less intense Aurora B expression. In follicular or papillary differentiated carcinomas a less intense signal was observed (Fig.11B). The expression of Aurora B in anaplastic thyroid carcinomas or in differentiated carcinomas was compared to the expression of a well known proliferative marker such as Ki-67, by using MIB-1 antibody (Table 1). Staining for KI-67 was most intense in thyroid anaplastic carcinomas, showing a correlation with Aurora B expression.

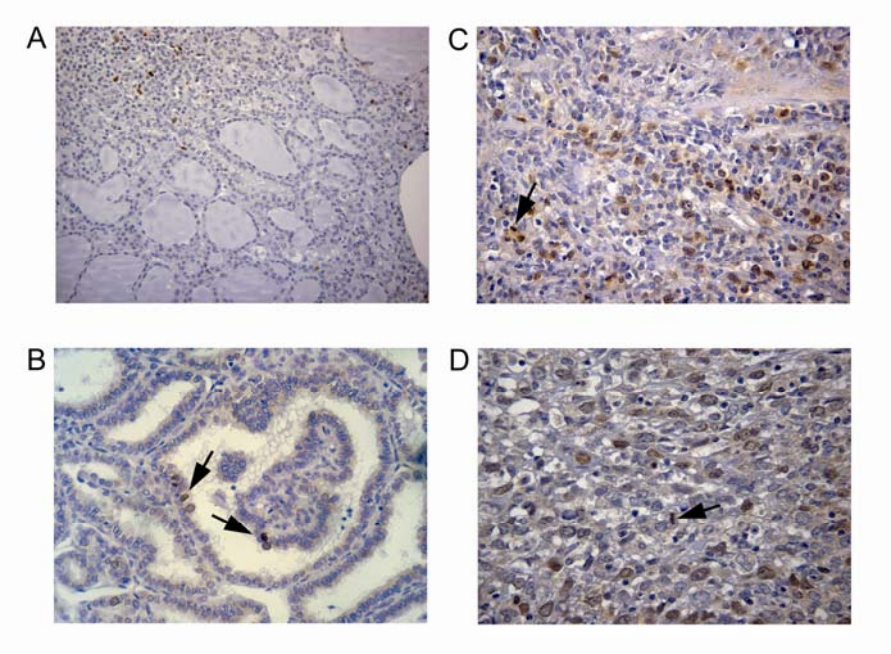

Figure 11 - Aurora B expression and localisation in human thyroid carcinomas

A Paraffin embedded section of a thyroid goitre. Expression of Aurora B protein was not observed.
B Section of thyroid papillary carcinoma, showing rare immunoreactivity for Aurora B protein.
C Section of anaplastic thyroid carcinoma, showing extensive immunoreactivity for Aurora B protein.
D Higher magnification of C, presence of a clear signal in neoplastic cells.

Table 1. Analysis of Aurora B and Ki-67 expression in thyroid specimen

Hystological type of thyroid specimen	Number of cases	Average immunostaining	
		Aurora B	Ki-67
Normal thyroid	1	0.5 ± 0.2	0.9 ± 0.3
Nodular goitre	3	1.2 ± 0.4	1.8 ± 0.6
Hashimoto's disease	3	0.8 ± 0.3	1.1 ± 0.6
Papillary carcinoma	10	2.3 ± 0.4	3.1 ± 0.5
Follicular carcinoma	10	2.8 ± 0.4	3.6 ± 0.6
Anaplastic carcinoma	15	29.6 ± 3.4	43.2 ± 6.6

Values are reported as percentage of immunopositive cells ± SD

These data paralleled the results obtained using cell lines and experimental tumours, showing that Aurora B expression is abundant in anaplastic carcinomas. Conversely, no or low expression was observed in benign adenomas or in non neoplastic thyroid lesions, such as Hashimoto's disease and in normal thyroid tissue. Our data extend to thyroid tumours the observation that the expression of Aurora B tends to group in higher grade of malignancy, as observed in seminona (Chieffi *et al.* 2006), colon carcinomas (Katayama *et al.* 1999), non small cell lung carcinoma (Smith et al 2005, Vischioni *et al.* 2006), mesothelioma (Lopez-Rios *et al*. 2006), glioblastoma (Araki *et al.* 2004, Zeng *et al.* 2007), oral cancer (Qi *et al.* 2007) and hepatocellular carcinoma (Kurai *et al.* 2005). It is possible that during tumour progression, in particular during the transition from differentiated to anaplastic thyroid carcinomas, Aurora B overexpression takes place and its over-

expression might confer a growth advantage to the neoplastic cells. Furthermore, our data indicate that Aurora B expression may serve as a prognostic marker in thyroid tumours. Recently, our observations have been confirmed by Ulisse et colleagues (2006), further validating Aurora B role in thyroid neoplastic progression.

Suppression of the Aurora B synthesis or function blocks cell proliferation

To establish whether Aurora-B expression is crucial for thyroid neoplastic cell growth and to assess whether Aurora B could represent a target for antineoplastic therapy, we performed selective gene silencing analysis using small interference RNA (RNAi). ARO cells were transfected with RNAi for Aurora B (RNAi) or scramble sequence (RNAc) or untreated (Ctr) and harvested after 24 and 48 hours, for both Western Blot and cell survival analysis. Aurora B-RNAi significantly decreased the synthesis of Aurora B protein in ARO cells at 48 hours (Fig.12A) and, consistently with its physiological role, histone H3 phosphorylation. The block of Aurora B protein synthesis is specific, since Aurora A levels were not affected (Fig.12A). The same lysates were probed with anti PARP antibody, to check if the treatment could induce apoptosis. As control for PARP pathway activation, ARO cells were treated for 24 (lane 7) or 48 h (lane 8) with paclitaxel 20nM (Yeung *et al.* 2000). As shown in figure 12A, lower panel, Aurora B RNAi does not induce PARP clivage. In figure 12B, cell survival of treated or untreated cells shows significant reduction in cell number after 48 hours of treatment.

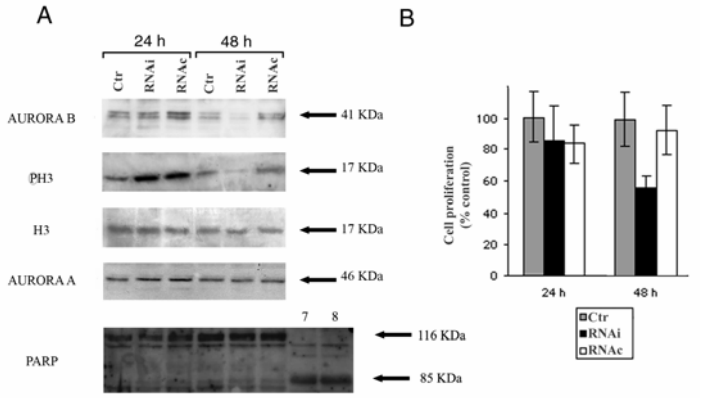

Figure 12- RNAi directed against Aurora B specifically inhibits its expression and blocks the proliferation of anaplastic thyroid carcinoma cells

A Inhibition of Aurora B expression by RNAi.

ARO cells were transfected with 200 nM annealed sense (RNA i) and aspecific control RNA (RNA c) 21-mer RNA oligonucleotides directed against Aurora B, or mock-transfected (Ctr). Cells were harvested at 24 and 48 h after transfection, and Western blot analysis was performed. A significant reduction of Aurora B expression and H3 phospshorylation was observed at 48 hours. Aurora A and H3 levels were not affected by the treatment.

B Time-dependent inhibition of ARO cell proliferation by Aurora B RNAi.

ARO cells were transfected with 200 nM annealed sense (RNA i) and control (RNAc) 21-mer RNA oligonucleotides directed against Aurora B, or mock-transfected (Ctr). The data are expressed as percentages of the control cell proliferation and the standard deviation was calculated (bar).The data are the mean of three different experiments.

To block Aurora B activity we also used the quinazolin derivative: N-[4-(6,7-dimethoxy-quinazolin-4-ylamino)-phenyl]-benzamide (Mortlock A *et al.*, 2001), here called AUR-inh. This compound is similar to AstraZeneca compound ZM1 (Girdler *et al.* 2006) and presents an I_c50 for Aurora A 20 fold higher than for Aurora B.

ARO and FRO cells were treated with 0 or 15 μM of the Aurora kinase inhibitor and, after 24 or 48 hours, cells were collected and lysed. Lysates were immunoblotted with anti-phospho-Ser-10 H3 histone antibody and anti α–tubulin antibody. As shown in figure 13A, a dramatic reduction in phosphorylation of the H3 histone was observed. To evaluate the effects of Aurora kinase inhibitor on cell proliferation, ARO and FRO cells were treated with 0, 5, 10 and 15 μM of Aurora inhibitor, and cell proliferation was evaluated after 24 and 48 hours. 10 and 15 μM of inhibitor significantly reduced cell proliferation (Fig.13B).

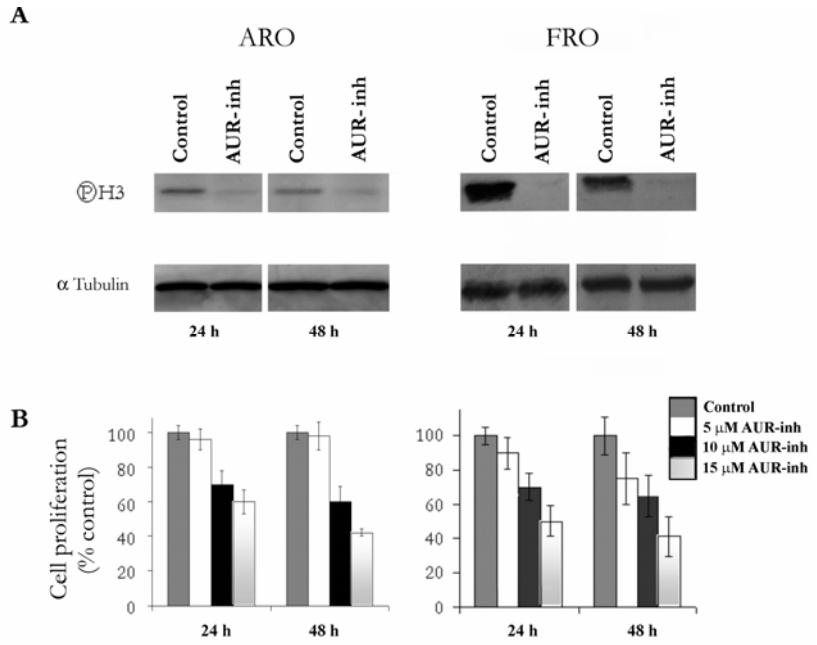

Figure 13 - Reduction in phosphorylation of the H3 histone and reduction in ARO and FRO cells proliferation by Aurora B kinase inhibitor

A ARO and FRO cells ($5x10^5$) were treated with 15 μM of Aurora kinase inhibitor, after 24 and 48 hours cells were lysed. Western blot analysis with anti-Ser-10 phosphorylated H3 histone antibody showed a dramatic reduction in the phosphorylation of the H3 histone, as a control untreated ARO and FRO cells were used. 50 μg of ARO lysate and 100 μg of FRO lysate were loaded in 12 % gel.

B ARO and FRO cells were treated with 0, 5, 10, 15 μM of the Aurora kinase inhibitor (AUR-inh) as a control untreated ARO and FRO cells were used. After 24 and 48 hours cell proliferation was evaluated. A significant reduction in cell proliferation was observed. The data are expressed as percentages of the control cell proliferation and the standard deviation was calculated (bar). The data are the mean of three different experiments.

Due to lack of a specific substrate for Aurora A, it was not possible to analyse Aurora A activity after AUR-inhibitor treatment. It is important to note that several studies (Girdler *et al.* 2006) indicate that the cellular events that occur following exposure to ZM1 are due to inhibition of Aurora-B, rather than Aurora-A. Furthermore in the present study we have observed that Aurora B inhibitor and RNAi showed quite similar effects. Therefore, although it is not possible to exclude that part of this effect is depending on Aurora A inhibition, we can suppose that the most part is due to Aurora B inhibition.

Aurora B antisense prolongs tumour latency but does not affect tumour incidence

Transfection of ARO cells with a construct containing AuroraB cDNA in sense or antisense orientation was also performed. Several clones were then selected for further experiments. The reduced expression of Aurora B protein in antisense expressing clones was confirmed by Western blot analysis (data not shown). The colony growth rate in semisolid medium was reduced in Aurora B-antisense expressing clones with respect of sense or empty vector transfected cells. Although no differences in tumour incidence were observed upon injection into athymic mice, tumour latency period of Aurora B-antisense expressing clones was increased (Table 2). It is worth to note that Aurora B overexpression does not affect colony-forming efficiency, tumour incidence and latency period. Likely, endogenous Aurora B expression levels in ARO cells are so high that further overexpression can not affect anymore their tumorigenicity. Transfection of an Aurora B antisense construct was not able to reduce tumour incidence and only the latency period was increased. This indicate that the block of Aurora B expression is not able to revert the neoplastic phenotype and acts only on the tumour growth rate. This observation probably reflects the role of Aurora B in thyroid carcinoma progression, being overexpressed only in late stages.

Table 2. Analysis of transformation markers of the ARO cells transfected with Aurora B cDNA in the sense or antisense orientation

Transfected DNA	Colony-forming efficiency (%)[a]	Tumour incidence[b]	Latency period (d)[c]
pCMV vector	56 ± 2	3/3	12 ± 1
pCMV Aurora B antisense clone 4	27 ± 1.4	4/4	31 ± 0.8
pCMV Aurora B antisense clone 6	30.6 ± 1.9	5/5	35.8 ± 0.8
pCMV Aurora B antisense clone 9	23 ± 2	3/3	28.7 ± 0.6
pCMV Aurora B sense clone 1	59 ± 1.8	4/4	12 ± 0.8
pCMV Aurora B sense clone 5	61.6 ± 2.1	5/5	11.4 ± 1.1

[a] Colonies larger than 64 cells were scored after 3 wk. Colony-forming efficiency was calculated with the formula: number of colonies formed/number of plated cells x 100.
[b] Tumorigenicity was assayed by injecting $1*10^6$ cells into athymic mice (6 weeks old).
[c] The animals were monitored for the appearance of tumors. The mean tumour latency is the time needed for tumours to reach 10 mm in diameter.

5. CONCLUSION

Anaplastic thyroid carcinoma is one of the most aggressive human neoplasia, that leads to death in few months. Surgery, radiotherapy and chemotherapy have no effects on its prognosis. Therefore, novel therapeutic approaches are required.

Oncolytic viruses are viral mutants able to selectively replicate in tumour cells. I have studied the oncolytic adenovirus *dl*1520 in combination with the HMG-Co reductase inhibitor lovastatin, demonstrating that lovastatin enhances the oncolytic activity of *dl*1520 *in vitro*. Furthermore, I have shown that lovastatin acts on viral gene expression, enhancing viral replication, but does not affect membrane CAR levels. *per os* administration of therapeutical dose of lovastatin statistically enhances *dl*1520 oncolytic effect *in vivo*. Lovastatin is a commonly used agent, with few major adverse effects, therefore we suggest that it could be used as adjuvant in *dl*1520 therapy.

I have also shown that Aurora B expression correlates with malignancy in human thyroid carcinoma and its inhibition blocks cell proliferation. Since Aurora B inhibitors act on proliferating cells and kill cells with non functional p53-mediated post-mitotic checkpoint, this class of drug should have a broad therapeutic index and we suggest that Aurora B could be a potential therapeutic target for anaplastic thyroid carcinoma.

6. ACKNOWLEDGEMENTS

I would like to express my sincere thanks to Prof. G. Portella for his competent supervision and support over the years. It has been a pleasure working with you - I very much appreciate your wisdom and patience.

Many thanks to Doctor S. Linardopoulos for giving me the opportunity to attend his lab in Breakthrough Breast Cancer Research Centre, London for 6 wonderful months.

Thank you my family – especially my parents and Luigi… you know why!

To all the people I have worked with and may have learnt from - thanks for tolerating the noise and disorder I bring with me!

Finally, I would like to thank all the people I have met in these years, starting from “Corpi Bassi” up to Spiros’ lab and those at Searles Close, going through “Dodicesimo”and “Tredicesimo piano”.

7. REFERENCES

Abbosh PH, Li X, Li L, Gardner TA, Kao C, Nephew KP. A conditionally replicative, Wnt/beta-catenin pathway-based adenovirus therapy for anaplastic thyroid cancer. Cancer Gene Ther. 2007 Apr;14(4):399-408. Epub 2007 Jan 12.

AbouEl Hassan MA, Braam SR, Kruyt FA. Paclitaxel and vincristine potentiate adenoviral oncolysis that is associated with cell cycle and apoptosis modulation, whereas they differentially affect the viral life cycle in non-small-cell lung cancer cells. Cancer Gene Ther. 2006 Dec;13(12):1105-14. Epub 2006 Jul 14.

Ain KB. Anaplastic thyroid carcinoma: behavior, biology, and therapeutic approaches. Thyroid. 1998 Aug;8(8):715-26. Review.

Anders M, Christian C, McMahon M, McCormick F, Korn WM. Inhibition of the Raf/MEK/ERK pathway up-regulates expression of the coxsackievirus and adenovirus receptor in cancer cells. Cancer Res. 2003 May 1;63(9):2088-95.

Andrews PD, Ovechkina Y, Morrice N, Wagenbach M, Duncan K, Wordeman L, Swedlow JR. Aurora B regulates MCAK at the mitotic centromere.Dev Cell. 2004 Feb;6(2):253-68.

Araki K, Nozaki K, Ueba T, Tatsuka M, Hashimoto N. High expression of Aurora-B/Aurora and Ipll-like midbody-associated protein (AIM-1) in astrocytomas. J Neurooncol. 2004 Mar-Apr;67(1-2):53-64.

Barzon L, Pacenti M, Taccaliti A, Franchin E, Bruglia M, Boscaro M, Palù G. A pilot study of combined suicide/cytokine gene therapy in two patients with end-stage anaplastic thyroid carcinoma. J Clin Endocrinol Metab. 2005 May;90(5):2831-4. Epub 2005 Feb 15.

Bergelson JM, Cunningham JA, Droguett G, Kurt-Jones EA, Krithivas A, Hong JS, Horwitz MS, Crowell RL, Finberg RW. Isolation of a common receptor for Coxsackie B viruses and adenoviruses 2 and 5. Science. 1997 Feb 28;275(5304):1320-3.

Bieler A, Mantwill K, Dravits T, Bernshausen A, Glockzin G, Köhler-Vargas N, Lage H, Gansbacher B, Holm PS. Novel three-pronged strategy to enhance cancer cell killing in glioblastoma cell lines: histone deacetylase inhibitor, chemotherapy, and oncolytic adenovirus *dl*1520. Hum Gene Ther. 2006 Jan;17(1):55-70.

Bischoff JR, Kirn DH, Williams A, Heise C, Horn S, Muna M, Ng L, Nye JA, Sampson-Johannes A, Fattaey A, McCormick F. An adenovirus mutant that replicates selectively in p53-deficient human tumor cells. Science. 1996 Oct 18;274(5286):373-6.

Bos JL. ras oncogenes in human cancer: a review. Cancer Res. 1989 Sep 1;49(17):4682-9. Review. Erratum in: Cancer Res 1990 Feb 15;50(4):1352.

Carmena M, Earnshaw WC. The cellular geography of aurora kinases. Nat Rev Mol Cell Biol. 2003 Nov;4(11):842-54. Review.

Catalano MG, Fortunati N, Pugliese M, Poli R, Bosco O, Mastrocola R, Aragno M, Boccuzzi G. Valproic acid, a histone deacetylase inhibitor, enhances sensitivity to doxorubicin in anaplastic thyroid cancer cells. J Endocrinol. 2006 Nov;191(2):465-72.

Catalano MG, Poli R, Pugliese M, Fortunati N, Boccuzzi G. Valproic acid enhances tubulin acetylation and apoptotic activity of paclitaxel on anaplastic thyroid cancer cell lines. Endocr Relat Cancer. 2007 Sep;14(3):839-45.

Chan KK, Oza AM, Siu LL. The statins as anticancer agents. Clin Cancer Res. 2003 Jan;9(1):10-9. Review

Chieffi P, Cozzolino L, Kisslinger A, Libertini S, Staibano S, Mansueto G, De Rosa G, Villacci A, Vitale M, Linardopoulos S, Portella G, Tramontano D. Aurora B expression directly correlates with prostate cancer malignancy and influence prostate cell proliferation. Prostate. 2006 Feb 15;66(3):326-33.

Chieffi P, Troncone G, Caleo A, Libertini S, Linardopoulos S, Tramontano D, Portella G. Aurora B expression in normal testis and seminomas. J Endocrinol. 2004 May;181(2):263-70.

Copland JA, Marlow LA, Kurakata S, Fujiwara K, Wong AK, Kreinest PA, Williams SF, Haugen BR, Klopper JP, Smallridge RC. Novel high-affinity PPARgamma agonist alone and in combination with paclitaxel inhibits human anaplastic thyroid carcinoma tumor growth via p21WAF1/CIP1. Oncogene. 2006 Apr 13;25(16):2304-17.

Dimitroulakos J, Thai S, Wasfy GH, Hedley DW, Minden MD, Penn LZ. Lovastatin induces a pronounced differentiation response in acute myeloid leukemias. Leuk Lymphoma. 2000 Dec;40(1-2):167-78.

Ditchfield C, Johnson VL, Tighe A, Ellston R, Haworth C, Johnson T, Mortlock A, Keen N, Taylor SS. Aurora B couples chromosome alignment with anaphase by targeting BubR1, Mad2, and Cenp-E to kinetochores. J Cell Biol. 2003 Apr 28;161(2):267-80.

Dowlati A, Robertson K, Cooney M, Petros WP, Stratford M, Jesberger J, Rafie N, Overmoyer B, Makkar V, Stambler B, Taylor A, Waas J, Lewin JS, McCrae KR, Remick SC. A phase I pharmacokinetic and translational study of the novel vascular targeting agent combretastatin a-4 phosphate on a single-dose intravenous schedule in patients with advanced cancer. Cancer Res. 2002 Jun 15;62(12):3408-16.

Earnshaw WC, Bernat RL. Chromosomal passengers: toward an integrated view of mitosis. Chromosoma. 1991 Mar;100(3):139-46.

Fechner H, Haack A, Wang H, Wang X, Eizema K, Pauschinger M, Schoemaker R, Veghel R, Houtsmuller A, Schultheiss HP, Lamers J, Poller W. Expression of coxsackie adenovirus receptor and alphav-integrin does not correlate with adenovector targeting in vivo indicating anatomical vector barriers. Gene Ther. 1999 Sep;6(9):1520-35.

Fulci G, Ishii N, Van Meir EG. p53 and brain tumors: from gene mutations to gene therapy. Brain Pathol. 1998 Oct;8(4):599-613. Review.

Fulci G, Van Meir EG. p53 and the CNS: tumors and developmental abnormalities. Mol Neurobiol. 1999 Feb;19(1):61-77. Review.

Furuya F, Shimura H, Suzuki H, Taki K, Ohta K, Haraguchi K, Onaya T, Endo T, Kobayashi T. Histone deacetylase inhibitors restore radioiodide uptake and retention in poorly differentiated and anaplastic thyroid cancer cells by expression of the sodium/iodide symporter thyroperoxidase and thyroglobulin. Endocrinology. 2004 Jun;145(6):2865-75.19.

Garcia-Rostan G, Zhao H, Camp RL, Pollan M, Herrero A, Pardo J, Wu R, Carcangiu ML, Costa J, Tallini G. ras mutations are associated with aggressive tumor phenotypes and poor prognosis in thyroid cancer. J Clin Oncol. 2003 Sep 1;21(17):3226-35.

Gassmann R, Carvalho A, Henzing AJ, Ruchaud S, Hudson DF, Honda R, Nigg EA, Gerloff DL, Earnshaw WC. Borealin: a novel chromosomal passenger required for stability of the bipolar mitotic spindle. J Cell Biol. 2004 Jul 19;166(2):179-91. Epub 2004 Jul 12.

Giet R, Petretti C, Prigent C. Aurora kinases, aneuploidy and cancer, a coincidence or a real link? Trends Cell Biol. 2005 May;15(5):241-50. Review.

Girdler F, Gascoigne KE, Eyers PA, Hartmuth S, Crafter C, Foote KM, Keen NJ, Taylor SS. Validating AuroraB as an anti-cancer drug target. JCell Sci.2006 Sep1;119(Pt 17):3664-75.

Girgert R, Vogt Y, Becke D, Bruchelt G, Schweizer P. Growth inhibition of neuroblastoma cells by lovastatin and L-ascorbic acid is based on different mechanisms. Cancer Lett. 1999 Apr 1;137(2):167-72.

Goldsmith ME, Kitazono M, Fok P, Aikou T, Bates S, Fojo T. The histone deacetylase inhibitor FK228 preferentially enhances adenovirus transgene expression in malignant cells. Clin Cancer Res. 2003 Nov 1;9(14):5394-401.

Gomez-Rivera F, Santillan-Gomez AA, Younes MN, Kim S, Fooshee D, Zhao M, Jasser SA, Myers JN. The tyrosine kinase inhibitor, AZD2171, inhibits vascular endothelial growth factor receptor signaling and growth of anaplastic thyroid cancer in an orthotopic nude mouse model. Clin Cancer Res. 2007 Aug 1;13(15 Pt 1):4519-27.

Goto H, Yasui Y, Kawajiri A, Nigg EA, Terada Y, Tatsuka M, Nagata K, Inagaki M. Aurora-B regulates the cleavage furrow-specific vimentin phosphorylation in the cytokinetic process.J Biol Chem. 2003 Mar 7;278(10):8526-30.

Goto H, Yasui Y, Nigg EA, Inagaki M. Aurora-B phosphorylates Histone H3 at serine28 with regard to the mitotic chromosome condensation.Genes Cells. 2002 Jan;7(1):11-7.

Greenberg VL, Williams JM, Cogswell JP, Mendenhall M, Zimmer SG. Histone deacetylase inhibitors promote apoptosis and differential cell cycle arrest in anaplastic thyroid cancer cells. Thyroid. 2001 Apr;11(4):315-25.

Grieco M, Santoro M, Berlingieri MT, Melillo RM, Donghi R, Bongarzone I, Pierotti MA, Della Porta G, Fusco A, Vecchio G. PTC is a novel rearranged form of the ret proto-oncogene and is frequently detected in vivo in human thyroid papillary carcinomas. Cell. 1990 Feb 23;60(4):557-63.

Hama Y, Shimizu T, Hosaka S, Sugenoya A, Usuda N. Therapeutic efficacy of the angiogenesis inhibitor O-(chloroacetyl-carbamoyl) fumagillol (TNP-470; AGM-1470) for human anaplastic thyroid carcinoma in nude mice. Exp Toxicol Pathol. 1997 Aug;49(3-4):239-47.

Hecht JR, Bedford R, Abbruzzese JL, Lahoti S, Reid TR, Soetikno RM, Kirn DH, Freeman SM. A phase I/II trial of intratumoral endoscopic ultrasound injection of ONYX-015 with intravenous gemcitabine in unresectable pancreatic carcinoma. Clin Cancer Res. 2003 Feb;9(2):555-61.

Heise C, Ganly I, Kim YT, Sampson-Johannes A, Brown R, Kirn D. Efficacy of a replication-selective adenovirus against ovarian carcinomatosis is dependent on tumor burden, viral replication and p53 status. Gene Ther. 2000 Nov;7(22):1925-9.

Heise C, Sampson-Johannes A, Williams A, McCormick F, Von Hoff DD, Kirn DH. ONYX-015, an E1B gene-attenuated adenovirus, causes tumor-specific cytolysis and antitumoral efficacy that can be augmented by standard chemotherapeutic agents. Nat Med. 1997 Jun;3(6):639-45.

Heise C, Sampson-Johannes A, Williams A, McCormick F, Von Hoff DD, Kirn DH. ONYX-015, an E1B gene-attenuated adenovirus, causes tumor-specific cytolysis and antitumoral efficacy that can be augmented by standard chemotherapeutic agents. Nat Med. 1997 Jun;3(6):639-45.

Hindler K, Cleeland CS, Rivera E, Collard CD. The role of statins in cancer therapy. Oncologist. 2006 Mar;11(3):306-15. Review.

Imanishi R, Ohtsuru A, Iwamatsu M, Iioka T, Namba H, Seto S, Yano K, Yamashita S. A histone deacetylase inhibitor enhances killing of undifferentiated thyroid carcinoma cells by p53 gene therapy. J Clin Endocrinol Metab. 2002 Oct;87(10):4821-4.

Ito T, Seyama T, Mizuno T, Tsuyama N, Hayashi T, Hayashi Y, Dohi K, Nakamura N, Akiyama M. Unique association of p53 mutations with undifferentiated but not with differentiated carcinomas of the thyroid gland. Cancer Res. 1992 Mar 1;52(5):1369-71.

Ito Y, Yoshida H, Uruno T, Nakano K, Miya A, Kobayashi K, Yokozawa T, Matsuzuka F, Matsuura N, Kakudo K, Kuma K, Miyauchi A. Survivin expression is significantly linked to the dedifferentiation of thyroid carcinoma. Oncol Rep. 2003 Sep-Oct;10(5):1337-40.

Kanda A, Kawai H, Suto S, Kitajima S, Sato S, Takata T, Tatsuka M. Aurora-B/AIM-1 kinase activity is involved in Ras-mediated cell transformation. Oncogene. 2005 Nov 10;24(49):7266-72.

Katz MS, Minsky BD, Saltz LB, Riedel E, Chessin DB, Guillem JG. Association of statin use with a pathologic complete response to neoadjuvant chemoradiation for rectal cancer. Int J Radiat Oncol Biol Phys. 2005 Aug 1;62(5):1363-70.

Keen N, Taylor S. Aurora-kinase inhibitors as anticancer agents. Nat Rev Cancer. 2004 Dec;4(12):927-36. Review.

Khuri FR, Nemunaitis J, Ganly I, Arseneau J, Tannock IF, Romel L, Gore M, Ironside J, MacDougall RH, Heise C, Randlev B, Gillenwater AM, Bruso P, Kaye SB, Hong WK, Kirn DH. A controlled trial of intratumoral ONYX-015, a selectively-replicating adenovirus, in combination with cisplatin and 5-fluorouracil in patients with recurrent head and neck cancer. Nat Med. 2000 Aug;6(8):879-85.

Kim S, Prichard CN, Younes MN, Yazici YD, Jasser SA, Bekele BN, Myers JN. Cetuximab and irinotecan interact synergistically to inhibit the growth of orthotopic anaplastic thyroid carcinoma xenografts in nude mice. Clin Cancer Res. 2006 Jan 15;12(2):600-7.

Kim S, Schiff BA, Yigitbasi OG, Doan D, Jasser SA, Bekele BN, Mandal M, Myers JN. Targeted molecular therapy of anaplastic thyroid carcinoma with AEE788. Mol Cancer Ther. 2005 Apr;4(4):632-40.

Kim S, Yazici YD, Barber SE, Jasser SA, Mandal M, Bekele BN, Myers JN. Growth inhibition of orthotopic anaplastic thyroid carcinoma xenografts in nude mice by PTK787/ZK222584 and CPT-11. Head Neck. 2006 May;28(5):389-99.

Kim S, Yazici YD, Calzada G, Wang ZY, Younes MN, Jasser SA, El-Naggar AK, Myers JN. Sorafenib inhibits the angiogenesis and growth of orthotopic anaplastic thyroid carcinoma xenografts in nude mice. Mol Cancer Ther. 2007 Jun;6(6):1785-92.

Kitazono M, Robey R, Zhan Z, Sarlis NJ, Skarulis MC, Aikou T, Bates S, Fojo T. Low concentrations of the histone deacetylase inhibitor, depsipeptide (FR901228), increase expression of the Na(+)/I(-) symporter and iodine accumulation in poorly differentiated thyroid carcinoma cells. J Clin Endocrinol Metab. 2001 Jul;86(7):3430-5.

Knox JJ, Siu LL, Chen E, Dimitroulakos J, Kamel-Reid S, Moore MJ, Chin S, Irish J, LaFramboise S, Oza AM. A Phase I trial of prolonged administration of lovastatin in patients with recurrent or metastatic squamous cell carcinoma of the head and neck or of the cervix. Eur J Cancer. 2005 Mar;41(4):523-30. Epub 2005 Jan 22.

Koyuturk M, Ersoz M, Altiok N. Simvastatin induces apoptosis in human breast cancer cells: p53 and estrogen receptor independent pathway requiring signalling through JNK. Cancer Lett. 2007 Jun 8;250(2):220-8. Epub 2006 Nov 27.

Koyuturk M, Ersoz M, Altiok N. Simvastatin induces proliferation inhibition and apoptosis in C6 glioma cells via c-jun N-terminal kinase. Neurosci Lett. 2004 Nov 11;370(2-3):212-7.

Kroll TG, Sarraf P, Pecciarini L, Chen CJ, Mueller E, Spiegelman BM, Fletcher JA. PAX8-PPARgamma1 fusion oncogene in human thyroid carcinoma [corrected] Science. 2000 Aug 25;289(5483):1357-60. Erratum in: Science 2000 Sep 1;289(5484):1474

Kurai M, Shiozawa T, Shih HC, Miyamoto T, Feng YZ, Kashima H, Suzuki A, Konishi I. Expression of Aurora kinases A and B in normal, hyperplastic, and malignant human endometrium: Aurora B as a predictor for poor prognosis in endometrial carcinoma. Hum Pathol. 2005 Dec;36(12):1281-8.

Kusama T, Mukai M, Iwasaki T, Tatsuta M, Matsumoto Y, Akedo H, Inoue M, Nakamura H. 3-hydroxy-3-methylglutaryl-coenzyme a reductase inhibitors reduce human pancreatic cancer cell invasion and metastasis. Gastroenterology. 2002 Feb;122(2):308-17.

Lamont JP, Nemunaitis J, Kuhn JA, Landers SA, McCarty TM. A prospective phase II trial of ONYX-015 adenovirus and chemotherapy in recurrent squamous cell carcinoma of the head and neck (the Baylor experience). Ann Surg Oncol. 2000 Sep;7(8):588-92.

Landriscina M, Fabiano A, Altamura S, Bagalà C, Piscazzi A, Cassano A, Spadafora C, Giorgino F, Barone C, Cignarelli M. Reverse transcriptase inhibitors down-regulate cell proliferation in vitro and in vivo and restore thyrotropin signaling and iodine uptake in human thyroid anaplastic carcinoma. J Clin Endocrinol Metab. 2005 Oct;90(10):5663-71.

Lersch C, Schmelz R, Erdmann J, Hollweck R, Schulte-Frohlinde E, Eckel F, Nader M, Schusdziarra V. Treatment of HCC with pravastatin, octreotide, or gemcitabine--a critical evaluation. Hepatogastroenterology. 2004 Jul-Aug;51(58):1099-103.

Libertini S, Iacuzzo I, Ferraro A, Vitale M, Bifulco M, Fusco A, Portella G. Lovastatin enhances the replication of the oncolytic adenovirus dl1520 and its antineoplastic activity against anaplastic thyroid carcinoma cells. Endocrinology. 2007 Nov;148(11):5186-94.

López-Aguilar E, Sepúlveda-Vildósola AC, Rivera-Márquez H, Cerecedo-Diaz F, Valdez-Sánchez M, Villasis-Keever MA. Security and maximal tolerated doses of fluvastatin in pediatric cancer patients. Arch Med Res. 1999 Mar-Apr;30(2):128-31.

López-Ríos F, Chuai S, Flores R, Shimizu S, Ohno T, Wakahara K, Illei PB, Hussain S, Krug L, Zakowski MF, Rusch V, Olshen AB, Ladanyi M. Global gene expression profiling of pleural mesotheliomas: overexpression of aurora kinases and P16/CDKN2A deletion as prognostic factors and critical evaluation of microarray-based prognostic prediction. Cancer Res. 2006 Mar 15;66(6):2970-9.

Luong QT, O'Kelly J, Braunstein GD, Hershman JM, Koeffler HP. Antitumor activity of suberoylanilide hydroxamic acid against thyroid cancer cell lines in vitro and in vivo. Clin Cancer Res. 2006 Sep 15;12(18):5570-7.

Margolis RL, Lohez OD, Andreassen PR. G1 tetraploidy checkpoint and the suppression of tumorigenesis. J Cell Biochem. 2003 Mar 1;88(4):673-83. Review.

Minden MD, Dimitroulakos J, Nohynek D, Penn LZ. Lovastatin induced control of blast cell growth in an elderly patient with acute myeloblastic leukemia. Leuk Lymphoma. 2001 Feb;40(5-6):659-62.

Minoshima Y, Kawashima T, Hirose K, Tonozuka Y, Kawajiri A, Bao YC, Deng X, Tatsuka M, Narumiya S, May WS Jr, Nosaka T, Semba K, Inoue T, Satoh T, Inagaki M, Kitamura T. Phosphorylation by aurora B converts MgcRacGAP to a RhoGAP during cytokinesis.Dev Cell. 2003 Apr;4(4):549-60.

Mitsiades CS, Poulaki V, McMullan C, Negri J, Fanourakis G, Goudopoulou A, Richon VM, Marks PA, Mitsiades N. Novel histone deacetylase inhibitors in the treatment of thyroid cancer. Clin Cancer Res. 2005 May 15;11(10):3958-65.

Modoni S, Landriscina M, Fabiano A, Fersini A, Urbano N, Ambrosi A, Cignarelli M. Reinduction of cell differentiation and 131I uptake in a poorly differentiated thyroid tumor in response to the reverse transcriptase (RT) inhibitor nevirapine. Cancer Biother Radiopharm. 2007 Apr;22(2):289-95.

Mortlock A, Keen N, Jung F, Brewster AG 2001 International Publication Number: WO01/21596A1 (www.european-patent-office.org)

Nahari D, Satchi-Fainaro R, Chen M, Mitchell I, Task LB, Liu Z, Kihneman J, Carroll AB, Terada LS, Nwariaku FE. Tumor cytotoxicity and endothelial Rac inhibition induced by TNP-470 in anaplastic thyroid cancer. Mol Cancer Ther. 2007 Apr;6(4):1329-37.

Nemunaitis J, Vorhies JS, Pappen B, Senzer N. 10-year follow-up of gene-modified adenoviral-based therapy in 146 non-small-cell lung cancer patients. Cancer Gene Ther. 2007 Aug;14(8):762-3. Epub 2007 May 18. No abstract available.

Nikiforov YE. Genetic alterations involved in the transition from well-differentiated to poorly differentiated and anaplastic thyroid carcinomas. Endocr Pathol. 2004 Winter;15(4):319-27. Review

You L, Yang CT, Jablons DM. ONYX-015 works synergistically with chemotherapy in lung cancer cell lines and primary cultures freshly made from lung cancer patients. Cancer Res. 2000 Feb 15;60(4):1009-13.

Ota T, Suto S, Katayama H, Han ZB, Suzuki F, Maeda M, Tanino M, Terada Y, Tatsuka M. Increased mitotic phosphorylation of histone H3 attributable to AIM-1/Aurora-B overexpression contributes to chromosome number instability. Cancer Res. 2002 Sep 15;62(18):5168-77.

Parato KA, Senger D, Forsyth PA, Bell JC. Recent progress in the battle between oncolytic viruses and tumours. Nat Rev Cancer. 2005 Dec;5(12):965-76. Review.

Portella G, Pacelli R, Libertini S, Cella L, Vecchio G, Salvatore M, Fusco A. ONYX-015 enhances radiation-induced death of human anaplastic thyroid carcinoma cells. J Clin Endocrinol Metab. 2003 Oct;88(10):5027-32.

Portella G, Scala S, Vitagliano D, Vecchio G, Fusco A. ONYX-015, an E1B gene-defective adenovirus, induces cell death in human anaplastic thyroid carcinoma cell lines. J Clin Endocrinol Metab. 2002 Jun;87(6):2525-31.

Prichard CN, Kim S, Yazici YD, Doan DD, Jasser SA, Mandal M, Myers JN. Concurrent cetuximab and bevacizumab therapy in a murine orthotopic model of anaplastic thyroid carcinoma. Laryngoscope. 2007 Apr;117(4):674-9.

Randal J. Antiangiogenesis drugs target specific cancers, mechanisms. J Natl Cancer Inst. 2000 Apr 5;92(7):520-2.

Reid T, Galanis E, Abbruzzese J, Sze D, Wein LM, Andrews J, Randlev B, Heise C, Uprichard M, Hatfield M, Rome L, Rubin J, Kirn D. Hepatic arterial infusion of a replication-selective oncolytic adenovirus (dl1520): phase II viral, immunologic, and clinical endpoints. Cancer Res. 2002 Nov 1;62(21):6070-9.

Rogulski KR, Freytag SO, Zhang K, Gilbert JD, Paielli DL, Kim JH, Heise CC, Kirn DH. In vivo antitumor activity of ONYX-015 is influenced by p53 status and is augmented by radiotherapy. Cancer Res. 2000 Mar 1;60(5):1193-6.

Sala SG, Munoz U, Bartolome F, Bermejo F, Martin-Requero A. 3HMG-CoA reductasa inhibitor, simvastatin, inhibits cell cycle progression at the G1-S checkpoint in immortalized lymphocytes from Alzheimer's disease patients independently of cholesterol lowering effects. J Pharmacol Exp Ther. 2007 Oct 10; [Epub ahead of print]

Schiff BA, McMurphy AB, Jasser SA, Younes MN, Doan D, Yigitbasi OG, Kim S, Zhou G, Mandal M, Bekele BN, Holsinger FC, Sherman SI, Yeung SC, El-Naggar AK, Myers JN. Epidermal growth factor receptor (EGFR) is overexpressed in anaplastic thyroid cancer, and the EGFR inhibitor gefitinib inhibits the growth of anaplastic thyroid cancer. Clin Cancer Res. 2004 Dec 15;10(24):8594-602.

Schmutzler C, Koehrle J. Innovative strategies for the treatment of thyroid cancer. Eur J Endocrinol. 2000 Jul;143(1):15-24. Review.

Segev DL, Umbricht C, Zeiger MA. Molecular pathogenesis of thyroid cancer. Surg Oncol. 2003 Aug;12(2):69-90. Review.

Seidman MA, Hogan SM, Wendland RL, Worgall S, Crystal RG, Leopold PL. Variation in adenovirus receptor expression and adenovirus vector-mediated transgene expression at defined stages of the cell cycle. Mol Ther. 2001 Jul;4(1):13-21.

She M, Jim Yeung SC. Combining a matrix metalloproteinase inhibitor, a farnesyltransferase inhibitor, and a taxane improves survival in an anaplastic thyroid cancer model. Cancer Lett. 2006 Jul 18;238(2):197-201.

Shellman YG, Ribble D, Miller L, Gendall J, Vanbuskirk K, Kelly D, Norris DA, Dellavalle RP. Lovastatin-induced apoptosis in human melanoma cell lines. Melanoma Res. 2005 Apr;15(2):83-9.

Sivaprasad U, Abbas T, Dutta A. Differential efficacy of 3-hydroxy-3-methylglutaryl CoA reductase inhibitors on the cell cycle of prostate cancer cells. Mol Cancer Ther. 2006 Sep;5(9):2310-6.

Smith SL, Bowers NL, Betticher DC, Gautschi O, Ratschiller D, Hoban PR, Booton R, Santibáñez-Koref MF, Heighway J. Overexpression of aurora B kinase (AURKB) in primary non-small cell lung carcinoma is frequent, generally driven from one allele, and correlates with the level of genetic instability. Br J Cancer. 2005 Sep 19;93(6):719-29.

Sorrentino R, Libertini S, Pallante PL, Troncone G, Palombini L, Bavetsias V, Spalletti-Cernia D, Laccetti P, Linardopoulos S, Chieffi P, Fusco A, Portella G. Aurora B overexpression associates with the thyroid carcinoma undifferentiated phenotype and is required for thyroid carcinoma cell proliferation. J Clin Endocrinol Metab. 2005 Feb;90(2):928-35

Spitzweg C, Morris JC. Approaches to gene therapy with sodium/iodide symporter. Exp Clin Endocrinol Diabetes. 2001;109(1):56-9. Review.

Suarez HG, du Villard JA, Severino M, Caillou B, Schlumberger M, Tubiana M, Parmentier C, Monier R. Presence of mutations in all three ras genes in human thyroid tumors. Oncogene. 1990 Apr;5(4):565-70.

Tatsuka M, Katayama H, Ota T, Tanaka T, Odashima S, Suzuki F, Terada Y. Multinuclearity and increased ploidy caused by overexpression of the aurora- and Ipl1-like midbody-associated protein mitotic kinase in human cancer cells. Cancer Res. 1998 Nov 1;58(21):4811-6.

Todo T, Rabkin SD, Sundaresan P, Wu A, Meehan KR, Herscowitz HB, Martuza RL. Systemic antitumor immunity in experimental brain tumor therapy using a multimutated, replication-competent herpes simplex virus. Hum Gene Ther. 1999 Nov 20;10(17):2741-55.

Tomko RP, Johansson CB, Totrov M, Abagyan R, Frisén J, Philipson L. Expression of the adenovirus receptor and its interaction with the fiber knob. Exp Cell Res. 2000 Feb 25;255(1):47-55.

Ulisse S, Delcros JG, Baldini E, Toller M, Curcio F, Giacomelli L, Prigent C, Ambesi-Impiombato FS, D'Armiento M, Arlot-Bonnemains Y. Expression of Aurora kinases in human thyroid carcinoma cell lines and tissues. Int J Cancer. 2006 Jul 15;119(2):275-82.

Vader G, Medema RH, Lens SM. The chromosomal passenger complex: guiding Aurora-B through mitosis. J Cell Biol. 2006 Jun 19;173(6):833-7. Epub 2006 Jun 12. Review.

Vischioni B, Oudejans JJ, Vos W, Rodriguez JA, Giaccone G. Frequent overexpression of aurora B kinase, a novel drug target, in non-small cell lung carcinoma patients. Mol Cancer Ther. 2006 Nov;5(11):2905-13**.**

Vitols S, Angelin B, Juliusson G. Simvastatin impairs mitogen-induced proliferation of malignant B-lymphocytes from humans-in vitro and in vivo studies.Lipids.1997Mar;32(3):255-62.

Walther W, Stein U. Viral vectors for gene transfer: a review of their use in the treatment of human diseases. Drugs. 2000 Aug;60(2):249-71. Review.

Wang CY, Zhong WB, Chang TC, Lai SM, Tsai YF. Lovastatin, a 3-hydroxy-3-methylglutaryl coenzyme A reductase inhibitor, induces apoptosis and differentiation in human anaplastic thyroid carcinoma cells. J Clin Endocrinol Metab. 2003 Jul;88(7):3021-6

Watanabe T, Hioki M, Fujiwara T, Nishizaki M, Kagawa S, Taki M, Kishimoto H, Endo Y, Urata Y, Tanaka N, Fujiwara T. Histone deacetylase inhibitor FR901228 enhances the antitumor effect of telomerase-specific replication-selective adenoviral agent OBP-301 in human lung cancer cells. Exp Cell Res. 2006 Feb 1;312(3):256-65. Epub 2005 Dec 13. \

Exp Cell Res. 2006 Feb 1;312(3):256-65. Epub 2005 Dec 13 White E, Sabbatini P, Debbas M, Wold WS, Kusher DI, Gooding LR. The 19-kilodalton adenovirus E1B transforming protein inhibits programmed cell death and prevents cytolysis by tumor necrosis factor alpha. Mol Cell Biol. 1992 Jun;12(6):2570-80.

White E. Mechanisms of apoptosis regulation by viral oncogenes in infection and tumorigenesis. Cell Death Differ. 2006 Aug;13(8):1371-7. Epub 2006 May 5. Review.

Xu G, Pan J, Martin C, Yeung SC. Angiogenesis inhibition in the in vivo antineoplastic effect of manumycin and paclitaxel against anaplastic thyroid carcinoma. J Clin Endocrinol Metab. 2001 Apr;86(4):1769-77.

Xu X, Quiros RM, Gattuso P, Ain KB, Prinz RA. High prevalence of BRAF gene mutation in papillary thyroid carcinomas and thyroid tumor cell lines. Cancer Res. 2003 Aug 1;63(15):4561-7.

Yeung SC, Xu G, Pan J, Christgen M, Bamiagis A. Manumycin enhances the cytotoxic effect of paclitaxel on anaplastic thyroid carcinoma cells. Cancer Res. 2000 Feb 1;60(3):650-6.

Yeung SC, She M, Yang H, Pan J, Sun L, Chaplin D. Combination chemotherapy including combretastatin A4 phosphate and paclitaxel is effective against anaplastic thyroid cancer in a nude mouse xenograft model. J Clin Endocrinol Metab. 2007 Aug;92(8):2902-9.

Yew PR, Berk AJ. Inhibition of p53 transactivation required for transformation by adenovirus early 1B protein. Nature. 1992 May 7;357(6373):82-5.

You L, Yang CT, Jablons DM. ONYX-015 works synergistically with chemotherapy in lung cancer cell lines and primary cultures freshly made from lung cancer patients. Cancer Res. 2000 Feb 15;60(4):1009-13.

Yu W, Fang H. Clinical trials with oncolytic adenovirus in China. Curr Cancer Drug Targets. 2007 Mar;7(2):141-8. Review.

Zeng WF, Navaratne K, Prayson RA, Weil RJ. Aurora B expression correlates with aggressive behaviour in glioblastoma multiforme. J Clin Pathol. 2007 Feb;60(2):218-21.

Zhong WB, Liang YC, Wang CY, Chang TC, Lee WS. Lovastatin suppresses invasiveness of anaplastic thyroid cancer cells by inhibiting Rho geranylgeranylation and RhoA/ROCK signaling. Endocr Relat Cancer. 2005 Sep;12(3):615-2

0013-7227/07/$15.00/0
Printed in U.S.A.

Endocrinology 148(11):5186–5194

doi: 10.1210/en.2007-0752

Lovastatin Enhances the Replication of the Oncolytic Adenovirus *dl*1520 and Its Antineoplastic Activity against Anaplastic Thyroid Carcinoma Cells

Silvana Libertini, Irma Iacuzzo, Angelo Ferraro, Mario Vitale, Maurizio Bifulco, Alfredo Fusco, and Giuseppe Portella

Dipartimenti di Biologia e Patologia Cellulare e Molecolare (S.L., I.I., A.Fu., G.P.) and Endocrinologia e Oncologia Molecolare e Clinica (M.V.), and Cattedra di Patologia Clinica (G.P.), Università di Napoli "Federico II," 80131 Napoli, Italy; Naples Oncogenomic Center-Centro Ingegneria Genetica (A.Fe., A.Fu.), Biotecnologie Avanzate, 80145 Naples, Italy; and Dipartimento di Scienze Farmaceutiche (M.B.), Università degli Studi di Salerno, 84084 Naples, Italy

Anaplastic thyroid carcinoma (ATC) is one of the most aggressive solid tumors and shows morphological features of a highly malignant, undifferentiated neoplasm. Patients with ATC have a poor prognosis with a mean survival time of 2–6 months; surgery, radiotherapy, and chemotherapy do not improve survival. Gene therapy approaches and oncolytic viruses have been tested for the treatment of ATC. To enhance the antineoplastic effects of the oncolytic adenovirus *dl*1520 (Onyx-015), we treated ATC cells with lovastatin (3-hydroxymethylglutaryl-CoA reductase inhibitor), a drug used for the treatment of hypercholesterolemia, which has previously been reported to exert growth-inhibitory and apoptotic activity on ATC cells. Lovastatin treatment significantly increased the effects of *dl*1520 against ATC cells. The replication of *dl*1520 in ATC cells was enhanced by lovastatin treatment, and a significant increase of the expression of the early gene *E1A 13 S* and the late gene *Penton* was observed in lovastatin-treated cells. Furthermore, lovastatin treatment significantly enhanced the effects of *dl*1520 against ATC tumor xenografts. Lovastatin treatment could be exploited to increase the efficacy of oncolytic adenoviruses, and further studies are warranted to confirm the feasibility of the approach in ATC patients. (*Endocrinology* 148: 5186–5194, 2007)

THYROID NEOPLASIAS INCLUDE well-differentiated follicular and papillary carcinomas, poorly differentiated papillary and follicular carcinomas, and undifferentiated anaplastic carcinomas (1).

Anaplastic carcinoma (ATC) constitutes 1–7% of all thyroid cancer cases. It arises from thyroid follicular cells showing morphological features of a highly malignant, undifferentiated neoplasm with multiple atypical mitotic figures; it reveals no follicular structures, colloid formation, or other features of thyroid differentiation (2). p53 and β-catenin mutations are the genetic alterations most frequently found in poorly differentiated and anaplastic carcinomas (3).

ATC represents one of the most aggressive human malignancies because it invariably has a fatal prognosis. In fact, the absence of active therapies is the major impediment to the successful control of the disease (2–4). Therefore, novel therapeutic approaches are required.

Selective replication oncolytic viruses represent a novel therapeutic approach; adenovirus and other viruses have been engineered for selective replication within neoplastic cells. The most common approach is the deletion of viral gene whose product is necessary for replication in normal cells but expendable in cancer cells. Unfortunately, due to the multifunctional nature of many viral proteins, the gene deletion approach for viral selective replication frequently results in a reduced replication and therapeutic potency (5).

The first replication-competent adenoviral mutant described, *dl*1520 (Onyx-015), contains a deletion of E1B-55K, which inhibits p53 and prevents apoptosis, allowing *dl*1520 replication in cancer cells lacking functional p53 pathway but not in normal cells. *dl*1520 was expected to replicate selectively in a high percentage of human cancers being the p53 pathway nonfunctional in about 50% of human neoplasia. However, the role of p53 in determining *dl*1520 selectivity has remained controversial for years because it was shown that *dl*1520 can replicate in tumor cell lines retaining wild-type p53 sequences, and its replication in primary cells is not restricted by p53.

Recently it has been shown that E1B-55K mediates late-viral RNA transport, and *dl*1520 tumor-selective replication is determined by a unique property of tumor cells to efficiently export late viral RNA in the absence of E1B-55K. Thus, loss of E1B-55K-mediated late viral RNA export, rather than p53 degradation, is the major determinant of *dl*1520 selective replication in neoplastic cells (5).

The use of *dl*1520 oncolytic virus as monotherapy has demonstrated limitations in efficacy, making more research necessary for the design of strategies that will increase its tumor-eradicating potential (6).

*dl*1520 has been used in conjunction with chemotherapeu-

First Published Online August 9, 2007

Abbreviations: AdGFP, GFP-transducing adenovirus; ATC, anaplastic thyroid carcinoma; CAR, coxsackievirus-adenovirus receptor; Ct, cycle threshold; FACS, fluorescence-activated cell sorter; FITC, fluorescein isothiocyanate; GFP, green fluorescent protein; HEK, human embryonic kidney; MEK, MAPK kinase; MOI, multiplicity of infection; pfu, plaque-forming unit.

***Endocrinology* is published monthly by The Endocrine Society (http://www.endo-society.org), the foremost professional society serving the endocrine community.**

tic agents in clinical trials with evidence for potential synergistic antitumor activity. The use of *dl*1520 in conjunction with cisplatin and 5-fluorouracil has been examined in a phase II clinical trial involving head and neck carcinoma patients. *dl*1520 has been used in combination with leucovorin and 5-fluorouracil in a phase II trial in patients with gastrointestinal carcinoma metastatic to the liver and with gemcitabine in a phase I/II trial in patients with unresectable pancreatic carcinoma (6, 7). All these studies have shown that combined treatment with *dl*1520 and chemotherapy increases the therapeutic effects.

We previously demonstrated an antineoplastic activity of *dl*1520 against ATC cell lines; however, high multiplicity of infections (MOIs) were used (8). Synergistic cell killing effects of *dl*1520 with doxorubicin or paclitaxel were observed in ATC cell lines, with the IC_{50} drug values reduced 1.75- to 11-fold in the presence of *dl*1520 (8). We have also shown increased efficacy of *dl*1520 followed by ionizing radiations, compared with either treatment alone (9). These data, previously obtained by us, suggest that *dl*1520 may be a valid tool in the treatment of anaplastic thyroid carcinoma in combination with other agents.

To develop novel therapeutic strategies based on replication selective adenoviruses, it is important to identify drugs able to enhance the oncolytic activity. In the present study, we evaluated the effects of lovastatin in combination with *dl*1520 against ATC cells.

Lovastatin (3-hydroxy-methylglutaryl-CoA reductase inhibitor), a drug used for the treatment of hypercholesterolemia, has been reported to exert growth-inhibitory activity *in vitro* and *in vivo*. Farnesyl- and geranylgeranylpyrophosphate, intermediates in the cholesterol synthetic pathway, are needed for isoprenylation, a crucial step for membrane attachment of cellular proteins like Ras, Rho, Cdc42, Rac, *etc.* (10, 11). By inhibiting protein isoprenylation, lovastatin induces a reduction of cell proliferation and apoptosis (10–11). Moreover, it has been demonstrated that low doses of lovastatin induce apoptosis of ATC cells (12, 13).

We have observed that lovastatin significantly enhanced the antineoplastic activity of *dl*1520 against ATC cells and its replication. Furthermore, a significant increase in viral gene expression was induced by lovastatin in ATC cells. Finally, the combined treatment induced a significant reduction of the growth of ATC tumor xenografts.

Materials and Methods

Cell lines and preparation of adenoviruses

The human anaplastic thyroid carcinoma cell lines used in the study are ARO, FRO, KAT-4, and Cal 62.

ARO and FRO human thyroid anaplastic carcinoma cell lines were established by Dr. G. J. Juillard (Department of Radiation Oncology, University of California, Los Angeles, Los Angeles, CA), and ARO and FRO cell lines were kindly provided by Professor J. A. Fagin (University of Cincinnati College of Medicine, Cincinnati, OH). KAT-4 cells were obtained from Dr. Ain (University of Kentucky, Lexington, KY). Cal 62 cell line was obtained from Deutsche Sammlung von Mikroorganismen und Zellkulturen GmbH (Braunschweig, Germany), German Collection of Microorganisms and Cell Cultures.

The NPA line derives from poorly differentiated papillary carcinoma and was obtained by Dr. G. J. Juillard. The FB1 cell line derives from a follicular carcinoma (14). Human embryonic kidney (HEK)-293 cells were obtained from American Type Culture Collection (Manassas, VA).

KAT-4 cells harbor a mutated *p53* gene, (273 Arg->His), whereas FRO cells express very low levels of p53, but no *p53* gene mutation was observed (8).

Cells were grown in DMEM supplemented with 10% fetal calf serum, glutamine, and ampicillin/streptomycin.

*dl*1520 (ONYX-015), a gift from Dr. A. Balmain (Cancer Research Institute, University of California, San Francisco, CA) and Dr. I. Ganly (Memorial Sloan-Kettering Cancer Center, New York, NY), is a chimeric human group C adenovirus (Ad2 and Ad5) that has a deletion between nucleotides 2496 and 3323 in the E1B region that encodes the 55-kDa protein. In addition, there is a C to T transition at position 2022 in region E1B that generates a stop codon at the third codon of the protein. Viral stocks were expanded in the HEK-293 cell line and purified, as previously reported (8).

Stocks were stored at −70 C after the addition of glycerol to a concentration of 50% (vol/vol). Virus titer was determined by plaque-forming units (pfu) on the HEK-293 cells.

Adenovirus infection

Cells were detached, counted, and plated in 6-well plate at 70% cell density. After 24 h, cells were infected with a green fluorescent protein (GFP)-transducing adenovirus (AdGFP), a nonreplicating E1 and E2-deleted adenovirus encoding GFP, diluted in growth medium at different MOIs; medium was replaced after 2 h. Cells were washed 24 h after infection and then trypsinized, washed, and resuspended in 300 μl PBS and analyzed for GFP expression on a fluorescence-activated cell sorter (FACS) cytometer (Dako Cytomation, Carpinteria, CA) and Summit version 4.3 software (Dako, Carpinteria, CA).

Different treatment conditions were used for the evaluation of lovastatin effects: antineoplastic effects were evaluated in the presence of lovastatin, whereas experiments designed to evaluate the effects of the drug on the early phases of viral infection were performed with a short treatment time.

For the evaluation of lovastatin effects on adenoviral entry and GFP expression, the cells were treated for 16 h with 10 μM lovastatin and then infected for 24 h with AdGFP. Cells were harvested and prepared for FACS analysis as previously described.

For the evaluation of the cytoxic effects of the *dl*1520 virus, 1×10^3 cells were seeded in 96-well plates, and 24 h later lovastatin was added to the incubation medium. After an additional 16 h, medium was replaced with a medium containing or not lovastatin plus *dl*1520 at different MOIs. After 14 d the cells were fixed with 10% trichloroacetic acid and stained with 0.4% sulforhodamine B in 1% acetic acid (15). The bound dye was solubilized in 200 μl of 10 mM unbuffered Tris solution, and the optical density was determined at 490 nm in a microplate reader (Bio-Rad Laboratories, München, Germany). The percent of survival rates of treated cells were calculated by assuming the survival rate of untreated cells to be 100%.

Quantitative PCR of dl1520

To quantify the amount of *dl*1520 virus genome on lovastatin treatment, ATC cells were treated with 10 μM lovastatin for 16 h and then media replaced with a medium containing different MOIs of *dl*1520 alone or with lovastatin. After 24 h of infection, cell media were collected and viral DNA extracted using a QIAamp DNA minikit (QIAGEN, Valencia, CA). Viral DNA was then quantified by real-time PCR using assay-specific primer and probe. A real-time-based assay was developed using the following primers: 5′-GCCACCGAGACGTACTTCAGC-CTG-3′ (upstream primer) and 5′-TTG TAC GAG TAC GC G GTA TCCT-3′ (downstream primer) for the amplification of 143 bp sequence of the viral hexon gene (from bp 99 to 242 bp). For quantification, a standard curve was constructed by assaying serial dilutions of *dl*1520 virus ranging from 0.1 to 100 pfu.

To quantify the amount of *dl*1520 virus genome in tumor xenografts, total DNA was extracted from 20 mg of each sample using a DNA purification system (Promega Corp., Madison, WI). DNA was resuspended in 200 μl of water and 2 μl used for the real-time PCR-based assay. For each experiment the DNA was extracted from three different samples of each treatment group.

Quantitative RT-PCR of dl1520 gene expression

Cells were infected with 10 or 100 pfu of *dl*1520, in the presence or in the absence of 10 μM of lovastatin, and harvested at 24 h after infection. Cells were dissolved in 1 ml Trizol (Invitrogen, Carlsbad, CA). RNA quality was evaluated by agarose gel electrophoresis; DNase treatment was performed. One microgram of total RNA was reverse transcribed and the expression of *E1A 13 S* and *Penton* genes monitored using real-time PCR with the following specific primers: E1A 13 S forward, 5′-AATGGCCGCCAGTCTTTT-3′ and reverse, 5′-ACACAGGACTG-TAGACAA-3′; Penton forward, 5′-TAACCAGTCACAGTCGCAAG-3′ and reverse, 5′-CCCGCGCCTTAAACTTATT-3′ (16). To calculate the relative expression levels, we used the $2^{-[\Delta][\Delta]}$cycle threshold (Ct) method. Negative controls, samples without RT-PCR, or CDNA template were included in every PCR run, always resulting negative (data not shown).

Detection of cell surface coxsackievirus-adenovirus receptor (CAR) receptor

Cells were grown in six-well plates. After 48 h cells were detached in PBS-EDTA 10 mM, washed with PBS, and then incubated 1.5 h in FACS buffer with a mouse anti-CAR monoclonal antibody RmcB (1:250) (17). After washing, the cells were incubated in FACS buffer containing the secondary antibody conjugated to fluorescein isothiocyanate (FITC) (1: 100; Sigma, St. Louis, MO) and analyzed for CAR expression on a Cyan cytometer (Dako Cytomation) and Summit version 4.3 software (Dako).

Human thyroid tissue samples and real time RT-PCR

Normal and neoplastic human thyroid tissues were obtained from surgical specimens and immediately frozen in liquid nitrogen. Thyroid tumors were collected at the Laboratoire d'Histologie et de Cytologie, Centre Hospitalier (Lyon Sud, France) and the Laboratoire d'Anatomie Pathologique, Hospital de L'Antiquaille (Lyon, France).

Total RNA was isolated and DNase digested using the RNeasy mini-kit (QIAGEN) according to the manufacturer's recommendations. One microgram of total RNA from each sample was reverse transcribed using random hexamers as primers and Moloney leukemia virus reverse transcriptase (Applied Biosystems, Foster City, CA) to yield cDNA.

To design a quantitative PCR assay, a human ProbeLibray system (Exiqon, Vedbaek, Denmark) was used. Probe and primers pair to amplify a fragment for real-time PCR of Cxadr mRNA were selected entering its accession number (NM001338.3) on the assay design page of the ProbeFinder software. ProbeFinder generated an intron-spanning assay identifying the exon-exon boundaries within submitted transcript. An amplicon of 93 nucleotides scattered among sixth and seventh exon was selected. The primer sequences were: Cxadr forward, 5′-AT-GAAAAGGAAGTTCATCAACGTA-3′, Cxadr reverse, 5′-AATGAT-TACTGCCGATGTAGCTT-3′. The same procedure was used to select probe and primes for housekeeping gene G6PDH, accession no. X03674. The primer sequences were: G6PDH forward, 5′-ACAGAGTGAGC-CCTTCTTCAA-3′, G6PDH reverse, 5′-GGAGGCTGCATCATCGTACT-3′. All fluorigenic probes were dual labeled with FAM at 5′end and with a black quencer at the 3′end.

Relative quantitative TaqMan RT-PCR was performed in a Chromo4 detector (MJ Research, Waltham, MA) in 96-well plates using a final volume of 25 μl. The conditions used for PCR were 10 min at 95 C and then 45 cycles of 20 sec at 95 C and 1 min at 60 C. Each reaction was performed in duplicate. To calculate the relative expression levels, we used the $2^{-[\Delta][\Delta]Ct}$ method, where $[\Delta][\Delta]C_t = [\Delta]C_{t,sample} - [\Delta]C_{t,reference.}$

Written informed consent was obtained from all participants. The study protocol was approved by the ethics committees of the Centre Hospitalier Lyon Sud and the University Federico II, Napoli, and conducted in accordance with the principles of the Declaration of Helsinki as revised in 2000.

Protein extraction and Western blot analysis

In all experiments 70% confluent cells were used. Cells were homogenized directly into lysis buffer (50 mM HEPES, 150 mM NaCl, 1 mM EDTA, 1 mM EGTA, 10% glycerol, 1% Triton X-100, 1 mM phenylmethylsulfonyl fluoride, 1 μg/ml aprotinin, 0.5 mM sodium orthovanadate, 20 mM sodium pyrophosphate). The lysates were clarified by 20 min centrifugation at 14,000 $\times$ *g*. Protein concentrations were estimated by a Bio-Rad assay, and then proteins were boiled in Laemmli buffer [Tris-HCl (pH 6.8) 0.125 M, sodium dodecyl sulfate 4%, glycerol 20%, 2-mercaptoethanol 10%, bromophenol blue 0.002%] for 5 min before electrophoresis. Proteins were subjected to SDS-PAGE (10% polyacrylamide) under reducing conditions. After electrophoresis, proteins were transferred to nitrocellulose membranes (Immobilon; Millipore Corp., Billerica, MA); complete transfer was assessed using prestained protein standards (Bio-Rad, Hercules, CA). After blocking with Tris-buffered saline-BSA [25 mM Tris (pH 7.4), 200 mM NaCl, 5% BSA], the membrane was incubated with the primary polyclonal rabbit antibody (Santa Cruz Biotechnology, Santa Cruz, CA) against CAR receptor SC-15–405 (1:200) for 1 h (at room temperature) or with the monoclonal antibody against against β-actin (Sigma). Membranes were then incubated with the horseradish peroxidase-conjugated secondary antibody (1:10,000) for 45 min (at room temperature), and the reaction was detected with an ECL system (Amersham Life Science, Buckinghamshire, UK).

Tumorigenicity assay

Experiments were performed with 6-wk-old female athymic mice (Charles River, Calco, Lecco, Italy). FRO cells (4×10^6) were injected into the right flank of 80 athymic mice. After 20 d, when tumors were clearly detectable, the animals were divided into four groups (20 animals/group), and tumor volume was evaluated. Two groups received lovastatin in the drinking water (40 mg/1000 ml) and after 6 d *dl*1520 (5×10^7 pfu) was injected in the peritumoral area in a group treated with lovastatin and in an untreated group.

Tumor diameters were measured with calipers every second day by two blind and neutral observers until the animals were killed. No mouse showed signs of wasting or other indications of toxicity. Tumor volumes were calculated by the formula of rotational ellipsoid: Tumor volume = $A \times B^2/2$, where A is the axial diameter and B is the rotational diameter.

All mice were maintained at the Dipartimento di Biologia e Patologia Cellulare e Molecolare Animal Facility. The animal experimentations described herein were conducted in accordance with accepted standards of animal care and in accordance with the Italian regulations for the welfare of animals used in studies of experimental neoplasia, and the study was approved by our institutional committee on animal care.

The amount of lovastatin administered was chosen considering that the average daily water intake for each mouse was 5–7.5 ml and 10 mg/kg/d was the best dose of lovastatin for obtaining biological effects in mice.

To evaluate the genome equivalent copies of *dl*1520 in tumor xenografts, three animals bearing FRO xenografts received lovastatin in the drinking water (40 mg per 1000 ml). After 6 d, *dl*1520 (5×10^7 pfu) was injected in the peritumoral area of the mice treated with lovastatin and in three untreated mice.

After 48 h animals were killed, tumors excised, DNA extracted, and viral replication evaluated by real-time PCR. DNA quality was analyzed by real-time PCR of the β-actin gene.

Statistical analysis

Comparisons among different treatment groups in the experiments *in vivo* were made by the ANOVA method and the Bonferroni *post hoc* test using a commercial software (Prism 4; GraphPad, San Diego, CA). Assessment of differences among rate of tumor growth in mice was made for each time point of the observation period; treatment groups were control, *dl*1520, lovastatin, and lovastatin plus *dl*1520.

The analysis of the cell-killing effect *in vitro* was also made by the ANOVA method and the Bonferroni *post hoc* test. For all the other experiments, comparisons among groups were made by the ANOVA method and *t* test.

Results

Analysis of adenoviral infectivity of human thyroid carcinoma cell lines

To evaluate the susceptibility of ATC cells to adenoviral infection, we infected a panel of thyroid carcinoma cell lines using an AdGFP; the results are shown in Fig. 1A.

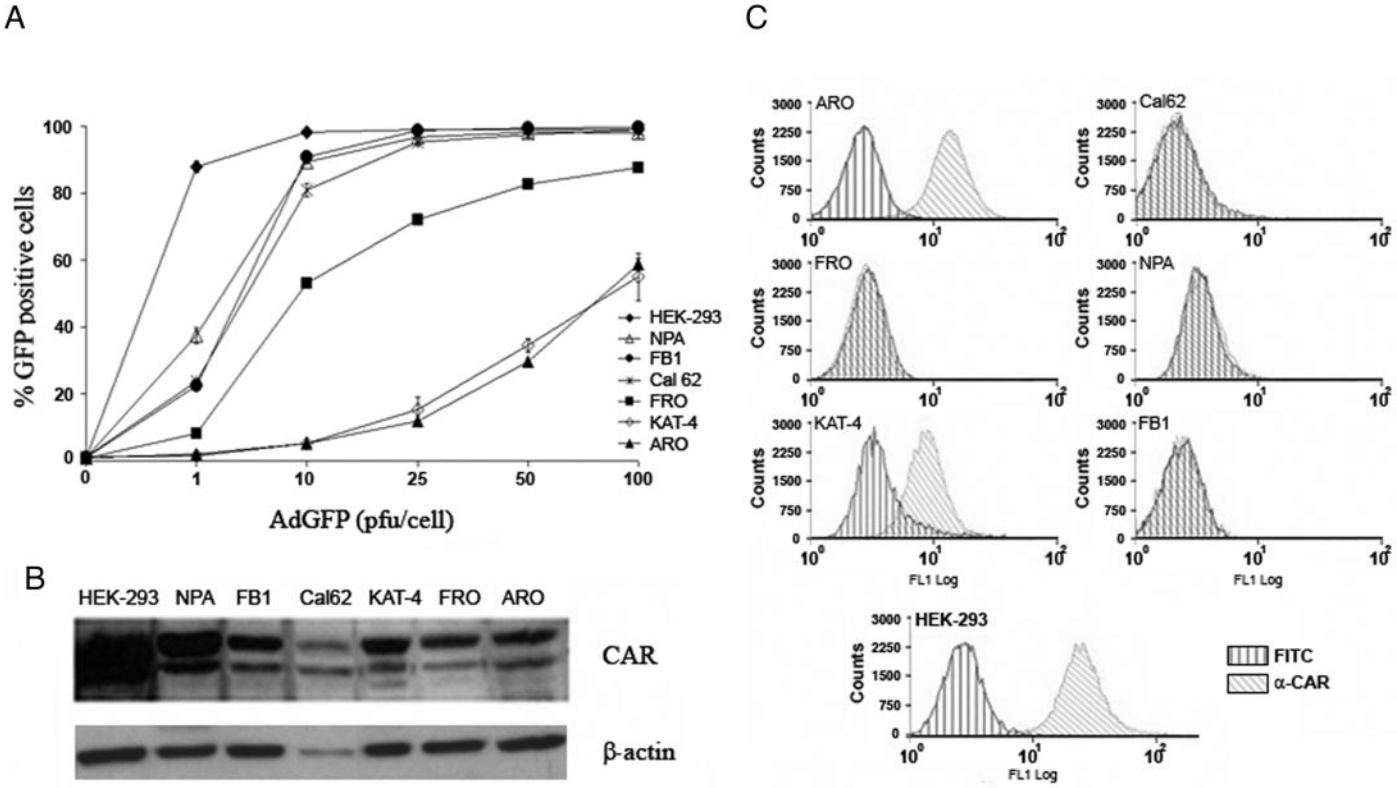

FIG. 1. A, Percentage of positive cells upon AdGFP infection. Cells were infected at different MOIs with AdGFP, and after 24 h the percentage of fluorescent cells was evaluated by FACS analysis. ATC cell lines ARO and KAT-4 were the less sensitive to AdGFP infection at all MOIs used, whereas FRO and Cal 62 cells displayed a higher percentage of GFP-expressing cells. FRO cells showed about 50% of GFP-positive cells at 10 MOI; conversely, Cal 62 at the same MOI showed about 80% of positive cells. Follicular thyroid carcinoma cell line FB1 and papillary thyroid carcinoma cell line NPA showed about 90% of GFP-positive cells at 10 MOI. HEK-293 cells were used as a positive control. The data are the mean of three different experiments; the *bar* represents the SD. B, Western blot analysis of CAR expression in thyroid carcinoma cell lines. Cal 62, FRO, and ARO cells showed low expression of total CAR levels, whereas FB1, KAT-4, and NPA cells expressed the higher of total CAR levels. Equal amounts of protein lysates (50 μg) were loaded. C, Cytofluorimetric analysis of CAR expression on the membrane of thyroid carcinoma cell lines. Flow cytometry analysis showed the absence of cell surface CAR expression in FRO, NPA, Cal 62, and FB1 thyroid cancer cell lines. ARO and KAT-4 cell lines showed the presence of CAR on the membrane. HEK-293 cells were used as positive control. Cells were incubated with a anti-CAR (RmcB) monoclonal antibody or FITC-labeled mouse alone. In all experiments, 70% confluent cells were used.

The anaplastic thyroid carcinoma cell lines ARO, FRO, and KAT-4 display the lowest percentage of fluorescent cells at all the MOIs used; indeed 100 pfu/cell are required to obtain greater than 50% ARO- and KAT-4-positive cells, whereas at 10 pfu/cell, about 50% of FRO cells are positive. Conversely, follicular thyroid carcinoma cell line FB1 and papillary thyroid carcinoma cell line NPA showed about 90% of GFP-positive cells at 10 MOI. As a positive control HEK-293 cells were used.

Because adenoviral infection occurs via the attachment to the CAR (18), we analyzed CAR expression by Western blot; two CAR-specific bands of 44 and 46 kDa, respectively, were detected in all the samples (Fig. 1B). However, certain differences were observed in their levels; in ATC cell lines, variable levels ranging from very low to intermediate were observed; the papillary thyroid carcinoma-derived NPA cell line, the follicular carcinoma-derived FB-1 cell lines, and the ATC-derived KAT-4 cell line express the highest CAR levels. A cytofluorimetric analysis was performed to evaluate the presence of CAR on the cell membrane (Fig. 1C), showing the absence of CAR on the cell surface in FRO, NPA, Cal 62, and FB1 cells. This observation suggests a CAR-independent entry of AdGFP in these cell lines. The cell lines ARO and KAT-4 showed the presence of CAR on the cell membrane despite being the less susceptible to adenoviral infection.

To confirm that anaplastic thyroid carcinomas express low levels of CAR, we evaluated the CAR mRNA levels in human thyroid carcinoma tissues by RT-PCR. Significantly lower levels (**, $P < 0.01$) in CAR gene expression were observed in papillary carcinomas, follicular carcinomas, and anaplastic thyroid carcinomas with respect to normal thyroid samples (Fig. 2).

Lovastatin enhances the cell killing effects and the replication of the oncolytic adenovirus dl1520

Because our data show that ATC are not readily infected by therapeutic adenoviruses, we decided to evaluate the effects of lovastatin in combination with *dl*1520. KAT-4 cells were chosen as representative of ATC cells at low sensitivity to the infection with *dl*1520; the FRO cell line was chosen as representative of an intermediate infectivity (8, 9).

In both cell lines, the combined treatment enhanced the cell-killing activity of *dl*1520. In FRO cells treated with 10 pfu/cell of *dl*1520, an additive and significant (2.5 μM) and

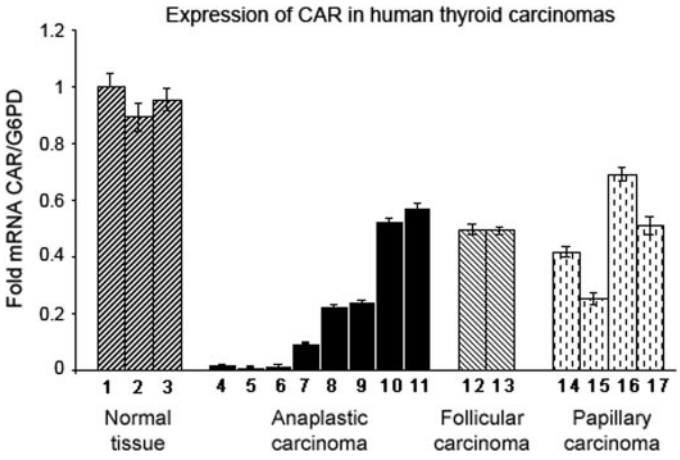

FIG. 2. CAR expression in thyroid carcinoma tissues. Three normal thyroid samples (1–3), eight anaplastic (4–11), two follicular (12 and 13), and four papillary (14–17) thyroid carcinomas were used for real-time RT-PCR analysis of CAR expression, showing a reduction in CAR mRNA levels in all neoplastic tissues with respect to normal thyroid samples.

highly significant (5 μM) increase in cell killing was observed. In KAT-4 cells a highly significant increase in cell killing was induced by lovastatin treatment at all MOIs and lovastatin concentrations used (Fig. 3A).

Next, we quantified the amount of *dl*1520 virus genome by real-time PCR in FRO and KAT-4 cells untreated, treated with lovastatin for 16 h (lovastatin 16 h) before infection, or kept in the presence of lovastatin after the infection (lovastatin) and infected with different MOIs. In FRO cells at 10 pfu/cell, both lovastatin treatments induced an highly significant (**, $P < 0.01$) increase in viral replication (Fig. 3B). KAT-4 cells kept in the presence of lovastatin also showed a highly significant increase in viral replication (**, $P < 0.01$), whereas 16 h treatment did not modify viral replication.

Lovastatin enhances the expression of viral genes

Because ATC cells infected in the presence of lovastatin show an increase in viral replication, we decided to evaluate the infectivity of ATC cells in the presence of lovastatin. KAT-4 and FRO cells were pretreated with a noncytotoxic concentration of lovastatin (10 μM) for 16 h and then infected with AdGFP at different MOIs. FACS analysis of treated or untreated cells showed that lovastatin treatment induced a highly statistically significant (**, $P < 0.01$) increase in the number positive cells ranging from 3 up to 10% (Fig. 4A).

Both cell lines showed a strong increase in fluorescence to cell ratio on lovastatin treatment (Fig. 4A).

Pharmacological inhibitors of the Raf-MAPK kinase (MEK)-ERK pathway up-regulates CAR expression on the cell surface of cancer cells (19); lovastatin is a well-known inhibitor of p21 Ras isoprenylation and activity. Therefore, we evaluated the effects of lovastatin on CAR expression in

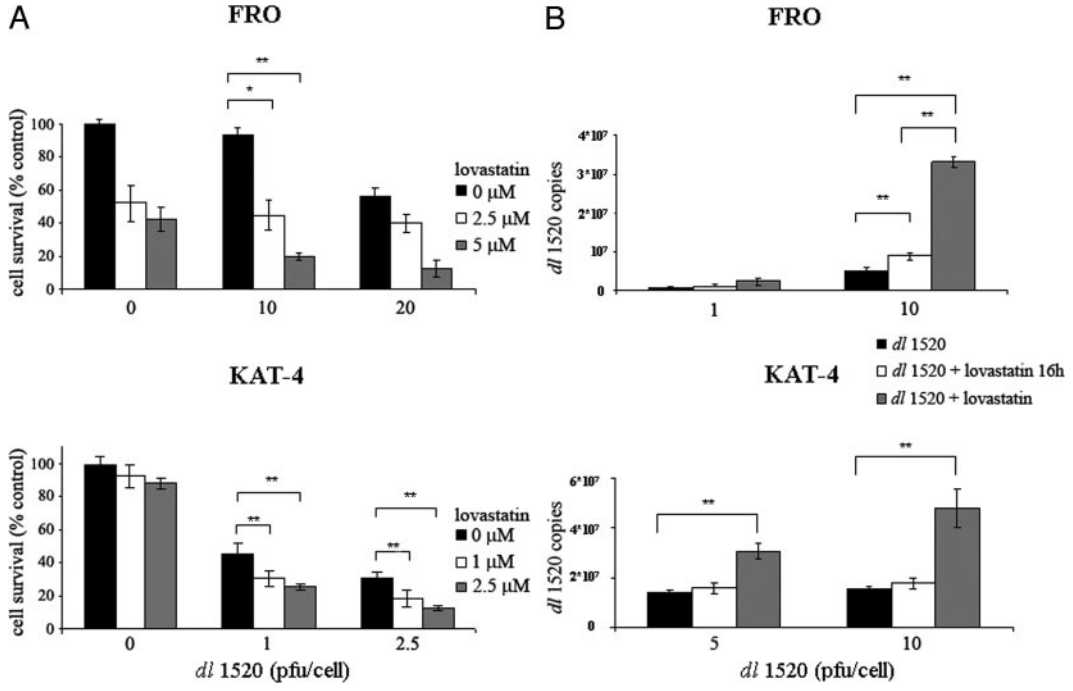

FIG. 3. A, Lovastatin treatment enhances the cell-killing effects of the oncolytic adenovirus *dl*1520. FRO and KAT-4 cells were treated with lovastatin and then infected with the oncolytic adenovirus *dl*1520 at different MOIs. In FRO cells kept in the presence of lovastatin, a highly significant increase (**, $P < 0.01$) in the cell-killing activity of 10 pfu/cell of *dl*1520 was observed in association with 5 μM of lovastatin. In KAT-4 cells kept in the presence of 1 and 2.5 μM of lovastatin, a highly significant increase (**, $P < 0.01$) of the cell-killing activity in combination with 1 and 2.5 pfu/cell of *dl*1520 was obtained. Viral concentration able to induce the same cell-killing in the two cell lines were used. The data are expressed as percentages of untreated control cells and are the mean of five different experiments; the *bar* represents the SD. B, Lovastatin treatment enhances the replication of the oncolytic adenovirus *dl*1520. FRO and KAT-4 cells were treated with lovastatin (10 μM) for 16 h and then infected with a medium containing *dl*1520 (lovastatin 16 h) or *dl*1520 plus lovastatin (lovastatin). FRO cells at 10 pfu/cell showed a highly significant increase (**, $P < 0.01$) of *dl*1520 replication in both groups. KAT-4 cells at 5 and 10 pfu/cell showed a highly significant increase (**, $P < 0.01$) of *dl*1520 replication only in the group kept in the presence of lovastatin. The data are the mean of three different experiments; the *bar* represents the SD.

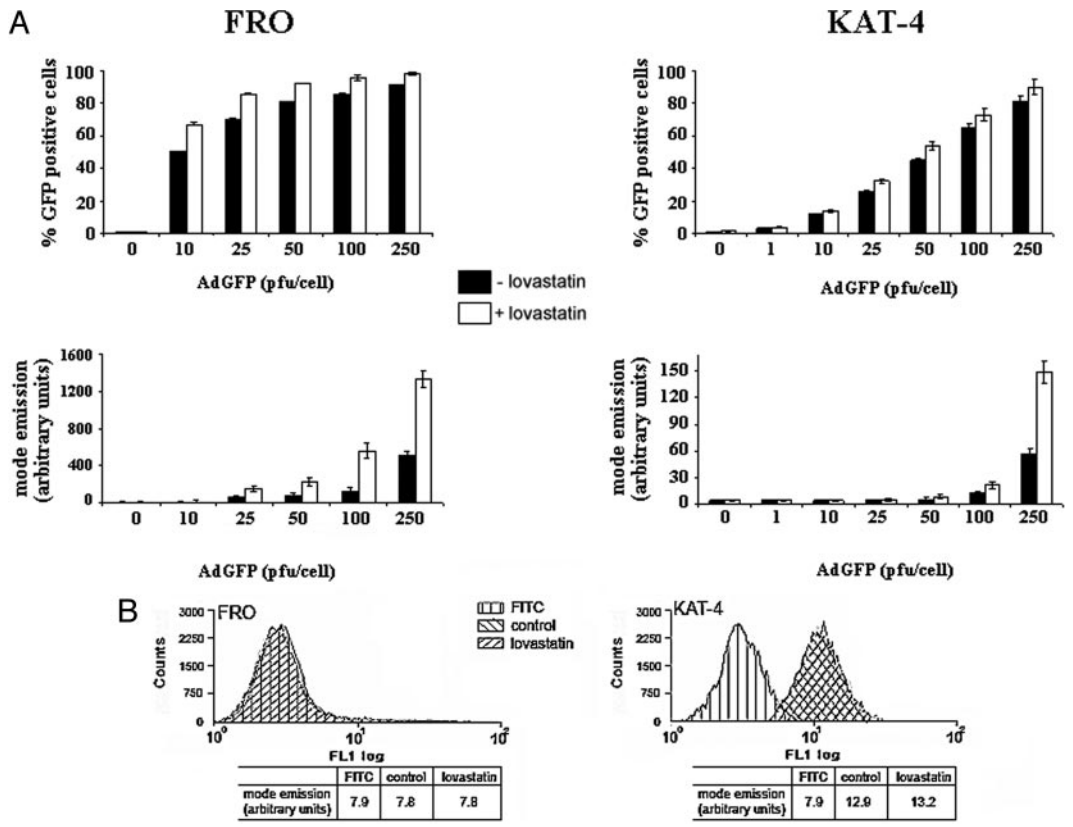

FIG. 4. A, Percentage of GFP-positive cells and fluorescence to cell ratio in lovastatin-treated cells. FRO and KAT-4 cells were treated with 10 μM of lovastatin for 16 h and then infected with AdGFP at different MOIs. FACS analysis was performed 24 h after the infection. Lovastatin increased the percentage of AdGFP-positive KAT-4 and FRO cells (*upper panel*). Highly significant difference between treated and untreated cells is observed in both cell lines starting from 10 pfu/cell point. Lovastatin-treated cells showed an increase in fluorescence to cell ratio (*lower panel*). The difference is statistically high ($P < 0.01$), starting from 25 pfu/cell (FRO cells) or 50 pfu/cell (KAT-4 cells).The data are the mean of five different experiments; the *bar* represents the SD. B, Lovastatin does not modify CAR expression on the cell surface of KAT-4 and FRO cells. KAT-4 and FRO cells were treated with 10 μM lovastatin for 16 h and then incubated with anti-CAR (RmcB) monoclonal antibody (lovastatin) and compared with untreated control cells (control). Background emission was assessed by incubating KAT-4 and FRO cells with FITC-labeled mouse alone (FITC). CAR expression was not modified by lovastatin treatment. The data are representative of three different experiments.

ATC cells. CAR levels on cell surface, evaluated by FACS analysis (Fig. 4B), were not modified by lovastatin treatment.

Because lovastatin-treated cells showed an increased in fluorescence to cell ratio, we hypothesized that lovastatin treatment could enhance viral gene expression. To monitor the expression of adenoviral genes in lovastatin-treated ATC cells we selected two adenoviral genes, whose expression is correlated with different stages of the adenoviral life-cycle: *E1A 13 S* representing genes transcribed from the immediate early region and *Penton* representing genes expressed from the late region.

FRO and KAT-4 cells were infected respectively with a MOI of 100 and 10 pfu of dl1520 in the presence or in the absence of lovastatin (10 μM). The expression levels of E1A 13 S and *Penton* gene were measured by real-time RT-PCR at 24 h. Cotreatment with lovastatin significantly (*, $P < 0.05$) enhanced the expression levels of *E1A 13 S* and *Penton* gene in both cell lines (Fig. 5).

Lovastatin in combination with dl1520 reduces the growth of ATC tumor xenografts

To demonstrate that the combined treatment lovastatin and *dl*1520 could potentially yield improved clinical efficacy, we evaluated the effects of lovastatin treatment *in vivo*.

FRO cells were injected into the right flank of athymic mice, and after 20 d, when tumors were clearly detectable (T = 0), animals were randomized into four groups and lovastatin was added in the drinking water of two groups. The animals received lovastatin until the end of the experiment. After 6 d *dl*1520 was injected within the tumor (T = 6), twice per week. In Fig. 6A, tumor growth is expressed as a percentage of growth relative to the volume observed at T = 0.

*dl*1520 treatment was able to significantly reduce (*, $P < 0.05$) the growth of tumor xenografts in the initial phase of the treatment (up to T = 30). Conversely, the combination lovastatin plus *dl*1520 was able to induce a highly significant reduction (**, $P < 0.01$) in tumor growth until the end of experiment, confirming that lovastatin enhances the antineoplastic effects of *dl*1520. No toxicities were observed in treated animals.

Finally, we evaluated by real-time PCR (Fig. 6B) the genome equivalent copies of *dl*1520 in animals bearing FRO xenografts and treated with *dl*1520 and *dl*1520 plus lovastatin. Lovastatin treatment was able to induce a 10-fold increase in viral replication.

Discussion

ATC represents one of the most lethal human neoplasia being refractory to conventional therapies, including sur-

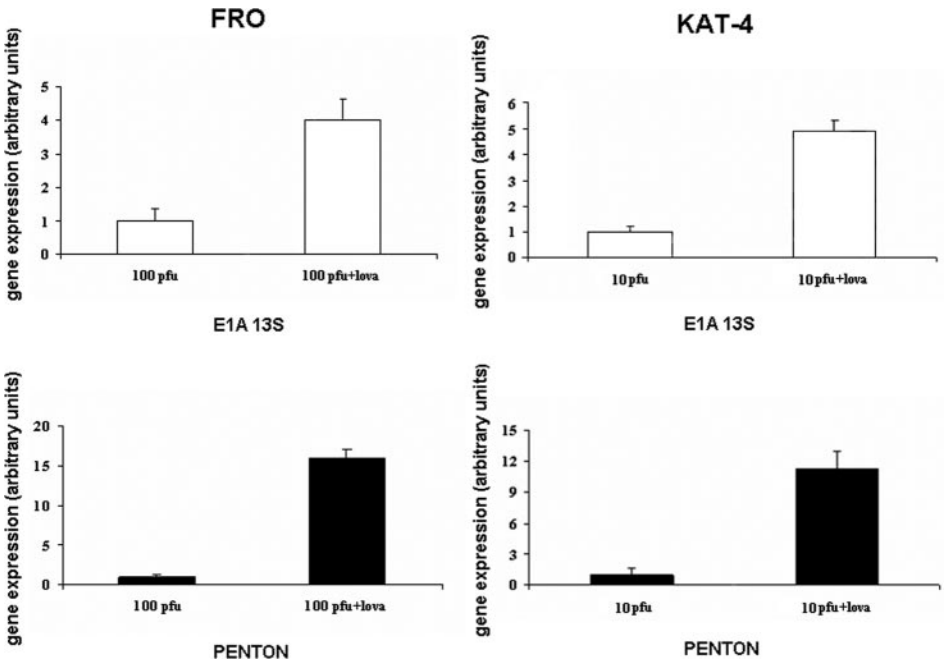

FIG. 5. Lovastatin increases viral gene expression in ATC cells. FRO and KAT-4 cells were treated with 10 μM of lovastatin; after 16 h cells were infected with *dl*1520. For FRO cells a MOI of 100 pfu was used; KAT-4 cells were infected with 10 pfu. After 24 h the levels of expression of the adenoviral immediate early region gene *E1A 13 S* and the adenoviral of late region gene *Penton* were measured by real-time RT-PCR. Lovastatin treatment significantly enhanced the expression levels of the *E1A 13 S* and Penton gene. In FRO cells a 4-fold increase of *E1A 13 S* expression levels and 16-fold increase of Penton gene were obtained. In KAT-4 cells, a 5-fold increase of *E1A 13 S* expression levels and 12-fold increase in Penton expression levels were observed. The data are the mean of three different experiments; the *bar* represents the SD.

gery, radioactive iodine, and chemotherapy (2–4). Development and evaluation of novel treatment strategies are needed.

Replication-selective oncolytic viruses (virotherapy) are being developed as a novel, targeted form of anticancer treatment. *dl*1520 (Onyx-015) was the first virus that had been genetically engineered for replication-selectivity for treatment in cancer patients. Recent results from a phase III clinical trial have confirmed the ability of an oncolytic adenovirus (H101) bearing an E1B-55kD gene deletion similar to that present in *dl*1520 to increase the response rate of nasopharyngeal carcinoma in combination with cisplatin (20).

Selective oncolytic replicating adenoviruses have been tested in ATC cell lines and tumor xenografts showing promising results (8, 9); however, high MOIs of *dl*1520 were required to efficiently kill ATC cells.

The efficacy of oncolytic adenoviruses as therapeutic agents relies on the capability of target neoplastic cells to bind, internalize, and sustain the replication of adenoviruses. We analyzed the infectivity of a panel of human thyroid carcinoma cell lines, showing a low infectivity in most ATC cell lines. Conversely, papillary or follicular thyroid carcinoma cells display a higher infectivity. In a previous study, we evaluated the infectivity of ATC cell lines ARO, KAT-4, and FRO infecting the cells for 48 h with a *lac*Z-transducing adenovirus and evaluating the percentage of infected cells counting stained cells in randomly selected fields. The different results obtained in the two studies can be explained with the use of different reporter genes, infection times, and detection techniques.

Adenovirus internalization relies on the presence of cell surface of the CAR; a Western blot analysis has been performed on total cell lysates showing discrete or high expression levels of CAR. However, cytofluorimetric assay for CAR expression on cell surface showed a low or absent expression of CAR, suggesting a CAR-independent adenoviral entry in thyroid carcinoma cells lines. Furthermore, a significant reduction in CAR gene expression was observed in anaplastic

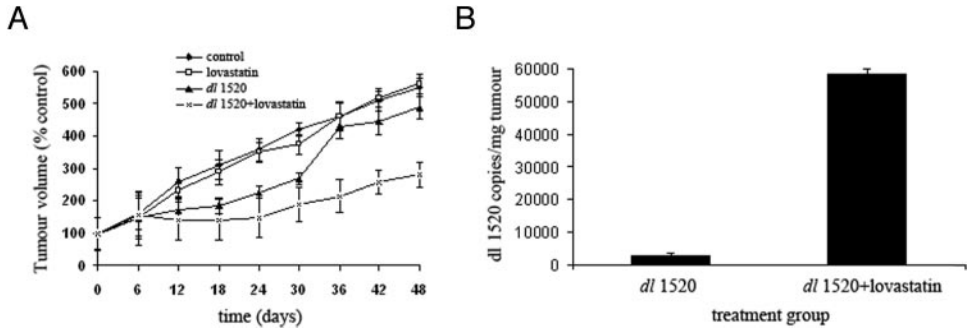

FIG. 6. Tumor growth delay induced by lovastatin and *dl*1520. A, Relative tumor growth of animals treated with *dl*1520 and lovastatin and control groups. Lovastatin treatment alone did not show statistically significant differences with the untreated control, whereas *dl*1520 induced a statistically significant reduction ($P < 0.05$) in the initial phase of the treatment (up to T = 30). The combination of *dl*1520 plus lovastatin significantly delayed tumor growth, compared with *dl*1520 single treatment group from T = 36 ($P < 0.01$). Data are presented as mean ± SD. B, Genome equivalent copies in tumor xenografts. A 10-fold increase in genome equivalent copies in tumor xenografts excised from lovastatin plus *dl*1520 group was observed. The data are the mean of three different experiments; the *bar* represents the SD.

thyroid carcinomas samples, compared with normal thyroid tissues.

Our observations are in agreement with previous studies and confirm a low susceptibility of ATC cells to therapeutic approaches based on adenoviral vectors (21).

It is worth noting that CAR expression is negatively regulated by TGF-β during the switch from epithelial to mesenchymal phenotype, and human pancreatic carcinoma cells show loss of epithelial differentiation and CAR surface localization on TGF-β treatment (22). In ATC cell lines, we observed discrete or high total expression levels of CAR and loss of surface localization of CAR. Our results indicate that the loss of thyroid differentiation, a typical feature of ATC, causes an intracellular localization of CAR receptor, probably by increasing the recycling of CAR receptors or shifting them to the cytosol.

Because ATC cells display a low infectivity and a high MOI of *dl*1520 is required to efficiently kill these cells, we decided to enhance the oncolytic activity by using lovastatin in combination with *dl*1520.

Lovastatin, a drug used for the treatment of hypercholesterolemia, has previously been reported to exert growth-inhibitory activity *in vitro* and *in vivo*. Farnesyl- and geranylgeranylpyrophosphate, intermediates in the cholesterol synthetic pathway, are needed for isoprenylation a crucial step for membrane attachment of cellular proteins like of p21 Ras, Rho, Cdc42, Rac, *etc.* (10). By inhibiting protein isoprenylation, lovastatin exerts its cellular effects, including a reduction of cell proliferation and induction of apoptosis (10). It is worth noting that low doses of lovastatin induce apoptosis or differentiation of ATC cells (11, 12).

Our study demonstrates that the treatment of ATC cell lines KAT-4 and FRO with lovastatin significantly increased the effects of *dl*1520.

A significant increase in viral replication was observed in lovastatin-treated cells. In FRO cells a significant increase was observed infecting lovastatin-treated cells with 10 pfu/cell, whereas at 1 pfu/cell, no significant differences were observed. In KAT-4 cells kept in the presence of lovastatin and infected with 5 or 10 pfu/cell, significant increase was observed; however, the pretreatment with lovastatin for 16 h was not able to increase viral replication.

These results suggest that the increase in viral replication observed treating ATC cells with lovastatin is viral dose or lovastatin treatment time dependent. Therefore, it is possible that higher MOIs of *dl*1520 in combination with a 16-h lovastatin pretreatment could result in enhanced viral replication in KAT-4 cells.

Increased infection efficacy could account for the increased oncolytic activity after lovastatin treatment; moreover, lovastatin inhibits the isoprenylation and the activity of p21 ras, blocking MEK activity, and it has been reported that MEK inhibitors, U0126 and PD184352, increase the expression of CAR protein and adenoviral entry in cancer cells (19). Therefore, we evaluated the adenoviral entry and CAR expression levels in ATC cell lines treated with lovastatin. We observed a modest, albeit significant, increase in adenoviral entry (3–10%), which that it is not sufficient to explain the effects of lovastatin on viral replication and cell survival.

CAR expression levels either total (data not shown) or on the cell surface were not modified by lovastatin treatment.

Cholesterol deprivation of FRO and KAT-4 cells did not modify adenoviral entry (data not shown), suggesting that the effects of lovastatin were not mediated by the inhibition of cholesterol synthesis.

It has been shown that lovastatin inhibits the invasiveness of an ATC cell line (ARO) and focal adhesion kinase phosphorylation, a nonreceptor tyrosine kinase playing a crucial role in integrin-mediated cell adhesion (23); therefore, it is not possible to exclude that lovastatin induces changes in integrin pattern on cell surface. Because it has been suggested that integrins can act as a coreceptor for adenovirus types 2 and 5 (24), the modest increase in adenoviral entry observed by us could be due to changes in integrins pattern induced by lovastatin. Further studies are required to verify this hypothesis.

A high increase in the fluorescence to cell ratio of lovastatin-treated cells was observed. This observation suggested to us that the drug could enhance the expression of viral genes, thereby increasing viral replication. To confirm this hypothesis, the expression of two viral genes, representing the early and the late phases, was analyzed in ATC cells infected with *dl*1520. Lovastatin increased significantly the expression of early gene *E1A 13 S* and a late gene *Penton*.

It has been proposed that drugs able to affect the cell cycle could enhance viral oncolysis by modulating viral gene expression (25). Lovastatin together with other clinically used statins (fluvastatin and simvastatin) induces a G_1 arrest of prostate cancer cells (26). A block of the cell cycle in ATC cells could enhance viral gene expression and increase the replication of *dl*1520. Further studies are required to clarify the mechanisms responsible for the effects of lovastatin on *dl*1520 gene expression and replication.

The administration of lovastatin *per os* to nude mice bearing ATC tumor xenografts enhances the antitumoral effects of *dl*1520 and increases the viral replication *in vivo*, confirming that this treatment could improve the clinical efficacy of replicating oncolytic adenoviruses. Interestingly, the injection of lovastatin and the virus within the tumor did not increase the effects of *dl*1520 (data not shown), indicating that a constant lovastatin blood concentration should be obtained to enhance the effects of *dl*1520.

The data presented here identify lovastatin as a promising agent for increasing the effects of oncolytic adenoviruses in ATC cells. It has been reported that FR901228 and trichostatin A, members of a new group of anticancer agents, the histone deacetylase inhibitors (27–29), or the MEK inhibitors U0126 and PD184352 (18) increase the antineoplastic effects of oncolytic adenoviruses. However, these agents have been used in a limited number of clinical trials, whereas 3-hydroxy-3-methylglutaryl coenzyme A reductase inhibitors have been widely used to reduce cardiovascular diseases without major adverse effects (10, 11). Lovastatin is generally well tolerated; the most important adverse effect is myotoxicity within the first 3 months of therapy (11). The risk of muscle dysfunction is increased by coadministration of other drugs able to interfere with lovastatin metabolism (11).

In the present study, in *in vitro* experiments, lovastatin was

used at final concentrations ranging from 2.5 to 10 μM, and in *in vivo*, we used a lovastatin concentration of 10 mg/kg/d.

Although the therapeutic dose for the treatment of hypercholesterolemia is about 1 mg/kg/d, which yields serum levels of 0.1 μM, it has been shown that serum concentrations of 2–4 μM of lovastatin are well tolerated in animal models, and clinical trials of phase I and II have been performed using 25 mg/kg/d with encouraging results (11). All these data indicate that lovastatin at a dose of 10 mg/kg/d could probably be used in ATC patients in combination with *dl*1520 without major side effects.

In conclusion, we have identified lovastatin as a drug that increases adenoviral replication and enhances the effects of an oncolytic adenovirus *in vitro* and *in vivo* against ATC cells. Therefore, lovastatin could be useful in the context of gene therapy for anaplastic thyroid carcinoma. Further studies are required to confirm the feasibility of this approach in ATC patients.

Acknowledgments

We thank Professor G. Vecchio and Dr. P. Formisano for their suggestions and a critical review of the manuscript. We thank Dr. G. Hallden for providing RmcB antibody. We also thank S. Sequino for technical assistance.

Received June 8, 2007. Accepted August 2, 2007.

Address all correspondence and requests for reprints to: Giuseppe Portella, Dipartimento di Biologia e Patologia Cellulare e Molecolare, Università di Napoli Federico II, via S. Pansini 5, 80131 Napoli, Italy. E-mail: portella@unina.it.

This work was supported by the Italian Ministry of Instruction, University, and Research (PRIN 2002) and the Associazione Italiana per la Ricerca sul Cancro.

Disclosure Statement: The authors have nothing to declare.

References

1. **Hedinger C, Williams ED, Sobin LH** 1989 The WHO histological classification of thyroid tumours: a commentary on the second edition. Cancer 63:908–911
2. **Ain KB** 2000 Management of undifferentiated thyroid cancer. Baillieres Best Pract Res Clin Endocrinol Metab 14:615–629
3. **Nikiforov YE** 2004 Genetic alterations involved in the transition from well-differentiated to poorly differentiated and anaplastic thyroid carcinomas. Endocr Pathol 15:319–327
4. **Sherman SI** 2003 Thyroid carcinoma. Lancet 361:501–511
5. **Parato KA, Senger D, Forsyth PA, Bell JC** 2005 Recent progress in the battle between oncolytic viruses and tumours. Nat Rev Cancer 12:965–976
6. **Kruyt FA, Curiel DT** 2002 Toward a new generation of conditionally replicating adenoviruses: pairing tumor selectivity with maximal oncolysis. Hum Gene Ther 13:485–495
7. **Post DE, Khuri FR, Simons JW, Van Meir EG** 2003 Replicative oncolytic adenoviruses in multimodal cancer regimens. Hum Gene Ther 14:933–946
8. **Portella G, Scala S, Vitagliano D, Vecchio G, Fusco A.** 2002 ONYX-015, an E1B gene-defective adenovirus, induces cell death in human anaplastic thyroid carcinoma cell lines. J Clin Endocrinol Metab 87:2525–2531
9. **Portella G, Pacelli R, Libertini S, Cella L, Vecchio G, Salvatore M, Fusco A** 2003 ONYX-015 enhances radiation-induced death of human anaplastic thyroid carcinoma cells. J Clin Endocrinol Metab 88:5027–5032
10. **Graaf MR, Richel DJ, Van Noorden CJ, Guchelaar HJ** 2004 Effects of statins and farnesyltransferase inhibitors on the development and progression of cancer. Cancer Treat Rev 30:609–641
11. **Chan KK, Oza AM, Siu LL**2003 The statins as anticancer agents. Clin Cancer Res 9:10–19
12. **Wang CY, Zhong WB, Chang TC, Lai SM, Tsai YF** 2003 Lovastatin, a 3-hydroxy-3-methylglutaryl coenzyme A reductase inhibitor, induces apoptosis and differentiation in human anaplastic thyroid carcinoma cells. J Clin Endocrinol Metab 88:3021–3026
13. **Zhong WB, Wang CY, Chang TC, Lee S** 2003 Lovastatin induces apoptosis of anaplastic thyroid cancer cells via inhibition of protein geranylgeranylation and *de novo* protein synthesis. Endocrinology 144:3852–3859
14. **Fiore L, Pollina LE, Fontani G, Casalone R, Berlingieri MT, Giannini R, Pacini F. Miccoli P, Toniolo A, Fusco A, Basolo F** 1997 Cytokine production by a new undifferentiated human thyroid carcinoma cell line, FB-1. J Clin Endocrinol Metab 82:4094–4100
15. **Skehan P, Storeng R, Scudiero D, Monks A, McMahon J, Vistica D, Warren J T, Bokesch H, Kenney S, Boyd MR** 1990 New colorimetric cytoxicity assay for anticancer-drug screening. J Natl Cancer Inst 82:1107–1112
16. **Abou El Hassan MA, Braam SR, Kruyt FA** 2006 Paclitaxel and vincristine potentiate adenoviral oncolysis that is associated with cell cycle and apoptosis modulation, whereas they differentially affect the viral life cycle in non-small-cell lung cancer cells. Cancer Gene Ther 12:1105–1114
17. **Hsu LK, Lonberg-Holm K, Alstein B, Crowell RL** 1988 A monoclonal antibody specific for the cellular receptor for the group B coxsackieviruses. J Virol 62:1647–1652
18. **Coyne CB, Bergelson JM** 2005 CAR: a virus receptor within the tight junction. Adv Drug Deliv Rev 57:869–882
19. **Anders M, Christian C, McMahon M, McCormick F, Korn WM** 2003 Inhibition of the Raf/MEK/ERK pathway up-regulates expression of the Coxsackie virus and adenovirus receptor in cancer cells. Cancer Res 63:2088–2095
20. **Crompton AM, Kirn DH** 2007 From ONYX-015 to armed vaccinia viruses: the education and evolution of oncolytic virus development. Curr Cancer Drug Targets 2:133–2139
21. **Marsee DK, Vadysirisack DD, Morrison CD, Prasad ML, Eng C, Duh QY, Rauen KA, Kloos RT, Jhiang SM** 2005 Variable expression of Coxsackie-adenovirus receptor in thyroid tumors: implications for adenoviral gene therapy. Thyroid 15:977–987
22. **Lacher MD, Tiirikainen MI, Saunier EF, Christian C, Anders M, Oft M, Balmain, A, Akhurst RJ, Korn WM** 2006 Transforming growth factor-beta receptor inhibition enhances adenoviral infectability of carcinoma cells via up-regulation of Coxsackie and adenovirus receptor in conjunction with reversal of epithelial-mesenchymal transition. Cancer Res 66:1648–1657
23. **Zhong WB, Liang YC, Wang CY, Chang TC, Lee WS** 2005 Lovastatin suppresses invasiveness of anaplastic thyroid cancer cells by inhibiting Rho geranylgeranylation and RhoA/ROCK signalling. Endocr Relat Cancer 3:615–629
24. **Li E, Brown SL, Stupack DG, Puente XS, Cheresh DA, Nemerow GR** 2001 Integrin $\alpha(v)\beta(1)$ is an adenovirus coreceptor. J Virol 75:5405–5409
25. **Abou El Hassan MA, Braam SR, Kruyt FA** 2006 A real-time RT-PCR assay for the quantitative determination of adenoviral gene expression in tumor cells. J Virol Methods 133:53–61
26. **Sivaprasad U, Abbas T, Dutta A** 2006 Differential efficacy of 3-hydroxy-3-methylglutaryl CoA reductase inhibitors on the cell cycle of prostate cancer cells. Mol Cancer Ther 5:2310–2316
27. **Goldsmith ME, Kitazono M, Fok P, Aikou T, Bates S, Fojo T** 2003 The histone deacetylase inhibitor FK228 preferentially enhances adenovirus transgene expression in malignant cells. Clin Cancer Res 9:5394–5401
28. **Bieler A, Mantwill K, Dravits T, Bernshausen A, Glockzin G, Kohler-Vargas N, Lage H, Gansbacher B, Holm PS** 2006 Novel three-pronged strategy to enhance cancer cell killing in glioblastoma cell lines: histone deacetylase inhibitor, chemotherapy, and oncolytic adenovirus dl520. Hum Gene Ther 17: 55–70
29. **Dion LD, Goldsmith KT, Tang DC, Engler JA, Yoshida M, Garver Jr RI** 1997 Amplification of recombinant adenoviral transgene products occurs by inhibition of histone deacetylase. Virology 231:201–209

***Endocrinology* is published monthly by The Endocrine Society (http://www.endo-society.org), the foremost professional society serving the endocrine community.**

The Prostate 66:326 –333 (2006)

Aurora B Expression Directly Correlates With Prostate Cancer Malignancy and Influence Prostate Cell Proliferation

Paolo Chieffi,[1]* Laura Cozzolino,[2] Annamaria Kisslinger,[3] Silvana Libertini,[4] Stefania Staibano,[2] Gelsomina Mansueto,[2] Gaetano De Rosa,[2] Antonia Villacci,[4] Mario Vitale,[5] Spiros Linardopoulos,[6] Giuseppe Portella,[4] and Donatella Tramontano[4]**

[1]*Dipartimento di Medicina Sperimentale, II Università di Napoli, Naples, Italy*
[2]*Dipartimento di Scienze Biomorfologiche e Funzionali, Università di Napoli "Federico II," Naples, Italy*
[3]*IEOS/CNR, Naples, Italy*
[4]*Dipartimento di Biologia e Patologia Cellulare e Molecolare, Università di Napoli "Federico II," Naples, Italy*
[5]*Dipartimento di Endocrinologia e Oncologia Molecolare e Clinica, Università di Napoli "Federico II," Naples, Italy*
[6]*The Breakthrough Breast Cancer Research Centre, London, United Kingdom*

BACKGROUND. Chromosomal instability is one of the most common features of prostate cancer (PC), especially in advanced stages. Recent studies suggest that defects in mitotic checkpoints play a role in carcinogenesis. Lack of mitotic regulation induces aneuploidy in cancer cells acting thereafter as a driving force for malignant progression. Serine/threonine protein kinases of the Aurora genes family play an important throughout the entire cell cycle. In that Aurora B regulates chromosome segregation by ensuring the orientation of sister chromatids. As a consequence, the overexpression of Aurora B in diploid human cells NHDF induces the appearance of multinucleate cells.

METHODS. Archive samples of normal and neoplastic prostate tissue, and prostate derived cell lines were screened for the expression of Aurora B.

RESULTS. Immunohistochemical analysis showed increased nuclear expression of Aurora-B in high Gleason grade PCs respect to low and intermediate grade cases and in all cancers in respect to hyperplastic and normal glands. Furthermore, in the high Gleason grade anaplastic cancer tissues Aurora B expression was accompanied by the phosphorylation of the histone H3. In analogy to the in vivo situation, Aurora B was vigorously expressed in the androgen independent PC cell lines PC3 and DU145, while a very modest expression of the kinase was observed in the androgen sensitive LnCap cells and in the EPN cells, a line of epithelial cells derived from normal prostate tissue. In addition, in PC3 cells Aurora B expression is accompanied the by the phosphorylation of the histone H3. The block of Aurora B expression induced by an inhibitor of Aurora kinase activity significantly reduced the growth of prostate carcinoma cells, but not that of non-transformed EPN cells.

Grant sponsor: Italian Ministry of Instruction, University and Research (MIUR); Grant sponsor: PRIN 2002; Grant sponsor: Associazione Italiana per la Ricerca sul Cancro (AIRC).

*Correspondence to: Paolo Chieffi, MD, PhD, Dipartimento di Medicina Sperimentale, Via Costantinopoli, 16, 80138 Napoli, Italy. E-mail: Paolo.Chieffi@unina2.it

**Correspondence to: Donatella Tramontano, PhD, Dipartimento di Biologia e Patologia Cellulare e Molecolare, Via Pansini, 5, 80131 Napoli, Italy. E-mail: Donatella.Tramontano@unina.it

Received 2 May 2005; Accepted 8 August 2005
DOI 10.1002/pros.20345
Published online 2 November 2005 in Wiley InterScience (www.interscience.wiley.com).

CONCLUSIONS. Our data are the first demonstration of a role of Aurora B in PC progression. In addition, the observation that Aurora B specific inhibitors interfere with PC cell proliferation but not with that of non-transformed prostate epithelial cells suggest that Aurora B is a potential therapeutic target for PC. *Prostate 66: 326–333, 2006.* © 2005 Wiley-Liss, Inc.

KEY WORDS: **prostatic tissue; anaplastic carcinoma; AIM-1**

INTRODUCTION

Prostate cancer (PC) is the most common neoplasia in men and the second leading cause of death after cardiovascular diseases [1]. Because the complex structure of the prostate gland and the lack of appropriate model systems the mechanisms underlying initial development and progression of PC are still largely unknown. In addition, a part from PSA, reliable biochemical or genetic markers for early cancer detection or for prognostic use are not available at the moment and the diagnosis, and the disease management are complicated by the multifocal presentation and the phenotypic and genotypic heterogeneity of PC [2–4].

The molecular model of PC progression from initial normal dysplasia to terminal late-stage metastatic disease suggests the involvement of multiple genetic alterations. High-grade prostate intraepithelial neoplasia (HPIN) is the most likely precursor of PC [5].

Currently there is no available clinical, immunohistochemical, or morphologic criteria that are predictive of this progression. As a consequence it is very important to recognize early markers enabling us to discriminate between the pre-neoplastic lesion, which will progress into invasive cancer and those that will not progress. Chromosomal instability leading to the generation of numerical and structural changes has been implicated in the pre-neoplastic and neoplastic stages of PC. Unstable chromosome number in cancer cells is currently believed to act as a driving force during the malignant progression and aneuploidy is the most prevalent genomic alteration identified in solid tumors [6,7]. A critical step for the maintenance of genetic stability is the chromosome segregation, which requires a high coordination of cellular process [8,9]. Loss of the mitotic regulation is a possible cause of aneuploidy in human epithelial malignancy and it is thought to create an abnormal nuclear morphology in cancer cells. Serine/threonine protein kinases of the Aurora genes family play a regulatory role from G2 to cytokinesis, encompassing key cell cycle events such as centrosome duplication, chromosome bi-orientation, and segregation [10,11]. The family of the Aurora genes includes Aurora A/STK-15, Aurora B/AIM-1, and Aurara C/AIK3. Aurora A is overexpressed in several solid tumors, and NIH 3T3 fibroblasts overexpressing Aurora A gene show an increase in centrosome number and aneuplody leading to neoplastic transformation [12–14].

Aurora B is a chromosome passenger protein, localized on the centromeres from prophase through the metaphase-anaphase transition [10,14–19]. Another chromosome passenger protein is INCENP, which tightly associates with Aurora B, probably regulating its activity. Survivin, a conserved inhibitor of apoptosis (IAP) like protein is a third member of the Aurora B complex [8,9]. Aurora B has been described to phosphorylate histone H3 at ser-10 and phosphorylation of histone H3 is required for proper chromosome dynamics during mitosis [14–19]. It has been also demonstrated that Aurora B overexpression in diploid human cells NHDF induces multinuclearity. Furthermore, Aurora B transfected cells have an unstable chromosome number and show an aggressive phenotype in vivo [18,19].

Since Aurora B plays a crucial role for chromosome dynamics, and aneuploidy is a common feature of prostate carcinomas, we analyzed Aurora B expression in archive prostate carcinoma tissue and in human prostate cell lines, originating from normal and neoplastic prostate tissue. All of prostate carcinoma cell lines showed increased Aurora B levels compared to the non-transformed cell line. Immunohistochemical studies performed on archive samples showed that Aurora B was detectable in normal prostate tissue and that its expression progressively increased with increasing of the Gleason Score, with a strong signal in anaplastic prostate carcinomas. The block of Aurora B kinase B activity by means of specific kinase inhibitors induced growth inhibition in human prostate anaplastic carcinoma cells but not in non-transformed prostate epithelial cells.

MATERIALS AND METHODS

Cell Culture

The two androgen-independent human PC cell lines PC3 [20] and DU145 [21] and the androgen-sensitive cell line, LnCap [22] used in these studies were grown in DMEM supplemented with 10% fetal bovine serum. EPN cells, a line of non-transformed epithelial cells derived by human normal prostate tissue spontaneously adapted to grow in culture, were routinely

cultured in Keratynocyte serum free medium (KSFM) supplemented with 3% fetal bovine serum (FBS) [23]. Growth curves were performed as previously described [23]. As for evaluation of the effect of the kinase inhibitor on cell proliferation the following method was applied. DU145, LnCap, PC3 cells were plated at a concentration of 1×10^3 cell/well in a 96-well plate and after 24 hr the cells were treated with 5, 10, 15 μM of the inhibitor. The quinazolin derivative: *N*-[4-(6,7-dimethoxy-quinazolin-4-ylamino)-phenyl]-benzamide [24] was dissolved in DMSO at a concentration of 10 mM. Cell proliferation was evaluated after 24 and 48 hr by using the Cell Titer 96® Aqueous cell proliferation assay (Promega, Milan, Italy). The values reported represent the mean ± SD of three independent samples per each experimental point.

FACS

Cytofluorimetric estimation of cell proliferation was performed as follows: the plates were washed in cold PBS and trypsin was added. Cells were collected, washed again in PBS and fixed in cold PBS, 70% ethanol for 30 min. Ethanol was removed by two PBS washes, and cells were incubated in PBS, 50 μg/ml propidium iodide, 10 μg/ml ribonuclease A, and deoxyribonuclease-free overnight at 4°C. Cells were then analyzed by flow cytometry using a FACScan (Becton Dickinson, Mountain View, CA). G_0–G_1, S, and G_2–M cell cycle phases were gated and the corresponding cells were counted.

Histology

Archival formalin-fixed, paraffin-embedded prostatectomy tissue was acquired from the files of the Pathology Section of the Biomorphological and Functional Sciences Department, University of Naples Federico II, Naples, Italy.

A total of 35 cases of PC were retrieved and, for each case, a paraffin block from the most representative area of the tumor was selected, as well as a block selected from different regions of the same prostate containing normal and/or hyperplastic prostatic glands. Four micrometer-thick serial sections were then cut from each block, and a hematoxylin and eosin section of each tumor was re-examined to confirm the original diagnosis and staging of PC. The Gleason sum scores for the cases ranged from 4 to 9.

Immunohistochemistry

Serial sections of each case were de-waxed, rehydrated through decreasing alcohols and treated with 3% hydrogen peroxide for 5 min to inactivate endogenous peroxidases, and then washed in distilled water. The slides were then pre-incubated in a microwave oven three times for 5 min in 10 mM, 6 pH buffer citrate. After quenching of endogenous peroxidase, antigen retrieval was achieved by boiling sections at 120°C at 3.4 atm for 10 min in 1% citrate buffer; the sections were then blocked for 2 hr at room temperature with 1.5% blocking serum (DAKO). Incubation with the primary antibody was carried out overnight, in a moist chamber, with the anti AIM-1 (Aurora B, 1:1,000, #611082,BD Transduction Laboratories, San Diego, CA). Finally, binding of the primary antibody was detected by the conventional streptavidin-biotin linked horseradish peroxidase (LSAB-HRP) procedure, using 3,3′-diaminobenzidine (DAB) as chromogen [25]. Negative controls were performed on serial sections of the same tissues, substituting the primary antibody with non-immune serum.

Slight nuclear counterstaining was performed with Harris' hematoxylin; slides were then coverslipped using a synthetic mounting medium.

The results of the immunohistochemical staining were evaluated separately by two observers. Only cells with a definite brown staining were judged as positive.

The immunohistochemical expression was quantified semi-quantitatively, using a 40× objective and expressed as percentage of positive nuclei. Then, tumors and respective normal and/or hyperplastic glandular tissue were assigned to one of the following arbitrary categories: (1) from 0% to <5% of positive cells; (2) from 5% <10%; (3) from 10% to 25%; (4) >25% of cells.

The data were analyzed utilizing the one-way Analysis of Variance (ANOVA) and Student-Newman–Keuls Multiple Comparisons Test (SPSS statistical software, version 6.1 for Windows. For the categorical parameters the Chi-square test was used; the non-parametric Mann–Whitney *U*-test was utilized for continuous variables). Only values of $P < 0.05$ were considered as significant.

Protein Extraction and Western Blot Analysis

Prostate samples or cells were homogenized directly into lysis buffer (50 mM HEPES, 150 mM NaCl, 1 mM EDTA, 1 mM EGTA, 10% glycerol, 1%Triton-X-100, 1 mM phenylmethylsulfonyl fluoride, 1 μg aprotinin, 0.5 mM sodium orthovanadate, 20 mM sodium pyrophosphate). The lysates were clarified by centrifugation at 14,000× 10 min. Protein concentrations were estimated by a Bio-Rad assay (Bio-Rad, München, Germany), and boiled in Laemmli buffer (Tris-HCl pH 6.8 0,125 M, SDS 4%, glycerol 20%, 2-mercaptoethanol 10%, bromophenol blue 0.002%) for 5 min before electrophoresis. Proteins were subjected to SDS–PAGE (10% polyacrylamide) under reducing condition. After

electrophoresis, proteins were transferred to nitrocellulose membranes (Immobilon Millipore Corporation); complete transfer was assessed using prestained protein standards (Bio-Rad, Hercules, CA). After blocking with TBS-BSA (25mM Tris, pH 7.4, 200 mM NaCl, 5% bovine serum albumin), the membrane was incubated with the primary antibody against: (1) Aurora B (1:400; # 611082, BD Transduction Laboratories); (2) Phospho H3 (ser 10) (1:250, # 06-570, Upstate, Lake Placid, NY); (3) β-Tubulin (1:500, # T-4026, SIGMA Chemical Corporation, St. Louis, MO) for 1 hr (at room temperature). Membranes were then incubated with the horseradish peroxidase-conjugated secondary antibody (1:2,000) for 45 min (at room temperature) and the reaction was detected with an ECL system (Amersham, Life Science, Chiltern Hills, UK).

RESULTS

Aurora B Expression in ProstateTissue

A total of 35 cases of archive prostate tissue comprising normal prostate and neoplastic tissues scoring Gleason 4 to 7/8 were retrieved and the original histological diagnosis and grading of PC was confirmed for all the cases examined. Tissues were stained with anti Aurora B antibodies. Results showed increased nuclear expression of Aurora-B in high-score PCs respect to low and intermediate score cases ($P < 0.05$) and in all cancers respect to hyperplastic ($P < 0.05$) and normal ($P < 0.01$) glands (Table I, Fig. 1a–c).

Four cases of PC showed a diffuse, strong cytoplasmic staining, in addition or instead of the nuclear staining. In two cases of benign hyperplasia a cytoplasmic localization of Aurora B immunostaining was observed in isolate epithelial cells. Dynamic exchange from cytoplasm and centrosome has been already reported for other members of the Aurora gene family [26,27]. In normal prostate tissue, few cells positive for Aurora B staining were observed (Fig. 1a). The expression of Aurora B was confined to the epithelial cells and no positive cells could be observed within the stromal part of the gland. Similarly to that of Aurora B the expression of Ki-67 increased in tumors tissues in respect to normal or hyperplastic areas (data not shown).

Western Blot analysis of total protein extracted from the frozen prostate tissue comprising normal prostate and neoplastic tissues scoring Gleason 4 to 7/8 confirmed the morphological results. A band of 41 kDa was observed in all the samples tested. Aurora B expression dramatically increased with the Gleason score, being extremely high in undifferentiated tumors (Fig. 2a). Aurora B has been described to phosphorylate histone H3 at Ser-10, therefore to investigate the biological activity of the kinase in the prostate tissue, the same samples were immunoblotted with anti-phospho-Ser-10 H3 histone antibodies. As shown in Figure 2b, an increased phosphorylation of the H3 histone was observed in the higher Gleason grade tissues. β-Tubulin was used to assess the equal amounts of protein (Fig. 2c).

Aurora B Expression in Human Prostate Cell Lines

The expression of Aurora B was investigated in prostate cell lines derived from normal and neoplastic tissues by Western blot. As shown in Figure 3a Aurora B was expressed in the androgen independent PC3 cell line and at a lesser extent in the DU145 cell lines while a much weaker expression of the kinase was observed the androgen sensitive LnCap cells. In the EPN cells, a line of non-transformed androgen sensitive epithelial cells the expression of Aurora B was consistently weaker then that of the tumor cell lines. In addition, in PC3 and in DU145 cell lines Aurora B expression is associated to an increase in the phosphorylation of histone H3 (Fig. 3b). β-Tubulin was used to assess the equal amounts of protein (Fig. 3c).

TABLE I. Immunohistoclinical expression and topographical localization of AURORA B in 35 cases of prostate cancer.

Cases	Gleason's score	Aurora B score	Normal prostaic glands	Benign hyperplastic glands
N = 14	≤4	2 (n = 6, N*)	1 (N = 7)	1 (N = 3)
		3 (n = 6, N)	2 (N = 7)	2 (N = 11)
		4 (n = 2, N)		
N = 12	>4 to ≤7	3 (n = 5, N)	1 (N = 2)	2 (N = 12)
		4 (n = 7, N)	2 (N = 10)	
N = 9	>7	4 (n = 7, 5N, 2N+C**)	2 (N = 9)	2 (N = 7) 3 (N = 2)
		4 (n = 2, C)		

*Nuclear.
**Cytoplasmic localization of Aurora B.

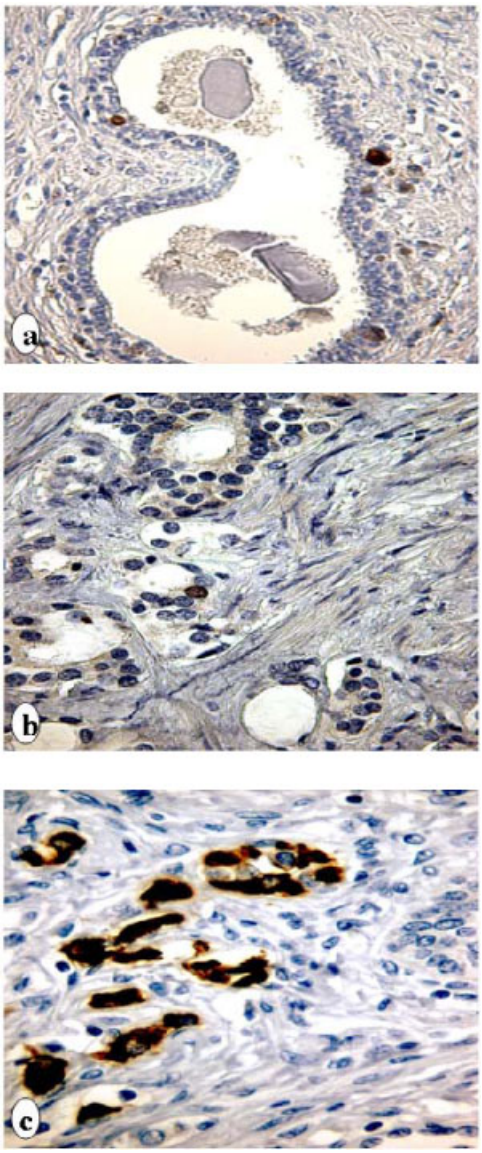

Fig. 1. Aurora B expression in human prostate tissues. Localization of the Aurora B protein in human prostate tissue by immunocytochemistry; **(a)** paraffin embedded section of normal prostate tissue. Expression of Aurora B protein was not observed; **(b)** section of intermediate Gleason grade prostate carcinoma, showing some nuclear immunoreactivity for Aurora B protein; **(c)** section of anaplastic prostate carcinoma, showing extensive nuclear immunoreactivity for Aurora B protein (400×). [Color figure can be viewed in the online issue, which is available at www.interscience.wiley.com.]

Aurora B Kinase Inhibitor and Prostate Cell Proliferation

A small molecule similar to the quinazolin derivative: *N*-[4-(6,7-dimethoxy-quinazolin-4-ylamino)-phenyl]-benzamide has been shown to inhibit the Aurora B kinase activity [24,28]. To evaluate the effects of Aurora kinase inhibitor on prostate cell proliferation, PC3, DU145, LnCap, and EPN cells were treated with 5, 10, and 15 μM, and cell proliferation was evaluated after 24 and 48 hr. The Aurora kinase inhibitor significantly reduced the proliferation of PC cells, while had no effects on the non-transformed EPN cells, which expressed only small concentrations of Aurora B

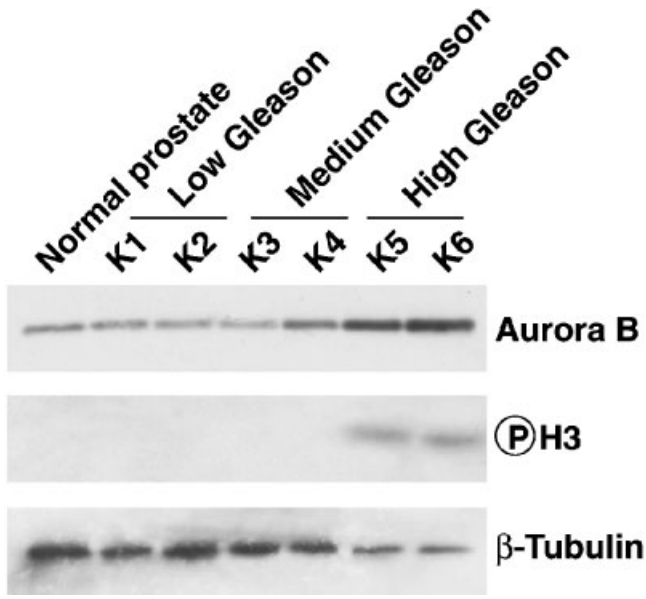

Fig. 2. Western blot analysis of Aurora B expression in prostate human tissues; **(a)** the expression of Aurora B protein increases with increasing Gleason score being maximal in anaplastic carcinomas; **(b)** in addition in the samples corresponding to high grade carcinoms it present a band corresponding to the phosphorylated hystone H3; **(c)** β-Tubulin was used to assess the equal amounts of protein.

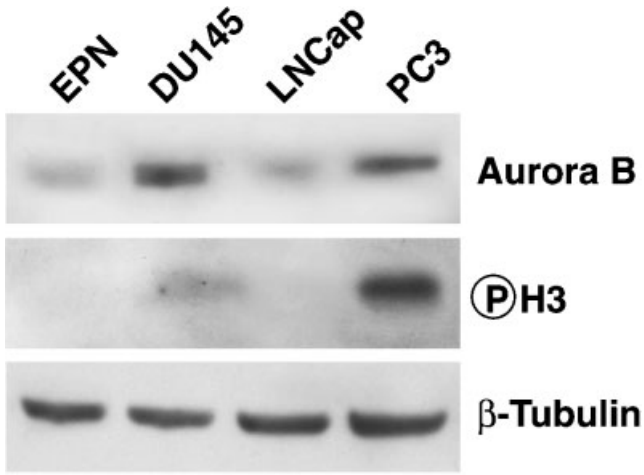

Fig. 3. Western blot analysis of Aurora B expression in human prostate cell lines; **(a)** the level of expression increased from normal differentiated androgen dependent to non-differentiated androgen independent cell lines. Aurora B was highly expressed in the PC3; at a lesser extent in the DUI45 cells, and it was basically absent in LnCap and in the EPN cells; **(b)** in the PC3 Aurora B mediated the phosphorylation of H3 hystone; **(c)** β-Tubulin was used to assess the equal amounts of protein.

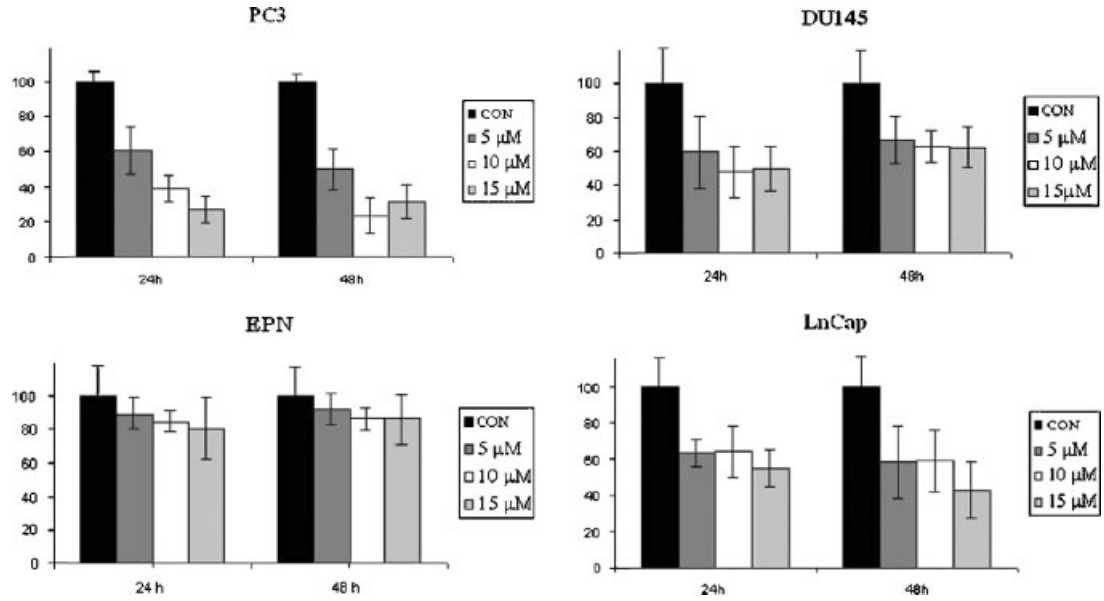

Fig. 4. Aurora kinase inhibitor reduced the growth of prostate tumor cells PC3, DU 145, and LnCap but not that of normal prostate epithelial cells, EPN.

kinase (Fig. 4). As expected FACS analysis showed that the kinase inhibitor blocked the cell cycle of PC3, DU145, and LnCap cells at the G_2/M phase.

DISCUSSION

In the present study we have evaluated the expression of Aurora B in prostate cell lines and human prostate tumors. The immunohistochemical analysis of neoplastic or non-neoplastic prostate tissues showed that the expression of Aurora B directly correlates with increase in the Gleason grade of the PC being abundant in undifferentiated carcinomas. Conversely, lower expression was observed in normal tissues and in low-grade prostate carcinomas. This observation suggests that during tumor progression, in particular during the transition from differentiated prostate carcinomas to undifferentiated prostate carcinomas, Aurora B overexpression takes place and Aurora B overexpression might confer a growth advantage to the neoplastic cells [29–33].

By using a selective Aurora B kinase inhibitor we demonstrated that the block of Aurora B activity dramatically reduces the proliferation of prostate carcinoma cells [24,28]. It is important to note that the growth of EPN cells, a line originated from normal epithelial prostate tissue, which express low levels of Aurora B, was not affected by the Aurora B inhibitor.

In LnCap cells the expression of Aurora B is weaker than that in PC3 and Du145. It is important to note that LnCap cells, although derived from a lymph node of an aggressive PC, are among the PC derived cell lines, the less aggressive and tumorigenic. Moreover, LnCap cells retain prostate differentiated markers including the sensitivity to androgen stimulation, also suggesting a less aggressive phenotype. In addition, the proliferation rate is much lower than that of PC3 and Du145 [22], therefore the expression of Aurora B correlates with the proliferative rate and the aggressiveness of the different cell lines.

Alterations of the mechanisms responsible for maintaining the chromosome balance are common in neoplastic cells [15,16]. Disruption of mitotic checkpoints induces unstable chromosome number or aneuploidy, which is thought to create abnormal nuclear morphology in cancer cells and contribute to genetic instability. Alterations in chromosome number have been described as a common feature of almost all solid tumors. Aneuploidy has been observed also in PC. Interestingly, studies using loss of heterozygosity analyses, CGH2 and fluorescent in situ hybridization revealed few recurrent chromosomal aberrations in early PCs [34–36]. Low-stage primary tumors tend to be near diploid with few clonal numerical and/or structural aberrations. In contrast, high-stage, advanced primary, or metastatic prostate tumors tend to be aneuploid with a high degree of chromosomal aberrations [2,8]. Moreover several chromosomal abnormalities have been reported and summarized in the expert reviews published on http://www.expert reviews.org in 2003 [37].

Although chromosomal instability is a key mechanism in the process of malignant transformation in human epithelial tissues, yet the molecular mechanisms responsible for chromosome destabilization during carcinogenesis are largely unknown [38–41].

Centrosome defects have been invoked to contribute to genomic instability during PC progression. Centrosomes are structurally and numerically abnormal in the vast majority of metastatic and invasive prostate carcinomas. The extent of centrosome abnormalities in invasive prostate carcinoma correlates with the Gleason grade [42].

Two recent set of data reported the potential role of STK15 (Aurora-A) a serine/threonine kinase found in centrosomes and involved in mitotic chromosomal segregation in PC. Overexpression of Aurora-A is present in some normal and in the majority of high-grade PIN lesions and is an early event leading to the genetic instability in prostate carcinogenesis [43,44].

Thus, dysfunction in mitotic checkpoints represent a primary cause of genomic instability and as a consequence of accumulation of structural and numeral chromosomal abnormalities present in tumor cells. Aurora B assuring the correct orientation of sister chromatides plays a crucial role in mitosis. A significant overexpression of Aurora B has been observed in human cancer cell lines, and in colorectal tumors a correlation between Aurora B expression levels and Duke's grade in colorectal tumors has been described [33]. Furthermore, it has been observed that the forced expression of Aurora B produced aneuploid cells with a malignant and aggressive phenotype, indicating that Aurora B is relevant in aneuploidy development during carcinogenesis [18,19]. Recently, we have demonstrated that high expression levels of Aurora B are a consistent feature of human seminomas and in thyroid anaplastic carcinomas a high expression of Aurora B was observed [45–47]. In these previous studies, the expression of Ki-67 was analyzed showing an increase in tumors tissues in respect to normal or hyperplastic areas similar to Aurora B. In agreement with our previous results a highly statistical correlation between expression Aurora B and that of Ki-67 with a percentage of Aurora-B positive cells lower than that of the Ki-67-positive cells (data not shown) was observed.

CONCLUSIONS

Although large efforts have been put in the research of appropriate therapy of PC the appearance in the population of the tumor of androgen insensitive cells vanishes the good result obtained by the hormonal therapy. The observation that in PC tissue Aurora B gene expression levels directly correlates to the stage of malignant progression, that the block of Aurora B expression or activity via an Aurora B inhibitor, reduces the proliferation of anaplastic prostatic carcinoma cells but not that of epithelial normal cells could contribute to the development of novel therapeutic strategies. The implications of these findings include Aurora B assessment as an useful biomarker in the gray zone for monitoring disease in prevention strategies and for improving early diagnosis.

REFERENCES

1. Jemal A, Kulldorff M, Devesa SS, Hayes RB, Fraumeni JF Jr. A geographic analysis of prostate cancer mortality in the United States, 1970–89. Int J Cancer 2002;101:168–174.
2. Arnold JT, Isacs JT. Mechanisms progression of androgen-independent prostate cancer: It is not only cancer cell's foult. Endocr Relat Cancer 2002;9:61–73.
3. Nwosu V, Carpten J, Trent JM, Sheridan R. Heterogeneity of genetic alterations in prostate cancer: Evidence of the complex nature of the disease. Hum Mol Genet 2001;10:2313–2318.
4. Ruijter ET, Miller GJ, van de Kaa CA, van Bokhoven A, Bussemakers MJ, Debruyne FM, Ruiter DJ, Schalken JA. Molecular analysis of multifocal prostate cancer lesions. J Pathol 1999;188:271–277.
5. Zitzelsberger H, Kulka U, Lehmann L, Walch A, Smida J, Aubele M, Lorch T, Hofler H, Bauchinger M, Werner M. Genetic heterogeneity in a prostatic carcinoma and associated prostatic intraepithelial neoplasia as demonstrated by combined use of laser-microdissection, degenerate oligonucleotide primed PCR and comparative genomic hybridization. Virchows Arch 1998; 433:297–304.
6. Sieber OM, Heinimann K, Tomlinson IP. Genomic instability-the engine of tumorigenesis? Nat Rev Cancer 2003;3:701–708.
7. Jallepalli P, Lengauer C. Chromosome segregation and cancer: Cutting through the mystery. Nat Rev Cancer 2001;1:109–117.
8. Nigg EA. Mitotic kinases as regulators of cell division and its checkpoints. Nat Rev Mol Cell Biol 2001;21:21–32.
9. Andrews PD, Knatko E, Moore WJ, Swedlow JR. Mitotic mechanics: The auroras come into view. Curr Opin Cell Biol 2003; 15:672–683.
10. Adams RR, Carmena M, Earnshaw WC. Chromosomal passengers and the (aurora) ABCs of mitosis. Trends Cell Biol 2001;11: 49–54.
11. Dutertre S, Descamps S, Prigent C. On the role of aurora-A in centrosome function. Oncogene 2002;21:6175–6183.
12. Bischoff JR, Anderson L, Zhu Y, Mossie K, Ng L, Souza B, Schryver B, Flanagan P, Clairvoyant F, Ginther C, Chan CS, Novotny M, Slamon DJ, Plowman GD. A homologue of Drosophila aurora kinase is oncogenic and amplified in human colorectal cancers. EMBO J 1998;17:3052–3065.
13. Zhou H, Kuang J, Zhong L, Kuo WL, Gray JW, Sahin A, Brinkley BR, Sen S. Tumour amplified kinase STK15/BTAK induces centrosome amplification, aneploidy and transformation. Nature Genet 1998;20:189–193.
14. Ewart-Toland A, Briassouli P, de Koning JP, Mao JH, Yuan J, Chan F, MacCarthy-Morrogh L, Ponder BA, Nagase H, Burn J, Ball S, Almeida M, Linardopoulos S, Balmain A. Identification of Stk6/STK15 as a candidate low-penetrance tumor-susceptibility gene in mouse and human. Nature Genet 2003;34:403–412.
15. Adams RR, Maiato H, Earnshaw WC, Carmena M. Essential roles of Drosophila inner centromere protein (INCENP) and aurora B in histone H3 phosphorylation, metaphase chromosome alignment, kinetochore disjunction, and chromosome segregation. J Cell Biol 2001;153:865–880.

16. Kaitna S, Pasierbek P, Jantsch M, Loidl J, Glotzer M. The aurora B kinase AIR-2 regulates kinetochores during mitosis and is required for separation of homologous chromosomes during meiosis. Curr Biol 2002;12:798–812.
17. Murata-Hori M, Wang YL. The kinase activity of aurora B is required for kinetochore-microtubule interactions during mitosis. Curr Biol 2002;12:894–899.
18. Ota T, Suto S, Katayama H, Han ZB, Suzuki F, Maeda M, Tanino M, Terada Y, Tatsuka M. Increased mitotic phosphorylation of histone H3 attributable to AIM-1/Aurora B overexpression contributes to chromosome number instability. Cancer Res 2002; 62:5168–5177.
19. Tatsuka M, Katayama H, Ota T, Tanaka T, Odashima S, Suzuki F, Terada Y. Multinuclearity and increased ploidy caused by overexpression of the aurora- and Ipl1-like midbody-associated protein mitotic kinase in human cancer cells. Cancer Res 1998; 58:4811–4816.
20. Kaingn ME, Narayan KS, Ohnuki Y, Lechner J, Jones LW. Establishment and characteritation of a human prostatic cancer cell line (PC3). Invest Urol 1979;17:16–23.
21. Stone KR, Mickey DD, Wunderli H, Mickey GH, Paulson DF. Isolation of human prostate carcinoma cell line (DU145). Int J Cancer 1987;21:274–281.
22. Horoszewicz JS, Leong SS, Kawinski E, Karr JP, Rosenthal H, Ming Chu T, Mirand A, Murphy GP. LNCaP model of human prostatic carcinoma. Cancer Res 1983;43:1809–1818.
23. Sinisi AA, Chieffi P, Pasquali D, Kisslinger A, Staibano S, Bellastella A, Tramontano D. EPN: A novel epithelial cell line derived from human prostate tissue. In Vitro Cell Dev Biol-An 2002;38:165–175.
24. Mortlock A, Keen N, Jung F, Brewster AG. International Publication Number: WO01/21596A1 (www.european-patent-office.org) 2001.
25. Hsu SM, Raine L, Fanger H. Use of avidin-biotin-peroxidase complex (ABC) in immunoperoxidase techniques: A comparison between ABC and unlabeled antibody (PAP) procedures. J Histoch Cytochem 1981;29:557–580.
26. Berdnik D, Knoblich JA. Drosophila Aurora-A is required for centrosome maturation and actin-dependent asymmetric protein localization during mitosis. Curr Biol 2002;12:640–647.
27. Stenoien DL, Sen S, Mancini MA, Brinkley BR. Dynamic association of a tumor amplified kinase, Aurora-A, with the centrosome and mitotic spindle. Cell Motil Cytoskeleton. 2003; 5:134–146.
28. Ditchfield C, Johnson VL, Tighe A, Ellston R, Haworth C, Johnson T, Mortlock A, Keen N, Taylor SS. Aurora B. Couples chromosome alignment with anaphase by targeting BubR1, Mad2, and Cenp-E to kinetochores. J Cell Biol 2003;161:267–280.
29. Miyoshi Y, Iwao K, Egawa C, Noguchi S. Association of centrosomal kinase STK15/BTAK mRNA expression with chromosomal instability in human breast cancers. Int J Cancer 2001;92: 370–373.
30. Li D, Zhu J, Firozi PF, Abbruzzese JL, Evans DB, Cleary K, Friess H, Sen S. Overexpression of oncogenic STK15/BTAK/Aurora A kinase in human pancreatic cancer. Clin Cancer Res 2003;9:991–997.
31. Gritsko TM, Coppola D, Paciga JE, Abbruzzese JL, Evans DB, Cleary K, Friess H, Sen S. Activation and overexpression of centrosome kinase BTAK/Aurora-A in human ovarian cancer. Clin Cancer Res 2003;9:1420–1426.
32. Hamada M, Yakushijin Y, Ohtsuka M, Kakimoto M, Yasukawa M, Fujita S. Aurora2/BTAK/STK15 is involved in cell cycle checkpoint and cell survival of aggressive non-Hodgkin's lymphoma. Br J Haematol 2003;12:439–447.
33. Katayama H, Ota T, Jisaki F, Ueda Y, Tanaka T, Odashima S, Suzuki F, Terada Y, Tatsuka M. Mitotic kinase expression and colorectal cancer progression. J Natl Cancer Inst 1999;91:1160–1162.
34. Nupponen NN, Hyytinen ER, Kallioniemi AH, Visakorpi T. Genetic alterations in prostate cancer cell lines detected by comparative genomic hybridization. Cancer Genet Cytogenet 1998;101:53–57.
35. Nupponen NN, Visakorpi T. Molecular cytogenetics of prostate cancer. Microsc Res Tech 2000;51:456–463.
36. Jenkins RB, Qian J, Lee HK, Huang H, Hirasawa K, Bostwick DG, Proffitt J, Wilber K, Lieber MM, Liu W, Smith DI. A molecular cytogenetic analysis of 7q31 in prostate cancer. Cancer Res 1998; 58:759–766.
37. http://www.expert last access April 2005.
38. Cahill DP, Kinzler KW, Vogelstein B, Lengauer C. Genetic instability and Darwinian selection in tumours. Trends Cell Biol 1999;9: M57–M60.
39. Fan R, Kumaravel TS, Jalali F, Marrano P, Squire JA, Bristow RG. Defective DNA strand break repair after DNA damage in prostate cancer cells: Implications for genetic instability and prostate cancer progression. Cancer Res 2004;64(23):8526–8533.
40. Mark A R, Angelo M De M. Molecular genetics of human prostate cancer. Mod Pathol 2004;17:380–388.
41. Gu Y, Kim KH, Ko D, Nakamura K, Yasunaga Y, Moul JW, Srivastava S, Arnstein P, Rhim JS. A telomerase-immortalized primary human prostate cancer clonal cell line with neoplastic phenotypes. Int J Oncol 2004;25:1057–1064.
42. Pihan GA, Purohit A, Wallace J, Malhotra R, Liotta L, Doxsey SJ. Centrosome defects can account for cellular and genetic changes that characterize prostate cancer progression Cancer Res 2001; 61:2212–2219.
43. McKlveen Buschhorn H, Klein RR, Chambers SM, Hardy MC, Green S, Bearss D, Nagle RB. Aurora-A over-expression in high-grade PIN lesions and prostate cancer. Prostate. 2005 Mar 7; [Epub ahead of print] 64(4): 341–346.
44. Ewart-Toland A, Dai Q, Gao YT, Nagase H, Dunlop MG, Farrington SM, Barnetson RA, Anton-Culver H, Peel D, Ziogas A, Lin D, Miao X, Sun T, Ostrander EA, Stanford JL, Langlois M, Chan JM, Yuan J, Harris C, Bowman E, Clayman GL, Lippman SM, Lee JJ, Zheng W, Balmain A. Aurora-A/STK15 T+91A is a general low penetrance cancer susceptibility gene: A meta-analysis of multiple cancer types. Carcinogenesis. 2005 Mar. 31; [Epub ahead of print] 26(8):1368–1373.
45. Chieffi P, Troncone G, Caleo A, Libertini S, Linardopoulos S, Tramontano D, Portella G, Aurora B. Expression in normal testis and seminomas. J Endocrinol 2004;181:263–270.
46. Nikiforov YE. Editorial: Anaplastic carcinoma of the thyroid–will aurora B light a path for treatment? J Clin Endocrinol Metab 2005;90(2):1243–1245.
47. Sorrentino R, Libertini S, Pallante PL, Troncone G, Palombini L, Bavetsias V, Spalletti-Cernia D, Laccetti P, Linardopoulos S, Chieffi P, Fusco A, Portella G. Aurora B over expression associates with the thyroid carcinoma undifferentiated phenotype and is required for thyroid carcinoma cell proliferation. J Clin Endocrinol Metab 2005;90(2):928–935.

0021-972X/05/$15.00/0
Printed in U.S.A.

The Journal of Clinical Endocrinology & Metabolism 90(2):928–935

doi: 10.1210/jc.2004-1518

Aurora B Overexpression Associates with the Thyroid Carcinoma Undifferentiated Phenotype and Is Required for Thyroid Carcinoma Cell Proliferation

Rosanna Sorrentino, Silvana Libertini, Pier Lorenzo Pallante, Giancarlo Troncone, Lucio Palombini, Vassilios Bavetsias, Daniela Spalletti-Cernia, Paolo Laccetti, Spiros Linardopoulos, Paolo Chieffi, Alfredo Fusco, and Giuseppe Portella

Dipartimenti di Biologia e Patologia Cellulare e Molecolare (R.S., S.Lib., P.L.P., D.S.-C., A.F., G.P.), Scienze Biomorfologiche e Funzionali-Istituto di Anatomia Patologica (G.T., L.P.), and Chimica Biologica (P.L.), Università Federico II, 80131 Naples, Italy; Cancer Research U.K. Centre for Cancer Therapeutics (V.B., S.Lin.), Institute of Cancer Research 15, Belmont, Sutton, Surrey SM2 5NG, United Kingdom; The Breakthrough Breast Cancer Research Centre (S.Lin.), Institute of Cancer Research, London SW3 6JB, United Kingdom; and Dipartimento di Medicina Sperimentale (P.C.), II Università di Napoli, 80138 Naples, Italy

Alterations in chromosome number (aneuploidy) are common in human neoplasias. Loss of mitotic regulation is believed to induce aneuploidy in cancer cells and act as a driving force during the malignant progression. The serine/theronine protein kinases of *aurora* family genes play a critical role in the regulation of key cell cycle processes. Aurora B mediates chromosome segregation by ensuring orientation of sister chromatids and overexpression of Aurora B in diploid human cells NHDF (normal human diploid fibroblast) induces multinuclearity.

We analyzed Aurora B expression in human thyroid carcinomas. Cell lines originating from different histotypes showed an increase in Aurora B expression. Immunohistochemical analysis of archive samples showed a high expression of Aurora B in anaplastic thyroid carcinomas; conversely, Aurora B expression was not detectable in normal thyroid tissue. Real-time PCR analysis confirmed a strong expression of Aurora B in anaplastic thyroid carcinomas.

The block of Aurora B expression induced by RNA interference or by using an inhibitor of Aurora kinase activity significantly reduced the growth of thyroid anaplastic carcinoma cells. (*J Clin Endocrinol Metab* 90: 928–935, 2005)

THYROID CARCINOMA IS the most frequent malignant endocrine tumor in humans. Thyroid neoplasia includes tumors with different molecular and clinical features including differentiated follicular and papillary carcinomas, poorly differentiated papillary and follicular carcinomas and undifferentiated anaplastic carcinomas (1, 2). Papillary carcinomas represent more than 70% of thyroid malignant tumors and rearrangements of RET gene have represented for years the most frequent genetic alterations found in papillary carcinomas (3, 4). More recently several studies (5–9) indicated a high percentage of B-RAF mutations in thyroid papillary carcinomas. Follicular carcinomas are differentiated thyroid tumors, which frequently show RAS genes activating mutations (10) and paired domain-containing transcription factor (PAX-8) and peroxisome proliferator-activated receptor (PPAR) gamma 1 rearrangements (11). Poorly differentiated and anaplastic carcinomas derive from differentiated carcinomas through a process of neoplastic progression. Alterations of the p53 tumor suppressor gene are a peculiar feature of anaplastic carcinomas (12–14). Although critical molecular mechanisms of thyroid tumorigenesis have been identified, other molecular steps of thyroid neoplastic progression need to be clarified. Unstable chromosome number in cancer cells is currently believed to act as a driving force during the malignant progression, and aneuploidy is the most prevalent genomic alteration identified in solid tumors (15, 16). Alterations in chromosome number are common in follicular thyroid carcinomas (17, 18); however, the cause of aneuploidy in many sporadic thyroid cancers is currently unknown.

A critical step for the maintenance of genetic stability is the chromosome segregation, which requires a high coordination of cellular process (19, 20). Loss of the mitotic regulation is a possible cause of aneuploidy in human epithelial malignancy, and it is thought to create an abnormal nuclear morphology in cancer cells. The serine/theronine protein kinases of the Aurora family genes play a regulatory role from G_2 to cytokinesis, encompassing key cell cycle events such as centrosome duplication, chromosome biorientation, and segregation (21, 22). The family of the Aurora genes includes Aurora A/STK-15, Aurora B/AIM-1, and AURORA C/AIK3. Aurora A is overexpressed in several solid tumors, and NIH 3T3 fibroblasts overexpressing Aurora A gene show an increase in centrosome number and aneuploidy, leading to neoplastic transformation (23, 24). A polymorphism in Aurora A gene has been also associated with a certain degree of aneuploidy in human tumors (25).

Aurora B (AIM1) is a chromosome passenger protein, localizing on centromeres from prophase through the met-

First Published Online November 23, 2004

Abbreviations: PTU, Propylthiouracil; RNAi, RNA interference; siRNA, small interfering RNA.

aphase-anaphase transition (21, 26–30). Another chromosome passenger protein is INCENP, which tightly associates with Aurora B, probably regulating its activity. Survivin, a conserved inhibitor of apoptosis-like protein, is a third member of the Aurora B complex (19, 20). Aurora B has been described to phosphorylate histone H3 at ser-10, and phosphorylation of histone H3 is required for proper chromosome dynamics during mitosis (26–30). It has also been demonstrated that Aurora B overexpression in diploid human cells normal human diploid fibroblast induces multinuclearity. Furthermore, Aurora B-transfected cells have an unstable chromosome number and show an aggressive phenotype *in vivo* (29, 30).

Because Aurora B plays a crucial role for chromosome dynamics and aneuploidy is a common feature of thyroid carcinomas, we analyzed Aurora B expression in human thyroid carcinoma cell lines, originating from different histotypes and archive thyroid carcinoma tissue. All of the thyroid carcinoma cell lines showed increased Aurora B levels. Immunohistochemical studies performed on archive samples showed a clear expression of Aurora B in thyroid carcinomas, with a strong signal in anaplastic thyroid carcinomas, whereas Aurora B was not detectable in normal thyroid tissue. The block of Aurora B synthesis by RNA interference (RNAi) induced growth inhibition in human thyroid anaplastic carcinoma cells. The same effect was achieved treating anaplastic thyroid carcinoma cells with an inhibitor of the Aurora kinases.

Materials and Methods

Cell lines, plasmids, and transfections

The human anaplastic thyroid carcinoma cell lines used in the study are ARO, FRO, 8550-C, BHT 101, KAT-18, Cal 62, and KAT-4.

ARO and FRO human thyroid anaplastic carcinoma cell lines were obtained by Dr. G. F. Juillard (University of California, Los Angeles). ARO and FRO cell lines were kindly provided by Prof. J. A. Fagin (University of Cincinnati College of Medicine, Cincinnati, OH).

KAT-4 and KAT-18 cell lines were established and obtained from Dr. K. B. Ain (University of Kentucky, Lexington, KY). 8505-C anaplastic thyroid cell line was established by Dr. M. Akiyama (Radiation Effects Research Foundation, Hiroshima, Japan), BHT 101 anaplastic thyroid carcinoma cell line was established by Dr. I. Palyi (National Institute of Oncology, Budapest, Hungary), and Cal 62 anaplastic thyroid carcinoma cell line was established by Dr. J. Gioanni (Centre A. Lacassagne, Nice, France). 8505-C, BHT 101, and Cal 62 cell lines were obtained from Deutsche Sammlung von Mikroorganismen und Zellkulturen GmbH, German Collection of Microorganisms and Cell Cultures (Braunschweig, Germany).

The NPA line derived from poorly differentiated papillary carcinoma and was obtained by Dr. Juillard, the TPC 1 cell line derived from a papillary thyroid carcinoma (31), and the WRO and FB1 cell lines derived from a follicular carcinoma (32, 33).

Cells were grown in DMEM medium supplemented with 10% fetal calf serum and ampicillin/streptomycin.

Cell proliferation was evaluated by using a colorimetric assay for determining the number of viable cells, Cell Titer 96 Aqueous cell proliferation assay (Promega, Madison, WI) according to the manufacturer's suggestions.

The pCMV-AIM1 construct, containing the human Aurora B gene cDNA (accession no. NM 004217), was obtained as follows: mRNA from human testis (Clontech, Palo Alto, CA) was reverse transcribed using random hexamers as primers and Muloney leukemia virus reverse transcriptase (Applied Biosystems, Foster City, CA) to yield cDNA. The forward (5′-CTCTGGATCCATGGCCCAGAAGGAGAAC-3′) and reverse (5′-ACAGGGATCCTCAGGCGACAGATTGAAG-3′) primers were used to amplify the cDNA. The PCR product was cloned into the *Bam*H1 site of the pcDNA His-tagged (Invitrogen Life Technologies, Carlsbad, CA).

The pCMV AIM-1 sense and antisense constructs were obtained by inserting the Aurora B cDNA in both sense and antisense orientation in the pCMV vector under the transcriptional control of the cytomegalovirus promoter. The vector also carries the gene for G418 resistance. The transfection was performed according to the calcium phosphate transfection protocol (32). After 36 h the cells were trypsinized and expanded, and stable transfectants were generated after selection with 400 μg/ml geneticin (G418) (Life Technologies, Italy). Six independent clones were isolated from pCMV AIM-1 sense, pCMV AIM-1 antisense, and control transfections. The clones carrying sense or antisense plasmid were then selected for further experiments.

The quinazoline derivative: *N*-[4-(6,7-dimethoxy-quinazolin-4-ylamino)-phenyl]-benzamide (34) was dissolved in dimethylsulfoxide at a concentration of 10 mM. Then 1×10^3 ARO cells were plated in a 96-well plate, and after 24 h the cells were treated with 5, 10, or 15 μM of the inhibitor. Cell proliferation was evaluated after 24 and 48 h by using the Cell Titer 96 aqueous cell proliferation assay (Promega). Soft agar colony assays were performed according to a previously described technique (35).

Synthesis of Aurora kinase inhibitor

For the synthesis of Aurora kinase inhibitor, the methodology described elsewhere (34) was followed.

RNAi and transfection of RNA oligonucleotides

For design of small interfering RNA (siRNA) oligos targeting Aurora B, the sequence AAG GAGAACUCCUACCCCUGG (RNAi) was selected, corresponding to the nucleotides located 67–87 bp of the human Aurora B gene. As a control of siRNA oligo, the following aspecific sequence was used AAG GUC CCC AUC CUC AAG AGG (RNAc). The siRNAs were purchased from Dharmacon Research (Lafayette, CO).

Approximately 6×10^5 cells were plated per 6-well plate in media containing 10% fetal bovine serum to give 30–50% confluence. Transfection of the RNA oligonucleotides was performed after 24 h to result in a final RNA concentration of 200 nM. Transfections were performed using Oligofectamine (Invitrogen, Carlsbad, CA).

Human thyroid tissue samples, semiquantitative RT-PCR, real-time PCR, and immunohistochemistry

Normal and neoplastic human thyroid tissue was obtained from surgical specimens and immediately frozen in liquid nitrogen. Thyroid tumors were collected at the Laboratoire d'Histologie et de Cytologie, Centre Hospitalier Lyon Sud, France, and the Laboratoire d'Anatomie Pathologique, Hospital de L'Antiquaille Lyon, France. Total RNA was isolated and DNase digested using the RNeasy minikit (Qiagen, Valencia, CA) according to the manufacturer's recommendations. Three micrograms of total RNA from each sample were reverse transcribed using random hexamers as primers and Moloney leukemia virus reverse transcriptase (Applied Biosystems) to yield cDNA. Semiquantitative RT-PCR was carried out on cDNA using the GeneAmp PCR System 9600 (Applied Biosystems). A RNA PCR core kit (Applied Biosystems) was used to perform PCR. The human β-actin gene primers, amplifying a 109-bp cDNA fragment, were used as a control with the following program: 95 C for 10 min; 25 cycles at 95 C for 30 sec, 60 C for 30 sec, and 72 C for 30 sec; and 72 C for 5 min for a final extension.

To amplify the Aurora B mRNA, RT-PCR was performed using two primers that amplified a 128-bp nucleotide cDNA fragment encompassing exons 5 and 6 with the following program: 95 C for 10 min; 29 cycles of 95 C for 30 sec, 59.5 C for 30 sec, and 72 C for 30 sec; and a final extension of 72 C for 5 min.

Quantitative PCR was performed in triplicate using iCycler (Bio-Rad Laboratories, München, Germany) with SYBR Green PCR master mix (Applied Biosystems) as follows: 95 C 10 min and 40 cycles (95 C 15 sec and 60 C 1 min). Fold mRNA overexpression was calculated according to the formula $2^{(Rt-Et)}/2^{(Rn-En)}$ as described previously (36), where Rt is the threshold cycle number for the reference gene (β-actin) in the tumor, Et for the experimental gene in the tumor, Rn for the reference

gene in the normal sample, and En for the experimental gene in the normal sample. Specific primers used are as follows. Aurora B forward, 5′-CTGGAATATGCACCACTTGGA, reverse, 5′CGAATGACAGTAAGACAGGG; and β-actin-forward, 5′-TCGTGCGTGACATTAAGGAG; β-actin-reverse, 5′-GTCAGGCAGCTCGTAGCTCT.

The cellular distribution of Aurora B protein was assessed by immunohistochemical analysis. Aurora B expression was evaluated in both nonneoplastic and neoplastic thyroid tissues. Hematoxylin and eosin-stained slides were retrieved from the files of the Department of Bio-Morphological Sciences at the University Federico II of Naples; in all cases the histological diagnosis was confirmed on review. Paraffin-embedded sections were obtained from these samples, and Aurora B expression was evaluated. Xylene-dewaxed and alcohol-rehydrated paraffin sections were placed in Coplin jars filled with a 0.01 M trisodium citrate solution and heated for 3 min in a conventional pressure cooker. After heating, slides were thoroughly rinsed in cool running water for 5 min and then washed in Tris-buffered saline (pH 7.4).

Aurora B protein was detected by using the polyclonal antibody raised in rabbit (no. 611082; BD Transduction Laboratories, San Diego, CA). The incubation with the primary antibody was followed by incubation with biotinylated antimouse immunoglobulins and by peroxidase-labeled streptavidin (LSAB-Dako, Carpinteria, CA). The signal was developed by using diaminobenzidine chromogen as substrate. Negative controls were run with normal rabbit serum instead of the primary antibody, or the antibody was preadsorbed with the cognate peptide (10^{-6} M). Cases were scored by assessing the percentage of labeled cells, and percentage of positive cells was evaluated by analyzing 1000 neoplastic cells in five different high power fields. The study was approved by the Ethics Committee of the Centre Hospitalier Lyon Sud and the University Federico II Napoli. In all cases written informed consent was obtained.

Protein extraction and Western blot analysis

Cells were homogenized directly into lysis buffer (50 mM HEPES, 150 mM NaCl, 1 mM EDTA, 1 mM EGTA, 10% glycerol, 1%Triton X-100, 1 mM phenylmethylsulfonyl fluoride, 1 μg/ml aprotinin, 0.5 mM sodium orthovanadate, and 20 mM sodium pyrophosphate). The lysates were clarified by centrifugation at 14,000 × 10 min. Protein concentrations were estimated by an assay (Bio-Rad) and boiled in Laemmli buffer [0.125 M Tris-HCl (pH 6.8), 4% SDS, 20% glycerol, 10% 2-mercaptoethanol, and 0.002% bromophenol blue] for 5 min before electrophoresis. Proteins were subjected to SDS-PAGE (10% polyacrylamide) under reducing conditions. After electrophoresis, proteins were transferred to nitrocellulose membranes (Immobilon, Millipore Corp., Bedford, MA); complete transfer was assessed using prestained protein standards (Bio-Rad, Hercules, CA). After blocking with Tris-buffered saline-BSA [25 mM Tris (pH7.4), 200 mM NaCl, and 5% BSA], the membrane was incubated with the primary antibody against Aurora B for 1 h (at room temperature). Membranes were then incubated with the horseradish peroxidase-conjugated secondary antibody (1:10,000) for 45 min (at room temperature), and the reaction was detected with an enhanced chemiluminescence system (Amersham Life Science, Buckinghamshire, UK).

Tumorigenicity assay

Experiments were performed in 6-wk-old male athymic mice (Charles River, Italy). Untransfected ARO cells (1×10^6) or respectively transfected with a plasmid-containing Aurora B in the sense or antisense orientation were injected into the right flank of the mice. The animals were monitored for the appearance of tumors and tumor latency evaluated. The mean tumor latency is the time needed for tumors to reach 10 mm in diameter. All mice were maintained at the Dipartimento di Biologia e Patologia Animal Facility. Animal experimentations described in the present paper have been conducted in accordance with accepted standards of animal care, in accordance with the Italian regulations for the welfare of animals used in studies of experimental neoplasia, and the study was approved by Ethics Committee on Animal Care of the University Federico II Napoli.

Results

Aurora B expression in thyroid carcinoma cell lines

Thyroid carcinoma cell lines derived from papillary carcinomas, follicular carcinomas, and anaplastic thyroid carcinomas were analyzed for Aurora B expression by Western blot. An Aurora B-specific band of 41 kDa was detected in all the samples. As shown in Fig. 1, A and B, the highest expression levels were observed in the cell lines derived from anaplastic thyroid carcinoma (ARO, FRO, 8505-C, BHT101, KAT-18, Cal 62, and KAT-4), whereas only a faint band of 41 kDa was observed in human thyroid primary culture cells.

Therefore, these data would indicate that the expression of

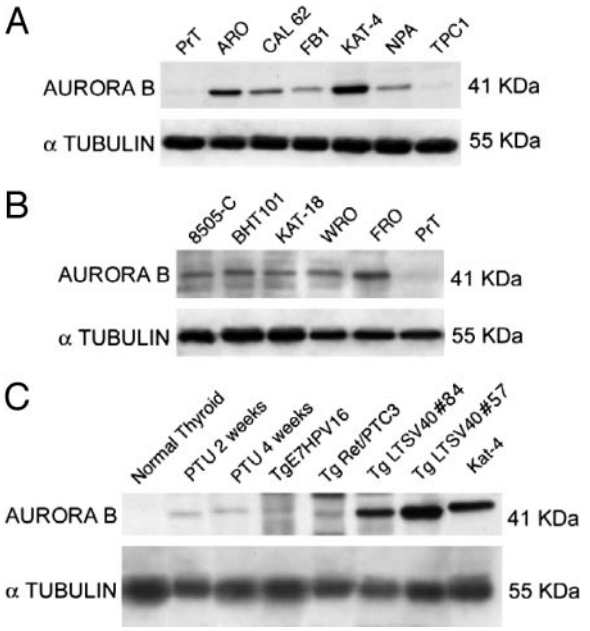

FIG. 1. Aurora B expression in thyroid carcinoma cell lines and experimental thyroid carcinomas. A, Western blot analysis of Aurora B expression in human thyroid cells: ARO, Cal 62, FB1, KAT-4, NPA, and TPC1. Expression levels were increased in the anaplastic thyroid carcinoma cell lines ARO, Cal 62, and KAT-4. In the papillary thyroid carcinoma-derived cell lines NPA and TPC 1 and the follicular thyroid carcinoma-derived cell line FB1, a clear band was observed. In the primary culture of human thyroid (PrT), a faint band was observed. B, Western blot analysis of Aurora B expression in human thyroid cells: 8505-C BHT101, KAT-18, WRO, and FRO. Expression levels were increased in the anaplastic thyroid carcinoma cell lines 8505-C, BHT101, KAT-18, and FRO. In follicular thyroid carcinoma-derived cell line WRO, Aurora B expression was clearly detectable. The primary culture of human thyroid (PrT) was used as a control. C, Western blot analysis of Aurora B expression in thyroid carcinoma excised from different experimental model of thyroid carcinogenesis. Normal thyroid: Normal thyroid gland excised from a 6-month-old wild-type mouse; PTU 2 weeks: thyroid gland excised from a mouse treated for 2 wk with the goitrogenic agent PTU; PTU 4 weeks: thyroid gland excised from a mouse treated for 4 wk with the goitrogenic agent PTU; Tg E7 HPV16: follicular carcinoma of the thyroid obtained from a transgenic mouse expressing in the gland HPV16 oncogene; Tg Ret/PTC3: papillary carcinoma of the thyroid obtained from a transgenic mouse expressing in the gland RET/PTC3 oncogene; Tg LTSV40: anaplastic thyroid carcinoma obtained from a transgenic mouse expressing in the gland SV 40 LT oncogene (animal 84); Tg LTSV40: anaplastic thyroid carcinoma obtained from a transgenic mouse expressing in the gland SV 40 LT oncogene (animal 57); KAT-4: positive control cells.

Aurora B is more abundant in cell lines characterized by a malignant and aggressive phenotype.

Aurora B expression in experimental models of thyroid carcinogenesis

To confirm that Aurora B gene expression is increased in highly malignant thyroid carcinomas, Aurora B expression in thyroid glands obtained from animal models of thyroid carcinogenesis was evaluated by Western blot. We used transgenic animals lines expressing RET/PTC3, HPV 16 E7, and LT SV40 oncogenes under the transcriptional control of the thyroglobulin promoter.

RET/PTC3 is an oncogene frequently activated in human thyroid papillary carcinomas, and it has been shown to induce thyroid papillary carcinomas when expressed in the thyroid cells of transgenic animals (37). Transgenic mice carrying HPV 16 E7 oncogene under the transcriptional control of the thyroglobulin gene promoter develop follicular carcinomas of the thyroid (38), whereas thyroid anaplastic carcinomas are obtained in animals with thyroid-targeted expression of LT SV40 oncogene (39). Thyroid glands of animals treated with the goitrogenic agent propylthiouracil (PTU) for 2 wk and 1 month (40) were used as a control for nonneoplastic proliferation. Furthermore, the thyroid gland of a 6-month-old wild-type mouse was used as a control (Fig. 1C). The results shown are representative of three different experiments.

Elevated levels of Aurora B protein expression were observed in the experimental thyroid anaplastic carcinomas. A weaker signal was observed in the papillary and follicular carcinomas. Conversely, very low levels of Aurora B were observed in normal thyroid tissue as in thyroid glands stimulated by PTU.

Aurora B expression in the normal human thyroid and thyroid neoplastic lesions

To evaluate the expression of Aurora B in human thyroid carcinoma tissues, a panel of matched tumor/normal tissues was analyzed by RT-PCR. No significant differences in Aurora B gene expression were observed in papillary carcinomas matched with normal thyroid tissue (Fig. 2A), whereas an increased Aurora B expression was observed in anaplastic thyroid carcinomas with respect to the normal thyroid tissue (Fig. 2B).

Quantitative PCR was performed to confirm overexpression of Aurora B in anaplastic thyroid carcinomas. About 15-fold mRNA overexpression was observed in ATC samples with respect to the β-actin reference gene. A 2-fold increase was observed in papillary thyroid carcinoma samples (Fig. 2C).

Archive thyroid tumors comprising adenoma (five cases), follicular (five cases), papillary (10 cases), and anaplastic thyroid carcinomas (15 cases) were stained for Aurora B. As a control three cases of nodular goitre and three cases of Hashimoto's thyroiditis were analyzed. In normal thyroid tissue, few positive cells for Aurora B staining were observed. Conversely, all of thyroid anaplastic carcinoma examined showed a very high expression of Aurora B (Fig. 3, C and D). Positive cells were irregularly distributed throughout the tumor. Occasionally, a heterogeneous pattern of expression was seen, with areas showing strong labeling adjacent to areas with less intense Aurora B expression. The signal was most intense in dividing cells, with mitotic figures depicted by the antibody.

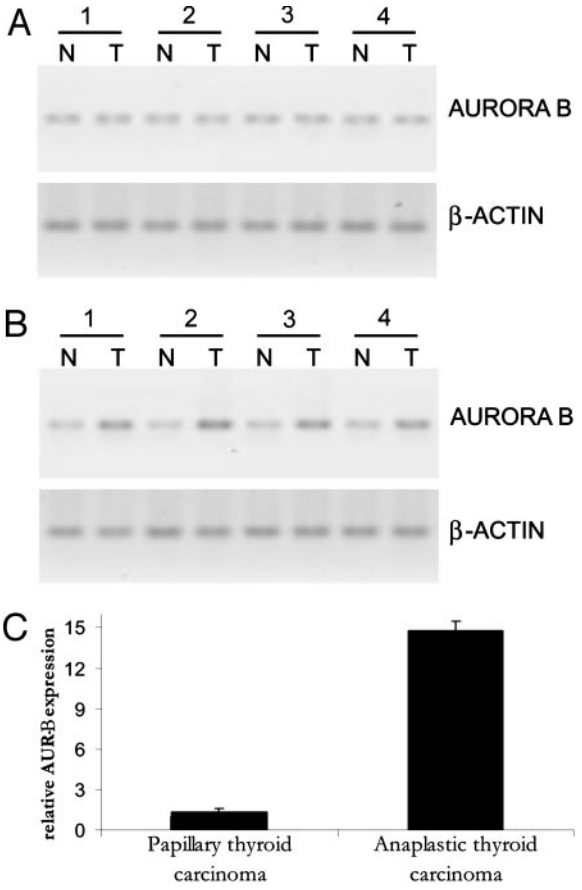

FIG. 2. Aurora B expression in matched tumor (T)/normal (N) tissues. A, RT-PCR analysis of Aurora B expression in papillary thyroid carcinomas samples 1–4. Papillary thyroid carcinomas matched with normal thyroid tissues. B, RT-PCR analysis of Aurora B expression in anaplastic thyroid carcinomas samples 1–4. Anaplastic thyroid carcinomas matched with normal thyroid tissues. Levels of Aurora B were increased in the anaplastic thyroid carcinomas. C, Real-time PCR analysis of Aurora B (AUR-B) expression in papillary thyroid and anaplastic thyroid carcinomas. A 15-fold increase of Aurora B expression was observed in anaplastic thyroid carcinomas.

In follicular or papillary differentiated carcinomas, a less intense signal was observed. Also in differentiated carcinomas, signal was most intense in dividing cells, and the cytoplasm of positive cells was devoid of signal (Fig. 3B). The expression of Aurora B in anaplastic thyroid carcinomas or differentiated carcinomas was compared with the expression of a well-known proliferative marker such as Ki-67, by using MIB-1 antibody (Table 1). Staining for Ki-67 was most intense in thyroid anaplastic carcinomas, showing a correlation with Aurora B expression.

Effects of the suppression of the Aurora B protein synthesis in anaplastic thyroid carcinoma cells

To establish whether Aurora B expression is crucial for thyroid neoplastic cell growth and assess whether Aurora B

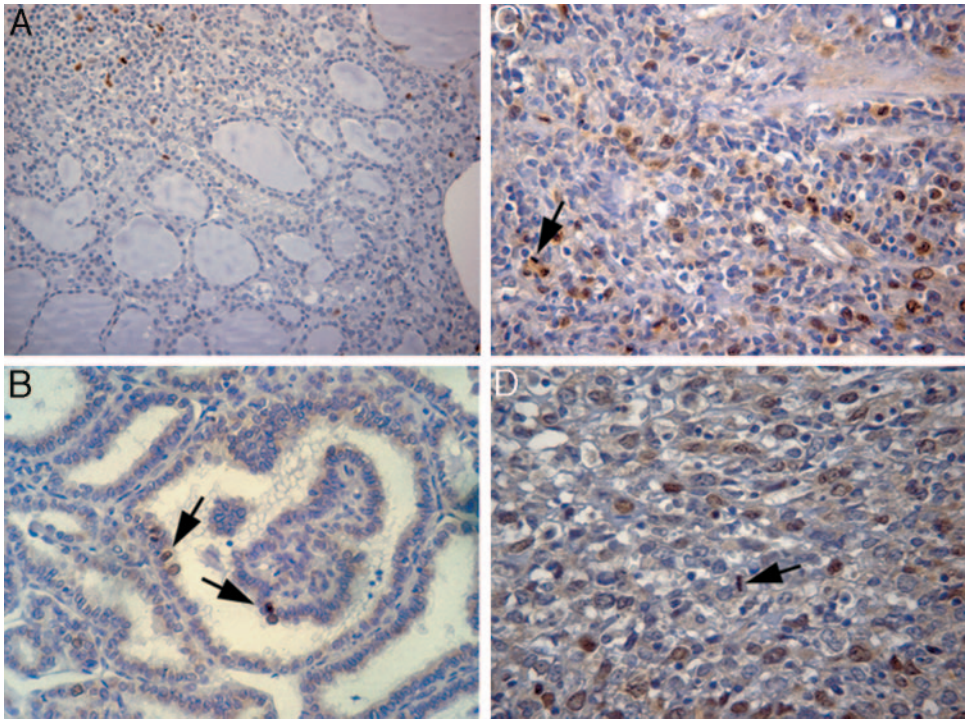

FIG. 3. Aurora B expression in human thyroid carcinomas. Localization of the Aurora B protein in human thyroid carcinomas by immunocytochemistry. A, Localization of the Aurora B protein in a paraffin-embedded section of a thyroid goitre. Expression of Aurora B protein was not observed. B, Section of thyroid papillary carcinoma (case 8), showing rare immunoreactivity for Aurora B protein. C, Section of anaplastic thyroid carcinoma (case 12), showing extensive immunoreactivity for Aurora B protein. D, Higher magnification of C, showing presence of a clear signal in neoplastic cells.

could represent a target for antineoplastic therapy, we performed an RNAi selective gene silencing analysis using siRNAs (41–43). We observed that Aurora B RNAi significantly decreased the synthesis of Aurora B protein in ARO cells at 48 h (Fig. 4A). The block of Aurora B protein synthesis is specific because Aurora A levels were not affected (Fig. 4A). Aurora B has been described to phosphorylate histone H3 at Ser-10 during mitosis *in vivo*. To confirm the effects of RNAi, cell lysates, respectively, obtained from RNAi treated, untreated control ARO cells, and aspecific RNA treated ARO cells were immunoblotted with anti-phospho-Ser-10 H3 histone antibody and anti-H3 histone antibody. As shown in Fig. 4A, a reduced phosphorylation of the H3 histone was observed in the RNAi-transfected cells at 48 h. RNAi treatment significantly reduced cell proliferation (Fig. 4B).

Transfection of ARO cells with an antisense construct (pCMV AIM-1 antisense) of the Aurora B DNA was also performed. Control transfections were performed using an Aurora B sense construct (pCMV AIM-1 sense) or an empty vector (pCMV). Clones were isolated from each transfection and the integration of the constructs was confirmed by Southern blot (data not shown). The reduced expression of Aurora B protein was confirmed in pCMV AIM-1 antisense clones by Western blot analysis (data not shown). The colony growth rate in semisolid medium was reduced in Aurora B antisense-expressing clones with respect to sense transfected or control cells. Although no differences in tumor incidence were observed on injection into athymic mice, tumor latency period of Aurora B antisense-expressing clones was increased (Table 2 and Fig. 5).

A small molecule similar to the quinazoline derivative: *N*-[4-(6,7-dimethoxy-quinazolin-4-ylamino)-phenyl]-benzamide has been shown to inhibit the Aurora B kinase activity (33, 44). To further evaluate the role of the Aurora B kinase activity on thyroid carcinoma cell proliferation, 5×10^5 ARO and 5×10^5 FRO cells were treated with 15 μM of the Aurora kinase inhibitor; after 24 and 48 h, cells were collected and lysed. Lysates were immunoblotted with anti-phospho-Ser-10 H3 histone antibody and antitubulin antibody. As shown in Fig. 6A, a dramatic reduction in phosphorylation of the H3 histone was observed in the treated cells. To evaluate the effects of Aurora kinase inhibitor on cell proliferation, ARO and FRO cells were treated with 5, 10, and 15 μM, and cell proliferation was evaluated after 24 and 48 h. Ten and 15 μM of Aurora kinase inhibitor significantly reduced cell proliferation (Fig. 6B).

TABLE 1. Analysis of Aurora B and Ki-67 expression in thyroid specimens

Histological type of thyroid specimen	No. of cases	Average immunostaining	
		Aurora B	Ki-67
Normal thyroid	1	0.5 ± 0.2	0.9 ± 0.3
Nodular goitre	3	1.2 ± 0.4	1.8 ± 0.6
Hashimoto's disease	3	0.8 ± 0.3	1.1 ± 0.6
Papillary carcinoma	10	2.3 ± 0.4	3.1 ± 0.5
Follicular carcinoma	10	2.8 ± 0.4	3.6 ± 0.6
Anaplastic carcinoma	15	29.6 ± 3.4	43.2 ± 6.6

Values are reported as percentage of immunopositive cells ± SD.

Discussion

Alterations of the mechanisms responsible for maintaining the chromosome balance are common in neoplastic cells (15, 16). Disruption of mitotic checkpoints induces unstable chromosome number or aneuploidy, which is thought to create abnormal nuclear morphology in cancer cells and contribute to genetic instability. It has been described that alterations in chromosome number are common in neoplasias from thyroid follicular cells; however, the mutational analysis of two

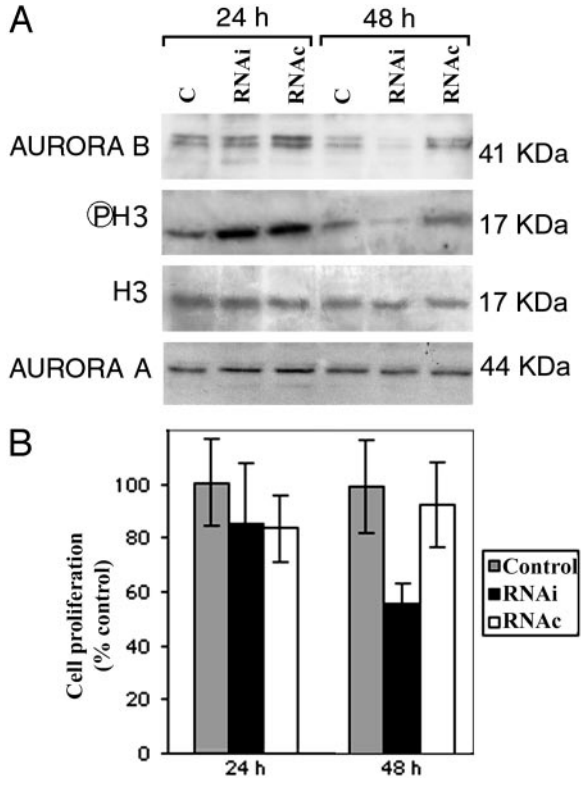

FIG. 4. RNAi directed against Aurora B specifically inhibits its expression and blocks the proliferation of anaplastic thyroid carcinoma cells. A, Inhibition of Aurora B expression by RNAi. ARO cells were transfected with 200 nM annealed sense (RNAi) and aspecific control RNA (RNAc) 21-mer RNA oligonucleotides directed against Aurora B or mock transfected (C). Cells were harvested at 24 and 48 h after transfection, and Western blot analysis was performed. A significant reduction of Aurora B expression and H3 phosphorylation (ⓅH3) was observed at 48 h. Aurora A and H3 levels were not affected by the treatment. B, Time-dependent inhibition of ARO cell proliferation by Aurora B RNAi. ARO cells were transfected with 200 nM annealed sense (RNAi) and control (RNAc) 21-mer RNA oligonucleotides directed against Aurora B or mock-transfected (control). The data are expressed as percentages of the control cell proliferation, and the SD was calculated (*bar*). The data are the mean of three different experiments.

components of the spindle assembly checkpoint pathway, BUB1 and BURBR1, has shown that these two proteins do not account for the development of aneuploidy in thyroid cancer (17).

The Aurora protein kinases play a crucial role in the regulation of the cell cycle processes. Three Aurora-related kinases have been described in mammals, Aurora A (STK15), Aurora B (AIM 1), and Aurora C (STK13) (19–21). All three mammalian members of this family are overexpressed in human cancer cells. Overexpression of Aurora A is thought to relate to multiple centrosome production, and its role has been evaluated in human mammary (45), pancreatic (46), and other neoplastic lesions (47, 48).

A significant overexpression of Aurora B has been observed in human cancer cell lines and colorectal tumors, and a correlation between Aurora B expression levels and Duke's grade in colorectal tumors has been described (30, 49). Furthermore, it has been observed that the forced expression of Aurora B produced aneuploid cells with a malignant and

TABLE 2. Analysis of transformation markers of the ARO cells transfected with the Aurora B cDNA in the sense or antisense orientation

Transfected DNA	Colony-forming efficiency (%)[a]	Tumor incidence[b]	Latency period (d)[c]
pCMV vector	56	3/3	12
pCMV Aurora B antisense clone 4	27	4/4	31
pCMV Aurora B antisense clone 6	31	5/5	36
pCMV Aurora B antisense clone 9	23	3/3	29
pCMV Aurora B sense clone 1	59	4/4	12
pCMV Aurora B sense clone 5	62	5/5	11

[a] Colonies larger than 64 cells were scored after 3 wk. Colony-forming efficiency was calculated with the formula: number of colonies formed/number of plated cells × 100.

[b] Tumorigenicity was assayed by injecting 1×10^6 cells into athymic mice (6 wk old).

[c] The animals were monitored for the appearance of tumors. The mean tumor latency is the time needed for tumors to reach 10 mm in diameter. In pCMV Aurora B antisense transfected cells, the median tumor latency differed significantly from that of control.

aggressive phenotype, indicating that Aurora B is relevant in aneuploidy development during carcinogenesis (29). Recently it has been shown that high expression levels of Aurora B are a consistent feature of human seminomas (50).

In the present study, we evaluated the expression of Aurora B in thyroid carcinoma cell lines and experimental and human thyroid tumors, and we observed that the expression of Aurora B is increased in cell lines derived from thyroid anaplastic carcinomas. An increase of Aurora B expression was observed in experimental anaplastic thyroid tumors, whereas in differentiated experimental thyroid tumors, a lower expression of the Aurora B gene was observed. It is important to note that a very low expression of Aurora B was observed in the glands of animals treated with PTU, despite the intense mitotic activity of the follicular cells (40). These data indicate that Aurora B-increased expression is associated with the late stages of thyroid tumor progression and suggest that the Aurora B overexpression could contribute to thyroid tumor progression.

The immunohistochemical analysis of neoplastic or nonneoplastic thyroid lesions paralleled the results obtained using cell lines and experimental tumors, showing that the expression is abundant in anaplastic carcinomas. Conversely, no or low expression was observed in benign adenomas, nonneoplastic thyroid lesions such as Hashimoto disease, and normal thyroid tissue. Our data on thyroid carcinomas extend to this type of tumor the observation that the expression of Aurora B displays a tendency to group in higher grade of malignancy as previously observed in colon carcinomas (49). This observation suggests that during tumor progression, in particular during the transition from differentiated thyroid carcinomas to anaplastic thyroid carcinomas, Aurora B overexpression takes place, and Aurora B overexpression might confer a growth advantage to the neoplastic cells. Furthermore, our data indicate that Aurora B expression may serve as a prognostic marker in thyroid tumors.

FIG. 5. Growth of tumor xenografts in nude mice injected with ARO control cells or Aurora B sense- or antisense-transfected ARO cells. Nontransfected ARO cells (control) or transfected with a plasmid containing Aurora B (Aur B) in the sense or antisense orientation were injected into the right flank of the mice. The animals were monitored for the appearance of tumors, and tumor latency was evaluated. No differences in tumor incidence were observed. Tumor latency period of Aurora B antisense-expressing clones was increased.

In our study, the functional consequences of RNAi-mediated decrease of Aurora B expression in anaplastic thyroid cancer cells were determined using assays of gene expression and cellular proliferation. Our results demonstrate that the Aurora B siRNA treatment induces a significant reduction in cell proliferation. No cells with apoptotic figures were observed, and the analysis of the apoptotic cascade indicated that the pathway was not activated by the Aurora B RNAi treatment (data not shown). It is possible to conclude that the block of Aurora B protein synthesis does not induce apoptosis in ARO cell line; moreover, an accumulation of Aurora B RNAi-treated cells in G_2/M phase was observed by flow cytometry (data not shown). The inhibition ARO cells proliferation was about 40% on RNAi treatment; these data indicate that cell proliferation is not completely dependent on Aurora B activity.

Aurora B cDNA antisense transfection decreased colony formation in soft agar and resulted in increased tumor latency. By using a selective Aurora B kinase inhibitor, we confirmed that the block of Aurora B activity dramatically reduces the proliferation of anaplastic thyroid carcinoma cells.

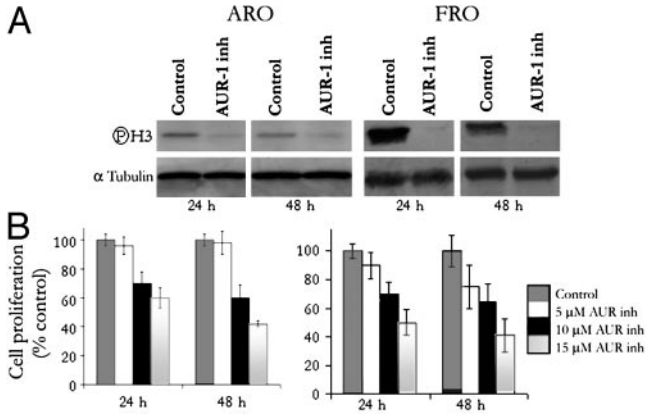

FIG. 6. Reduction in phosphorylation of the H3 histone and reduction in ARO and FRO cell proliferation by Aurora B kinase inhibitor. A, ARO and FRO cells (5×10^5) were treated with 15 μM of Aurora kinase inhibitor; after 24 and 48 h, cells were lysed. Western blot analysis with anti-Ser-10 phosphorylated H3 histone antibody showed a dramatic reduction in the phosphorylation of the H3 histone (ⓅH3); as a control, untreated ARO and FRO cells were used. B, ARO and FRO cells were treated with 5, 10, or 15 μM of the Aurora kinase inhibitor (AUR inh); as a control, untreated ARO and FRO cells were used. After 24 and 48 h, cell proliferation was evaluated. A significant reduction in cell proliferation was observed. The data are expressed as percentages of the control cell proliferation, and the SD was calculated (*bar*). The data are the mean of three different experiments.

Anaplastic thyroid carcinoma is resistant to currently available therapeutic agents. The observation that the block of Aurora B expression or activity reduces the proliferation of anaplastic thyroid carcinoma cells could contribute to the development of novel therapeutic strategies.

In conclusion, our data indicate that in thyroid carcinomas Aurora B gene expression levels are correlated to the stage of malignant progression, and the block of Aurora B expression or its kinase activity significantly reduces the growth of thyroid anaplastic carcinoma cells, suggesting that Aurora B is a potential therapeutic target.

Acknowledgments

We thank Professor G. Vecchio and Dr. P. Formisano for their suggestions and a critical review of the manuscript. We are indebted to S. Sequino for his excellent technical assistance.

Received July 31, 2004. Accepted November 11, 2004.

Address all correspondence and requests for reprints to: Giuseppe Portella, Dipartimento di Biologia e Patologia Cellulare e Molecolare, Facoltà di Medicina e Chirurgia di Napoli, Università Federico II, via S. Pansini 5, 80131 Napoli, Italy. E-mail: portella@unina.it.

This work was supported by the Italian Ministry of Instruction, University and Research, PRIN 2002, and the Associazione Italiana per la Ricerca sul Cancro.

References

1. **Hedinger C, Williams ED, Sobin LH** 1989 The WHO histological classification of thyroid tumours: a commentary on the second edition. Cancer 63:908–911
2. **Wynford-Thomas D** 1997 Origin and progression of thyroid epithelial tumours. Cellular and molecular mechanisms. Horm Res 47:145–157
3. **Grieco M, Santoro M, Berlingieri MT, Melillo RM, Donghi R, Bongarzone I, Pierotti MA, Della Porta G, Fusco A, Vecchio G** 1990 PTC is a novel rearranged form of the ret proto-oncogene and is frequently detected *in vivo* in human thyroid papillary carcinomas. Cell 60:557–563
4. **Tallini G, Asa SL** 2001 RET oncogene activation in papillary thyroid carcinoma. Adv Anat Pathol 6:345–354
5. **Cohen Y, Xing M, Mambo E, Guo Z, Wu G, Trink B, Beller U, Westra WH,**

Ladenson PW, Sidransky D 2003 BRAF mutation in papillary thyroid carcinoma. J Natl Cancer Inst 95:625–627
6. **Kimura ET, Nikiforova MN, Zhu Z, Knauf JA, Nikiforov YE, Fagin JA** 2003 High prevalence of BRAF mutations in thyroid cancer: genetic evidence for constitutive activation of the RET/PTC-RAS-BRAF signaling pathway in papillary thyroid carcinoma. Cancer Res 63:1454–1457
7. **Xu X, Quiros RM, Gattuso P, Ain KB, Prinz RA** 2003 High prevalence of BRAF gene mutation in papillary thyroid carcinomas and thyroid tumor cell lines. Cancer Res 63:4561–4567
8. **Fukushima T, Suzuki S, Mashiko M, Ohtake T, Endo Y, Takebayashi Y, Sekikawa K, Hagiwara K, Takenoshita S** 2003 BRAF mutations in papillary carcinomas of the thyroid. Oncogene 22:6455–6457
9. **Nikiforova MN, Kimura ET, Gandhi M, Biddinger PW, Knauf JA, Basolo F, Zhu Z, Giannini R, Salvatore G, Fusco A, Santoro M, Fagin JA, Nikiforov YE** 2003 BRAF mutations in thyroid tumors are restricted to papillary carcinomas and anaplastic or poorly differentiated carcinomas arising from papillary carcinomas. J Clin Endocrinol Metab 88:5399–5404
10. **Suarez HG, du Villard JA, Severino M, Caillou B, Schlumberger M, Tubiana M, Parmentier C, Monier R** 1990 Presence of mutations in all three ras genes in human thyroid tumors. Oncogene 5:565–570
11. **Kroll TG, Sarraf P, Pecciarini L, Chen CJ, Mueller E, Spiegelman BM, Fletcher JA** 2000 PAX8-PPAR-1 fusion in oncogene human thyroid carcinoma. Science 289:1357–1360
12. **Ito T, Seyama T, Mizuno T, Tsuyama N, Hayashi Y, Dohi K, Nakamura N, Akiyama M** 1992 Unique association of p53 mutations with undifferentiated but not differentiated carcinomas of the thyroid gland. Cancer Res 52:1369–1371
13. **Fagin JA, Matsuo K, Karmakar A, Chen DL, Tang SH, Koeffler HP** 1993 High prevalence of mutations of p53 gene in poorly differentiated human thyroid carcinomas. J Clin Invest 91:179–184
14. **Dobashi Y, Sakamoto A, Sugimura H, Mernyei M, Mori M, Oyama T, Machinami R** 1993 Overexpression of p53 as a possible prognostic factor in human thyroid carcinoma. Am J Surg Pathol 17:375–381
15. **Sieber OM, Heinimann K, Tomlinson IP** 2003 Genomic instability-the engine of tumorigenesis? Nat Rev Cancer 3:701–708
16. **Jallepalli P, Lengauer C** 2001 Chromosome segregation and cancer: cutting through the mystery. Nat Rev Cancer 1:109–117
17. **Ouyang B, Knauf JA, Ain K, Nacev B, Fagin JA** 2002 Mechanisms of aneuploidy in thyroid cancer cell lines and tissues: evidence for mitotic checkpoint dysfunction without mutations in BUB1 and BUBR1. Clin Endocrinol (Oxf) 56:341–350
18. **Stoler DL, Datta RV, Charles MA, Block AW, Brenner BM, Sieczka EM, Hicks Jr WL, Loree TR, Anderson GR** 2002 Genomic instability measurement in the diagnosis of thyroid neoplasms. Head Neck 24:290–295
19. **Nigg EA** 2001 Mitotic kinases as regulators of cell division and its checkpoints. Nat Rev Mol Cell Biol 21:21–32
20. **Andrews PD, Knatko E, Moore WJ, Swedlow JR** 2003 Mitotic mechanics: the auroras come into view. Curr Opin Cell Biol 15:672–683
21. **Adams RR, Carmena M, Earnshaw WC** 2001 Chromosomal passengers and the (aurora) ABCs of mitosis. Trends Cell Biol 11:49–54
22. **Dutertre S, Descamps S, Prigent C** 2002 On the role of aurora-A in centrosome function. Oncogene 21:6175–6183
23. **Bischoff JR, Anderson L, Zhu Y, Mossie K, Ng L, Souza B, Schryver B, Flanagan P, Clairvoyant F, Ginther C, Chan CS, Novotny M, Slamon DJ, Plowman GD** 1998 A homologue of *Drosophila* aurora kinase is oncogenic and amplified in human colorectal cancers. EMBO J 17:3052–3065
24. **Zhou H, Kuang J, Zhong L, Kuo WL, Gray JW, Sahin A, Brinkley BR, Sen S** 1998 Tumour amplified kinase STK15/BTAK induces centrosome amplification, aneuploidy and transformation. Nat Genet 20:189–193
25. **Ewart-Toland A, Briassouli P, de Koning JP, Mao JH, Yuan J, Chan F, MacCarthy-Morrogh L, Ponder BA, Nagase H, Burn J, Ball S, Almeida M, Linardopoulos S, Balmain A** 2003 Identification of Stk6/STK15 as a candidate low-penetrance tumor-susceptibility gene in mouse and human. Nat Genet 34:403–412
26. **Adams RR, Maiato H, Earnshaw WC, Carmena M** 2001 Essential roles of Drosophila inner centromere protein (INCENP) and aurora B in histone H3 phosphorylation, metaphase chromosome alignment, kinetochore disjunction, and chromosome segregation. J Cell Biol 153:865–880
27. **Kaitna S, Pasierbek P, Jantsch M, Loidl J, Glotzer M** 2002 The aurora B kinase AIR-2 regulates kinetochores during mitosis and is required for separation of homologous chromosomes during meiosis. Curr Biol 12:798–812
28. **Murata-Hori M, Wang YL** 2002 The kinase activity of aurora B is required for kinetochore-microtubule interactions during mitosis. Curr Biol 12:894–899
29. **Ota T, Suto S, Katayama H, Han ZB, Suzuki F, Maeda M, Tanino M, Terada Y, Tatsuka M** 2002 Increased mitotic phosphorylation of histone H3 attributable to AIM-1/Aurora B overexpression contributes to chromosome number instability. Cancer Res 62:5168–5177
30. **Tatsuka M, Katayama H, Ota T, Tanaka T, Odashima S, Suzuki F, Terada Y** 1998 Multinuclearity and increased ploidy caused by overexpression of the aurora- and Ipl1-like midbody-associated protein mitotic kinase in human cancer cells. Cancer Res 58:4811–4816
31. **Ishizaka Y, Ushijima T, Sugimura T, Nagao M** 1990 cDNA cloning and characterization of ret activated in a human papillary thyroid carcinoma cell line. Biochem Biophys Res Commun 16:402–408
32. **Estour B, Van Herle AJ, Juillard GJ, Totanes TL, Sparkes RS, Giuliano AE, Klandorf H** 1989 Characterization of a human follicular thyroid carcinoma cell line (UCLA RO 82 W-1). Virchows Arch B Cell Pathol Incl Mol Pathol 57:167–174
33. **Fiore L, Pollina LE, Fontanini G, Casalone R, Berlingieri MT, Giannini R, Pacini F, Miccoli P, Toniolo A, Fusco A, Basolo F** 1997 Cytokine production by a new undifferentiated human thyroid carcinoma cell line, FB-1. J Clin Endocrinol Metab 82:4094–4100
34. **Mortlock A, Keen N, Jung F, Brewster AG** 2001 International publication no. WO01/21596A1 (www.european-patent-office.org)
35. **Macpherson I, Montagnier L** 1964 Agar suspension culture for the selective assay of the cells transformed by Polyoma virus. Virology 23:291–294
36. **El-Rifai W, Frierson Jr HF, Moskaluk CA, Harper JC, Petroni GR, Bissonette EA, Jones DR, Knuutila S, Powell SM** 2001 Genetic differences between adenocarcinomas arising in Barrett's esophagus and gastric mucosa. Gastroenterology 121:592–598
37. **Powell Jr DJ, Russell J, Nibu K, Li G, Rhee E, Liao M, Goldstein M, Keane WM, Santoro M, Fusco A, Rothstein JL** 1998 The RET/PTC3 oncogene: metastatic solid-type papillary carcinomas in murine thyroids. Cancer Res 58:5523–5528
38. **Ledent C, Marcotte A, Dumont JE, Vassart G, Parmentier M** 1995 Differentiated carcinomas develop as a consequence of the thyroid specific expression of a thyroglobulin-human papillomavirus type 16 E7 transgene. Oncogene 10:1789–1797
39. **Ledent C, Dumont J, Vassart G, Parmentier M** 1991 Thyroid adenocarcinomas secondary to tissue-specific expression of simian virus-40 large T-antigen in transgenic mice. Endocrinology 129:1391–1401
40. **Portella G, Ferulano G, Santoro M, Grieco M, Fusco A, Vecchio G** 1989 The Kirsten murine sarcoma virus induces rat thyroid carcinomas *in vivo*. Oncogene 4:181–188
41. **Bass BL** 2000 Double-stranded RNA as a template for gene silencing. Cell 101:235–238
42. **Caplen NJ, Parrish S, Imani F, Fire A, Morgan RA** 2001 Specific inhibition of gene expression by small double-stranded RNAs in invertebrate and vertebrate systems. Proc Natl Acad Sci USA 98:9742–9747
43. **Elbashir SM, Harborth J, Lendeckel W, Yalcin A, Weber K, Tuschl T** 2001 Duplexes of 21-nucleotide RNAs mediate RNA interference in cultured mammalian cells. Nature 411:494–498
44. **Ditchfield C, Johnson VL, Tighe A, Ellston R, Haworth C, Johnson T, Mortlock A, Keen N, Taylor SS** 2003 Aurora B couples chromosome alignment with anaphase by targeting BubR1, Mad2, and Cenp-E to kinetochores. J Cell Biol 161:267–280
45. **Miyoshi Y, Iwao K, Egawa C, Noguchi S** 2001 Association of centrosomal kinase STK15/BTAK mRNA expression with chromosomal instability in human breast cancers. Int J Cancer 92:370–373
46. **Li D, Zhu J, Firozi PF, Abbruzzese JL, Evans DB, Cleary K, Friess H, Sen S** 2003 Overexpression of oncogenic STK15/BTAK/Aurora A kinase in human pancreatic cancer. Clin Cancer Res 9:991–997
47. **Gritsko TM, Coppola D, Paciga JE, Abbruzzese JL, Evans DB, Cleary K, Friess H, Sen S** 2003 Activation and overexpression of centrosome kinase BTAK/Aurora-A in human ovarian cancer. Clin Cancer Res 9:1420–1426
48. **Hamada M, Yakushijin Y, Ohtsuka M, Kakimoto M, Yasukawa M, Fujita S** 2003 Aurora2/BTAK/STK15 is involved in cell cycle checkpoint and cell survival of aggressive non-Hodgkin's lymphoma. Br J Haematol 12:439–447
49. **Katayama H, Ota T, Jisaki F, Ueda Y, Tanaka T, Odashima S, Suzuki F, Terada Y, Tatsuka M** 1999 Mitotic kinase expression and colorectal cancer progression. J Natl Cancer Inst 91:1160–1162
50. **Chieffi P, Troncone G, Caleo A, Libertini S, Linardopoulos S, Tramontano D, Portella G** 2004 Aurora B expression in normal testis and seminomas. J Endocrinol 181:263–270

JCEM is published monthly by The Endocrine Society (http://www.endo-society.org), the foremost professional society serving the endocrine community.

Oncogene (2005) 24, 7012–7021

www.nature.com/onc

Raised expression of the antiapoptotic protein ped/pea-15 increases susceptibility to chemically induced skin tumor development

Pietro Formisano[1], Giuseppe Perruolo[1], Silvana Libertini[1], Stefania Santopietro[1], Giancarlo Troncone[2], Gregory Alexander Raciti[1], Francesco Oriente[1], Giuseppe Portella[1], Claudia Miele[1] and Francesco Beguinot*[,1]

[1]*Dipartimento di Biologia e Patologia Cellulare e Molecolare, Università di Napoli Federico II, Istituto di Endocrinologia ed Oncologia Sperimentale del CNR, Via Sergio Pansini, 5, Naples 80131, Italy;* [2]*Dipartimento di Scienze Biomorfologiche e Funzionali of the Federico II University of Naples, Naples, Italy*

ped/pea-15 is a cytosolic protein performing a broad antiapoptotic function. We show that, upon DMBA/TPA-induced skin carcinogenesis, transgenic mice overexpressing *ped/pea-15* ($Tg_{ped/pea-15}$) display early development of papillomas and a four-fold increase in papilloma number compared to the nontransgenic littermates ($P<0.001$). The malignant conversion frequency was 24% for the $Tg_{ped/pea-15}$ mice and only 5% in controls ($P<0.01$). The isolated application of TPA, but not that of DMBA, was sufficient to reversibly upregulate *ped/pea-15* in both untransformed skin and cultured keratinocytes. ped/pea-15 protein levels were also increased in DMBA/TPA-induced papillomas of both $Tg_{ped/pea-15}$ and control mice. Isolated TPA applications induced Caspase-3 activation and apoptosis in nontransformed mouse epidermal tissues. The induction of both Caspase-3 and apoptosis by TPA were four-fold inhibited in the skin of the $Tg_{ped/pea-15}$ compared to the nontransgenic mice, accompanied by a similarly sized reduction in TPA-induced JNK and p38 stimulation and by constitutive induction of cytoplasmic ERK activity in the transgenics. *ped/pea-15* expression was stably increased in cell lines from DMBA/TPA-induced skin papillomas and carcinomas, paralleled by protection from TPA apoptosis. In the A5 spindle carcinoma cell line, antisense inhibition of *ped/pea-15* expression simultaneously rescued sensitivity to TPA-induced Caspase-3 function and apoptosis. The antisense also reduced A5 cell ability to grow in semisolid media by 65% ($P<0.001$) and increased by three-fold tumor latency time ($P<0.01$). Thus, the expression levels of *ped/pea-15* control Caspase-3 function and epidermal cell apoptosis *in vivo* and determine susceptibility to skin tumor development.

Oncogene (2005) **24,** 7012–7021. doi:10.1038/sj.onc.1208871; published online 25 July 2005

Keywords: ped/pea-15; transgenic mice; chemical carcinogenesis; skin cancer; apoptosis

*Correspondence: F Beguinot; E-mail: beguino@unina.it
Received 26 January 2005; revised 6 May 2005; accepted 20 May 2005; published online 25 July 2005

Introduction

There is evidence that deregulation of apoptosis plays an important role in tumorigenesis. Indeed, alterations of apoptosis-related genes have been identified in a number of human cancers (Debatin and Krammer, 2004). ped/pea-15 is a 15 kDa, death effector domain (DED)-containing protein featuring ubiquitous expression, and originally identified as a major astrocytic phosphoprotein (Araujo *et al*., 1993; Condorelli *et al*., 1998). ped/pea-15 exerts a broad antiapoptotic action through at least three distinct mechanisms. Firstly, it inhibits the formation of the death-inducing signaling complex (DISC) and Caspase-3 activation triggered by FASL, tumor necrosis factor alpha, and the tumor necrosis factor-related apoptosis-inducing ligand (TRAIL) (Condorelli *et al*., 1999; Kitsberg *et al*., 1999; Hao *et al*., 2001). Secondly, ped/pea-15 inhibits stress-induced apoptosis by simultaneously blocking stress-activated protein kinases (SAPK) and increasing the function of cytosolic extracellular signal-regulated kinases (ERK1/2) (Condorelli *et al*., 2002). Thirdly, ped/pea-15 prevents degradation of the antiapoptotic protein XIAP caused by release of proapoptotic mitochondrial proteins (Trencia *et al*., 2004).

Studies in our own and other laboratories have shown that elevated expression of *ped/pea-15* occurs in several tumor-derived cell lines. Indeed, *ped/pea-15* is highly expressed in human glioma and metastatic breast cancer cell lines and induces resistance to chemotherapic agents in these cells (Ramos *et al*., 2000; Hao *et al*., 2001; Condorelli *et al*., 2002; Trencia *et al*., 2004). *ped/pea-15* is also expressed at high levels in tumor cell lines derived from human larynx, cervix, and skin tumors (Condorelli *et al*., 1998), and in human mammary carcinomas as well (Tsukamoto *et al*., 2000). Finally, the *ped/pea-15* gene was demonstrated to be increasingly expressed during tumor progression in murine squamous carcinomas (Dong *et al*., 2001). However, despite these mounting evidence supporting the role of *ped/pea-15* in neoplastic transformation and tumor progression, whether *ped/pea-15* has a direct role in tumorigenesis and progression *in vivo* has not been investigated yet.

Transgenic mice overexpressing *ped/pea-15* ubiquitously have recently been generated (Vigliotta *et al*., 2004). These mice feature reduced glucose tolerance due to both impaired insulin action and secretion. We have now used these transgenics and a well-characterized mouse model of chemically induced multistep skin carcinogenesis (Balmain and Harris, 2000) to explore the role of *ped/pea-15* in the initiation, promotion and progression of skin tumors. Our study shows, for the first time, that *ped/pea-15* expression level has a significant impact on skin tumor development in a mouse model of chemically induced skin carcinogenesis.

Results

Skin carcinogenesis in ped/pea-15 *transgenic mice*

We have investigated whether the variation in *ped/pea-15* expression levels affects skin tumorigenesis. To this end, we have used transgenic mice overexpressing the human cDNA of *ped/pea-15* ($Tg_{ped/pea\text{-}15}$; Vigliotta *et al*., 2004). Based on Western blot analysis, ped/pea-15 protein was overexpressed by about four-fold ($P<0.001$) in the epidermis of these transgenics, as compared to their nontransgenic littermates (WT) (Figure 1a).

$Tg_{ped/pea\text{-}15}$ and control mice ($n=40$/group; M/F = 1) were subjected to a single DMBA topical application followed by repeated applications of the tumor promoter TPA. This treatment resulted in the development of papillomatous lesions. Visible papillomas began to appear on the dorsal skin of both the $Tg_{ped/pea\text{-}15}$ and WT mice at 7 weeks of promotion, indicating no difference in the benign tumor latency between the two groups of mice (Figure 1b). The incidence of papilloma development reached 100% at 10 weeks of promotion in the $Tg_{ped/pea\text{-}15}$, and at week 12 in the WT mice ($P<0.001$; Figure 1b). Interestingly, there was a significant increase in the average number of papillomas per mouse in the $Tg_{ped/pea\text{-}15}$ compared to WT mice throughout the entire promoter treatment period. The difference in papilloma number was already significant at week 8. By the end of promotion (week 15), $Tg_{ped/pea\text{-}15}$ mice showed 18.4 ± 10.7 papillomas per mouse compared to 4.9 ± 4.8 in the WT mice ($P<0.001$) (Figure 1c). No gender-related difference was evidenced in either the incidence or the number of papillomas in transgenic and control mice (data not shown).

At 35 weeks after promoter treatment suspension, the lesions from $Tg_{ped/pea\text{-}15}$ and WT mice were subjected to histological examination. The malignant conversion frequency was 24% in the $Tg_{ped/pea\text{-}15}$ mice (12 out of 50 analysed lesions, Figure 2A). As in previous studies (Burns *et al*., 1978), the frequency was only 5% (two out of 40 analysed lesions) in the control mice ($P<0.001$), however. Sections of the lesions from $Tg_{ped/pea\text{-}15}$ mice more frequently showed the presence of a poorly differentiated epithelial neoplasm composed of nests of small undifferentiated cells with minimal keratinization, occasional squamous pearl formation and extremely

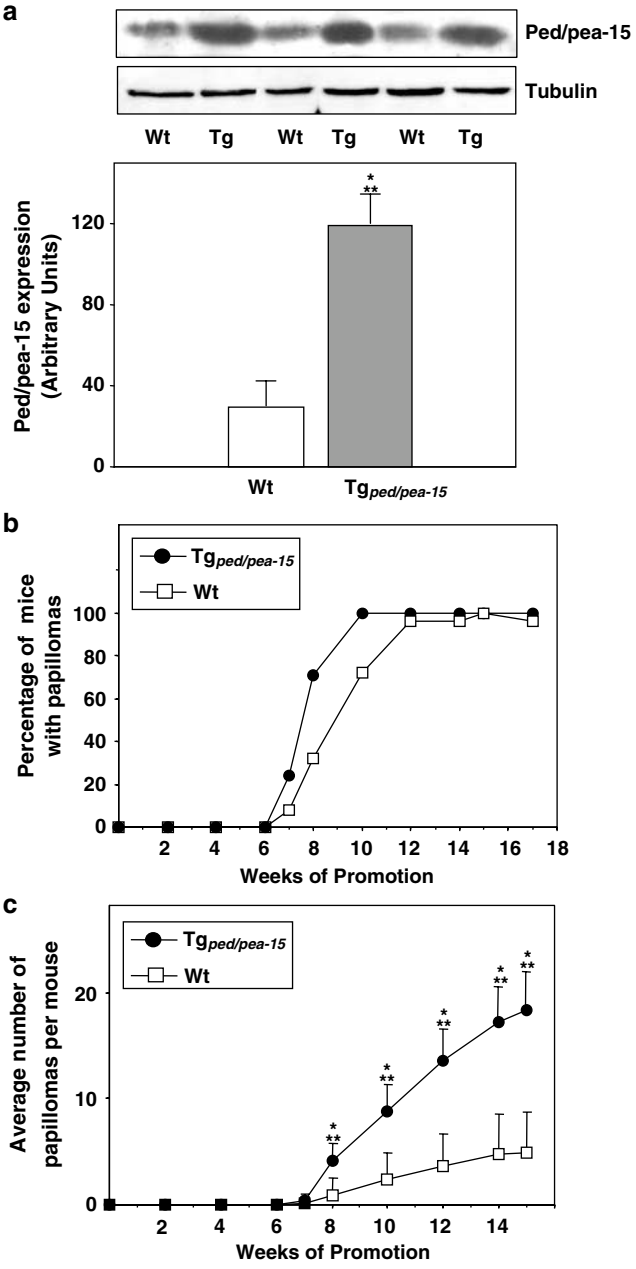

Figure 1 Chemically induced skin carcinogenesis in $Tg_{ped/pea\text{-}15}$ mice. (**a**) Duplicate samples from the dorsal skin of *ped/pea-15* transgenic mice ($Tg_{ped/pea\text{-}15}$) and the nontransgenic littermates ($n=40$ animals/group; male/female = 1) were solubilized and proteins (50 μg) analysed by Western blotting with ped/pea-15 antibodies as in Vigliotta *et al*. (2004). To ensure normalization, aliquots from the samples were also blotted with tubulin antibodies. Bars represent the average values ($\pm$s.d.) obtained from ped/pea-15 band densitometry, normalized for tubulin band densitometry. A representative blot is also shown on the top. (**b** and **c**) $Tg_{ped/pea\text{-}15}$ and control mice (three independent experiments; $n=40$ animals/group in each; male/female = 1) were subjected to skin carcinogenesis as described under Materials and methods. The number of papillomas was recorded weekly and is expressed either as percentage of mice containing at least one papilloma (**b**) or the average number ($\pm$s.d.) of papillomas per mouse (**c**). Statistical significance was assessed by *t*-test analysis

A

Mouse line	No. of mice At 35 weeks by the end of promotion	No. of carcinomas per no. of papillomas	Frequency of malignant conversion
Wt	20	2/40	5%
$Tg_{ped/pea-15}$	12	12/50	24%

B

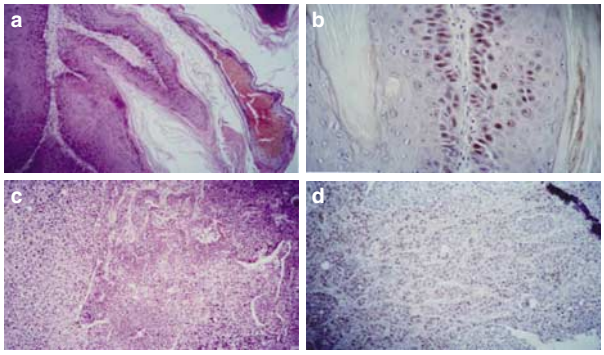

Figure 2 Malignant conversion frequency in $Tg_{ped/pea-15}$ mice. (**A**) ped/pea-15 transgenic and control mice were subjected to chemical carcinogenesis as described under Materials and methods. Total papilloma and carcinoma numbers were recorded. Carcinoma numbers were scored by morphological appearance on collection followed by histological confirmation after H&E staining of paraffin sections. (**B**) Representative H&E stained paraffin sections ($\times 100$ magnification) of tumors at 35 weeks after the end of promotion treatment from control (a) and $Tg_{ped/pea-15}$ mice (c). In the transgenics, PCNA immunostaining ($\times 100$ magnification) was scattered throughout the the tumour tissue (d), while limited to the basal cells in the control mice (b), as evidenced at higher magnification ($\times 400$). Representative microphotographs are shown

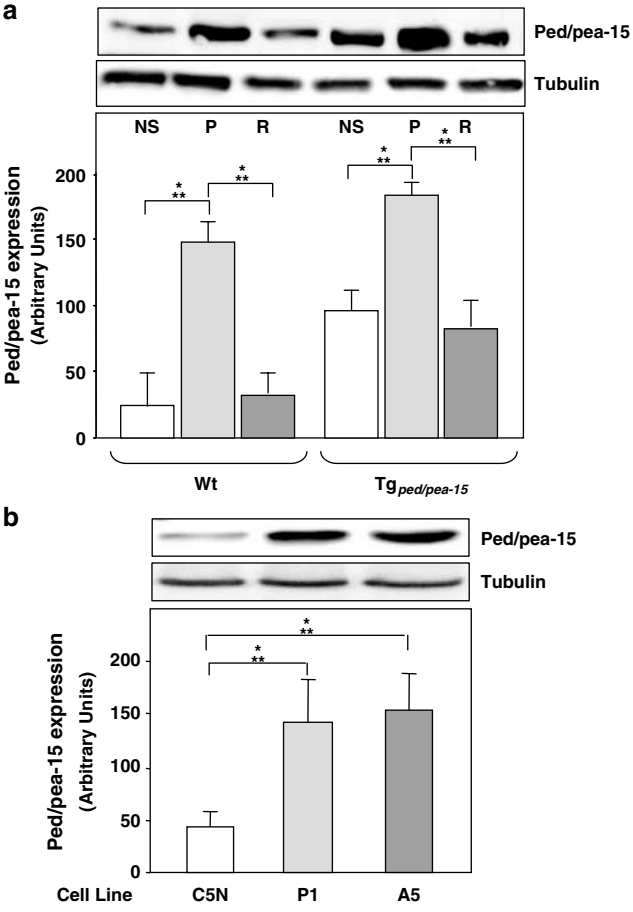

Figure 3 *ped/pea-15* expression in cell lines from chemically induced skin tumors and papillomas from $Tg_{ped/pea-15}$ mice. (**a**) Papillomatous lesions (P; $n=32$), samples from unaffected skin of the surrounding areas (NS; $n=34$), or from the skin corresponding to the papillomatous base upon regression of the lesion (R; $n=28$) from control (WT) and *ped/pea-15* transgenic mice ($Tg_{ped/pea-15}$) animals ($n=27$/group) were excised and lysed as described in the legend to Figure 1. ped/pea-15 and tubulin expression were detected in the lysates (50 μg of proteins/sample) by Western blotting and autoradiography. Blots were revealed by ECL and autoradiography and analysed by laser densitometry. Bars represent the average (values $\pm$ s.d.) of the tubulin-normalized expression of ped/pea-15 in duplicate determinations from four independent experiments. The difference between P and NS was significant at the $P=0.001$ (Wt) and $P<0.001$ (Tg). (**b**) The C5N, P1 and A5 cell lines derived, respectively, from normal keratinocytes, DMBA/TPA-induced papillomas and spindle cell carcinomas, were cultured as described under Materials and methods. Cell proteins (50 μg) were Western blotted with ped/pea-15 or tubulin antibodies as indicated. Blots were revealed and further analysed as in (**a**). Bars represent the average (values $\pm$ s.d.) of the tubulin-normalized expression of ped/pea-15 in duplicate determinations from four independent experiments. The difference between the P1 and C5N cells and between the A5 and C5N cells were significant at the $P<0.001$ level. A representative autoradiograph is also shown

intense mitotic activity (Figure 2B(c)). As shown in Figure 2B(d), the majority of the neoplastic cells displayed intense PCNA nuclear labeling, and stained cells were scattered throughout the tissue, reflecting the neoplastic modifications. At variance, lesions from WT mice more commonly showed benign hyperplastic proliferation of the epidermis, with epithelial cells featuring normal morphological characteristics, without significant nuclear atypia (Figure 2B(a)). Based on PCNA immunostaining, cycling cells were present only at the basal epidermal level (Figure 2B(b)). Differentiating squamous cells exhibited no staining, consistent with lack of dysplatic/neoplastic changes in the WT mouse skin.

ped/pea-15 levels during skin tumor initiation and promotion

To investigate the significance of *ped/pea-15* expression to skin tumor development and malignant progression, we have first analysed ped/pea-15 levels in papillomatous lesions and in the corresponding skin upon regression of the lesions. Despite the four-fold increase in the normal skin of $Tg_{ped/pea-15}$ *versus* control mice, ped/pea-15 was raised to comparable absolute levels in papillomas from WT and $Tg_{ped/pea-15}$ mice (Figure 3a). Immunohistochemical analysis with ped/pea-15 antibodies revealed comparable distribution of ped/pea-15 between the stromal and epithelial components of the epidermal tissues from transgenic and control mice (data not shown). After papilloma regression, there were no longer differences in ped/pea-15 levels between the skin

where the lesion had originated and the surrounding normal skin, in both the $Tg_{ped/pea-15}$ and the WT mice.

We next analysed mouse cell lines derived from DMBA/TPA-induced skin tumors at different stages of carcinogenesis (Portella *et al*., 1998). By Western blotting, ped/pea-15 protein was similarly overexpressed (almost three-fold; $P<0.001$) in both the P1 benign papilloma cells and the A5 highly anaplastic, invasive spindle carcinoma cells compared to the C5N immortalized nontumorigenic keratinocytes (Figure 3b). Thus, in the cell lines as well as *in vivo*, the increase in ped/pea-15 protein level appeared to occur at an early stage during skin carcinogenesis.

Repeated applications of the DMBA initiator on the mouse skin did not change ped/pea-15 levels either in the $Tg_{ped/pea-15}$ or in WT mice (Figure 4a). Also, transfection of the constitutively active H-*Ras61* mutant in keratinocytes showed no effect on ped/pea-15 levels (Figure 4b), indicating that *Ras* activation is not sufficient to upregulate ped/pea-15. At variance with DMBA, TPA treatment raised ped/pea-15 expression in skin cells, both in the absence and in the presence of the H-Ras61 mutant (Figure 4b). Indeed, exposure of the nontumorigenic C5N keratinocytes to 100 μg/ml TPA increased ped/pea-15 protein level in a time-dependent manner (Figure 5a). The effect achieved a plateau (five-fold increase) within 24 h and was maintained for 24 more hours, returning to baseline upon TPA withdrawal. Also, a single TPA application to the skin of both WT and $Tg_{ped/pea-15}$ mice caused a five-fold elevation of ped/pea-15 protein for up to 48 h, declining thereafter and returning to the pretreatment level by 144 h (still four-fold higher in transgenic compared to WT mice; Figure 5b). Previous studies showed that phosphorylation by both Akt/PKB and PKC increases intracellular stability of ped/pea-15 (Trencia *et al*., 2003). Based on immunoblotting with specific pSer116 and pSer104 ped/pea-15 antibodies, these increased ped/pea-15 levels in TPA-treated skin were accompanied by 2.5- and four-fold increased phosphorylation of ped/pea-15 on the Akt/PKB and PKC sites (Ser116 and Ser104, respectively). There were no differences in these phosphorylations in Wt and transgenic mice suggesting that increased ped/pea-15 stability may, at least in part, account for the effect of TPA in these animals (Figure 5c).

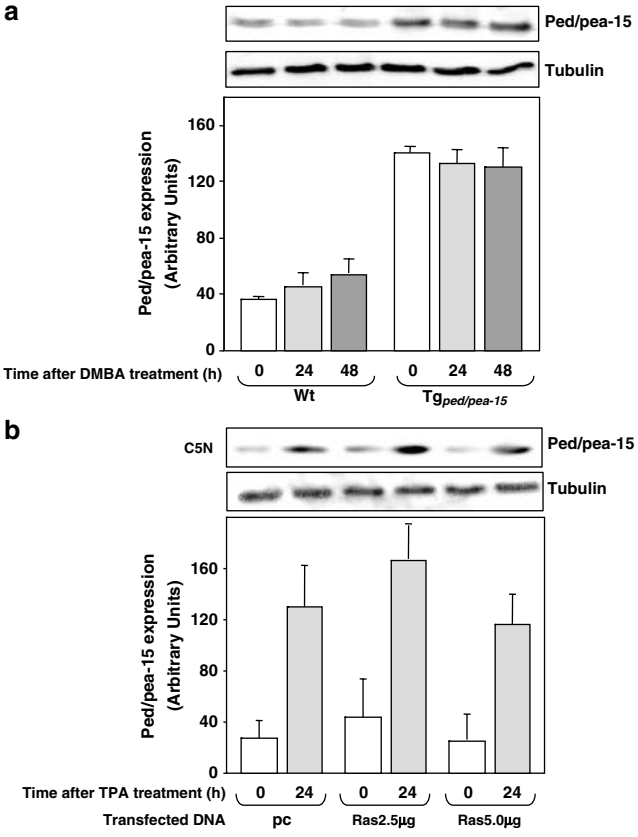

Figure 4 Effect of DMBA application and of constitutively active Ras mutant on *ped/pea-15* expression. (**a**) Mouse dorsal skin was treated by repeated DMBA applications at times 0, 6 and 12 h. ped/pea-15 and tubulin expression was determined at the indicated times upon the first application of DMBA, as described above. Bars represent the mean $\pm$ s.d. of duplicate determinations of the tubulin-normalized expression of ped/pea-15 in 2 (**a**: $n=20$ mice/time point) independent experiments. Representative blots are also shown in the insets. (**b**) The C5N cells were transfected with 2.5 or 5.0 μg of H-Ras61 or with 5.0 μg of the empty vector (pc) as described under Materials and methods. After TPA treatment, cells were lysed and cell proteins (50 μg) were Western blotted with ped/pea-15 or tubulin antibodies as indicated. Blots were revealed by ECL and autoradiography and analysed by laser densitometry. Bars represent the average (values $\pm$ s.d.) of the tubulin-normalized expression of ped/pea-15 in duplicate determinations from three independent experiments. Representative blots are also shown in the insets

Effect of ped/pea-15 on skin tissue apoptosis

To examine the consequences of *ped/pea-15* overexpression and its role in skin tumorigenesis, we compared *in vivo* apoptosis in the skin of $Tg_{ped/pea-15}$ and WT mice upon the application of TPA. Based on skin lysate determination, $Tg_{ped/pea-15}$ mice showed a significant decrease in the number of apoptotic cells compared to WT animals (Figure 6a). Importantly, TPA application to the skin of WT mice induced the appearance of the 20K fragment of the terminal caspase Caspase-3 in the lysates, evidencing Caspase-3 activation (Figure 6b). Activation of Caspase-3 by TPA was barely detectable in the skin of $Tg_{ped/pea-15}$ mice, however. Consistently, cleavage of the Caspase-3 substrate PARP was well evident upon treating WT mouse skin with TPA, but >10-fold less measurable in $Tg_{ped/pea-15}$ mice (Figure 6c).

At variance with Caspase-3, TPA treatment exhibited very little effect on the activation of the upstream caspase, Caspase-8, in both WT and $Tg_{ped/pea-15}$ mouse skin (data not shown).

In different cell types, ped/pea-15 protects the inhibitor of apoptosis XIAP from the intracellular degradation following certain apoptotic stimuli, thereby preventing Caspase-3 activation (Trencia *et al*., 2004). However, skin lysates from WT and $Tg_{ped/pea-15}$ mouse showed no difference in XIAP levels (Figure 7a),

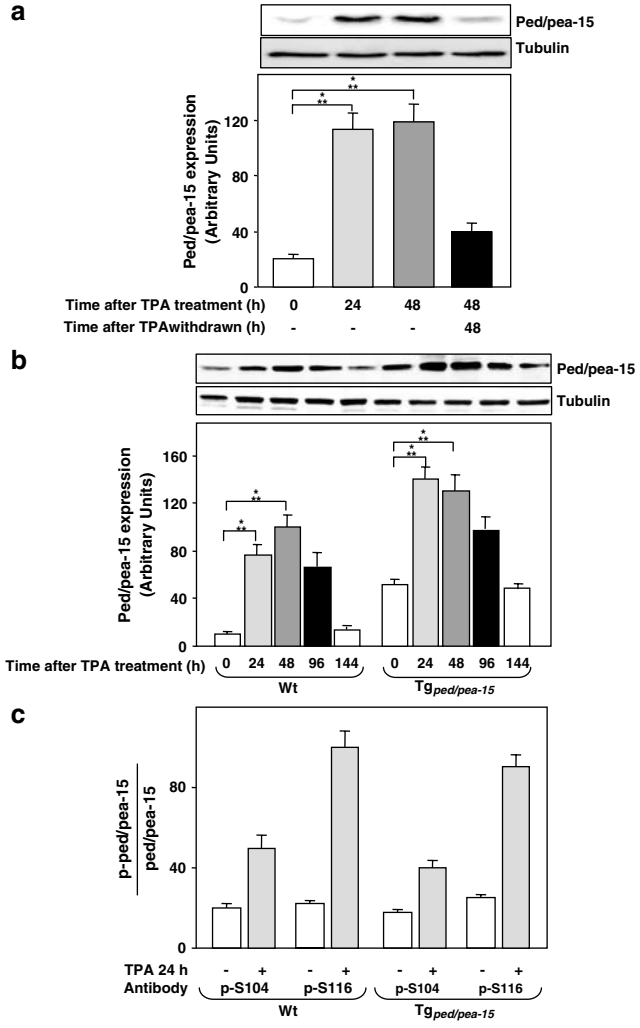

Figure 5 Effect of isolated applications of TPA on *ped/pea-15* expression and phosphorylation. C5N keratinocytes (**a**) and shaved dorsal skin of WT and Tg mice (**b**) were exposed to TPA, respectively, by addition to the culture medium (**a**) and topical application (**b**) as described under Materials and methods. Upon 48 h, TPA was removed from the cell cultures by medium replacement (**a**). At the indicated times, cells (**a**) and tissue samples (**b**) were lysed and analysed by Western blotting with ped/pea-15 and tubulin antibodies. Skin lysate filters were also reblotted with specific phosphoserine$_{104}$ and phosphoserine$_{116}$ antibodies (**c**). Blots were revealed by ECL and autoradiography and subjected to densitometric quantitation. Bars represent the mean $\pm$ s.d. of duplicate determinations of the tubulin-normalized expression of ped/pea-15 in three (**a, b**: $n = 20$ mice/time point) and two (**c**) independent experiments. Representative blots are also shown in the insets

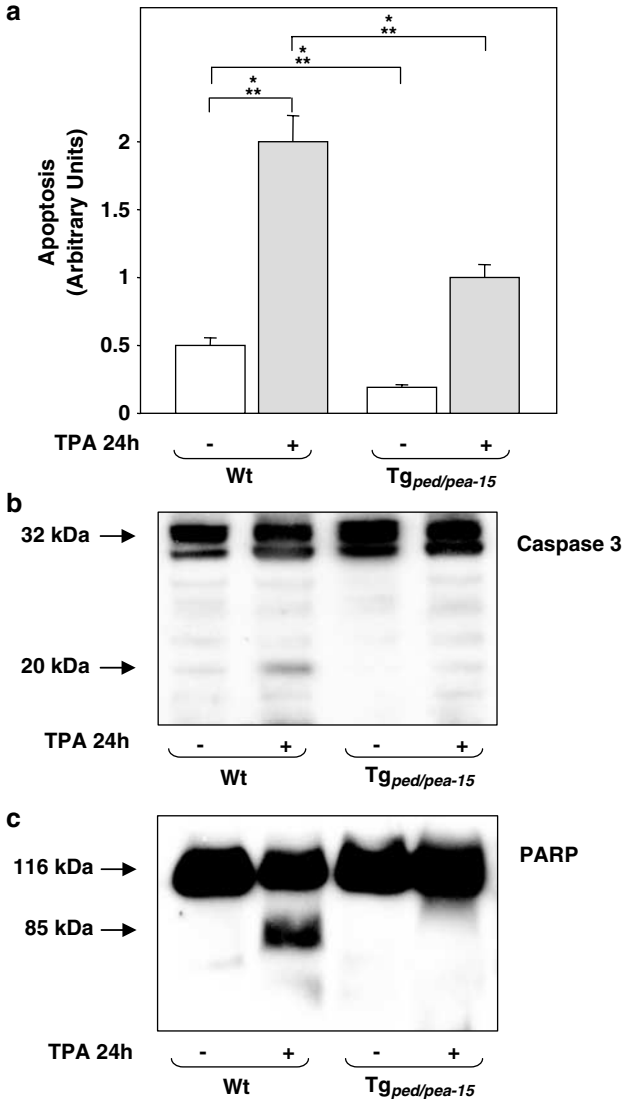

Figure 6 TPA-induced apoptosis and activation of Caspase 3 in Tg$_{ped/pea-15}$ mice. (**a**) Transgenic and control mice ($n = 30$/group; M/F ratio = 1 in each group) were subjected to TPA applications (6.25 μg of TPA in 200 μl acetone for 24 h) as described under Materials and methods. Samples of squamous stratified epithelium from the treated areas were solubilized and analysed with the ELISA^{PLUS} kit for detection of apoptosis. Bars represent the mean values ($\pm$ s.d.) of triplicate determinations in three independent experiments. (**b**) The dorsal skin of Tg$_{ped/pea-15}$ and control mice was treated with TPA as above. Samples from the treated skin were excised and analysed by Western blotting with Caspase-3 (**b**) or PARP antibodies (**c**). Blots were revealed by ECL and autoradiography. A representative autoradiography is shown; same results were obtained in three further experiments

suggesting that alternative mechanisms are responsible for the reduced apoptosis occurring in the Tg$_{ped/pea-15}$ mouse skin after TPA exposure. Indeed, previous studies in 293 cells indicated that ped/pea-15 antiapoptotic function requires ped/pea-15 simultaneous inhibition of the SAPK signaling system of JNK/p38 and activation of ERK1/2 (Condorelli *et al*., 2002). In WT mouse skin, TPA elicited a 10-fold increase in phosphorylation of the key activation sites of JNK (Thr183 and Tyr185) and those of p38 (Thr180, Thr182), indicating activation of these kinases (Figure 7b). Interestingly, the effect of TPA was five-fold reduced in Tg$_{ped/pea-15}$ mouse skin, despite normal expression of both JNK and p38. ERK1/2 phosphorylation was also constitutively increased in Tg$_{ped/pea-15}$ compared to Wt mouse skin (Figure 7c). Despite the eight-fold induction in the WT mouse, ERK phosphorylation in response to TPA showed little further increase in the transgenics, with no significant difference in ERK1/2 expression.

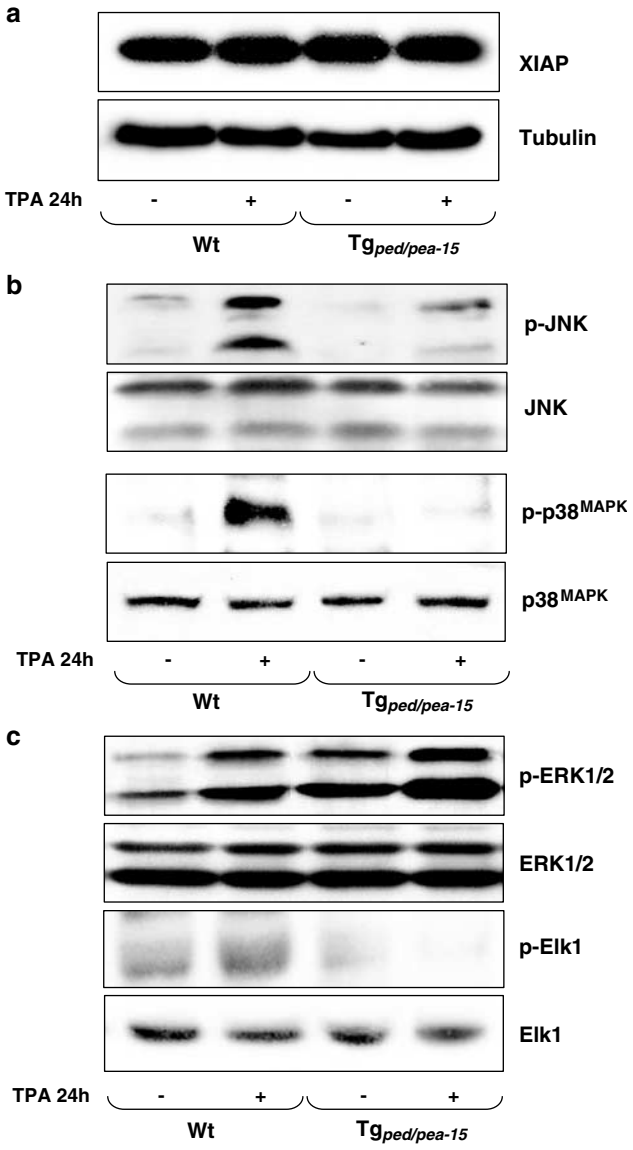

Figure 7 Effects of TPA on XIAP expression and JNK, p38, ERK1/2 and ELK1 phosphorylations. Transgenic and control mice ($n = 12$/group; M/F ratio = 1 in each group) were subjected to TPA applications (6.25 μg of TPA in 200 μl acetone for 24 h) as described under Materials and methods. Samples from the treated skin were excised and analysed by Western blotting with XIAP, tubulin (**a**), phospho-JNK, JNK, phospho-p38, p38 (**b**), phospho-ERK1/2, ERK1/2, phospho-Elk1, and Elk-1 antibodies (**c**). Blots were revealed by ECL and autoradiography. The autoradiographs shown are representative of four (**a** and **b**) and three (**c**) independent experiments

Consistent with the reported ability of ped/pea-15 to prevent nuclear migration of ERK1/2, phosphorylation of the ELK substrate in response to TPA was drastically reduced in tissues from $Tg_{ped/pea\text{-}15}$ compared to control mice. At variance with ELK, TPA phosphorylation of the H3 histone target of the ERK1/2-downstream and ped/pea-15 binding kinase RSK2 (Vaidayanathan and Ramos, 2003) showed no difference in $Tg_{ped/pea\text{-}15}$ and control mice (data not shown). Thus, at least in part, overexpression of ped/pea-15 may inhibit TPA-induced apoptosis by dysregulating selective pathways of the MAPK signaling and by inhibiting Caspase-3.

The role of caspase-3 inhibition in chemically induced skin tumorigenesis

To further address the involvement of impaired Caspase-3 activation in the increased susceptibility to skin carcinogenesis of the $Tg_{ped/pea\text{-}15}$ mice, we first compared TPA effect in the C5N nontumorigenic mouse keratinocytes and the A5 highly malignant invasive spindle carcinoma cells. Based on its own cleavage and that of the PARP substrate, TPA induction of Caspase-3 was barely detectable in the *ped/pea-15* overexpressing A5 cells, despite the evident effect occurring in the C5N keratinocytes (Figure 8a). The reduced activation of Caspase-3 in the A5 carcinoma cells was paralleled by a six-fold decrease in TPA-induced apoptosis, compared to the C5N keratinocytes (Figure 8b). We then silenced the expression of ped/pea-15 using a specific antisense cDNA (Hao *et al*., 2001). In the A5 cells, the antisense inhibited ped/pea-15 expression to levels comparable to those of the untreated C5N keratinocytes (Figure 8c). In parallel, the antisense rescued TPA apoptosis in the A5 cells, rendering the A5 as responsive to TPA as the C5N cells (Figure 8b). Caspase-3 and PARP cleavage in response to TPA was similarly rescued in antisense-transfected A5 cells (Figure 8a).

The colony growth rate in semisolid medium was also reduced in the antisense expressing A5 clones compared to cells tansfected with the empty vector (65% reduction; $P < 0.001$) (Table 1). Importantly, injection of A5 cells transfected with either the *ped/pea-15* antisense cDNA or the empty vector into athymic mice showed no significant difference in tumor incidence. However, the tumor latency period of the antisense expressing clones was almost three-fold increased compared to that of control cells ($P < 0.01$).

Discussion

There is evidence that increased expression of the antiapoptotic protein *ped/pea-15* is associated to development of malignancy (Condorelli *et al*., 1998; Ramos *et al*., 2000; Tsukamoto *et al*., 2000; Dong *et al*., 2001; Hao *et al*., 2001). However, no information is available, to date, to assess whether modulation of *ped/pea-15* expression may directly affect tumorigenesis and/or progression *in vivo*. Chemically induced skin carcinogenesis studies have provided valuable information concerning the impact of genetic alterations on multistep tumorigenesis and progression in genetically modified mice (Balmain and Harris, 2000). In the present paper, we have addressed the role of ped/pea-15 in skin tumor initiation, promotion and progression and used transgenic mice overexpressing the *ped/pea-15* gene. These mice express three- to four-fold higher skin levels of *ped/pea-15* compared to their nontransgenic littermates. We now report that, in parallel with the increased *ped/pea-15* expression, the transgenics show

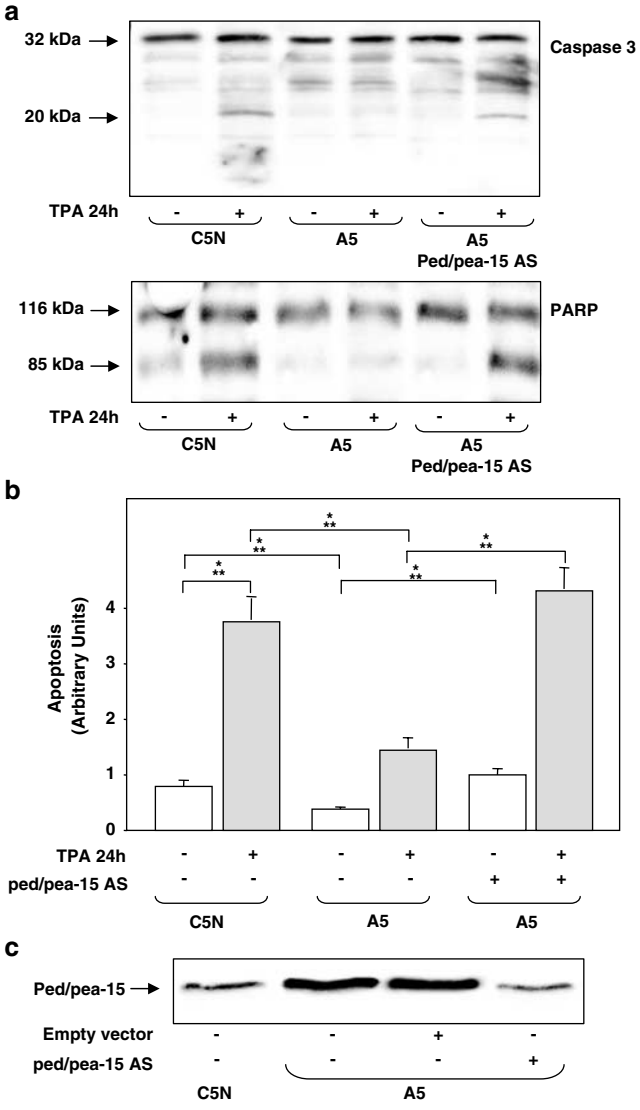

Figure 8 Effect of ped/pea-15 silencing on TPA apoptosis in C5N and A5 cells. (**a**) C5N and A5 cells stably transfected with ped/pea-15 antisense cDNA were obtained as described under Materials and methods. Antisense-expressing and control cells were exposed to TPA for 24 h and then solubilized. Cell lysates (50 μg per point) were then analysed by Western blotting with Caspase-3 or PARP antibodies, as indicated. The effect of the antisense on *ped/pea-15* expression was controlled in the same cell lysates by Western blotting with ped/pea-15 antibodies as described in the legend to Figure 3(c). Filters were revealed by ECL and autoradiography. The autoradiographs shown are representative of three independent experiments. Alternatively (**b**), TPA-stimulated cells were solubilized and analysed with the ELISA^{PLUS} kit for detection of apoptosis as described under Materials and methods. Bars represent the mean values ($\pm$s.d.) of triplicate determinations in three independent experiments

anticipated as well as increased occurrence of benign papillomatous lesions upon being topically treated with the tumor initiator DMBA followed by repeated applications of the tumor promoter TPA. Interestingly, *ped/pea-15* expression is also increased in papillomas from WT mice, compared to the adjacent normal skin. The significance of the increased ped/pea-15 levels to skin tumorigenesis is further strengthened by the finding that, upon papilloma regression, ped/pea-15 returns to basal levels in the skin where the lesions have been produced. In addition, the malignant conversion frequency of the papillomatous lesion was significantly higher in *ped/pea-15* transgenic compared to the control animals. These results indicate, for the first time, that increased levels of ped/pea-15 confer greater susceptibility to skin carcinogenesis *in vivo* and may enhance cutaneous tumor progression toward malignancy. Indeed, after suspension of TPA treatment, the transgenic mice maintain stably elevated ped/pea-15 levels compared to the WT animals where the effect of TPA vanishes.

We show that the constitutively active H-*Ras61* mutant does not affect *ped/pea-15* expression levels in keratinocytes. Consistently, DMBA application did not upregulate *ped/pea-15* in mouse skin, indicating that *Ras* mutation is not sufficient to cause *ped/pea-15* overexpression. At variance, treatment with TPA alone rapidly increased *ped/pea-15* expression levels in the skin of both transgenic and control mice, suggesting that ped/pea-15 overexpression represents an early event during cutaneous tumor promotion, though not initiation. At least in part, the effect of TPA may be mediated by induction of PKB/Akt and PKC. Indeed, (i) phosphorylation of ped/pea-15 on PKB/Akt and PKC sites is increased in TPA-treated skin; and (ii) previous studies (Trencia *et al*., 2003) demonstrated that phosphorylation of these sites increases cellular stability of ped/pea-15. In addition, transformed cell lines derived from DMBA/TPA-induced skin tumors consistently show higher ped/pea-15 levels compared to immortalized nontumorigenic keratinocytes. It is conceivable, therefore, that higher *ped/pea-15* levels may confer a distinctive advantage to the cells upon DMBA initiation, leading to selection of those overexpressing ped/pea-15.

Transgenic mice overexpressing *ped/pea-15* feature insulin-resistance and decreased glucose tolerance (Vigliotta *et al*., 2004). Considerable epidemiological evidence exists indicating that these metabolic abnormalities have a role in determining the occurrence of a

Table 1 Analysis of transformation markers of A5 carcinoma cells

Transfected DNA/caspase inhibitor	*Colony-forming efficiency (%)*[a]	*Tumor incidence*[b]	*Latency period (days)*[c]
—	58	5/5	14
pcDNA vector	56	6/6	14
pcDNA AS	20	6/6	39
Z-DEVD-FMK	14	—	—

[a]Colonies larger than 64 cells were scored after 3 weeks. Colony-forming efficiency was calculated by dividing the number of colonies formed by the number of plated cells $\times 100$. [b]Tumorigenicity was assayed by injecting 1×10^6 cells into 6-week-old athymic mice. [C]The animals were monitored for the appearance of tumors. The mean tumor latency is the time needed for tumors to reach 10 mm in diameter. The tumor latency of the antisense (AS)-transfected cells differed significantly from controls ($P<0.001$)

number of tumors in humans (Calle and Kaaks, 2004). Transgenic mice overexpressing *ped/pea-15* show no greater prevalence of spontaneous tumors, but whether insulin-resistance and/or impaired glucose tolerance contribute to the increased susceptibility to skin carcinogenesis cannot be concluded from the present study. Different mechanisms likely play a greater role, however, as TPA-induced upregulation of *ped/pea-15* also accompanies skin tumor development in nontransgenic mice featuring normal insulin sensitivity and glucose tolerance.

ped/pea-15 performs a broad antiapoptotic action in cultured cells (Condorelli *et al*., 1999, 2002; Kitsberg *et al*., 1999; Hao *et al*., 2001; Trencia *et al*., 2004). At least in part, ped/pea-15 antiapoptotic action is due to inhibition of the induction of the terminal caspase, Caspase-3 (Hao *et al*., 2001; Condorelli *et al*., 2002). In this paper, we show that TPA-induced apoptosis in squamous stratified epithelium *in vivo* is also significantly inhibited in *ped/pea-15* transgenic mice. This decrease is accompanied by reduced activation of Caspase-3 and cleavage of the Caspase-3 substrate PARP in response to TPA. Reduced apoptosis and Caspase-3 activation in response to TPA also occur in the A5 cells, which are derived from DMBA/TPA-induced spindle cell carcinomas and overexpress ped/pea-15. Consistently, in the normal C5N keratinocytes that express lower levels of endogenous *ped/pea-15*, transfection of *ped/pea-15* cDNA and treatment with the specific Caspase-3 inhibitor Z-DEVD-FMK prevented TPA apoptosis in a nonadditive manner (data not shown). Expression of a specific ped/pea-15 antisense cDNA in the A5 cells simultaneously reduced ped/pea-15 levels and rescued TPA-induced apoptosis and Caspase-3 activation. Importantly, the antisense significantly increased the latency preceding tumor formation upon A5 cell injection in nude mice. The A5 cell growth in semisolid medium was also significantly reduced by decreasing *ped/pea-15* expression. Thus, the impaired apotosis determined by inhibition of Caspase-3 activity in *ped/pea-15* overexpressing skin cells might affect the malignant progression as well as tumorigenesis.

Previous studies by other investigators and by us have shown that ped/pea-15 may inhibit Caspase-3 function by preventing the activation of Caspase-8 (Condorelli *et al*., 1999; Kitsberg *et al*., 1999) as well as by increasing stability of the inhibitor of apoptosis protein XIAP (Trencia *et al*., 2004). These events do not account for ped/pea-15 inhibition of Caspase-3 in TPA-treated skin, as *ped/pea-15* overexpression does not affect TPA action on either Caspase-8 function or XIAP levels. In certain cell types, block of the JNK and p38 members of the MAPK family also plays an important role in mediating the ped/pea-15 protection from apoptosis (Condorelli *et al*., 2002), which may lead to Caspase-3 inhibition (Kamata *et al*., 2005). Full antiapoptotic function in these cells requires concomitant *ped/pea-15* induction of the ERK1/2 MAPKs and/or ERK1/2 anchoring into the cytoplasm (Formstecher *et al*., 2001; Condorelli *et al*., 2002). Impaired JNK and p38 activation and increased ERK1/2 cytoplasmic activity have also been detected in the skin of $Tg_{ped/pea-15}$ mice upon exposure to TPA, indicating they may mediate the decreased susceptibility to apoptosis caused by overexpression of *ped/pea-15* in these cells. Indeed, same as in other cell types (Condorelli *et al*., 2002), in the A5, the rescue of JNK function by overexpression of the upstream kinase MKK6 significantly enhanced the apoptotic response to TPA (data not shown).

Intriguingly, Gaumont-Leclerc *et al*. (2004) have very recently reported evidence that *ped/pea-15* may exert a tumor suppressor function in the IMR90 fibroblasts. It is possible that this function is also exerted in the mouse keratinocyte model. Upon DMBA/TPA exposure of these cells, the antiapoptotic function of ped/pea-15 seems to prevail, however. Consistently, ped/pea-15 overexpression confers raised susceptibility to chemical carcinogenesis in the skin. Thus, different settings may lead ped/pea-15 to have its pro- or antioncogenic functions overriding.

Deregulated apoptosis has been suggested to play an important role in tumorigenesis and malignant progression of transformed cells by contributing the cells with the capability to skip cell death programs, accumulating DNA damage (Debatin and Krammer, 2004). In certain tumors, these abnormalities may occur because of loss of proapoptotic molecules such as Bax, Apaf-1 or Caspase-8 (Harada and Grant, 2003; Baldi *et al*., 2004). In other situations, impaired apoptosis has been associated to increased expression of antiapoptotic molecules of the Bcl-2 family (Harada and Grant, 2003). In this paper, we have shown that increased expression levels of the antiapoptotic protein ped/pea-15 may also determine susceptibility to skin tumorigenesis and tumor progression by inhibiting Caspase-3-dependent apoptosis in DMBA/TPA-treated mice. Several alterations occurring in these chemically induced mouse skin tumors have also been observed in the homologous cutaneous tumors in humans (Balmain and Harris, 2000). ped/pea-15 might represent a novel target for cutaneous cancer treatment and prevention.

Materials and methods

Transgenic ped/pea-15 *mice*

The C57BL/6JxDBA/2J *ped/pea-15* transgenic mice were described in Vigliotta *et al*. (2004). The animals were maintained in the animal facility at the Dipartimento di Biologia e Patologia Cellulare e Molecolare, Federico II University of Naples. Experiments involving animals were conducted in accordance with accepted standards of animal care and the Italian regulations for the welfare of animals. The study protocol was approved by the Institutional Committee on Animal Care of the University of Naples.

Two-stage skin carcinogenesis

The dorsal skin of 8-week-old mice were shaved, and, 2 days later, a single dose of 50 μg of 7,12-dimethylbenz[a]anthracene (DMBA) in 200 μl of acetone was applied. At 1 week after initiation, the mice were treated with 6.25 μg of 12-*O*-tetradecanoylphorbol-13-acetate (TPA) in 200 μl of acetone

twice a week for 15 weeks. The number of papillomas detected by palpation was recorded once a week.

At 1 week after termination of TPA treatment, mice were killed, and skin tissues snap frozen in liquid nitrogen and/or fixed in freshly prepared 4% paraformaldehyde followed by paraffin embedding. Mice were maintained for 35 additional weeks after TPA discontinuation, and tumor progression was investigated. Tumors were scored as papillomas or carcinomas by histological analysis after H&E staining of paraffin sections.

Histology

Tissues were fixed in formalin, dehydrated, blocked in paraffin and sectioned at 6 μm. The tissue sections were stained with hematoxylin and eosin. A total of 76 nonmalignant papillomas and all malignant tumors were examined. Malignant skin tumors were densely cellular spindle cell tumors in the dermis underlying the papilloma, often exhibiting invasion through skeletal muscle and sometimes associated with lymph node metastasis. Premalignant lesions were squamous cells showing atypia (enlarged nuclei, mitotic activity) but not associated with spindle cell proliferation, invasion and metastasis.

Cell culture and growth, transfection and Western blot analysis

The C5N, P1 and A5 cells have been previously described (Portella *et al*., 1998) and were kindly provided by Dr A Balmain (University of California, San Francisco, Comprehensive Cancer Center, USA). Cells were cultured in DMEM supplemented with 10% foetal calf serum, 10 000 U/ml penicillin, 10 000 μg/ml streptomycin and 2% L-glutamine in a humidified CO_2 incubator as described in Portella *et al*. (1998). Transfection of the constitutively active H-Ras61 in C5N cells, tissue collection and Western blots were performed as described in Vigliotta *et al*. (2004). The pcDNA-*ped/pea-15* antisense construct has been previously described (Hao *et al*., 2001). Clones expressing the antisense were selected as in Hao *et al*. (2001). Soft agar colony assays were performed according to a previously described technique (Macpherson and Montagnier, 1964). The antibodies used include ped/pea-15 antibodies (Vigliotta *et al*., 2004), phosphoserine$_{104}$ped/pea-15 and phosphoserine$_{116}$ped/pea-15 antibodies (Trencia *et al*., 2004), tubulin, caspase-3, XIAP and PARP antibodies (Santa Cruz Biotechnology, CA, USA).

Detection of apoptosis

Animals were subjected to topical applications of acetone-dissolved TPA (6.25 μg) or DMBA (50 μg) or acetone alone, as indicated. The animals were killed, skin tissues were removed and then solubilized as in Vigliotta *et al*. (2004) and processed for the apoptosis assay using the Cell Death Detection ELISA^{PLUS} Kit (Roche Diagnostics GmbH, Mannheim, Germany), according to the manufacturer instructions. For studies in isolated cells, apoptosis was investigated as previously described (Trencia *et al*., 2004).

Tumorigenicity assay

Experiments were performed in 6-week old male athymic mice (Charles River, Italy). A5 cells (1×10^6), either transfected with the *ped/pea-15* antisense cDNA or not, were injected into the right flank of the mice. The animals were monitored for the appearance of tumors and tumor latency was evaluated. The mean tumor latency is the time needed for tumors to reach 10 mm in diameter. All mice were maintained at the animal facility of the Dipartimento di Biologia e Patologia Cellulare e Molecolare of the Federico II University of Naples.

Densitometry and statistical analysis

Densitometric analysis was performed using a Scion Image Analyser. All the data were expressed as mean$\pm$s.d. Significance was assessed by Student's *t*-test for comparison between two means.

Acknowledgements
We thank Dr A Balmain for kindly providing C5N, P1 and A5 cells and Dr S Linardopoulos for critical reading of the manuscript. The technical help of Maria Russo, Salvatore Sequino and Dr Antonio Baiano is also acknowledged. This work was supported by the European Community's FP6 EUGENE2 (LSHM-CT-2004-512013), grants from the Associazione Italiana per la Ricerca sul Cancro (AIRC) to FB and PF, and the Ministero dell'Università e della Ricerca Scientifica (PRIN to FB, GiPo and PF and FIRB RBNE0155LB to FB). The financial support of Telethon – Italy is gratefully acknowledged.

References

Araujo H, Danziger N, Cordier J, Glowinski J and Chneiweiss H. (1993). *J. Biol. Chem.*, **268,** 5911–5920.

Baldi A, Santini D, Russo P, Catricala C, Amantea A, Picardo M, Tatangelo F, Botti G, Dragonetti E, Murace R, Tonini G, Natali PG, Baldi F and Paggi MG. (2004). *Exp. Dermatol.*, **13,** 93–97.

Balmain A and Harris CC. (2000). *Carcinogenesis*, **21,** 371–377.

Burns FJ, Vanderlaan M, Snyder E and Albert RE. (1978). *Carcinogenesis, Mechanisms of Tumour Promotion and Co-Carcinogenesis* Slaga TJ and Boutwell RK (eds). Raven Press, Ltd: New York.

Calle EE and Kaaks R. (2004). *Nat. Rev. Cancer*, **4,** 579–591.

Condorelli G, Trencia A, Vigliotta G, Perfetti A, Goglia U, Cassese A, Musti AM, Miele C, Santopietro S, Formisano P and Beguinot F. (2002). *J. Biol. Chem.*, **277,** 11013–11018.

Condorelli G, Vigliotta G, Iavarone C, Caruso M, Tocchetti CG, Andreozzi F, Cafieri A, Tecce MF, Formisano P, Beguinot L and Beguinot F. (1998). *EMBO J.*, **17,** 3858–3865.

Condorelli G, Vigliotta G, Cafieri A, Trencia A, Andalo P, Oriente F, Miele C, Caruso M, Formisano P and Beguinot F. (1999). *Oncogene*, **18,** 4409–4415.

Debatin KM and Krammer PH. (2004). *Oncogene*, **23,** 2950–2966.

Dong G, Loukinova E, Chen Z, Gangi L, Chanturita TI, Liu ET and Van Waes C. (2001). *Cancer Res.*, **61,** 4797–4808.

Formstecher E, Ramos JW, Fauquet M, Calderwood DA, Hsieh JC, Canton B, Nguyen XT, Barnier JV, Camonis J, Ginsberg MH and Chneiweiss H. (2001). *Dev. Cell.*, **2,** 239–250.

Gaumont-Leclerc MF, Mukhopadhyay UK, Goumard S and Ferbeyre G. (2004). *J. Biol. Chem.*, **279,** 46802–46809.

Hao C, Beguinot F, Condorelli G, Trencia A, Van Meir EG, Yong VW, Parney IF, Roa WH and Petruk KC. (2001). *Cancer Res.*, **61,** 1162–1170.

Harada H and Grant S. (2003). *Rev. Clin. Exp. Hematol.*, **7,** 117–138.

Kamata H, Honda S, Maeda S, Chang L, Hirata H and Karin M. (2005). *Cell*, **120,** 649–661.

Kitsberg D, Formstecher E, Fauquet M, Kubes M, Cordier J, Canton B, Pan G, Rolli M, Glowinski J and Chneiweiss H. (1999). *J. Neurosci.*, **19,** 8244–8251.

Macpherson I and Montagnier L. (1964). *Virology*, **23,** 291–294.

Portella G, Cumming SA, Liddell J, Cui W, Ireland H, Akhurst RJ and Balmain A. (1998). *Cell Growth Differ.*, **9,** 393–404.

Ramos JW, Hughes PE, Renshaw MW, Schwartz MA, Formstecher E, Chneiweiss H and Ginsberg MH. (2000). *Mol. Biol. Cell*, **11,** 2863–2872.

Trencia A, Fiory F, Maitan MA, Vito P, Barbagallo AP, Perfetti A, Miele C, Ungaro P, Oriente F, Cilenti L, Zervos AS, Formisano P and Beguinot F. (2004). *J. Biol. Chem.*, **279,** 46566–46572.

Trencia A, Perfetti A, Cassese A, Vigliotta G, Miele C, Oriente F, Santopietro S, Giacco F, Condorelli G, Formisano P and Beguinot F. (2003). *Mol. Biol. Cell*, **23,** 4511–4521.

Tsukamoto T, Yoo J, Hwang SI, Guzman RC, Hirokawa Y, Chou YC, Olatunde S, Huang T, Bera TK, Yang J and Nandi S. (2000). *Cancer Lett.*, **149,** 105–113.

Vaidayanathan H and Ramos WJ. (2003). *J. Biol. Chem.*, **278,** 32367–32372.

Vigliotta G, Miele C, Santopietro S, Portella G, Perfetti A, Maitan MA, Cassese A, Oriente F, Trencia A, Fiory F, Romano C, Tiveron C, Tatangelo L, Troncone G, Formisano P and Beguinot F. (2004). *Mol. Cell. Biol.*, **24,** 5005–5015.

Aurora B expression in normal testis and seminomas

P Chieffi, G Troncone[1], A Caleo[1], S Libertini[2], S Linardopoulos[3], D Tramontano[4] and G Portella[2]

Dipartimento di Medicina Sperimentale, II Università di Napoli, Naples, Italy

[1]Dipartimento di Scienze Biomorfologiche e Funzionali, Università di Napoli 'Federico II', Naples, Italy

[2]Dipartimento di Biologia e Patologia Cellulare e Molecolare, Università di Napoli 'Federico II', Naples, Italy

[3]The Breakthrough Breast Cancer Research Centre, London, United Kingdom

[4]Dipartimento di Scienze Biologiche ed Ambientali, Università del Sannio, Benevento, Italy

(Requests for offprints should be addressed to P Chieffi, Dipartimento di Medicina Sperimentale, Via Costantinopoli 16, 80138 Napoli, Italy; Email: Paolo.Chieffi@unina2.it)

Abstract

Aurora/Ipl1-related kinases are a conserved family of proteins that have multiple functions during mitotic progression. High levels of Aurora kinases are characteristic of rapidly dividing cells and tumours. Aurora B encodes a protein that associates with condensing chromatin, concentrates at centromeres, and then relocates onto the central spindle at anaphase. In this study the expression and the localisation of Aurora B throughout germinal epithelial progression in normal testis and its neoplastic counterpart were analysed.

Immunocytochemistry and RT-PCR analysis of mouse germinal epithelium cells showed the presence of Aurora B in spermatogonia and occasionally in spermatocytes. Western blot analysis revealed the typical Aurora B isoform (~41 kDa) in the same cellular types. A similar distribution was observed in human testis by immunohistochemistry. Moreover, the distribution and the expression of Aurora B were investigated in neoplasms derived from germ cells. Surgical samples of seminomas were analysed, and a high percentage of Aurora B positive cells (51%) was detected; the expression of Aurora B was significantly related to the MIB-1 proliferation marker ($R = 0{\cdot}816$).

The data presented here demonstrate that Aurora B expression occurs in spermatogonial division. Furthermore, our results indicate that the expression of Aurora B is a consistent feature of human seminomas.

Journal of Endocrinology (2004) **181,** 263–270

Introduction

Mitosis is a highly coordinated process that ensures the fidelity of chromosome segregation and is characterised by dramatic morphological changes which occur in a strictly sequential order (Cao & Wang 1990). The mechanisms that coordinate the cycle of chromosome condensation and decondensation with the assembly, function, and subsequent disassembly of the mitotic spindle are poorly understood. Highly conserved genes essential for chromosome condensation have been found through genetic screens in yeasts and *Drosophila* (Bhat *et al.* 1996, Sutani *et al.* 1999). Protein phosphorylation has been suggested as an important regulatory mechanism for cytokinesis. Among the protein kinases, serine/threonine protein kinase of the Aurora family (Aurora A/STK-15, Aurora B/AIM-1, Aurora C/AIK-3) are known to be required for the progression through the M phase. It has been shown that the products of the Aurora family genes are expressed in proliferating cells and are overexpressed in neoplastic cells (Tanaka *et al.* 1999). In particular, Aurora B has been found overexpressed in human cancer cells of different origin such as HeLa, Lovo, HT29, and in cell lines derived from colorectal tumours (Tatsuka *et al.* 1998). Moreover, high expression levels of Aurora B were detected in primary human colorectal cancers at various pathologic stages with a tendency to group in higher grades of malignancy defined by pathological observation (Katayama *et al.* 1999). Finally, overexpression of Aurora B in diploid human cells NHDF induced multinuclearity, which is one of the most common features of tumour cells (Tatsuka *et al.* 1998, Terada *et al.* 1998).

During the cell cycle Aurora B (AIM-1) peaks after Aurora A and is prominent at the midzone during anaphase and in postmitotic bridges during telophase. The two kinases display distinct subcellular localisations. Aurora B and its corresponding proteins, *Caenorhabditis elegans* AIR-2, *Xenopus laevis* AIRK2, and *Drosophila* IAL, have roles in cytokinesis (Terada *et al.* 1998). Moreover, double-stranded RNA interference analysis has revealed that Aurora B plays a critical role in chromosome segregation as well as in cytokinesis (Adams *et al.* 2001).

Online version via http://www.endocrinology.org
0022–0795/04/0181–263

Spermatogenesis is a hormonally regulated and unique developmental process whereby diploid stem cells differentiate through an ordered sequence of steps into haploid spermatozoa, highly specialised in structure and function. This process can be divided into mitotic, meiotic, and postmeiotic phases that are synchronised and are an ideal model for studying the control of cellular growth and differentiation. The molecular mechanisms that regulate and coordinate the expression of genes throughout spermatogenesis in vertebrates are not completely understood (Sharpe 1994, Sassone-Corsi 1997).

The aim of this study is to clarify the spatio-temporal localisation of Aurora B kinase in the mouse germinal epithelium progression, and its expression in normal human testis and in testicular neoplastic lesions. Our results document that Aurora B is detected in the germinal epithelium in the spermatogonia and occasionally in spermatocytes. In addition, these data support the notion that Aurora B is involved in germ cell proliferation of normal and neoplastic testis. A high percentage of Aurora B-positive cells in seminomas was detected and the expression of Aurora B was significantly related to the MIB-1 proliferation marker.

Materials and Methods

Preparation of testicular cells

Germ cells were prepared from testes of adult CD1 mice (Charles River Italia, Calco, Italy). Testes were removed from the albuginea membrane and digested for 15 min in 0·25% (w/v) collagenase (type IX, Sigma) at room temperature under constant shaking. They were then washed twice in Minimum Essential Medium (Life Technologies, Inc.), seminiferous tubules were cut into pieces with a sterile blade and further digested in Minimum Essential Medium containing 1 mg/ml trypsin for 30 min at 30 °C. Digestion was stopped by adding 10% fetal calf serum and the germ cells released were collected after sedimentation (10 min at room temperature) of tissue debris. Germ cells were centrifuged for 13 min at 1500 r.p.m. at 4 °C and the pellet resuspended in 20 ml elutriation medium (120·1 mM NaCl, 4·8 mM KCl, 25·2 mM $NaHCO_3$, 1·2 mM $MgSO_4$ ($7H_2O$), 1·3 mM $CaCl_2$, 11 mM glucose, 1 × essential amino acid (Life Technologies, Inc.), penicillin, streptomycin, 0·5% bovine serum albumin). Pachytene spermatocyte and spermatid germ cells were obtained by elutriation of the unfractionated single cell suspension as described elsewhere (Meistrich 1977). Homogeneity of cell populations ranged between 80 and 85% for pachytene spermatocytes, 95% for spermatids, and was routinely monitored morphologically. Mature spermatozoa were obtained from the cauda of the epididymus of mature mice as described previously (Sette *et al.* 1997). Spermatogonia were obtained from prepubertal mice as previously described (Grimaldi *et al.* 1993, Rossi *et al.* 1993).

The NIH-3T3 mouse fibroblasts used in these studies were cultured as recommended by the American Type Culture Collection (Rockville, MD, USA).

Tissue samples

As a source of normal tissue, ten CD1 adult mice were killed and the testes were removed and fixed in Bouin's fluid. Samples were serially dehydrated in ethanol and cleared in xylene before processing on a commercial automated tissue processor. The animals used in the present study were maintained at the Department of Biology and Pathology Animal Facility. The animal experimentations described herein were conducted in accordance with accepted standards of animal care and in accordance with the Italian regulations for the welfare of animals used in experimental studies. The study was approved by our institutional committee on animal care. As a source of neoplastic tissues, paraffin-embedded blocks from ten cases of classic seminoma were retrieved from the files of the Department of Bio-Morphological Sciences at the University 'Federico II' of Naples on the basis of the Faculty of Medicine and Surgery Ethical Committee approval; in all instances, the diagnosis was confirmed on review.

Immunohistochemistry and quantitative analysis

In normal and neoplastic testis the cellular distribution of Aurora B protein was assessed by the polyclonal antibody raised in rabbits (no. 611082; BD Transduction Laboratories, San Diego, CA, USA). The conditions of pretreatment of the histological samples most suitable for Aurora B staining have been determined by preliminary experiments on colon cancer paraffin-embedded sections that express high levels of this protein (Bischoff *et al.* 1998). We observed that regardless of the length of fixation, a proceeding step of the heat-induced antigen retrieval technique yielded a larger number of cells with specific Aurora B nuclear staining (data not shown). Based on these observations, xylene-dewaxed and alcohol-rehydrated paraffin sections were placed in Coplin jars filled with a 0·01 M tri-sodium citrate solution, and heated for 3 min in a conventional pressure cooker. After heating, slides were thoroughly rinsed in cool running water for 5 min. They were then washed in Tris–buffered saline (TBS) pH 7·4 before incubating overnight with the Aurora B (1:1000) antibody. The incubation with the primary antibody was followed by incubation with biotinylated anti-mouse immunoglobulins and by peroxidase-labelled streptavidine (LSAB-DAKO, Copenhagen, Denmark); the signal was developed by using diaminobencidine chromogen as substrate. Negative controls were run

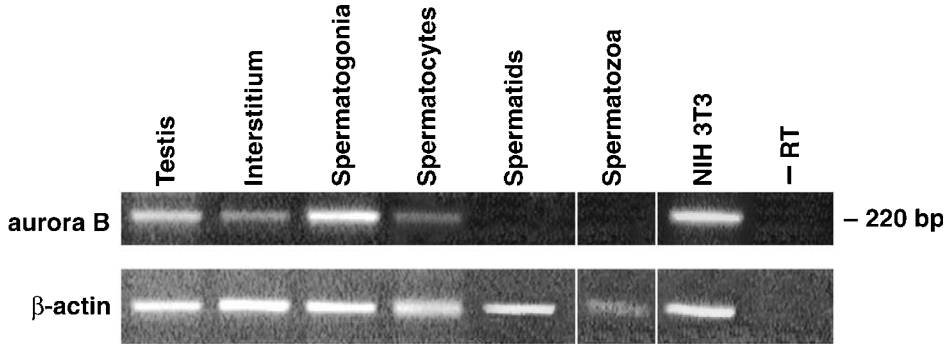

Figure 1 Expression of Aurora B mRNA in mouse testis. RT-PCR analysis of aurora B mRNA in adult mouse testis (lane 1), interstitium (lane 2), normal mouse testis germ cells (lane 3–6), NIH-3T3 cells as a positive control (lane 7), and without reverse transcriptase (− RT, lane 8). Total mRNA was then extracted, reversed transcribed and subjected to PCR analysis using primers (see Materials and Methods). The integrity of mRNA samples was determined by using β-actin as control (lower frame). The RT-PCR analysis is representative of three separate experiments.

with normal mouse serum instead of the primary antibody or the antibody was preabsorbed with the cognate peptide (10^{-6} M).

In order to assess the relationship between Aurora B expression and cell proliferation, seminomas were also stained with the MIB-1 antibody. The antibody (Immunotech, Marseille, France; diluted 1:50) recognised Ki-67, a nuclear protein expressed in the G1, S and G2/M phases; this antibody, known to stain spermatogonia, was also used as a control of antigenic preservation and of successful antigenic retrieval. Labelling indices for Aurora-B and MIB-1 antibodies were determined in the same manner. Adjacent sections were used and counting was performed in similar areas. Quantitative analysis performed with a computerised analyser system (CAS 200, Becton Dickinson, Chicago, USA) was used to score the nuclei of individual cells for expression of Aurora B and MIB-1 proteins. As already described, nuclear boundary optical density and antibody threshold were adjusted for each case examined (Bischoff *et al.* 1998). A minimal threshold was established by counting at least 1000 neoplastic cells per seminoma sample. In each case the distributions of Aurora B and MIB-1 proteins were evaluated and expressed as percentages of the total cell population. Data are reported as median and ranges. Statistical analysis was performed by means of the SPSS Inc. package (SPSS, Chicago, IL, USA). The relationship between Aurora B and MIB-1 immunostaining was analysed by calculating the nonparametric Spearman R coefficient. A P value less than 0·05 was considered significant.

Protein extraction and Western blot analysis

Mouse testes were homogenised directly into lysis buffer (50 mM HEPES, 150 mM NaCl, 1 mM EDTA, 1 mM EGTA, 10% glycerol, 1% Triton-X-100, 1 mM phenylmethylsulphonyl fluoride, 1 μg aprotinin, 0·5 mM sodium orthovanadate, 20 mM sodium pyrophosphate). The lysates were clarified by centrifugation at 14 000 × **g** for 10 min. Protein concentrations were estimated by a Bio-Rad assay (Bio-Rad, München, Germany), and boiled in Laemmli buffer (Tris–HCl (pH 6·8) 0·125 M, SDS 4%, glycerol 20%, 2-mercaptoethanol 10%, Bromophenol Blue 0·002%) for 5 min before electrophoresis. Proteins were subjected to SDS-PAGE (10% polyacrylamide) under reducing conditions. After electrophoresis, proteins were transferred to nitrocellulose membranes (Immobilon Millipore Corporation, Bedford, MA, USA); complete transfer was assessed using prestained protein standards (Bio-Rad, Hercules, CA, USA). After blocking with TBS-BSA (25 mM Tris, pH 7·4, 200 mM NaCl, 5% bovine serum albumin), the membrane was incubated with the primary antibody against Aurora B (1:400; #611082, BD Transduction Laboratories) and α-tubulin (1:500; clone DM1A, Sigma-Aldrich, Milan, Italy) for 1 h (at room temperature). Membranes were then incubated with the horseradish peroxidase-conjugated secondary antibody (1:10 000) for 45 min (at room temperature) and the reaction was detected with an ECL system (Amersham Life Science, UK).

RNA extraction and RT-PCR

Total RNA was extracted from cells and tissue using the RNAzol kit (Tel-Test, Inc., Friendswood, TX, USA) according to standard procedures. Total RNA (1 mg) was extracted from specimens (Tel-Test, Inc.) and reverse transcribed (Life Technologies Italia srl). cDNA was amplified using Aurora B specific primers. The primers used were as follows: Aurora B forward: 5′-TTG ACA ACT TTG AGA TTG GG-3′; Aurora B reverse: 5′-GCT GGT CGT AGA AGT AGT TGT-3′. Expression of the

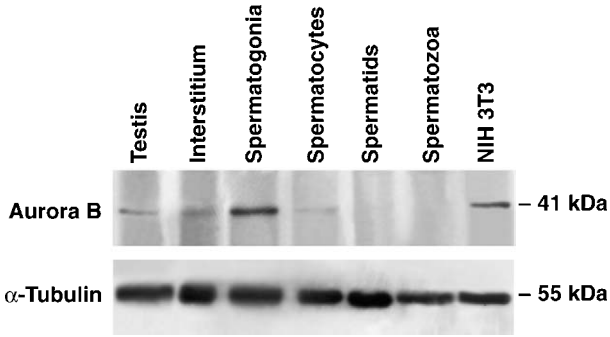

Figure 2 Distribution of Aurora B protein in mouse testis. Western blot analysis of aurora B protein in mouse adult testis (lane 1), interstitium (lane 2), normal mouse testis germ cells (lane 3–6), and NIH-3T3 cells as a positive control (lane 7) (40 μg/lane). Whole lysates were detected by Western blotting with anti-Aurora B polyclonal serum. The specific band of about 41 kDa was identified by comparison with comigrating size markers (Bio-Rad, Melville, NY, USA). α-Tubulin (Sigma) was used to assess the equal amounts of protein. The blots are representative of three separate experiments.

β-actin gene was utilised as an internal control for the amount of cDNA in the PCRs by using the following primers: β-actin forward: 5′-GTC AGG CAG CTC ATA GCT CT-3′; β-actin reverse: 5′-TCG TGCGTG ACATTA AAG AG-3′. PCR amplification was performed at 94 °C (1 min), 52 °C (1 min), and 72 °C (1 min) for 30 cycles. Reaction products were subjected to agarose gel electrophoresis. Samples amplified without previous reverse transcription were used to confirm that the signal was not due to amplification of contaminating DNA (data not shown).

Results

Aurora B expression in the mouse testicular cells

Aurora B expression in various mouse testis cells was evaluated by the RT-PCR method. Aurora B mRNA was expressed in germ cells almost exclusively in spermatogonia (spg) with a faint band present in spermatocytes (spc) (Fig. 1); a band was also detected in the interstitial cells (Fig. 1).

Western blot analysis of whole mouse testis and cell extracts from fractionated adult testis cells showed a single product migrating as a 41 kDa protein (Fig. 2). Among germ cells, it was abundant in spg, present in a few spc, and absent in spermatids (spt) and spermatozoa (spz), in agreement with the RT-PCR results. Aurora B protein was also present in the interstitial extract cells indicating a proliferative activity of these cells (Fig. 2).

Immunohistochemical analysis of Aurora B protein in mouse testis

Immunocytochemistry was performed on serial mouse testis sections using an antibody against Aurora B protein.

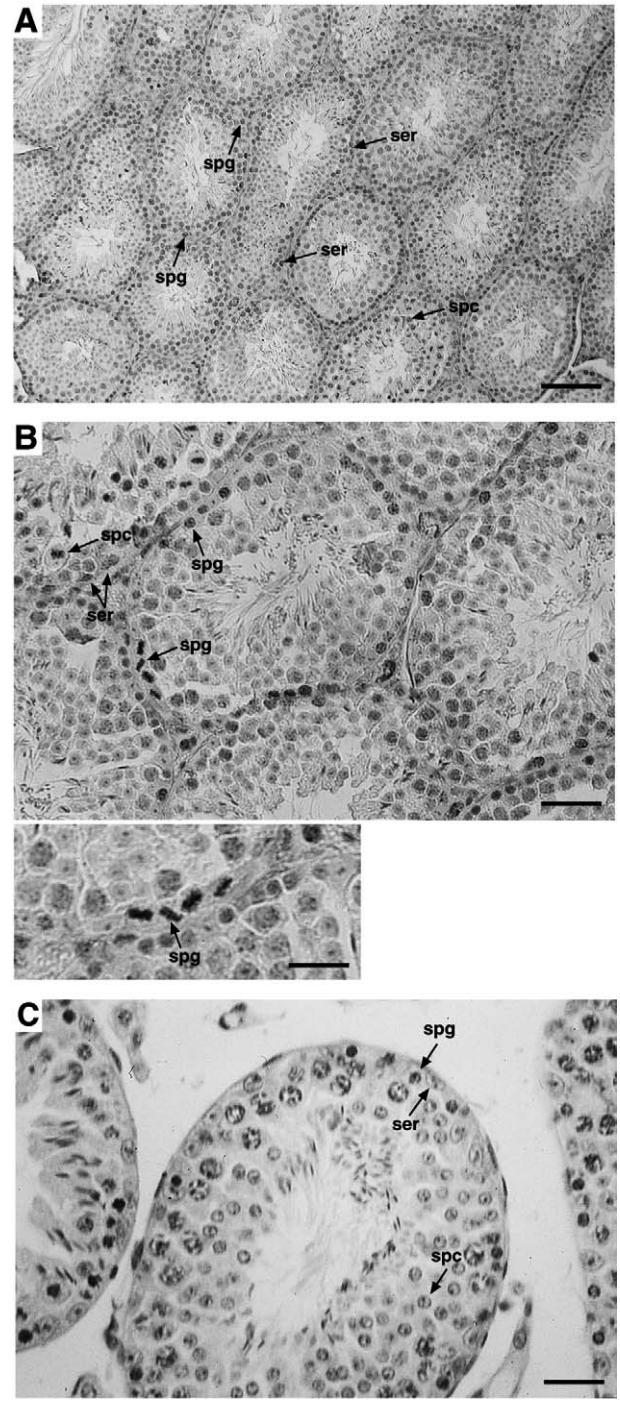

Figure 3 (A) Localisation of the Aurora B protein in sections of adult mouse testis by immunocytochemistry. Representative seminiferous tubules show staining in the spermatogonia (spg) and spermatocytes (spc). ser, Sertoli cells. Bar=100 μm. (B) Higher magnification showing specific staining for Aurora B in spg, spc and Sertoli cells (ser). Bar=50 μm. Lower panel: spg in mitotic metaphase showing Aurora B immunostaining. Bar=25 μm. (C) Control section using the antibody preabsorbed with the cognate peptide (10^{-6} M); symbols are as indicated above. Bar=50 μm.

A

	Ki-67	Aurora B
Number of cases	10	10
mean	62	46
median	66	51
range	41 - 79	29 - 55

B

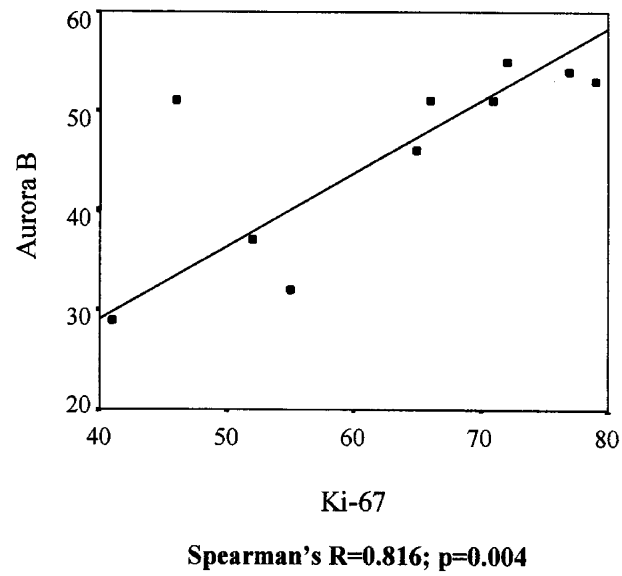

Figure 4 (A) Analysis of Ki-67 and Aurora B expression in seminomas. Values are reported as percentage of immunopositive cells. (B) Spearman analysis of the relationship between Ki-67 and Aurora B.

A topological regular expression of Aurora B was observed in seminiferous tubules with complete spermatogenesis (Fig. 3A). The protein was found in the spg and occasionally in spc (pachytene stage) and Sertoli cells (ser, Fig. 3B). In particular, immunoreactive spg showed intense metaphase mitotic figures (Fig. 3B, lower panel). On the other hand, Aurora B expression was not detectable in maturing germ cells. In fact, no labelling was seen in many primary and secondary spc, spt and spz (Fig. 3B).

The antiserum used in this study fulfils the criteria of specificity. In particular, immunoabsorption tests revealed that the labelling was quenched by preincubating antibody with 10^{-6} M of the cognate peptide (Fig. 3C).

Aurora B expression in the normal human testis and in seminomas

The vast majority of testicular cancers arise from germ cells. Premeiotic germ cells have been suggested to be the precursor for male germ cell tumours; therefore Aurora B expression was examined in a series of seminomas (Chaganti *et al.* 1994). Immunohistochemical analysis was performed in 10 cases of 'classical type' seminomas. In all cases examined a variable percentage of the neoplastic population was stained (range 29–55) as shown in Fig. 4A. The pattern of Aurora B staining in seminomas differed significantly from the pattern observed in mouse testis. Also, in the non neoplastic tissue adjacent to the neoplasia the staining pattern was limited to the basal spg and a few spc, with maturing cells being devoid of signal (Fig. 5A). As shown in Fig. 3, Aurora B-positive cells were irregularly distributed throughout the neoplastic tissue with a strong signal (Fig. 5B). Interestingly, individual dividing cells showed the most intense signal (Fig. 5B, insert).

We next compared the expression in seminomas of Aurora B to Ki-67, a well known proliferation marker, by using MIB-1 antibody. Similar to Aurora B, MIB-1 antibody was also more evident in tumours than in adjacent areas, with the percentage of Ki-67 stained cells ranging from 41–79 (Fig. 4A). Taking into account the overall data, Aurora-B expression showed a highly statistical correlation with Ki-67 ($R=0{\cdot}816$; $P=0{\cdot}004$, Fig. 4B).

It is noteworthy that the percentage of Aurora-B-positive cells was lower than the Ki-67-positive cell population, indicating that a subset of Ki-67-positive cells is also positive for Aurora B. In fact, Ki-67 was expressed by the very large majority of tumour cells (median percentage 66%), whereas the median percentage of Aurora B-positive cells was 51% of the total tumour cells (Fig. 4A).

Discussion

Spermatogenesis in mammals is characterised by a well-defined sequence of mitotic and meiotic divisions that lead to the production of mature spermatozoa. However, testicular development and normal spermatogenesis require specialised molecular mechanisms that ensure stringent stage-specific gene expression (McCarrey 1993, Chieffi *et al.* 2002).

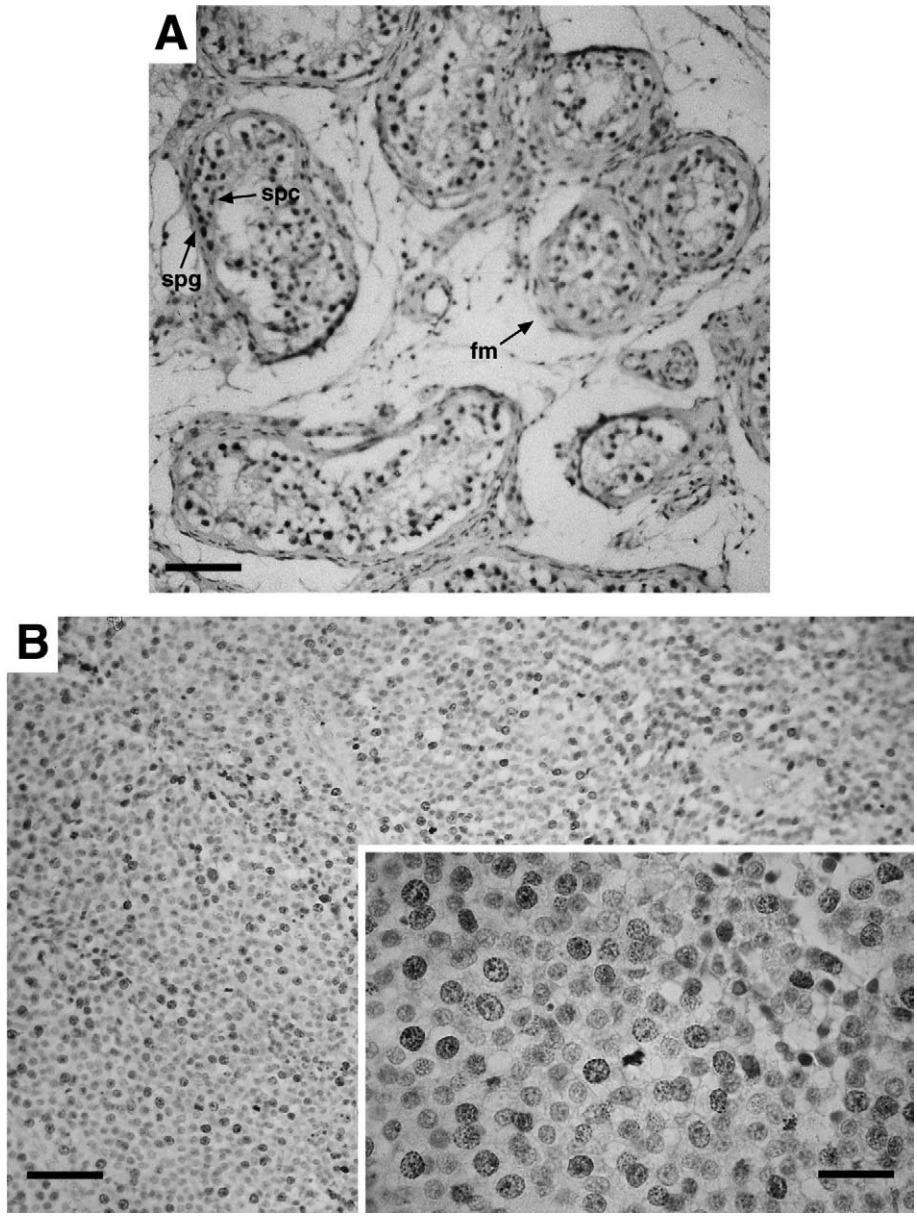

Figure 5 (A) Localisation of the Aurora B protein in sections of normal human testis by immunocytochemistry. Representative seminiferous tubules show staining in the spg and spc whereas stromal cells and fibromyocytes (fm) are devoid of signal. Bar=75 μm. (B) Paraffin-embedded section of seminoma (seminoma #6) showing extensive immunoreactivity for Aurora B protein. Bar=75 μm. Insert: at high magnification note the presence of a clear signal in neoplastic germ cells. Bar=25 μm.

In this study we have characterised the expression and the localisation of Aurora B in the testis and have demonstrated that mRNA and protein are present strongly and specifically in mitotic mouse germinal and interstitial cells, and absent in the meiotic and post-meiotic lineage cells.

Testicular tumours are rare, comprising 2% of all cancers in men; however, testicular cancer is the most common malignancy affecting males aged 20–35 years (Senturia 1987, Leendert *et al.* 1999). Because the molecular basis of these cancers needs to be elucidated, identification of cellular genes involved in testicular tumorigenesis could

increase our understanding of the development of testicular tumours, thus providing the basis for new targeted therapies.

There are at least three Aurora–related kinases in mammals, Aurora A (STK-15), Aurora B (AIM-1), and Aurora C (STK-13). All three mammalian members of this family are overexpressed in human cancer cells. Aurora A (STK-15) has been found to be overexpressed in half of all colorectal and breast cancers (mapped to 20q13) and it is highly expressed in the meiotic testicular cells. Aurora A (STK-15) is predominantly localised to centrosomes and its overexpression is supposed to be related to multiple centrosome production (Yanai *et al.* 1997, Bischoff *et al.* 1998, Giet & Prigent 1999, Zhou *et al.* 1998). Aurora C (STK-13) is also overexpressed in colorectal cancers (Takahashi *et al.* 2000).

Overexpression of Aurora B (AIM-1) has been observed in human neoplastic cell lines and in colorectal tumours (Tatsuka *et al.* 1998, Katayama *et al.* 1999). Recently, Aurora B has been shown to phosphorylate histone H3 at Ser-10 during mitosis *in vivo* (Ota *et al.* 2002). Expression of a kinase-negative form of Aurora B in Chinese hamster embryo cells (CHE) suppresses mitotic phosphorylation of histone H3 at Ser-10 (Terada *et al.* 1998). Mitotic phosphorylation of histone H3 at Ser-10 is critical for proper chromosome condensation and segregation (Terada *et al.* 1998). This has been demonstrated in *Tetrahymena* by abnormal chromosome segregation in a histone H3 mutant unable to undergo Ser-10 phosphorylation (Wei *et al.* 1999). Recent experiments performed by Sassoni-Corsi and coworkers clearly showed that Aurora B physically interacts with the H3 tail (Crosio *et al.* 2002); these data are of particular interest since the amino-terminal tail of histone H3 is able to bind its mitotic kinase from *Xenopus* egg extract (de la Barre *et al.* 2000). It has been clearly demonstrated that Aurora B overexpression induces increased mitotic H3 phosphorylation at Ser-10 (Ota *et al.* 2002), and phosphorylation imbalance induced by Aurora B overexpression might explain the errors in cytokinesis responsible for the appearance of multinuclear cells (Tatsuka *et al.* 1998). It is noteworthy that a significant overexpression of Aurora B has been observed in human cancer cell lines and in colorectal tumours in these lesions elevated expression was clearly observed in the neoplastic mitotic cells and Aurora B expression levels were increased as a function of Dukes' stage. (Tatsuka *et al.* 1998, Katayama *et al.* 1999)

In the present study, we show that Aurora B expression is a consistent feature of human seminomas, where its topological staining pattern is lost. The increase in Aurora B expression showed a positive correlation with the Ki-67 protein. It is important to note that Aurora B-positive staining in human seminomas does not completely overlap with the expression of Ki-67. The expression of Ki-67 occurs in all phases of the cell cycle excluding G0; therefore, Ki-67 immunostaining identifies all proliferating cells. Conversely, immunostaining against Aurora B may be capable of identifying, with more specificity, those cells progressing to G2/M, beyond the restriction point, indicating that Aurora B staining could provide different biological and clinical information. However, further experiments are required to assess the different expression of Aurora B and other proliferative markers.

Aurora B expression levels are regulated at both the mRNA and protein levels, with maximal mRNA and protein levels occuring during the G2/M phases (Terada *et al.* 1998). This cyclical pattern of regulation is conserved in cancer cells (Tatsuka *et al.* 1998). This indicates that the effects of Aurora B overexpression may be of critical importance during the G2/M phases of the cell cycle. The sequence of these events is essential for normal mitotic cell division in spermatogenesis and clearly overexpression of Aurora B may have implications for the abnormalities in germ cell maturation, such as those that occur in testicular cancer. Taken together, our data support a role for Aurora B in testicular mitotic germ cell maturation and, possibly, in the initiation and/or progression of testicular cancers.

In conclusion, we have shown that Aurora B expression occurs during spematogonial proliferation; in addition, expression of Aurora B is a consistent feature of human seminomas. This observation is of clinical interest since Aurora B might be a target for cancer treatment and may serve as a prognostic marker.

Funding

This work was supported by a Grant from the Second University of Naples, by the Associazione Italiana per la Ricerca sul Cancro (AIRC), and by COFIN-PRIN (2002).

References

Adams, RR, Carmena M & Earnshaw WC 2001 Chromosomal passengers and the (aurora) ABCs of mitosis. *Trends in Cellular Biology* **11** 49–54.

de la Barre AE, Gerson V, Gout S, Creaven M, Allis D & Dimitrov S 2000 Core histone N-termini play an essential role in mitotic condensation. *EMBO Journal* **19** 379–391.

Bhat MA, Philip AV, Glover DM & Bellen HJ 1996 Chromatid segregation at anaphase requires the barren product, a novel chromosome-associated protein that interacts with Topoisomerase II. *Cell* **87** 1103–1114.

Bischoff JR, Anderson L, Zhu Y, Mossie K, Ng L, Souza B, Schryver B, Flanagan P, Clairvoyant F, Ginther C, Chan CS, Novotny M, Slamon DJ & Plowman GD 1998 A homologue of *Drosophila* aurora kinase is oncogenic and amplified in human colorectal cancers. *EMBO Journal* **17** 3052–3065.

Cao LG & Wang YL 1990 Mechanism of the formation of contractile ring in dividing cultured animal cells. II. Cortical movement of microinjected actin filaments. *Journal of Cell Biology* **111** 1905–1911.

Chaganti RSK, Rodriguez E & Mathew S 1994 Origin of adult male mediastinal germ-cell tumors. *Lancet* **343** 1130–1132.

Chieffi P, Battista S, Barchi M, Di Agostino S, Pierantoni MG, Fedele M, Chiariotti L, Tramontano D & Fusco A 2002 HMGA1 and HMGA2 protein expression in mouse spermatogenesis. *Oncogene* **21** 3644–3650.

Crosio C, Fimia GM, Loury R, Kimura M, Okano Y, Zhou H, Sen S, Allis D & Sassone-Corsi P 2002 Mitotic phosphorylation of histone H3: spatio-temporal regulation by mammalian aurora kinase. *Molecular Cellular Biology* **22** 874–885.

Giet R & Prigent C 1999 Aurora/Ipl1-related kinases, a new oncogenic family of mitotic serine-threonine kinases. *Journal of Cell Science* **112** 3591–3601.

Grimaldi P, Piscitelli D, Albanesi C, Blasi F, Geremia R & Rossi P 1993 Identification of 3′,5′-cyclic adenosine monophosphate-inducible nuclear factors binding to the human urokinase promoter in mouse Sertoli cells. *Molecular Endocrinology* **7** 1217–1225.

Katayama H, Ota T, Jisaki F, Ueda Y, Tanaka T, Odashima S, Suzuki F, Terada Y & Tatsuka M 1999 Mitotic kinase expression and colorectal cancer progression. *Journal of the National Cancer Institute* **91** 1160–1162.

Leendert HJ, Looijenga J & Wolter Oosterhius J 1999 Pathogenesis of testicular germ cell tumours. *Journal of Reproduction and Fertility* **4** 90–100.

McCarrey JR 1993 Development of germ cell. In *Cell and Molecular Biology of the Testis*, pp 58–89. Eds C Desjardins & LL Ewing. New York: Oxford University Press.

Meistrich ML 1977 Separation of spermatogenic cells and nuclei from rodent testes. *Methods in Cell Biology* **15** 15–54.

Ota T, Suto S, Katayama H, Han ZB, Suzuki F, Maeda M, Tanino M, Terada Y & Tatsuka M 2002 Increased mitotic phosphorylation of histone H3 attributable to AIM-1/Aurora B overexpression contributes to chromosome number instability. *Cancer Research* **62** 5168–5177.

Rossi P, Dolci S, Albanesi C, Grimaldi P, Ricca R & Geremia R 1993 Follicle-stimulating hormone induction of steel factor (SLF) mRNA in mouse Sertoli cells, and stimulation of DNA synthesis in spermatogonia by soluble SLF. *Developmental Biology* **155** 68–74.

Sassone-Corsi P 1997 Transcriptional checkpoints determining the fate of male germ cells. *Cell* **88** 163–166.

Senturia YD 1987 The epidemiology of testicular cancer. *British Journal of Urology* **60** 285–291.

Sette C, Bevilacqua A, Bianchini A, Mangia F, Geremia R & Rossi P 1997 Parthenogenetic activation of mouse eggs by microinjection of a truncated c-kit tyrosine kinase present in spermatozoa. *Development* **124** 2267–2274.

Sharpe RM 1994 Regulation of spermatogenesis. In *The Physiology of Reproduction*, pp 1363–1434. Eds E Knobil & JD Neil. New York: Raven Press.

Sutani T, Yuasa T, Tomonaga T, Dohomae N, Takio K & Yanagida M 1999 Fission yeast condensin complex: essential roles of non-SMC subunits for condensation and Cdc2 phosphorylation of Cut3/SMC4. *Genes and Development* **13** 2271–2283.

Takahashi T, Futamura M, Yoshimi N, Sano J, Katada M, Takagi Y, Kimura M, Yoshioka T, Okano Y & Saji S 2000 Centrosomal kinases, HsAIRK1 and HsAIRK3, are overexpressed in primary colorectal cancers. *Japanese Journal of Cancer Research* **91** 1007–1014.

Tanaka T, Kimura M, Matsunaga K, Fukada D, Mori K & Okano Y 1999 Centrosomal kinase AIK1 is overexpressed in invasive ductal carcinoma. *Cancer Research* **59** 2041–2044.

Tatsuka M, Katayama H, Ota T, Tanaka T, Odashima S, Suzuki F & Terada Y 1998 Multinuclearity and increased ploidy caused by overexpression of the aurora- and Ipl1-like midbody-associated protein mitotic kinase in human cancer cells. *Cancer Research* **58** 4811–4816.

Terada Y, Tatsuka M, Suzuki F, Yasuda Y, Fujita S & Otsu MA 1998 AIM-1: a mammalian midbody-associated protein required for cytokinesis. *EMBO Journal* **17** 667–676.

Wei Y, Yu L, Bowen J, Gorovsky MA & Allis CD 1999 Phosphorylation of histone H3 is required for proper chromosome condensation and segregation. *Cell* **97** 99–109.

Yanai A, Arama E, Kilfin G & Motro B 1997 Ayk1, a novel mammalian gene related to *Drosophila* aurora centrosome separation kinase, is specifically expressed during meiosis. *Oncogene* **14** 2943–2950.

Zhou H, Kuang J, Zhong L, Kuo WL, Gray JW, Sahin A, Brinkley BR & Sen S 1998 Tumour amplified kinase STK15/BTAK induces centrosome amplification, aneploidy and transformation. *Nature Genetics* **20** 189–193.

Received 26 November 2003
Accepted 6 February 2004

0021-972X/03/$15.00/0
Printed in U.S.A.

The Journal of Clinical Endocrinology & Metabolism 88(10):5027–5032

doi: 10.1210/jc.2003-030385

ONYX-015 Enhances Radiation-Induced Death of Human Anaplastic Thyroid Carcinoma Cells

GIUSEPPE PORTELLA, ROBERTO PACELLI, SILVANA LIBERTINI, LAURA CELLA, GIANCARLO VECCHIO, MARCO SALVATORE, AND ALFREDO FUSCO

Dipartimento di Biologia e Patologia Cellulare e Molecolare (G.P., S.L., G.V., A.F.), Università di Napoli Federico II, Istituto di Biostrutture e Bioimmagini Consiglio Nazionale delle Ricerche (R.P., L.C.), and Dipartimento di Diagnostica per Immagini e Radioterapia (M.S.), Università di Napoli Federico II, 80131 Naples

ONYX-015 is a genetically modified adenovirus with a deletion of the E1B early gene and therefore is designed to replicate preferentially in p53-mutated cells causing their death. We previously demonstrated that the ONYX-015 virus kills anaplastic thyroid carcinoma (ATC) cells and enhances the antineoplastic effects of doxorubicin and paclitaxel. Here we report that ONYX-015 increased the cytopathic effect of radiotherapy in three ATC cell lines. In fact, ONYX-015 and radiation induced a significant cytopathic effect on ATC cells. DNA fragmentation analysis showed that ATC ONYX-015-treated cells were very sensitive to radiation-induced apoptosis. In addition, low doses of ONYX-015 associated with a single radiation dose of 10 Gy delayed the growth of a xenograft tumor induced by ARO cells in athymic mice. Our results suggest that the combination of ONYX-015 and radiotherapy should be considered for experimental trials in patients with anaplastic thyroid carcinoma. (*J Clin Endocrinol Metab* 88: 5027–5032, 2003)

ANAPLASTIC THYROID CARCINOMA (ATC) accounts for about 2% of all human thyroid neoplasias (1, 2) and, being resistant to conventional antineoplastic therapy (3), it is one of the most lethal human neoplasms. ONYX-015 is an attenuated adenovirus that does not replicate efficiently in cells bearing a normal p53 gene; however, it replicates efficiently in tumor cells that lack either functional p53 or p14 Arf, so causing their death (4–6). Because mutations in the p53 gene are a feature of ATC (7–12), ONYX-015 seems a prime candidate as an antineoplastic agent in this type of tumor. The ONYX-015 virus has already been tested in phase II and III clinical trials for the treatment of squamous cell cancers of the head and neck (13, 14), in phase I and II trials for primary and secondary liver tumors (15–17), and in a phase I trial for primary carcinoma of the pancreas (18).

We previously showed that the ONYX-015 virus kills ATC cells and reduces the growth of ATC tumor xenografts (19). We also showed that ONYX-015 enhances the antineoplastic effects of doxorubicin and paclitaxel in ATC cells. These results suggested that ONYX-015 might be envisaged for the treatment of ATC. However, although the ONYX-015 virus has proven to be biologically active and safe in cancer patients (20), it is unlikely to be effective as monotherapy because few cancers are cured with a single agent. For example, treatment with ONYX-015, cisplatin, and 5-fluorouracil resulted in a higher number of complete responses *vs.* ONYX-015 alone in patients with head and neck cancer (13). In addition, ONYX-015 enhanced the effect of standard chemotherapy in primary lung cancer cells and in nude mice human tumor xenografts (21, 22).

The aim of our study was to investigate the effect of ONYX-015 plus radiotherapy, which is frequently used to control local tumor growth, on the proliferation of human ATC cell lines. Here we report that ONYX-015 therapy enhanced radiation-induced cell death. The combination of ONYX-015 and radiotherapy also significantly delayed the growth of xenograft tumors induced in athymic mice by the injection of ATC cells.

Abbreviations: ATC, Anaplastic thyroid carcinoma; CMV, cytomegalovirus; MOI, multiplicity of infection; pfu, plaque-forming units.

Materials and Methods

Viruses

ONYX-015 (a gift from Dr. A. Balmain, University of California San Francisco Cancer Center and Cancer Research Institute, San Francisco, California; and Dr. I. Ganly, Cancer Research UK Beatson Laboratories, Bearsden, UK) is a chimeric human group C adenovirus (Ad2 and Ad5) that has a deletion between nucleotides 2496 and 3323 in the E1B region that encodes the 55-kDa protein. In addition, there is a C to T transition at position 2022 in region E1B that generates a stop codon at the third codon of the protein. These alterations prevent the expression of the 55-kDa protein in ONYX-015-infected cells (4).

Ad5 CMV *lacZ* (Quantum Biotechnology, Carlsbad, CA) is a nonreplicating E1-deleted adenovirus in which the reporter construct *lacZ* has been inserted in the E1 region under the control of the cytomegalovirus (CMV) promoter. We used the Ad5 CMV *lacZ* adenovirus as a control in clonogenic assays and *in vivo* experiments. Viral stocks were expanded in the human embryonic kidney 293 cell line, which expresses the E1 region of Ad2, and purified, as previously reported (19). Stocks were stored at −70 C after the addition of glycerol to a concentration of 50% vol/vol. Virus titer was determined by plaque-forming units (pfu) on the human embryonic kidney 293 cells.

Cell lines

ARO (23) and FRO (8), human thyroid anaplastic carcinoma cell lines, were obtained by Dr. G. Juillard (University of California Los Angeles); ARO and FRO cell lines are a kind gift of Prof. J. A. Fagin (University of Cincinnati College of Medicine, Cincinnati, OH); and KAT-4 (24) cells were obtained from Dr. K. B. Ain (University of Kentucky, Lexington, KY). Cells were grown in DMEM supplemented with 10% fetal calf serum and ampicillin/streptomycin.

ARO and KAT-4 harbor a mutated *p53* gene, *i.e.* 273 Arg->His,

whereas FRO cells express very low levels of p53 but do not have a p53 gene mutation (19).

Clonogenic assay

Cells were seeded at a density of 2×10^5 in 60-mm plates and infected with ONYX-015 or with a nonreplicating E1-deleted adenovirus with the lac Z reporter construct (Ad5 CMV *lacZ* virus) at multiplicity of infection (MOI) of 0.1 and 0.5 per cell for ARO, 0.5 and 1 per cell for KAT-4 cell line. FRO cell line was infected with a MOI of 0.5 and 2.5. An uninfected dish was used as a control. Cells were harvested 24 h later, plated at a density of 200 cells/plate (three replicates), and irradiated at a dose of 2, 4, or 6 Gy. Cells were incubated for 12 d to allow colony formation to occur. The colonies were stained with crystal violet, and colonies constituted by more than 40 cells were counted. The mean colony count in the three different plates per MOI, Gy dose, and both was calculated and expressed relative to the uninfected and untreated control. The results shown are the average of three different experiments

DNA fragmentation

To analyze the time dependency of apoptotic DNA fragmentation, ARO cells were plated in 96-well plates (1×10^3 in 100-μl medium) and treated with ONYX-015 (0.1 or 0.5 pfu/cell), radiation, or both. Cells were left for 48 h and then lysed. Apoptosis was measured in triplicate samples using the Cell Death Detection ELISA plus kit (Roche, Mannheim, Germany). This photometric sandwich enzyme-immunoassay determines cytoplasmic histone-associated DNA fragments (mono and oligo nucleosomes) upon induction of cell death. Briefly, a mixture of biotin-labeled antihistone and peroxidase-conjugated anti-DNA antibodies was added to the cell lysates and placed in a streptavidin-coated microtiter plate. During incubation, the antihistone antibody binds to the histone-competent apoptotic nucleosomes and links the immunocomplex to the streptavidin-coated plates via its biotinylation. The amount of nucleosomes by peroxidase activity was determined spectrophotometrically at 405 nm with 2,2′-azino-*bis*(3-ethylbenzthiazoline-6-sulfonic acid) as a substrate (Microplate reader, Bio-Rad, Munich, Germany). Results were expressed as relative amounts of apoptosis, being the results of the negative control equalized to 1.

Tumorigenicity assay

All experiments were performed with 6-wk-old male athymic mice (Charles River, Calco, Lecco, Italy). ARO cells (5×10^5) were injected into the right flank of 60 athymic mice. After 15 d, the animals were divided into four groups (15 animals/group), and tumor volume was evaluated. ONYX-015 (5×10^6 pfu) was injected in the peritumoral area in two groups for a consecutive 4 d. On d 5, at the end of viral treatment, a control group and a virus-treated group were anesthetized, and a single radiation dose of 10 Gy was administered on the tumor volume at a distance of 80 cm with a bolus interposition to avoid lower doses at the tumor external edge. Tumor diameters were measured with calipers every second day by two blind and neutral observers until the animals were killed. No mouse showed signs of wasting or other indications of toxicity.

Tumor volumes (V) were calculated with the rotational ellipsoid formula: $V = A \times B2/2$ (A, axial diameter; B, rotational diameter).

The same schedule was used for a control experiment with the replication-defective virus Ad5 CMV *lacZ* virus. Briefly, 40 athymic mice were inoculated sc with 1×10^6 ARO cells, and 15 d later, when tumors became detectable, 5×10^6 pfu of Ad5 CMV *lacZ* virus were injected peritumorally for a consecutive 4 d in 20 animals. Ten animals treated with Ad5 CMV *lacZ* virus and 10 untreated animals were then irradiated with a single dose of 10 Gy.

All mice were maintained at the Dipartimento di Biologia e Patologia Animal Facility. The animal experimentations described herein were conducted in accordance with accepted standards of animal care and in accordance with the Italian regulations for the welfare of animals used in studies of experimental neoplasia, and the study was approved by our institutional committee on animal care.

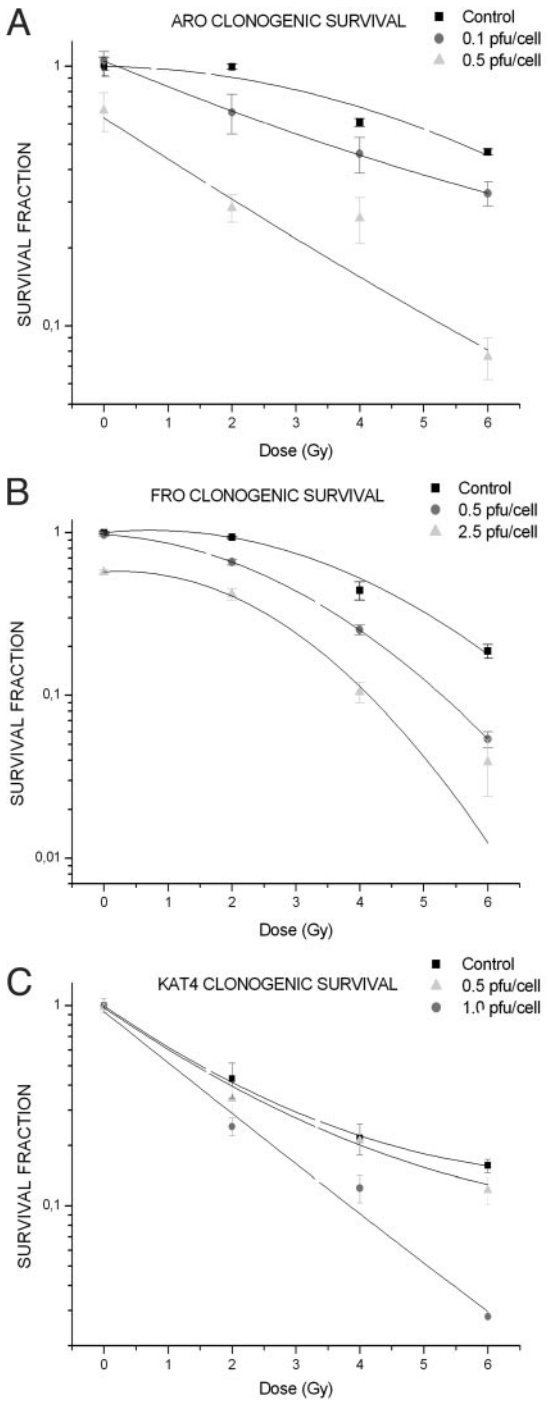

FIG. 1. ONYX-015 and radiation induced cell killing of human anaplastic thyroid carcinoma cell lines. ARO cells were infected with a MOI of 0.1 and 0.5 per cell, KAT-4 with a MOI of 0.5 and 1 per cell. FRO cell line was infected with a MOI of 0.5 and 2.5 per cell. After 24 h cells were irradiated with 2, 4, or 6 Gy. Control cells were irradiated at the indicated doses. Cells were incubated for 12 d to allow colony formation to occur, and colonies greater than 40 cells were counted. A, Clonogenic survival of ARO cells treated with ONYX and radiation. B, Clonogenic survival of FRO cells treated with ONYX and radiation. C, Clonogenic survival of KAT-4 cells treated with ONYX and radiation. Data are presented as mean ± SE of three replicate cultures. The lines are statistically significant bi-exponential fit.

Statistical analysis

Comparison among different treatment groups in the experiments was made by the ANOVA method and the Dunnett's *post hoc* test using a commercial software (SPSS Inc., Chicago, IL). For each cell line, comparison among cell survivals at different doses was made using ONYX-015 concentration as the grouping variable. Assessment of differences among rate of tumor growth in mice was made for each time point of the observation period; treatment groups were control, ONYX-015, radiotherapy, and ONYX-015 + radiotherapy.

Results

ONYX-015 increases the radiation-induced death of human thyroid anaplastic carcinoma cells

To evaluate the efficacy of ONYX-015 combined with radiation treatment, three ATC-derived human cell lines (ARO, KAT-4, and FRO) were used. ARO cells were infected with a MOI of 0.1 and 0.5 per cell, KAT-4 with a MOI of 0.5 and 1 per cell. FRO cell line was infected with a MOI of 0.5 and 2.5 per cell.

Twenty-four hours later, cells were irradiated with different doses (2, 4, or 6 Gy), and the cytotoxicity and the synergistic effects were evaluated. At these doses, radiation does not affect ONYX-015 DNA replication or DNA integrity. In fact, even a dose as high as 20 Gy does not alter virus integrity (25). A MOI of 1 or 2.5 was required to obtain an adjuvant effect of ONYX-015 on FRO cells. This is consistent with our previous finding that FRO cells are more resistant than ARO cells to adenovirus infection (19). However, in this previous study FRO cells were treated with 10 pfu/cell of ONYX-015 for 7 d, and a viability assay was used to assess the effects of the treatment yielding a survival fraction of about 90%. In the present study, FRO cells yield a survival fraction 55% at 2.5 pfu/cell of ONYX-015. The different treatment time and the different methods used to assess the effect of the replicating virus ONYX-015 can explain the discrepancy between these studies.

ONYX-015 enhanced the cytopathic effects of radiotherapy in all cell lines tested (Fig. 1). This enhancement was statistically significant at the doses of 2, 4, and 6 Gy for ARO cells (Dunnett's *post hoc* test, $P < 0.01$) with a MOI of 0.5, and for FRO cells (Dunnett's *post hoc* test, $P < 0.05$) with a MOI of 2.5. For KAT-4 cells a significant effect (Dunnett's *post hoc* test, $P < 0.05$) was observed at a dose of 6 Gy with a MOI of 1.0. In particular, the enhancement factor for a radiation-induced clonogenic inhibition of 50% in ARO cells pretreated with 0.1 pfu/cell of ONYX-015 was 1.55. Conversely, infection with a replication-defective virus bearing deletions of E1A and E1B that contains a *lac*Z reporter gene does not induce any significant additive or synergistic effects upon radiation treatment (Table 1). These results indicate that ONYX-015 could be used in association with radiotherapy to treat ATC because low viral concentration results in significant cell killing upon radiation.

DNA fragmentation of human thyroid anaplastic carcinoma cells infected with ONYX-015 and irradiated

We evaluated the capability of ONYX-015 to induce apoptosis in irradiated ATC cells using an ELISA-based assay to measure cytosolic apoptotic nucleosomes. ARO cells were infected with 0.1 or 0.5 pfu/cell of ONYX-015, and 24 h later the cells were irradiated with 2 Gy. Cells were left for 48 h and then lysed. The infection of ARO cells with 0.1 or 0.5 pfu/cell of ONYX-015 greatly increased the DNA fragmentation of ARO with respect of untreated or not infected control cells (Fig. 2).

Reduced growth of tumor xenografts of ATC cells treated with ONYX-015 and irradiated

To evaluate whether radiation treatment had a synergistic effect with ONYX-015 also *in vivo*, we inoculated 60 athymic mice sc with 5×10^5 ARO cells, and 15 d later, when tumors became detectable, animals were randomly assigned to four groups. Two groups were injected with 5×10^6 pfu of ONYX-015 peritumorally for a consecutive 4 d. One group not treated with ONYX-015 and one group treated with ONYX-015 were then irradiated with a single dose of 10 Gy. Tumor growth was then followed. In Fig. 3 tumor growth is expressed as a percentage of growth relative to the volume observed at radiation (T = 0). As expected, in the group that received either ONYX-015 or radiation only, tumor growth was not significantly inhibited compared with the control group (Dunnett's *post hoc* test, $P > 0.1$). Only the combination of ONYX-015 viral plus radiation therapy significantly delayed tumor growth compared with the control (Dunnett's *post hoc* test, $P < 0.05$).Conversely, the combination of Ad5 CMV *lacZ* plus a single dose of 10 Gy did not significantly delay tumor growth (Fig. 4).

Discussion

ATC is one of the most aggressive solid tumors, and patients with ATC have a very poor prognosis (3, 26). Consequently, several novel therapeutic approaches have been proposed. Manumycin, a farnesyl:protein transferase inhibitor, has proved to be effective against ATC cells alone and in combination with paclitaxel (27, 28). Moreover, there is evidence that suppression of HMGA1 protein synthesis leads to ATC cell death (29). More recently, we found that the replication defective ONYX-015 virus is highly efficient in

TABLE 1. Effects of infection of ATC cells with Ad5 CMV *lacZ*, an adenovirus lacking E1A and E1B regions, and radiation

Cell line	Untreated	Ad5 *lacZ*	2 Gy	Ad5 *lacZ*/2 Gy	4 Gy	Ad5 *lacZ*/4 Gy	6 Gy	Ad5 *lacZ*/6 Gy
ARO	285 ± 21	267 ± 27	215 ± 26	204 ± 31	175 ± 28	160 ± 19	110 ± 13	94 ± 11
KAT-4	305 ± 32	292 ± 28	273 ± 33	280 ± 27	215 ± 31	196 ± 25	138 ± 17	125 ± 23
FRO	324 ± 35	305 ± 28	286 ± 29	295 ± 32	210 ± 22	219 ± 28	157 ± 21	146 ± 19

ARO and KAT-4 cells were infected with a replication-defective virus at an MOI of 0.5 pfu/cell, whereas FRO cells were infected at an MOI of 2.5 pfu/cell. After 24 h, cells were irradiated with 2, 4, or 6 Gy and incubated for 12 d to allow colony formation to occur. Control cells were irradiated at the indicated doses. The total number of colonies obtained are indicated. No additive or synergistic effects of Ad5 CMV *lacZ* virus and radiation were observed on the different cell lines.

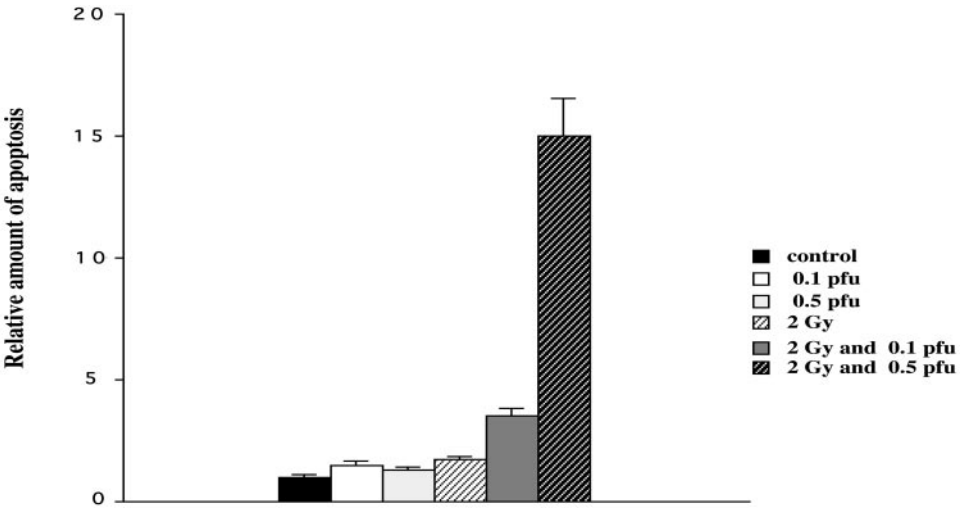

FIG. 2. DNA fragmentation of ARO thyroid anaplastic carcinoma cells infected with ONYX-015 and irradiated. ARO carcinoma cells were treated with ONYX-015 (0.1 or 0.5 pfu/cell) and irradiated. DNA fragmentation was measured after 48 h. Results are the means ± SD of duplicate determinations of three independent experiments. Results were expressed as relative amounts of apoptosis, being the results of the negative control equalized to 1.

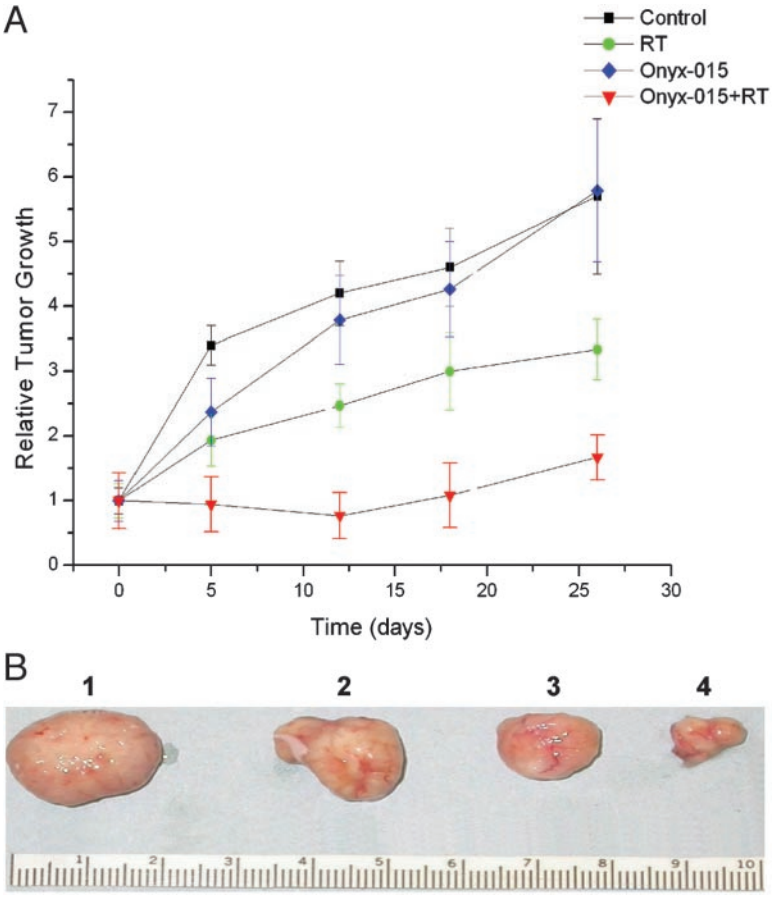

FIG. 3. Tumor growth delay induced by ONYX-015 and radiation. A, Relative tumor growth of animals treated with ONYX-015 and radiation, and control groups. Data are presented as mean ± SE. B, Representative tumors excised from mice after treatment: 1) control; 2) 5×10^6 pfu ONYX-015; 3) 10 Gy radiotherapy; and 4) 5×10^6 pfu of ONYX-015 and 10 Gy radiotherapy. RT, Radiotherapy.

killing human ATC cell lines either alone or in combination with doxorubicin and paclitaxel (19), and that this effect results from impairment of p53 function, which is a general feature of ATC cells (7–11).

The ONYX-015 plus radiation combination was used in a human colon carcinoma cell line carrying a wt p53 gene (RKO) and in a subclone that expresses an inactivating mutation of p53 gene (RKO p53.13). In this study, the authors have shown that ONYX-015 exerted a neoadjuvant effect to radiation against xenograft induced by the cell line carrying a mutant p53 gene (25). These findings prompted us to evaluate the effects of combined ONYX-015/radiation treatment on ATC cells.

Here, we report that ONYX-015 at a low MOI is an effective neoadjuvant to radiotherapy in ATC treatment. Our finding confirms that ONYX-015 could be beneficial in the treatment of this very aggressive disease. We found that very low viral concentrations (from 0.1–2.5 MOI), which are suitable for the clinical setting, enhanced the radiation-induced killing of ATC cells. Moreover, low doses of ONYX-015 associated

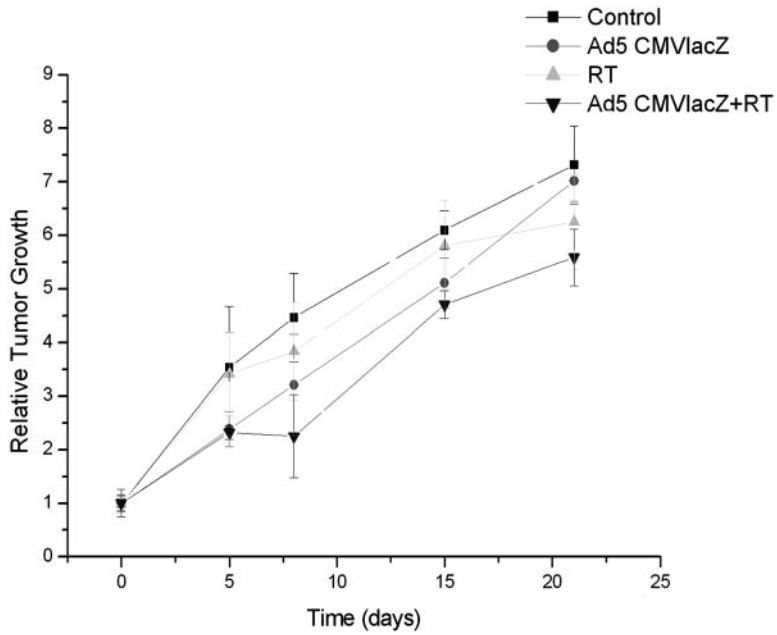

FIG. 4. Ad5 CMV *lacZ* does not modify the growth of xenograft tumors. Growth of xenograft tumors induced in nude mice treated with Ad5 CMV *lacZ* and radiation and control groups. RT, Radiotherapy.

with a single 10 Gy dose of radiation drastically delayed the growth of established xenograft tumors in athymic mice. Conversely, infection of ATC cells with Ad5 CMV *lac*Z virus, a replication-defective virus bearing deleted E1A and E1B sequences and treated with various doses of radiation, did not have any additive or synergistic cell killing; furthermore Ad5 CMV *lacZ* virus associated with a single 10 Gy dose of radiation was not able to delay the growth of established xenograft tumors in athymic mice. Consequently, the antineoplastic effects reported herein are specific for ONYX-015.

A DNA fragmentation assay showed that ATC ONYX-015-treated cells were very sensitive to radiation-induced apoptosis, which explains the synergistic effects observed in this study. The enhanced sensitivity to antineoplastic drugs or radiation observed in ONYX-015-infected cells has been attributed to the expression of E1A (30). Ad5 E1A expression has been shown to sensitize cells to radiotherapy and anticancer agents by inducing apoptosis (31–34), and E1A mediates apoptosis by inducing p53 accumulation (35, 36). However, E1A *per se* is sufficient to induce apoptosis regardless of p53 (36). Further experiments are required to elucidate how ONYX-015 and radiation activate apoptosis in ATC cells.

The necessity for p53 pathways to be nonfunctional in order for ONYX-015 replication to occur is an ongoing controversy. Despite the original design of the virus as selectively replication-competent only in p53-deficient cells, there are several reports indicating that the ONYX-015 virus is capable of replicating in p53 wild-type cells (37, 38). However, inactivation of the p53 pathway can be induced by changes in other components of the pathway, such as p14ARF or MDM2, and these alterations are functional surrogates for p53 mutation. Recently, in abdominal wall implants from a primary gall bladder carcinoma injected with ONYX-015, replication of the virus has been observed, not only in tumor cells, but in adjacent stromal cells presumably normal and bearing 53 wild type (39). Further studies are required to clarify whether these cells represented tumor cell variants or normal stromal cells, and the p53 status of these cells needs to be assessed.

The treatment of advanced or recurrent ATC is complex because the tumor invades the trachea and causes death by asphyxiation. Monotherapy usually fails to control local and regional ATC, and a multidisciplinary strategy consisting of surgery, chemotherapy, and radiotherapy is preferred (26). Clinical trials indicate that treatment with ONYX-015 helps to control locally aggressive neoplasms. Moreover, ONYX-015 administered iv has been found to be clinically safe and effective (20). Therefore, we propose that our results indicate that ONYX-015 plus radiation should be attempted to control local and regional ATC without increasing the toxic effects of radiation.

Acknowledgments

We are indebted to Dr. A. Balmain (University of California San Francisco Cancer Center and Cancer Research Institute, San Francisco, CA) and Dr. I. Ganly (Cancer Research UK Beatson Laboratories, Bearsden, UK) for providing the ONYX-015 adenovirus. We are indebted to S. Sequino and J. A. Gilder (Dipartimento di Biologia e Patologia Cellulare e Molecolare Università Federico II Napoli) for excellent technical assistance and for editing the text, respectively.

Received March 5, 2003. Accepted July 14, 2003.

Address all correspondence and requests for reprints to: Giuseppe Portella, Dipartimento di Biologia e Patologia Cellulare e Molecolare, Facoltà di Medicina e Chirurgia, Università di Napoli Federico II, via S. Pansini 5, 80131 Napoli, Italy. E-mail: portella@unina.it.

This study was supported by the Associazione Italiana per la Ricerca sul Cancro, by the Programa Italia-USA sulla Terapia dei Tumori coordinated by Prof. C. Peschle.

References

1. **Hedinger C, Williams ED, Sobin LH** 1989 The WHO histological classification of thyroid tumours: a commentary on the second edition. Cancer 63:908–911
2. **Wynford-Thomas D** 1997 Origin and progression of thyroid epithelial tumours. Cellular and molecular mechanisms. Horm Res 47:145–157

3. **Ain KB** 1999 Anaplastic thyroid carcinoma: a therapeutic challenge. Semin Surg Oncol 16:64–69
4. **Bischoff J R, Kirn D H, Williams A, Heise C, Horn S, Muna M, Ng L, Nye JA, Sampson-Johannes A, Fattaey A, McCormick F** 1996 An adenovirus mutant that replicates selectively in p53 deficient human tumor cells. Science 274:373–376
5. **Ries SJ, Brandts CH, Chung A S, Biederer CH, Hann BC, Lipner EM, McCormick F, Korn WM** 2000 Loss of p14ARF in tumor cells facilitates replication of the adenovirus mutant dl1520 (ONYX-015). Nat Med 6:1128–1133
6. **Nemunaitis J, Ganly I, Khuri F, Arseneau J, Kuhn J, McCarty T, Landers S, Maples P, Romel L, Randlev B, Reid T, Kaye S, Kirn D** 2000 Selective replication and oncolysis in p53 mutant tumors with ONYX-015, an E1B-55kD gene-deleted adenovirus, in patients with advanced head and neck cancer: a phase II trial. Cancer Res 15:6359–6366
7. **Ito T, Seyama T, Mizuno T, Tsuyama N, Hayashi T, Hayashi Y, Dohi K, Nakamura N, Akiyama M** 1992 Unique association of p53 mutations with undifferentiated but not differentiated carcinomas of the thyroid gland. Cancer Res 52:1369–1371
8. **Fagin JA, Matsuo K, Karmakar A, Chen DL, Tang SH, Koeffler HP** 1993 High prevalence of mutations of p53 gene in poorly differentiated human thyroid carcinomas. J Clin Invest 91:179–184
9. **Dobashi Y, Sakamoto A, Sugimura H, Mernyei M, Mori M, Oyama T, Machinami R** 1993 Overexpression of p53 as a possible prognostic factor in human thyroid carcinoma. Am J Surg Pathol 17:375–381
10. **Donghi R, Longoni A, Pilotti S, Michieli P, Della Porta G, Pierotti MA** 1993 p53 mutations are restricted to poorly differentiated and undifferentiated carcinomas of the thyroid gland. J Clin Invest 91:1753–1760
11. **Matias-Guiu X, Cuatrecasas M, Musulen E, Prat J** 1994 p53 expression in anaplastic carcinomas arising from thyroid papillary carcinomas. J Clin Pathol 47:337–339
12. **Fusco A, Santoro M** 1997 Human thyroid carcinogenesis. Forum 7.2:214–229
13. **Khuri F R, Nemunaitis J, Ganly I, Arseneau J, Tannock IF, Romel L, Gore M, Ironside J, MacDougall RH, Heise C, Randlev B, Gillenwater AM, Bruso P, Kaye SB, Hong WK, Kirn DH** 2000 A controlled trial of intratumoral ONYX-015, a selectively-replicating adenovirus, in combination with cisplatin and 5-fluorouracil in patients with recurrent head and neck cancer patients. Nat Med 6:879–885
14. **Nemunaitis J, Khuri F, Ganly I, Arseneau J, Posner M, Vokes E, Kuhn J, McCarty T, Landers S, Blackburn A, Romel L, Randlev B, Kaye S, Kirn D** 2001 Phase II trial of intratumoral administration of ONYX-015, a replication-selective adenovirus, in patients with refractory head and neck cancer. J Clin Oncol 19:289–298
15. **Habib NA, Mitry RR, Sarraf CE, Habib NA, Mitry RR, Sarraf CE, Jiao LR, Havlik R, Nicholls J, Jensen SL** 2002 Assessment of growth inhibition and morphological changes in in vitro and in vivo hepatocellular carcinoma models post treatment with dl1520 adenovirus. Cancer Gene Ther 9:414–420
16. **Reid T, Galanis E, Abbruzzese J, Sze D, Wein LM, Andrews J, Randlev B, Heise C, Uprichard M, Hatfield M, Rome L, Rubin J, Kirn D** 2002 Hepatic arterial infusion of a replication-selective oncolytic adenovirus (dl1520): phase II viral, immunologic, and clinical endpoints. Cancer Res 62:6070–6079
17. **Reid T, Galanis E, Abbruzzese J, Sze D, Andrews J, Romel L, Hatfield M, Rubin J, Kirn D** 2001 Intra-arterial administration of a replication-selective adenovirus (dl1520) in patients with colorectal carcinoma metastatic to the liver: a phase I trial. Gene Ther 21:1618–1626
18. **Mulvihill S, Warren R, Venook A, Adler A, Randlev B, Heise C, Kirn D** 2001 Safety and feasibility of injection with an E1B-55 kDa gene-deleted, replication-selective adenovirus (ONYX-015) into primary carcinomas of the pancreas: a phase I trial. Gene Ther 8:308–315
19. **Portella G, Scala S, Vitagliano D, Vecchio G, Fusco A** 2002 ONYX-015, an E1B gene-defective adenovirus, induces cell death in human anaplastic thyroid carcinoma cell lines. J Clin Endocrinol Metab 87:2525–2531
20. **Nemunaitis J, Cunningham C, Buchanan A, Blackburn A, Edelman G, Maples P, Netto G, Tong A, Randlev B, Olson S, Kirn D** 2001 Intravenous infusion of a replication-selective adenovirus (ONYX-015) in cancer patients: safety, feasibility and biological activity. Gene Ther 8:746–759
21. **Heise C, Sampson-Johannes A, Williams A, McCormick F, Von Hoff DD, Kirn DH** 1997 ONYX-015, an a E1B gene-attenuated adenovirus, causes tumor-specific cytolysis and antitumoral efficacy that can be augmented by standard chemotherapeutic agents. Nat Med 3:639–645
22. **You L, Yang C, Jablons DM** 2000 ONYX-015 works synergistically with chemotherapy in lung cancer cell lines and primary cultures freshly made from lung cancer patients. Cancer Res 60:1009–1013
23. **Pang X J, Hershman M, Chung M, Pekary AE** 1989 Characterization of tumor necrosis factor-α receptors in human and rat thyroid cells and regulation of the receptors by thyrotropin. Endocrinology 125:1783–1788
24. **Ain KB, Tofiq S, Taylor KD** 1996 Antineoplastic activity of taxol against human anaplastic thyroid carcinoma cell lines in vitro and in vivo. J Clin Endocrinol Metab 81:3650–3653
25. **Rogulski KR, Freytag SO, Zhang K Gilbert JD, Paielli DL, Kim JH, Heise CC, Kirn DH** 2000 In vivo antitumor activity of ONYX-015 is influenced by p53 status and is augmented by radiotherapy. Cancer Res 60:1193–1196
26. **Haigh PI** 2000 Anaplastic thyroid carcinoma. Curr Treat Options Oncol 1:353–357
27. **Yeung SJ, Xu G, Pan J, Christgen M, Bamiagis A** 2000 Manumycin enhances the cytotoxix effect of paclitaxel on anaplastic thyroid carcinoma cells. Cancer Res 60:650–656
28. **Xu G., Pan J, Martin C, Yeung SJ** 2001Angiogenesis inhibition in the in vivo antineoplastic effect of manumycin and paclitaxel against anaplastic thyroid carcinoma. J Clin Endocrinol Metab 86:1769–1777
29. **Scala S, Portella G, Fedele M, Chiappetta G, Fusco A** 2000 Adenovirus–mediated suppression of HMGI (Y) protein synthesis as potential therapy of human malignant neoplasias. Proc Nat Acad Sci USA 97:4256–4261
30. **Lowe SW, Ruley HE, Jacks T, Housman DE** 1993 p53-Dependent apoptosis modulates the cytotoxicity of anticancer agents. Cell 74:957–967
31. **Shao R, Karunagaran D, Zhou BPLi K, Lo SS, Deng J, Chiao P, Hung MC** 1997 Inhibition of nuclear factor-κB activity is involved in E1A-mediated sensitization of radiation-induced apoptosis. J Biol Chem 272:32739–32742
32. **Zhou Z, Jia S F, Hung MC, Kleinerman ES** 2001 E1A sensitizes HER2/neu overexpressing Ewing's sarcoma cells to topoisomerase II-targeting anticancer drugs. Cancer Res 61:3394–3398
33. **Frisch S, Mymryk J** 2002 Adenovirus-5 E1A: paradox and paradigm. Nat Rev Mol Cell Biol 6:441–452
34. **Deng J, Xia W, Hung MC** 1998 Adenovirus 5 E1A-mediated tumor suppression associated with E1A-mediated apoptosis in vivo. Oncogene 17:2167–2175
35. **Debbas M, White E** 1993 Wild-type p53 mediates apoptosis by E1A, which is inhibited by E1B. Genes Dev 7:546–554
36. **Putzer BM, Stiewe T, Parssanedjad K, Rega S, Esche H** 2000 E1A is sufficient by itself to induce apoptosis independent of p53 and other adenoviral gene products. Cell Death Differ 7:177–188
37. **Rothmann T, Hengstermann A, Whitaker NJ, Scheffner M, Zur Hausen H** 1998 Replication of ONYX-015, a potential anticancer adenovirus, is independent of p53 status in tumor cells. J Virol 72:9470–9478
38. **Goodrum FD, Ornelles DA** 1998 p53 status does not determine outcome of E1B 55-kilodalton mutant adenovirus lytic infection. J Virol 72:9479–9490
39. **Wadler S, Yu B, Tan JY, Kaleya R, Rozenblit A, Makower D, Edelman M, Lane M, Hyjek E, Horwitz M** 2003 Persistent replication of the modified chimeric adenovirus ONYX-015 in both tumor and stromal cells from a patient with gall bladder carcinoma implants. Clin Cancer Res 9:33–43